Biochemical Analysis of the Nuclease Module of the Human Ccr4-Not Deadenylase Complex

Maryati Maryati

Thesis submitted to the University of Nottingham for the degree of Doctor of Philosophy

December 2014

Abstract

In eukaryotic cells, the shortening and removal of the poly(A) tail (deadenylation) of cytoplasmic mRNA is a key step in mRNA degradation. The Ccr4-Not complex is well-characterised as a major deadenylase enzyme involved in mRNA deadenylation. The complex contains two catalytic subunits: Ccr4 and Caf1. Currently, it is unclear whether the Ccr4 and Caf1 catalytic subunits work cooperatively, or whether the nuclease components have unique roles in deadenylation. To facilitate the biochemical analysis of deadenylase enzymes, we have developed a fluorescence-based deadenylase assay, which is sensitive, quantitative and suitable for micro-well plate formats. We demonstrate the utility of the new assay for the discovery of small molecule inhibitors of the human Caf1/CNOT7 deadenylase enzyme. These compounds may become useful tools to investigate the contribution of the Caf1/CNOT7 in deadenylation. Furthermore, to understand the requirement and relative contributions of the ccr4 and Caf1 catalytic subunits, we therefore developed a method to express and purify a minimal human BTG2•Caf1•Ccr4 nuclease sub-complex from bacterial cells. By using chemical inhibition and well-characterised inactivating amino acid substitutions, we demonstrate that the enzyme activities of Caf1 and Ccr4 are both required for deadenylation. We propose a mechanism, in which the Caf1 and Ccr4 subunits cooperatively participate in mRNA deadenylation by the Ccr4-Not complex.

Acknowledgements

I would first like to thank my supervisor, Dr Sebastiaan Winkler, for giving me the opportunity and big support to complete my PhD. I would also like to thank Dr G. Jadhav & Prof P.M. Fisher, School of Pharmacy, University of Nottingham for providing the chemical compounds for screening Caf1 inhibitors and discussing the result. I would also like to thank Dr I. Kaur and Dr O. Loyin for the nice collaboration during the screening of Caf1 inhibitors. I would like to thank Dr Ingrid Dreveny for assistance with size exclusion chromatography. I would like to thank Dr Sebastiaan Winker for assistance with the analysis of protein structures. I would like to thank Blessing Airhihen for the generous gift of PARN protein. I would also like to thank the members of Winkler Groups, Dario, Heba, Vanessa and Lorenzo. I would also like to thank Prof David Heery and all the members of the Gene Regulation and RNA Biology Groups: Joel Fulton, Alex, Hilary, Hannah, Asma, Shoaib and Barbara Rampersad. I would also thank to Rachel and Ashley for their help during my first and second year of my study. I must thank the IDB (Islamic Development Bank) for funding me through this project. I also thank to Muhammadiyah University of Surakarta for the support during my study. Finally I need to thank big family, Mum, Dad, my brothers and sisters. Especially I need to thank my husband Hasto Widiharto and my three boys Rafi, Daffa and Nabil.

Table of Contents

List of Figures

Chapter 1

Chapter 3

Chapter 4

Chapter 5

Chapter 6

Chapter 7

List of Tables

Chapter 1

Chapter 2

Chapter 3

Chapter 4

Chapter 5

Chapter 6

Abbreviations List

Ago	Argonaute
ARE	A-U rich element
ARE-BP	ARE binding protein
ATP	Adenosine triphosphate
BMP	Bone morphogenic protein
BSA	Bovine serum alumin
CCR4	Carbon catabolite repression 4
CF I	Cleavage factors I
CF II	Cleavage factors II
CPEB3	Cytoplasmic polyadenylation element-binding protein 3
CPSF	Cleavage and polyadenylation specificity factor
CstF	Cleavage stimulation factor
Dcp1	Decapping enzyme 1
Dcp2	Decapping enzyme 2
DMSO	Dimethyl sulfoxide
DNA	Deoxyribonucleic acid
E. Coli	*Escherichia coli*
EDTA	Ethylenediaminetetraacetic acid
EDC3	Enhancer of decapping-3
EEP	Exonuclease-endonuclease-phosphatase

eIF4	Elongation initiation factor 4
FEN 1	Flap Endonuclease-1
Flc	Fluorescein
FRET	*Förster* resonance energy transfer
GST	*Glutathione S-transferase*
HIV	Human immunodeficiency virus
IMAC	Immobilised metal affinity chromatography
IPTG	Isopropyl β-D-1-thiogalactopyranoside
LB	Lysogeny Broth
LRR	Leucin-rich repeat
MCS	Multi cloning sites
m^7G	7-methyl-guanosine
mRNA	Messanger RNA
miRNA	MicroRNA
miRISC	MicroRNA induced silencing complex
NMD	Nonsense mediated decay
NSD	Nonstop mediated decay
NAR	Not Anchoring Region
PABP	Poly(A) binding protein
PAN	Poly(A) specific nuclease
PAN2	Poly(A) specific ribonuclease subunit 2
PAN3	Poly(A) specific ribonuclease subunit 3

PAP	Poly(A) polymerase
PABN1	Poly(A)-binding protein nuclear 1
PARN	Poly(A) specific ribonuclease
PAS	Polyadenylation signal
PCR	Polymerase Chain Reaction
Poly(A)	Poly adenosine tail
PTC	premature termination codon
RNA	Ribonucleic acid
RNAP II	RNA polymerase II
rRNA	Ribosomal RNA
RRM	RNA recognition motif
SDS-PAGE	Sodium dodecyl sulfate polyacrylamide gel electrophoresis
SEC	Size exclusion chromatography
snRNA	Small nuclear RNA
TAMRA	Tetramethylrhodamine
TGF-β	Transforming growth factor β
TTP	Tristetraprolin
UTR	Untranslated region
UPF	Up-frameshift

Chapter 1

Introduction

Chapter 1. Introduction

1.1 Overview of eukaryotic gene regulation

Gene regulation includes a wide range of processes that are used by cells to regulate the production of RNAs and proteins. The survival and development of multicellular organism is directly linked to the control of gene expression. Transcription is the first step in gene regulation in which DNA is copied into messenger RNA by the RNA polymerase. Eukaryotes have three RNA polymerases (RNAPI-III) (Cooper and Hausman, 2000). The immature messenger RNA (mRNA) molecule produced by RNA polymerase II (RNAPII) is known as pre-mRNA. The pre-mRNA undergoes three modifications in order to convert it to mature mRNA. These modifications include capping, splicing and polyadenylation (Bentley, 2005). The first process, capping, is the modification of the 5' end of eukaryotic mRNA. A guanylyl transferase forms a 5' to 5' triphosphate bridge, attaching a guanidine residue to the 5' end of the mRNA. Then, the guanidine residue is methylated at position seven by a methyl transferase to form the 5' cap which stabilizes the mRNA (Cowling, 2010). The second process, splicing, is the step by which the pre-mRNA is modified to remove the introns, leaving the protein coding exon sequences. This process is catalyzed by the spliceosome, a multi-subunit complex of protein and small nuclear RNA (snRNA) molecules (McManus and Graveley, 2011). The final step to produce mature mRNA is polyadenylation, which is the addition of a 3'polyadenosine (poly(A)) tail. The poly(A) tail is the key element responsible for the stability of mRNA. Messenger RNA with longer poly(A) tail are more stable with increased half-lives (Colgan and Manley, 1997, Mandel et al., 2008, Proudfoot, 2011). After mature mRNA is formed, the mRNA is exported to the cytoplasm. In the cytoplasm, the mRNA undergoes translation to form protein product or mRNA degradation (Figure 1.1).

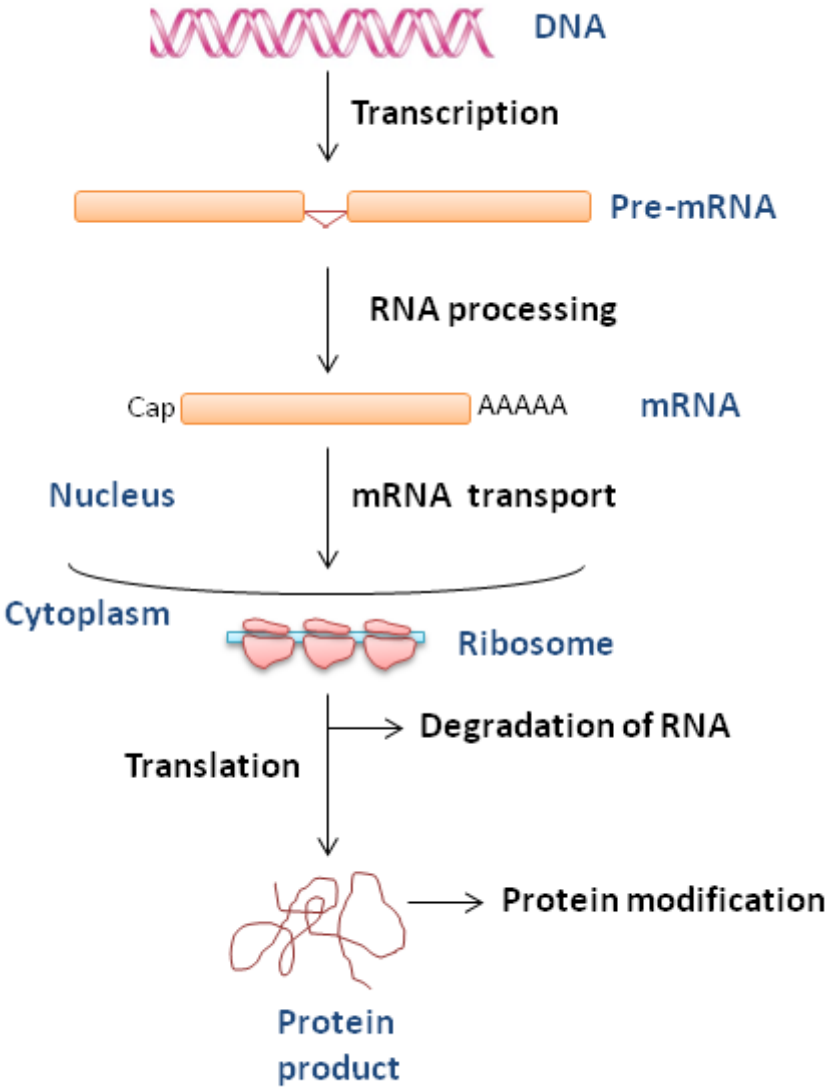

Figure 1.1 Overview of eukaryotic gene regulation. The pre-mRNA undergoes three modification processes: capping, splicing and polyadenylation to convert it into a mature mRNA. After mature mRNA is formed, the mRNA then exported to the cytoplasm for subsequent translation to produce a protein or degradation of the mRNA.

1.2 Polyadenylation

As part of gene regulation, the poly(A) tail of mRNA has multiple roles, such as promoting efficient translation, transport from the nucleus to the cytoplasm, and conferring stability. Stability of the mRNA in the cytoplasm is maintained by the presence of the poly(A) tail along with poly(A) binding proteins. Both of these features protect the mRNA from ribonuclease attack (Colgan and Manley, 1997, Chen and Shyu, 2011). The control of poly(A) tail length occurs in both the nucleus (nuclear polyadeanylation) and the cytoplasm (cytoplasmic polyadenylation). During nuclear polyadenylation, a poly(A) tail is added to the RNA at the end of transcription. Cytoplasmic polyadenylation is the elongation of the poly(A) tail after export of the mRNA to the cytoplasm. Polyadenylation follows the cleavage of the newly transcribed messenger RNA. The cleavage of nascent mRNA is required for normal transcription termination and for polyadenylation. In mammalian cells, the 3' end of the mRNA is processed by cleavage of the pre-mRNA at the polyadenylation site, followed by the addition of a non-templated polyadenylated tail, approximately 200–300 adenosine residues long (Sheets and Wickens, 1989, Zhang et al., 2010). Almost all eukaryotic pre-mRNAs undergo cleavage/polyadenylation at their 3' ends, except the histone mRNAs, which are cleaved but not polyadenylated (Gilmartin, 2005). The cleavage/polyadenylation machinery requires specific signal sequences in the pre-mRNA together with a large number of protein factors (Figure 1.2) (Zhang et al., 2010). The polyadenylation signal (PAS) was the first identified sequence element which plays an important role in 3’ mRNA processing. This sequence is an AAUAAA hexamer located around 10-30 bases upstream of the cleavage/polyadenylation site (Colgan and Manley, 1997, Mandel et al., 2008, Proudfoot, 2011)

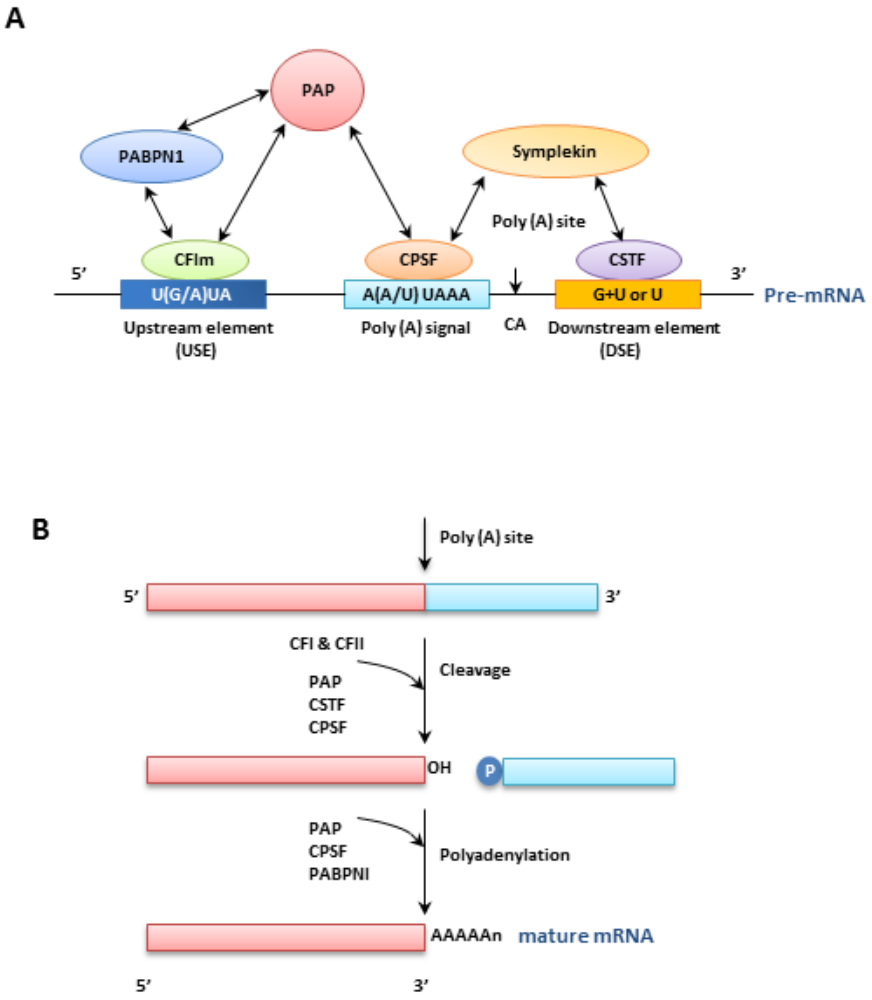

Figure 1.2 Mammalian pre-mRNA 3'end processing machinery. A. The nuclear cleavage and polyadenylation complex. The CPSF complex binds to the poly(A) signal. The Cleavage Factor 1 complex (CFIm) recognizes the upstream element and the CSTF complex recognized the GU- or U-rich downstream element. The interaction of CPSF, CStF, symplekin and CFIm stabilizes RNA binding, resulting in correct cleavage and polyadenylation site recognition and recruitment of the poly(A) polymerase (PAP). The nuclear poly(A) binding protein (PABPN1) interacts with CFIm and PAP and contributes to the efficiency of polyadenylation. **B.** The cleavage and polyadenylation process to form mature mRNA. The 3' end of the mRNA is processed by the cleavage of the pre-mRNA at the polyadenylation site followed by the addition of a non-templated polyadenylated tail.

The cleavage step requires cleavage-polyadenylation specificity factor (CPSF), cleavage stimulation factor (CSTF), cleavage factors I and II (CFI_m and $CFII_m$) and poly(A) polymerase (PAP). The polyadenylation signal (PAS) is recognised by the CPSF complex (CPSF 160 subunit) (Proudfoot, 2011). At the polyadenylation stage, the proteins required are: CPSF, PAP, symplekin and poly(A)-binding protein nuclear 1 (PABN1) (Zhao et al., 1999, Mandel et al., 2008, Charlesworth et al., 2013). The binding of PABN1 to the poly(A) stimulates PAP processivity and prevents degradation of mRNAs thereby preserving the length of the poly(A).

1.3 Regulated mRNA degradation

The abundance of an mRNA is not only dependent on the function of its synthesis, processing, and nuclear export rates, but also on the rate of mRNA degradation in the cytoplasm (Wu and Brewer, 2012). The degradation of eukaryotic mRNAs plays a key role in the control of gene expression. The stability of eukaryotic mRNAs are influenced by the 5′ 7-methylguanosine cap and the 3′ poly(A) tail. These two structures protect the mRNA from exonucleases. The 5′ 7-methylguanosine cap interacts with the cytoplasmic proteins eIF4E, and the 3′ poly(A) tail interacts with the poly(A) binding protein (PABP), both of which protect the transcript from exonucleases and enhance translation initiation. To initiate mRNA decay, either one of these two components must be disturbed, or the mRNA must be cleaved internally by endonuclease enzymes (Garneau et al., 2007). There are three classes of RNA-degrading enzymes: endonucleases that cut RNA internally, 5’ exonucleases that hydrolyse RNA from the 5’ end, and 3’ exonucleases that degrade RNA from the 3’ end (Houseley and Tollervey, 2009).

Shortening of the poly(A) tail of mRNA is an initial step in cytoplasmic mRNA degradation, which involves several deadenylases (Parker and Song, 2004, Garneau et al., 2007, Wahle and Winkler, 2013). Degradation of cytoplasmic

eukaryotic mRNA involves two general pathways, which both begin with deadenylation (Figure 1.3). In the first pathway decapping follows the deadenylation. After deadenylation, the Lsm 1-7 proteins bind to the 3' end of deadenylated product and assist the decapping enzyme complex, Dcp1-Dcp2, to remove the 5'cap structure. This results in the degradation of the mRNA body via 5'-3'digestion by XRN1. In the second pathway, deadenylation exposes the mRNA body to 3'-5' degradation by the cytoplasmic exosome (Parker and Song, 2004, Garneau et al., 2007, Goldstrohm and Wickens, 2008, Wu and Brewer, 2012). The enzymes involved in cytoplasmic mRNA are presented in Table 1.1.

Protein	**Human names**	**Function**
Deadenylase enzyme	CNOT7 (Caf1)	DEDD-type deadenylases of Ccr4-Not complex
	CNOT8 (Caf1b)	DEDD-type deadenylases of Ccr4-Not complex
	TOE1 (Caftz)	DEDD-type deadenylases
	PARN	DEDD-type deadenylases
	PAN2	DEDD-type deadenylases that form a dimeric complex with PAN3
	CNOT6 (Ccr4a)	EEP-type deadenylases of Ccr4-Not complex
	CNOT6L (Ccr4b)	EEP-type deadenylases of Ccr4-Not complex
	Nocturnin	EEP-type deadenylases
	Angel	EEP-type deadenylases
	Angel 2	EEP-type deadenylases
Decapping enzyme	Dcp1a, Dcp1b	Member of Dcp decapping enzyme
	Dcp2	Catalytic subunit of decapping enzyme
	Lsm 1-7	Lsm RNA binding complex containing Lsm subunits 1 to 7
Exoribunuclease enzymes	XRN1	Cytoplasmic 5' –3' exoribonuclease
	Exosome	Multi subunits exonuclease

Table 1.1 Enzymes involved in cytoplasmic mRNA degradation

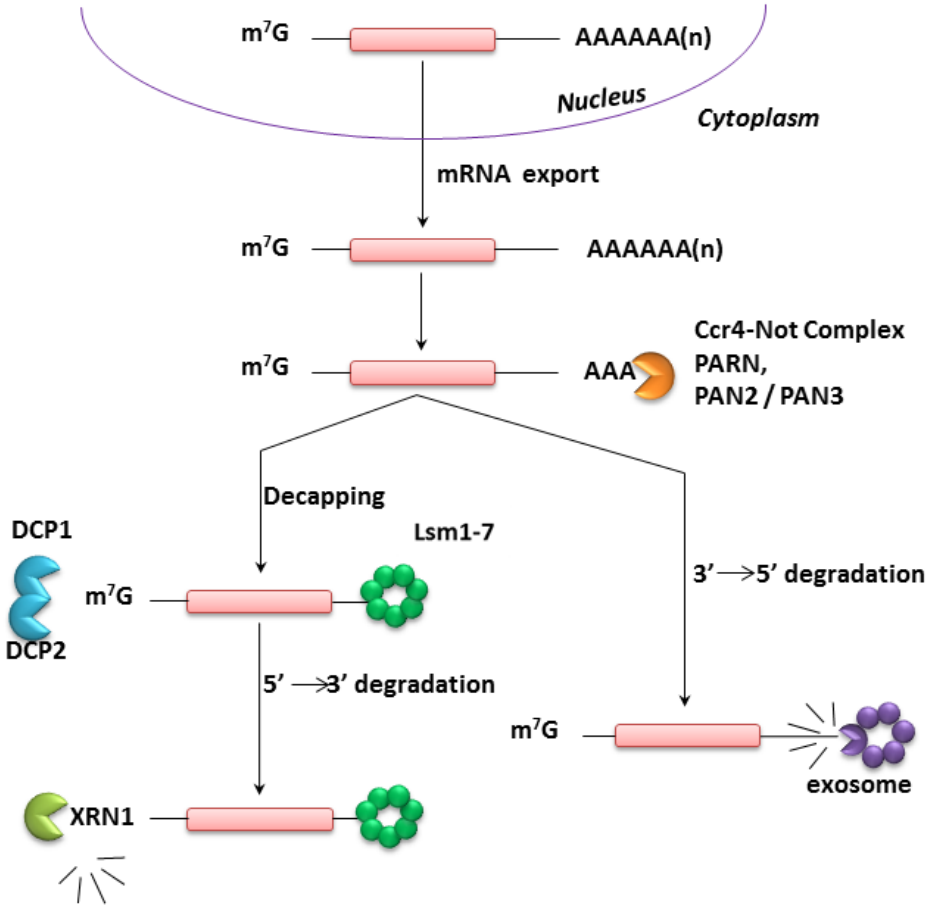

Figure 1.3 mRNA degradation pathways. In the cytoplasm, deadenylases shorten the poly(A) tail. Deadenylation of the poly(A) tail of mRNA stimulates mRNA degradation via two pathways, mRNA decapping by DCP1/DCP2 followed by 5'→3' degradation by XRN1, or 3 →5 degradation via the exosome enzyme.

1.3.1 The enzymes involved in deadenylation

Deadenylases, which degrade the poly(A) tail of mRNA, are Mg^{2+}-dependent exoribonucleases that use the poly(A) tail as their main substrate and hydrolyse RNA in a 3'→5' direction, producing the 5'-AMP. In recent years, biochemical and genetic analysis has increased the number of known deadenylases. Through the advance of bioinformatics, ten different deadenylase enzymes were identified in human cells (Goldstrohm and Wickens, 2008). Based on their nuclease domain, deadenylases are now categorized into two groups. The first group consists of DEDD-type nucleases, which contain Asp and Glu residues in the exonuclease motifs. The enzymes require two metal ions for their activity. The DEDD-type nucleases consist of many subfamilies, such as RNase D, RNase T and and oligoribunuclease. The RNase D is required in the maturation of small stable RNAs and denaturation of tRNA molecules. RNase T, a 3' to 5'exoribunuclease has important role in *E.coli* for maturation of small, stable RNAs and 23S rRNA. The enzyme also involved in the end of tRNA turnover. The third member, oligoribonuclease is a 3' to 5' exonuclease specific for small oligonucleotides. This enzyme is required for growth, because none of other enzymes can act efficiently on small substrates (Li et al., 1998, Li et al., 1999, Zuo and Deutscher, 2001). DEDD-type deadenylases include POP2 (also known Caf1a/CNOT7, Caf1b/CNOT8, TOE1/CAF1Z), poly(A)-specific ribonulease (PARN) and PAN2. The second group of deadenylases belongs to the exonuclease-endonuclease-phosphatase (EEP) family. The founding member of the EEP family is DNase I. Other proteins containing an EEP domain include apurinic/apyrimidinic (AP) DNA-repair endonucleases and human AP endonuclease (HAP1). These nucleases have 20% sequence identity and different cleavage preferences. The EEP family have conserved catalytic Asp and His residues in their nuclease domains, and use these amino acids to coordinate Mg^{2+} ions. EEP-type deadenylase enzymes include Ccr4a/CNOT6,

Ccr4b/CNOT6L, Nocturnin, ANGEL (Table 1.1)(Dlakic, 2000, Zuo and Deutscher, 2001).

The range of deadenylases varies among species. The POP2, Ccr4, PAN2 and ANGEL deadenylases are present in all eukaryotes, however other deadenylases are less prevalent. For example, PARN and CAF1Z are less conserved in *Drosophila melanogaster*. As a result of gene duplications the POP2, Ccr4, PARN and ANGEL families have developed in vertebrates, (Goldstrohm and Wickens, 2008). In several species, many of the enzymes are presented in multiple forms because of genome-duplication events. For example, Caf1a/CNOT7 and Caf1b/CNOT8 in humans share 89% similarity, Ccr4a/CNOT6 and Ccr4b/CNOT6L share 88% similarity at the amino acid level (Doidge et al., 2012b, Winkler and Balacco, 2013). Until now, the advantage of having so many different deadenylases remains unclear. There is a possibility that specific deadenylases target unique mRNA. On the other hand, multiple deadenylases may have overlapping functions and work on the same mRNA.

Poly (A) specific ribonuclease (PARN) is one of the mammalian nucleases that specifically degrades the poly(A) of mRNA (Goldstrohm and Wickens, 2008). PARN is a member of the DEDD family of nucleases in which the enzyme activity depends on divalent metal ions. This enzyme can be found in both the nucleus and cytoplasm (Korner et al., 1998). Interaction with the 5'cap structure increases the rate of mRNA degradation (Dehlin et al., 2000, Martinez et al., 2000, Martinez et al., 2001).

Structural and biochemical studies indicated that the structure of PARN is composed of at least three structural domains: the catalytic domain, the R3H domain and the RNA recognition motif (RRM). Acidic amino acids Asp-28, Glu-30, Asp-292 and Asp-382 are essential for the catalytic activity of PARN because they are directly involved in coordinating the divalent metal ions (Ren et al., 2002b, Ren et al., 2004). Asp-28 is the most important amino acid

in the binding of the two Mg^{2+} ions (He et al., 2011). Amino acids important for PARN cap binding are located within the RRM (Nilsson et al., 2007, Wu et al., 2009). Studies showed that the presence of a 5' cap structure in the substrate significantly increased the deadenylation activity of PARN (Dehlin et al., 2000, Gao et al., 2000, Martinez et al., 2001). The changes in the active site of PARN by metal binding or mutations might lead to a change in the conformation of PARN (He et al., 2011). Previous research has also showed that none of the alanine substitutions in the four conserved acidic residues was essential for PARN binding to the RNA substrate. It was indicated that the inability of the mutant to degrade the substrate was not due to a reduced RNA binding capacity (Ren et al., 2002b). Other research indicated that the poly(A) binding protein (PABP) inhibits PARN activity at a physiological salt concentration (Korner and Wahle, 1997).

Poly(A) specific nuclease (PAN) was first identified as a DEDD type nuclease in yeast. In yeast and mammals, PAN deadenylase is formed by two different subunits; Pan2 and Pan3 (Boeck et al., 1996, Garneau et al., 2007). Pan2/Pan3 is predominantly found in the cytoplasm. Pan2 is a 127 kDa protein and it acts as the catalytic subunit. Deadenylase activity of Pan2 is stimulated by the presence of Pan3 and PABP. The enzyme activity of Pan2 requires Mg^{2+} and a 3′-OH group in its substrate. The product of the reaction is 5′-AMP. This enzyme is specific for poly(A), and it is unable to degrade the body of the mRNA. Recruitment of mRNA for Pan2/Pan3 occurs via the Pan3-PABP interaction. Pan3 interacts with PABP (poly(A) binding protein) through the PAM2 motif (PABP-interacting motif 2) to stimulate Pan2 activity (Wolf and Passmore, 2014). In *S. cerevisiae*, the PAN deadenylases were required to trim poly(A) tails of nascent mRNAs to the standard length of 60–80 nucleotides (Brown et al., 1996, Garneau et al., 2007). In mammalian cells, cytoplasmic mRNA degradation is reported to be conducted

in two phases, an initial step by PAN2–PAN3 enzyme followed by CCR4–NOT (Yamashita et al., 2005, Bartlam and Yamamoto, 2010).

The Ccr4-NOT complex is the main mRNA deadenylase and is conserved from yeast to humans. The enzyme complex contains two deadenylase enzymes, Caf1a (CNOT7), Caf1b (CNOT8) DEDD-type and Ccr4a (CNOT6), Ccr4b (CNOT6L) EEP-type enzymes. These enzymes were first identified as the predominant cytoplasmic deadenylases in yeast (Caf1 and Ccr4). They regulate deadenylation and mRNA turnover (Tucker et al., 2001). Caf1a (CNOT7) and Caf1b (CNOT8) bind directly to the Ccr4-Not complex, but only one of these DEDD–type nucleases can be bound at any one time (Lau et al., 2009b). Caf1a (CNOT7)/Caf1b (CNOT8) interacts with Ccr4a (CNOT6)/Ccr4b (CNOT6L) through the leucine-rich repeat (LRR) domains of Ccr4 (Basquin et al., 2012).

Deadenylation can take place both in the nucleus and the cytoplasm. In the nucleus, deadenylation is thought to restrict the length of a newly added mRNA poly(A) tail, while, in the cytoplasm deadenylation initiates the degradation and repression of mRNA (Bianchin et al., 2005, Goldstrohm and Wickens, 2008, Bartlam and Yamamoto, 2010). Following deadenylation, other enzymes then continue with the mRNA degradation.

1.3.2 Decapping enzymes and their regulation

Removal of the 5' cap structure of mRNA (decapping) initiates the 5'→3' mRNA decay pathway. In eukaryotic cells, there are two types of decapping enzymes. First is the scavenger decapping enzyme (DcpS), which decaps short capped oligonucleotides to release m^7GMP. DcpS is unable to decap long substrates. It was suggested that long mRNAs are unable to fit into the active site of DcpS. The inability of DcpS to decap long mRNAs might be important in preventing the mRNA from being prematurely decapped (Coller and Parker, 2004). The other decapping enzyme is a dimer complex that

consists of two sub-units, Dcp1 and Dcp2 proteins. Dcp2 is the catalytic sub-unit, and Dcp1p functions to enhance Dcp2p activity. This decapping enzyme prefers substrates more than 25 nucleotides in sequence. Removal of the cap structure by Dcp1–Dcp2, or by Dcp2 alone, produces m^7GDP and leaves an mRNA with a 5′ monophosphate. The production of mRNA with 5′ monophosphate is a preferred substrate for XRN1, a 5' to 3' exonuclease. In yeast, loss of either sub-unit (Dcp1 or Dcp2) causes a complete block of decapping *in vivo*. This information suggests that there are no other important decapping enzymes that act on the mRNA . In human and yeast both sub-units physically interact with each other. In mammals, there are two version of Dcp1, hDcp1a and hDcp1b. These two versions might have different functions (Parker, 2004). Efficient decapping requires several factors, such as Lsm1-7 complex, LSM16 (EDC3, enhancer of decapping-3), PABP1 and Lsm 14 (mammalian RAP55, RNA associated protein of 55 kDa). The heptameric Lsm1-7 promotes decapping by interacting with the 3'end of mRNA (Garneau et al., 2007).

1.3.3 Protein-mediated mRNA decay.

It has been shown that some proteins mediate mRNA decay, for instance the tristetraprolin (TTP) protein, pumilio and Nanos proteins (Inada and Makino, 2014). The TTP protein mediates mRNA decay via an interaction with AU-rich elements (AREs). AREs are an important signal motif for rapid mRNA degradation in mammalian cells (Chen and Shyu, 1995). Bioinformatic analysis showed that between 5-8% of the transcriptome contains AREs (Halees et al., 2008). AREs are found in the 3' UTR of many mRNAs and are characterised by sequence regions which are rich in adenosines and uridines and often include one or more copies of the pentamer sequence AUUUA (Wu and Brewer, 2012, Chen and Shyu, 1995). AREs are abundant in mRNAs which encode interleukins, proto-oncogens and cytokines (Chen and Shyu, 1995, Shim and Karin, 2002). The sequence of AREs is diverse but can be

classified into three broad (Chen and Shyu, 1995, Wilusz et al., 2001) .Class I AREs contain 1–3 interspersed copies of the AUUUA pentamer surrounded by U-rich regions. This type is found in mRNAs for FOS and MYC. Class II AREs consist of multiple overlapping copies of the AUUUA motif, and are found in cytokine mRNAs such as GM-CSF and tumor necrosis factor α (TNFα). Class III AREs contain a predominantly U-rich sequence but lack AUUUA pentamers (Wu and Brewer, 2012). Each class of AREs has a specificity for RNA binding proteins that act as cofactors for recruiting deadenylases enzymes. Protein tristetrapolin (TTP) and its homolog BRF-1 are examples of protein that associate with AREs to promote mRNA decay. TTP binds to AREs and activates mRNA decay, by acting as a bridge to recruit the mRNA decay enzymes (Lykke-Andersen and Wagner, 2005). To recruit the CCR4-Not deadenylase complex, TTP protein directly binds to the scaffold of the deadenylase complex, CNOT1 (Fabian et al., 2013). In yeast, a pumilio family protein, Mpt5 recognizes the 3'UTRs of mRNA. This protein recruits the Ccr4-Not complex to mediate the mRNA decay by interaction with the Caf1 sub-unit (Goldstrohm et al., 2006).

1.3.4 MicroRNA-mediated decay

MicroRNAs (miRNAs) are short (20 to 22 nucleotides) non-coding RNAs that play an important role in post-transcriptional gene regulation. Most miRNAs repress translation by base-pairing to target mRNAs. Binding of the miRNA results in translational repression, often followed by degradation of the target mRNA (Bushati and Cohen, 2007, Chen and Shyu, 2011, Huntzinger and Izaurralde, 2011). During miRNA biogenesis, the newly synthesised single stranded miRNA is incorporated into the microRNA induced silencing complex (miRISC). The argonaute family protein (AGO) forms the core of the miRISC complex and recruits the GW182 proteins (Eulalio et al., 2008, Huntzinger and Izaurralde, 2011). The miRISC complex facilitates translation

silencing and mRNA degradation via two pathways. Within the first pathway, miRNAs direct endonucleolytic cleavage of fully complementary strands between the mRNA and the miRNA (Figure 1.4A). In this process, miRNAs direct their targets for 5′ to 3′mRNA decay by XRN1 and the exosome (Huntzinger and Izaurralde, 2011, Wu and Brewer, 2012). The second pathway of mRNA degradation via miRNA binding is through the recruitment of deadenylation enzymes (Figure 1.4B). This pathway requires GW182, Argonaute (AGO1), the Ccr4-Not complex and the Dcp1-Dcp2 complex (Behm-Ansmant et al., 2006).

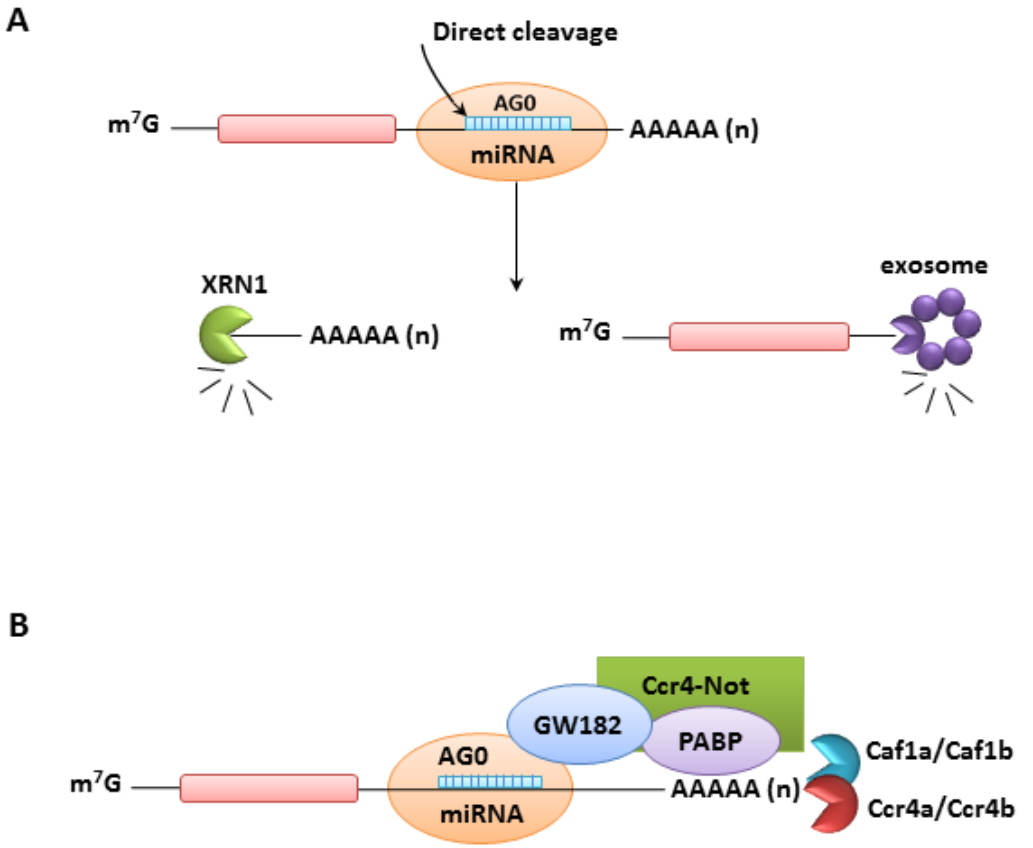

Figure 1.4 MicroRNA-mediated mRNA decay. **A**. AGO catalysed endoribonunuclease degradation. AGO acts as slicer activity to catalyse endonuclease activity when there is full complementarity between the mRNA and miRNA. The endoribonuclease generates 5' and 3' mRNA cleavage products which are degraded by XRN1 and the exosome. **B.** miRNA-mediated recruitment of the Ccr4-Not complex to mRNA. miRNA bound to AGO recruits GW182. GW182 interact with PABP and recruits the Ccr4-Not complex.

1.4 Quality control of mRNA

Messenger RNA surveillance consists of pathways in an organism that ensure the quality of mRNA by degrading the transcripts that have not been properly processed. In general, there are three surveillance mechanisms present in cells; nonsense-mediated decay, nonstop mRNA decay and no-go decay (Wu and Brewer, 2012).

1.4.1 Nonsense-mediated decay (NMD)

Nonsense-mediated mRNA decay is the most well-studied surveillance mechanism that has been found in all eukaryotes (Garneau et al., 2007). The NMD is a surveillance pathway that detects and degrades mRNAs containing premature termination codons (PTCs). This pathway is important in reducing the chance of producing truncated and potentially harmful proteins (Conti and Izaurralde, 2005, Chang et al., 2007). The core proteins of the NMD complex consist of three trans-acting factors, up-frameshift 1 (UPF1), UPF2 and UPF (Conti and Izaurralde, 2005). In mammalian cells, SMG5 and SMG7 proteins mediate the rapid degradation of NMD targeted mRNA. By interaction with Caf1 sub-units, this protein recruits the Ccr4-Not complex to premature termination codon containing mRNAs (Loh et al., 2013).

1.4.2 Nonstop mediated decay (NSD) and No go decay

Messenger RNA, which lacks a termination codon is unstable and subject to degradation. Nonstop mediated decay is a surveillance mechanism to detect and degrade mRNA transcripts lacking a stop codon (van Hoof et al., 2002, Wu and Brewer, 2012). Currently, there are two known pathways of NSD; Ski7 pathway and non Ski7 pathway. The Ski7 pathway, which is conserved in yeast and mammalian cells, requires the cytoplasm exosome, the SKI complex (Ski2, Ski3 and Ski8) and the adaptor protein Ski7. The stalled ribosome at the 3' end of the transcript initiates NSD. Ski7 binds to the empty A site on the ribosome. Ski7 then forms a complex with the SKI complex,

which in turn recruits the exosome which initiates 3'→5' mRNA decay (van Hoof et al., 2002, Wu and Brewer, 2012). The second pathway occurs in the absence of Ski7, and the MRNA is degraded in a 5'→3 direction (Figure 1.5) (Inada and Makino, 2014).

The other mRNA-surveillance mechanism is no-go decay, which has only been discovered in yeast and currently is not well understood. No go decay detects stalled ribosomes on mRNA in order to prevent the sequestration of translation factors to faulty transcripts. The mRNA is then cleaved near the stall site (Doma and Parker, 2007).

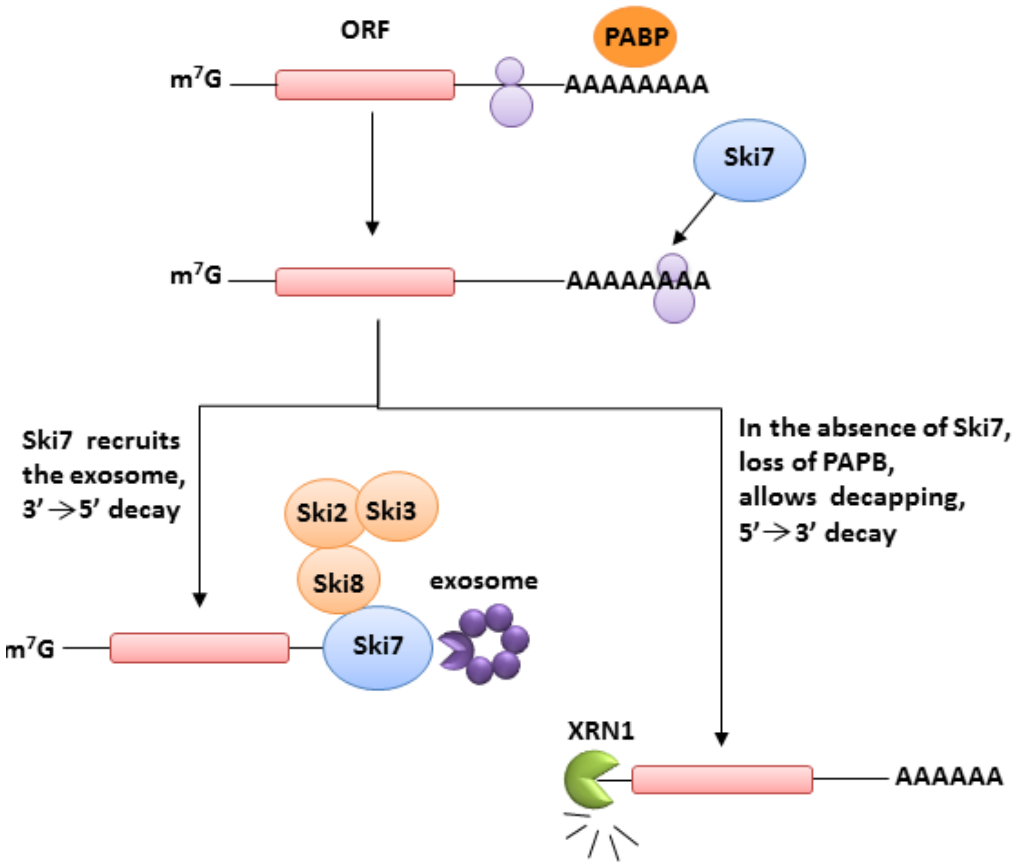

Figure 1.5 Nonstop-mediated mRNA decay. Upon translation of mRNAs lacking a stop codon, the ribosome is allowed to transverse the 3' UTR and stall within the poly(A) tail. In the presence of Ski7, Ski7 binds to the stalled ribosome, then forms a complex with Ski2, Ski3 and Ski8 before recruiting the exosome to stimulate 3'→5' mRNA degradation. In the absence of Ski7, it allows decapping and then the 5'→3 mRNA decay mediate the NSD.

1.5 The Ccr4-Not complex

1.5.1 Overview of the Ccr4-Not complex

The Ccr4-Not complex is conserved from yeast to humans. The conserved core of the Ccr4-Not complex consists of at least two modules: a catalytic module (nuclease module) and a NOT module. In *Saccharmyces cerevisiae*, the complex exists in two forms of 1.0 and 1.9 MDa, and consists of five NOT proteins (Not1-Not5), two catalytic subunits, Ccr4 and Caf1 (Pop2) and additional subunits including Caf40 and Caf130. The Caf130 subunit is specific to yeast (Liu et al., 1998, Chen et al., 2001, Collart, 2003, Lau et al., 2009). In human cells, orthologues for most of the yeast Ccr4-Not subunits have been identified (Albert et al., 2000)(Albert et al., 2000)(Albert et al., 2000). The human Ccr4-Not complex consists of two deadenylase enzymes, Caf1a (CNOT7) or Caf1b (CNOT8) and Ccr4a (CNOT6) or Ccr4b (CNOT6L) and several non-catalytic components (CNOT1 to CNOT4). In yeast Not3 and Not 5 are similar proteins, but humans only have one ortholog protein, CNOT3 (Albert et al., 2000, Lau et al., 2009). Additional subunits of the complex have been identified and include CNOT9/RCD1/Caf40, CNOT10 and CNOT11 (C2orf29). CNOT10 and CNOT11 are specific to humans, they are not found in yeast (Tabel 1.2) (Lau et al., 2009).

Yeast				Human					
Subunit		**MW (kDa)**	**amino acids**	**Subunit**		**MW (kDa)**	**amino acids**	**Domain/motifs**	**Other names**
Not1	Cdc39	240	2108	CNOT1		267	2376	LxxLL	human Not1
Not2	Cdc36	22	191	CNOT2		60	540		human Not2
Not3		94	836	CNOT3		82	609		human Not3
Not4	Mot2	65	587	CNOT4		71	433	RING	human Not4
Not5		66	560					Homology with Not3	
Ccr4		95	837	CNOT6	Ccr4a	63	557	LRR; EEP	Human Ccr4
				CNOT6L	Ccr4b	63	555	LRR; EEP	
Pop2	Caf1	50	433	CNOT7	Caf1	33	285	DEDD	human Caf1
				CNOT8	Caf1b	34	292	DEDD	Calif, human Pop2
Caf40		41	373	RQCD1		34	299		Rcd1, CNOT9
Caf130		129	1122						
				CNOT10		82	744		
				CNOT11		55	510		C2ORF29

Table 1.2 Ccr4-Not components in yeast and human cells.

Three-dimensional structure of the Ccr4-Not complex was first determined from yeast in 2011. Structural studies were carried out using electron microscopy and image reconstruction. The overall structure of the yeast 1.0 MDa Ccr4-Not complex isolated using Not1 as bait is an L-shape with two arms of similar length. The Caf1 and Ccr4 components are located in the hinge region connecting the two arms (Figure 1.6A.B) (Nasertorabi et al., 2011, Basquin et al., 2012).

Interactions between the individual subunits of the Ccr4-Not complex of *Drosophila melanogaster* was mapped by Bawankar et al (2013) using co-immunoprecipitation and pull-down assays (Figure 1.6C). The result showed that CNOT1 is the largest subunit of the Ccr4-Not complex and that it is assumed to be a scaffold protein in which several modules are attached. CNOT1 contains three main regions, the N-terminal region (CNOT1-N), the middle region (CNOT1-M) and the C-terminal region (CNOT1-C) (Bawankar et al., 2013). The CNOT1-M region consists of two domains: a middle domain of eukaryotic initiation factor 4G (MIF4G) and an unknown function domain (DUF3819). The DUF3819 was then termed CN9BD (CNOT9 binding domain). The nuclease module of Ccr4-Not complex binds to the middle domain via the MIF4G domain of NOT1. In this interaction, Caf1 acts as an adaptor between CNOT1 and Ccr4 (Basquin et al., 2012, Petit et al., 2012, Bawankar et al., 2013). Another protein, CNOT9/Caf40, which contains highly conserved domain encompassing six armadillo repeats binds to the middle region of CNOT1 via the unknown function domain DUF3819 (Bawankar et al., 2013). It has been shown that the CNOT1-M region mediates the interaction of Ccr4-Not with the silencing domain of TNRC6/GW182 (Huntzinger et al., 2013). Recent research indicates that the CNOT1-M region plays a role in the recruitment of Ccr4-Not complex to miRNA target through the W-binding pockets in the CN9BD-CNOT9 module. This study also provides the crystal structure of CNOT1-CNOT9 complex. The crystal shows tandem W-binding pockets in CNOT9 (Figure 1.7A) (Chen et al., 2014).

The N-terminal domain of CNOT1 interacts with two proteins, CNOT10 and CNOT11 (C2orf29) (Mauxion et al., 2013, Bawankar et al., 2013). CNOT10 and CNOT11 were originally identified as subunits of human Ccr4-Not complex (Lau et al., 2009b). Analysis using immunoprecipitation assays indicated that CNOT10 and CNOT11 have strong interaction. It suggests that CNOT10 and CNOT11 form a complex, then bind to the NOT1 scaffold via an interaction between CNOT11 and the N-terminal domain of NOT1 (Bawankar et al., 2013). The NOT module of the Ccr4-Not complex associates with C-terminal domain of CNOT1. CNOT2 and CNOT3 are related proteins that share a NOT-box in their conserved C-terminal region. In addition to the NOT-box, CNOT3 contains a highly conserved N-terminal domain which is linked to the NOT-box by a linker region. CNOT2 contains less-conserved N-terminal region. CNOT2 interacts with CNOT3 through the NOT-boxes in their C-terminal region. Moreover, CNOT2/CNOT3 interacts with CNOT1 through their C-terminal regions which contain the NOT-boxes (Bawankar et al., 2013). Recent study provides crystal structure of human NOT module containing C-terminal of the CNOT1, CNOT2 and CNOT3 (Figure 1.7B). The structure shows that the C-terminal of CNOT1 provides a rigid scaffold. The C-terminals of CNOT2 and CNOT3 contain a conserved domain named NOT-BOX, which is responsible for dimerization. The C-terminal also presents a region responsible for the interaction with CNOT1. This region is designated Not Anchoring Region (NAR) .

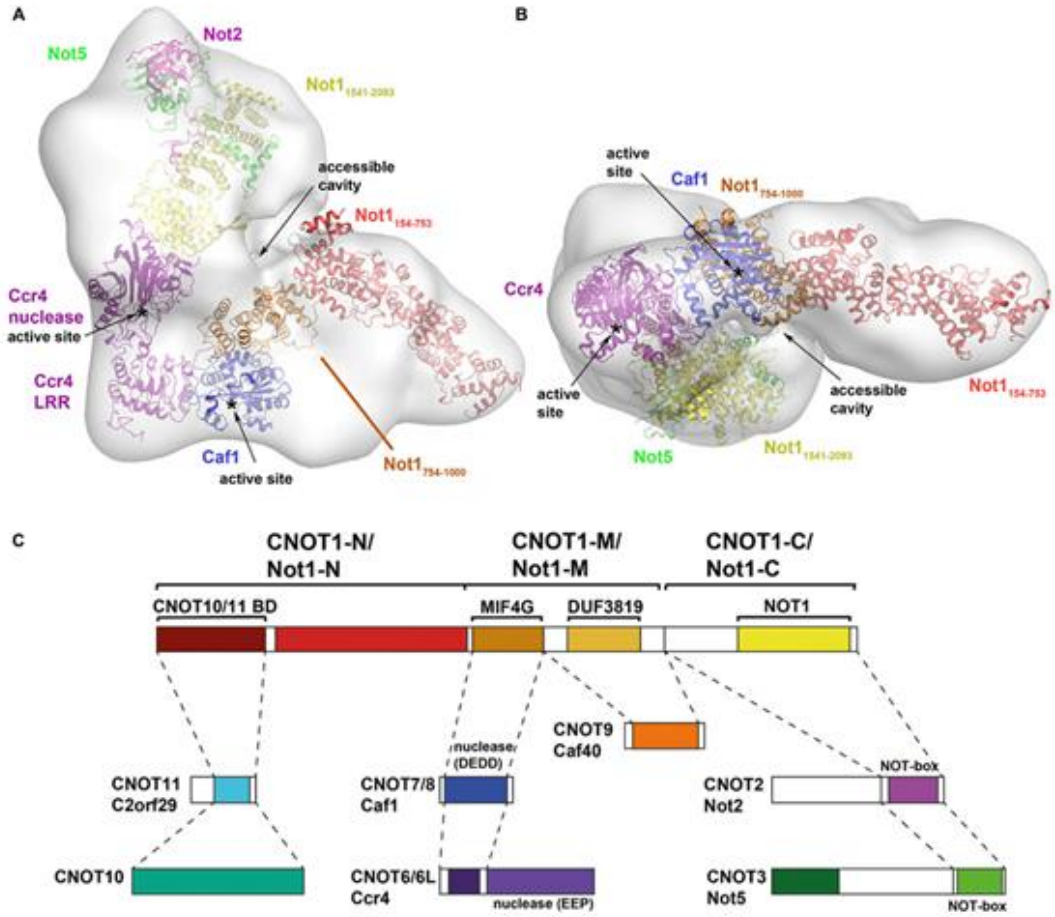

Figure 1.6 Overview of Ccr4-Not complex. A. B. Model of Ccr4-Not complex using electron microscopy (EM) and image reconstruction (Nasertorabi et al., 2011). **C.** Interactions maps between CNOT1 with other subunits of Ccr4-Not complex. Figure as originally published in Xu K, Bai Y, Zhang A, Zhang Q and Bartlam MG (2014) Insights into the structure and architecture of the CCR4–NOT complex Front. Genet. 5:137. doi: 10.3389/fgene.2014.00137. The figure was reproduced under the terms of the Creative Commons Attribution License, (CC-BY 3,0).

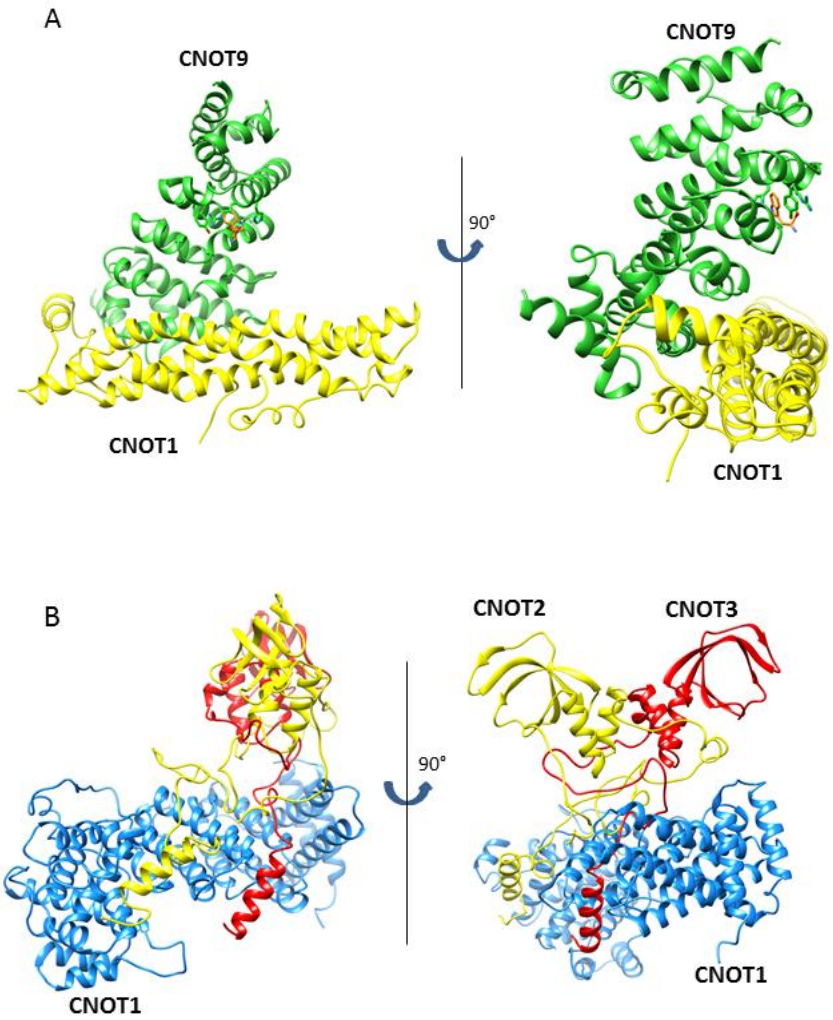

Figure 1.7 Crystal structure of the CNOT1 (DUF3819 domain)-CNOT9 complex and the NOT module. **A.** Crystal structure of CNOT1-CNOT9 complex. Shown are CNOT1 (amino acids residues 1353-1587; yellow) and CNOT9/RQCD1 (amino acid residues 15-285 green). Also shown is a W-binding pocket in CNOT9 (orange). PDB accession number: 4CRV. **B.** Structure of the human Not-module. Shown are the C-terminal part of CNOT1 (amino acid residues 1842-2353; blue), CNOT2 (residues 350-540; yellow) and CNOT3 (amino acids 607-748; red). PDB accession code used: 4C0D. Structure was visualized using the UCSF Chimera package (http://cgl.ucsf.edu/chimera; (Pettersen et al., 2004).

The nuclease module of the Ccr4-Not complex contains two distinct deadenylase enzymes. In yeast, the Ccr4-Not complex encompasses two deadenylases, Ccr4 and Caf1 (Pop2). In humans, the Ccr4-Not complex has two orthologs for each of the yeast deadenylases. The two human orthologs of Caf1 are CNOT7 (Caf1a) and CNOT8 (Caf1b). CNOT7 and CNOT8 have 76% identity and 89% similarity. The Caf1 subunit is characterized by the presence of DEDD (Asp-Glu-Asp-Asp) domain. The orthologs of yeast Ccr4 are CNOT6 (Ccr4a) and CNOT6L (Ccr4b). They share 78% identity and 88% similarity (Figure 1.8) (Albert et al., 2000, Dupressoir et al., 2001, Winkler and Balacco, 2013). CNOT7 (Caf1a) and CNOT8 (Caf1b) bind directly to the Ccr4-Not complex but only one of these DEDD–type nucleases can be bound at any one time (Lau et al., 2009).

The crystal structures of Caf1 were determined from *Saccharomyces cerevisiae* (Thore et al., 2003) and *Schizosaccharomyces pombe* (Jonstrup et al., 2007, Anderson and Kedersha, 2009). The crystal structure of Caf1 forms a kidney-shape. Two divalent metal ions are found in the active sites and coordinated by a single glutamate and three aspartate residues (Jonstrup et al., 2007, Anderson and Kedersha, 2009). In the Ccr4-Not complex, Caf1 binds to NOT1 via the MIF4G domain (Bawankar et al., 2013). The crystal structure of MIF4G domain of human CNOT1 in complex with Caf1/CNOT7 shows that Caf1 binding domain of NOT1 adopts on MIF4G fold and it consist of five helical hairpains. This domain was termed the NOT1 MIF4G. The crystal also indicates that the MIF4G domain binds Caf1 opposite to the catalytic site of Caf1 and leaves the Caf1 catalytic site fully accessible to RNA substrates (Figure 1.9A)(Petit et al., 2012).

It has been identified that the Ccr4 subunit is the main deadenylase in yeast (Draper et al., 1994, Tucker et al., 2001, Chen et al., 2002). Biochemical studies indicated that the Ccr4 protein has three major functional domains; N-terminal region, central terminal region and carboxy-terminal endonuclease-exonuclease-phosphatase (EEP) region. The N-terminal region

contains rich glutamines and asparagines. The central region has five tandem copies of leucine rich repeat (LRR) domain. This domain has been shown to interact with the other deadenylase subunits, Caf1. The stable interaction of the Ccr4 subunit to the Ccr4-Not complex requires interaction between Caf1 and the LRR domain of Ccr4. The carboxy-terminal region is associated with its ribonuclease activity (Dupressoir et al., 2001, Chen et al., 2002, Tucker et al., 2002, Draper et al., 1994). The crystal structure of human Ccr4 nuclease domain shows that the C-terminus forms a two layer α/β sandwich fold. The active site residues of Ccr4 are very similar with another hydrolysis such as apurinic/apyrimidinic endonuclease (APE)1. Crystal structure of Ccr4 showed that there are two Mg^{2+} ions in the active site. The Mg^{2+} ions are coordinated by five conserved residues, asparagine, glutamate, two aspartates and histidine (Figure 1.9C) (Wang et al., 2010). A partial structure of yeast Ccr4 nuclease domain has been reported as part of the Not1-Caf1-Ccr4 complex (Basquin et al., 2012). The sub complex contains N-terminal arm of Not1, Ccr4 and Caf1. The N-terminal arm of yeast Not1 has a HEAT repeat structure related to the MIF4G (middle domain of initiation factor 4G) fold. Not1 recognises Caf1 via the MIF4G domain and Caf1 interact with Ccr4 through the LRR domain of Ccr4 (Figure 1.9B) (Basquin et al., 2012). Figure 1.9A and 1.9B shows that human Caf1-CNOT1 was very similar with yeast Caf1-CNOT1. Structural overview of nuclease sub-complex was obtained by alignment of the crystal structures of the MIF4G domain of human CNOT1 in complex with Caf1/CNOT7 and the EEP nuclease domain of human Ccr4/CNOT6L on the structure of the yeast Not1-Caf1-Ccr4 complex (Figure 1.9D and 1.9E).

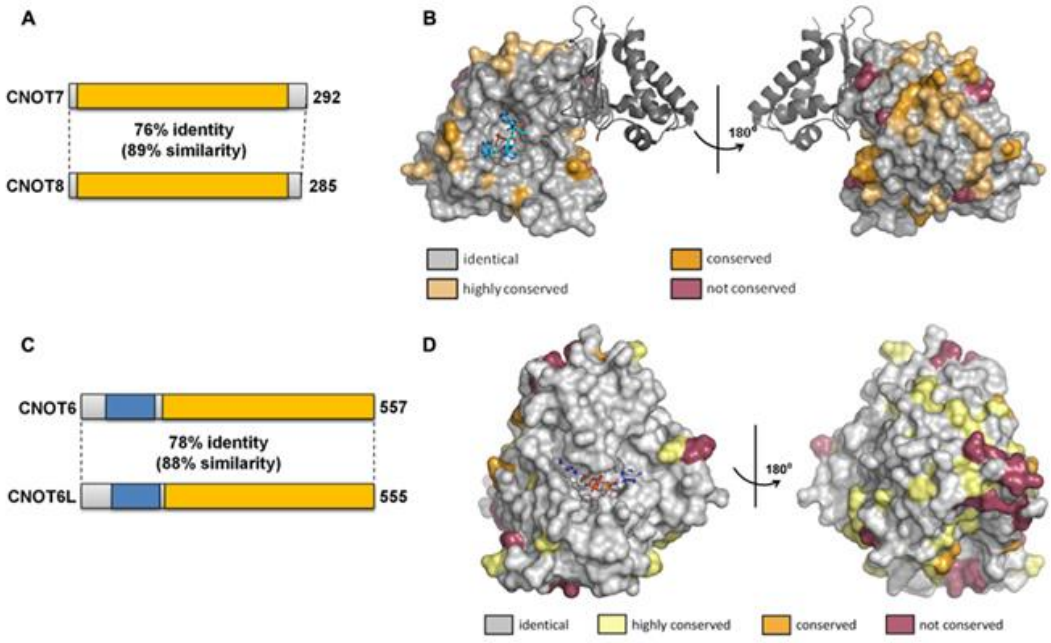

Figure 1.8 The Caf1 and Ccr4 subunits. **A**. Schematic overview of human CNOT7 and CNOT8. **B**. Conservation of surface residues between CNOT7 and CNOT8 subunits. The surface of human CNOT7 is shown with identical residues in CNOT7 and CNOT8 (grey colour), conserved residues (tan and dark yellow) and not conserved residues (purple). **C**. Schematic overview of human CNOT6 and CNOT6L. **D.** Conservation of surface residues between CNOT6 and CNOT6L subunits. The surface of human CNOT6L is shown with identical residues in CNOT6 and CNOT6L (grey colour), conserved residues (tan and dark yellow) and not conserved residues (purple). Figure as originally published in Balacco DL and Winkler GS (2013) Heterogeneity and complexity within the nuclease module of the Ccr4-Not complex. Front. Genet. 4:296. doi: 10.3389/fgene.2013.0029. The figure was reproduced under the terms of the Creative Commons Attribution License, (CC-BY 3,0)

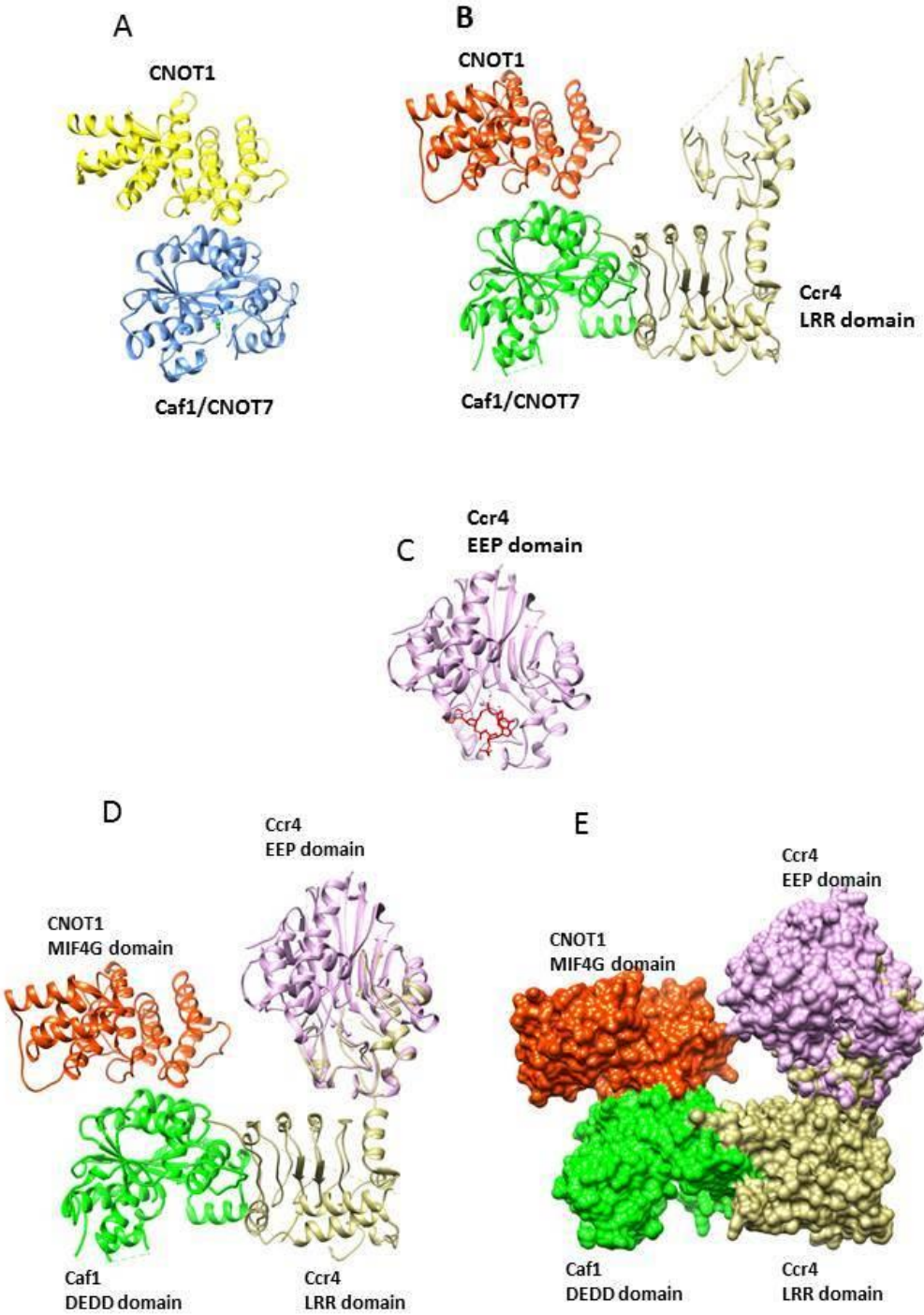
A
CNOT1
Caf1/CNOT7
B
CNOT1
Ccr4
LRR domain
Caf1/CNOT7
C
Ccr4
EEP domain
D
Ccr4
EEP domain
CNOT1
MIF4G domain
Caf1
DEDD domain
Ccr4
LRR domain
E
Ccr4
EEP domain
CNOT1
MIF4G domain
Caf1
DEDD domain
Ccr4
LRR domain

Figure 1.9 Crystal structure of the nuclease module of the Ccr4-Not complex. **A.** Crystal structure of MIF4G domain of CNOT1-Caf1/CNOT7 complex (PDB accession number 4GMJ)**.** Indicated are Caf1/CNOT7 (blue) and the MIF4G domain of CNOT1 (yellow). **B**. The structure of the yeast Not1-Caf1-Ccr4 complex (PDB accession number 4B8C). Indicated are the MIF4G domain of CNOT1 (orange), Caf1/CNOT7 (green) and Ccr4 (tan). **C**. Crystal structure of nuclease domain of human Ccr4 (pink) (PDB accession number 3NGO). **D.** Structure of nuclease sub-complex. Indicated are the catalytic EEP domain of human Ccr4 (pink), the LRR domain of Ccr4 (tan), Caf1/CNOT7 (green) and the MIF4G domain of CNOT1 (orange). **E.** Surface representation of nuclease sub-complex. The model was generated by alignment the crystal structures of the MIF4G domain of human CNOT1 in complex with Caf1/CNOT7 (PDB accession number 4GMJ) and the EEP nuclease domain of human Ccr4/CNOT6L (PDB accession number 3NGO) on the structure of the yeast Not1-Caf1-Ccr4 complex (PDB accession number 4B8C). Structure was visualized using the UCSF Chimera package (http://cgl.ucsf.edu/chimera; (Pettersen et al., 2004).

1.5.2 The role of the Ccr4-Not complex in mRNA degradation

mRNA degradation is initiated by shortening the poly(A) tail. Following deadenylation, a decapping enzyme removes the 5' cap structure of the mRNA, then the mRNA body is exposed and subjected to digestion by a 5'→3' exonuclease, XRN1. In an alternative pathway, following the deadenylation, cytoplasmic exonucleases degrade the mRNAs body in a 3′→5′ direction (Parker and Song, 2004a). The deadenylase activity of the Ccr4-Not complex is provided by Ccr4 and Caf1 in yeast, and its human homologues are Ccr4a/CNOT6, Ccr4b/CNOT6L, Caf1a/CNOT7 and Caf1b/CNOT8 (Dupressoir et al., 2001, Collart and Panasenko, 2011).

Analysis of the enzymatic activity of human and yeast Ccr4 indicates that the enzyme has a strong preference for poly(A) substrate *in vitro* and its deadenylase activity is independent, *in vitro* (Chen et al., 2002, Wang et al., 2010). Ccr4 is active as a monomer and remains active in the absence of Caf1(Bianchin et al., 2005, Chen et al., 2002).

The human Ccr4-Not complex contains one DEDD type deadenylase, either Caf1a/CNOT7 or Caf1b/CNOT8, and one EEP-type subunit, either Ccr4a/CNOT6 or Ccr4b/CNOT6L. The human Ccr4-Not complex can only contain two deadenylase enzyme, one from the EEP family and one from the DEDD family (Lau et al., 2009). By using genome-wide expression analysis, it is clear that Caf1a/CNOT7 and Caf1b/CNOT8 regulate largely identical gene sets (Aslam et al., 2009). The same investigation was done for Ccr4a/CNOT6 and Ccr4b/CNOT6L. The results also indicate that Ccr4a/CNOT6 and Ccr4b/CNOT6L regulate the mRNA abundance of identical gene sets (Aslam et al., 2009).

1.5.3 Regulation and recruitment of the Ccr4-Not complex

It has been identified that some proteins interact with sub-units of the Ccr4-Not complex in order to mediate the recruitment of the Ccr4-Not complex to specific mRNA (Doidge et al., 2012a).

The antiproliferative BTG/TOB protein family can bind to Caf1a/CNOT7 or Caf1b/CNOT8 through a conserved N-terminal domain (Yoshida et al., 2001, Prevot et al., 2001). The C-terminal domain of the BTG/TOB protein mediates this protein-protein interaction. In the Tob1 protein, the C-terminal domain has a PAM2 motif which acts as mediator for the interaction with the C-terminal domain of PABP. Through this interaction, Tob1 facilitates the recruitment of the Ccr4-Not complex to specific RNA (Figure 1.10A) (Ezzeddine et al., 2007, Funakoshi et al., 2007, Mauxion et al., 2008, Hosoda et al., 2011)). Moreover, Tob1 regulates recruitment of the Ccr4-Not complex to a specific mRNA. Tob1 directly binds to a sequence-specific RNA-binding protein, cytoplasmic polyadenylation element-binding protein 3 (CPEB3). Through its carboxyl-terminal region, Tob1 interacts with the carboxyl-terminal RNA-binding domain of CPEB3. Following this, Tob1 recruits the Ccr4-Not complex to CPEB3 via an interaction with the Caf1 sub-unit (Figure 1.10B). Recruitment of CPEB3 to the 3' UTR of mRNA results in shortening of the poly(A) tail and mRNA degradation, which is dependent on the presence of Caf1a (CNOT7)/Caf1b (CNOT8). This suggests that recruitment of Caf1a (CNOT7)/Caf1b (CNOT8) to a specific mRNA is mediated by a RNA binding protein and Tob1. Section 1.6 will discuss the BTG/TOB protein in more detail.

In addition, tritetraprolin (TTP) also mediates the recruitment of the Ccr4-Not complex. TTP binds to AREs and activates mRNA decay. During this process TTP acts as bridge to recruit the Ccr4-Not complex via an interaction with the scaffold protein CNOT1 (Figure 1.10C).

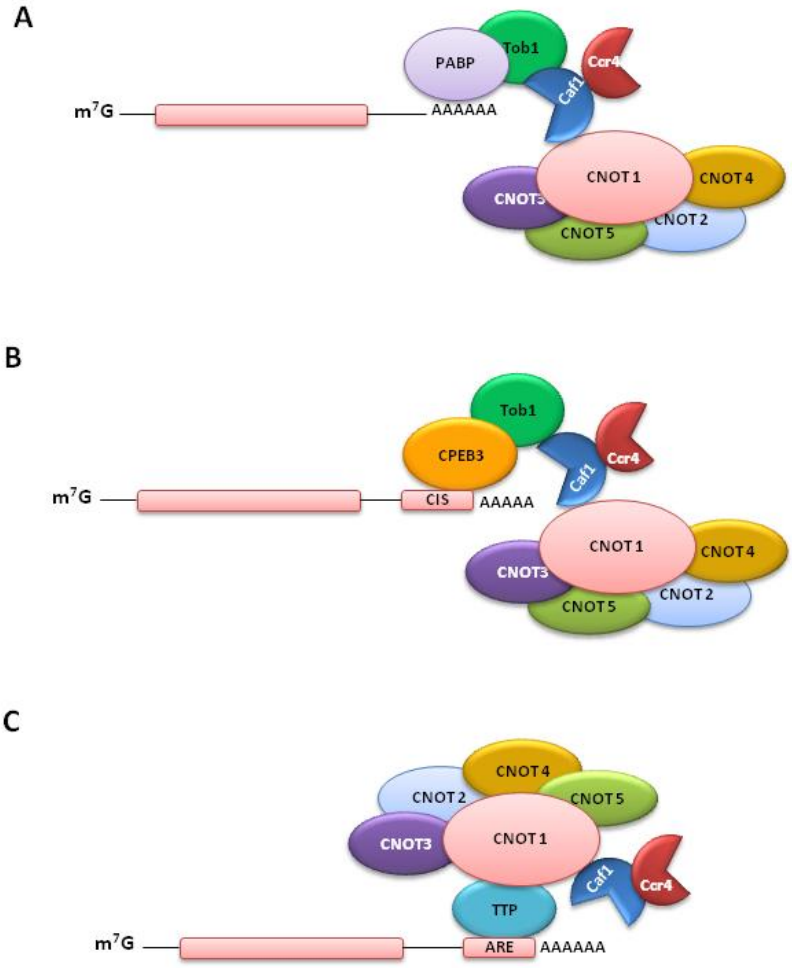

Figure 1.10 Models for recruitment of the Ccr4-Not complex. A. Tob1 facilitates the recruitment of the Ccr4-Not complex to specific RNA. The PAM2 motif of Tob 1 mediates the interaction of Tob1 with the C-terminal domain of PABP. **B**. Tob1 recruits the Ccr4-Not complex to a sequence-specific RNA-binding protein (CPEB3) by an interaction with the Caf1 sub-unit. **C** ARE mediates mRNA decay by binding with the tristoprolin (TTP) protein. The TTP acts as a bridge to recruit the mRNA decay enzyme. TTP protein directly binds to the scaffold protein of the deadenylase complex, CNOT1.

1.5.4 Regulation of physiological processes by Ccr4-Not complex

Structural and biochemical analysis of the mammalian Ccr4-Not complex indicates that it regulates various physiological processes (Shirai et al., 2014). Caf1 and Ccr4 are ubiquitously expressed, however evidence suggests that some of the subunits are particularly important for specific physiological processes (Chen and Shyu, 2011). It was proposed that the Ccr4-Not complex plays a role in cellular processes including cell growth and survival (Ito et al., 2011a, Morita et al., 2007, Fabian et al., 2011, Mittal et al., 2011). Moreover, analysis of knockout mice deficient in CNOT7 showed that the sub-unit of the Ccr4-Not complex plays a role in the regulation of bone mass (Washio-Oikawa et al., 2007).

Further evidence suggests that other components of Ccr4-Not possess specific physiological roles. CNOT1 does not have any catalytic domains. A study in HeLa cells indicated that depletion of CNOT1 compromises deadenylase activities and reduces the number of P-bodies, in which mRNA degradation is thought to take place. Moreover, depletion of CNOT1 induces apoptosis of Hela cells (Ito et al., 2011b).

CNOT3 has an essential function in metabolic regulation. CNOT3 +/- mice are protected against obesity and have a reduced fat content in adipocytes. Reduction of the Cnot3 gene in mice caused leanness and decreased liver and adipose tissue weight. Furthermore, it was identified that CNOT3 is involved in the recruitment of the Ccr4–Not deadenylase to mRNAs (Morita et al., 2011).

1.5.5 Other Roles of the Ccr4-Not complex

The Ccr4-Not complex displays two enzymatic activities: ubiquitination and deadenylation. The CNOT4 protein has an N-terminal RING domain that can interact with the UbcH5b E2 enzymes and provide ubiquitin protein ligase activity (Albert et al., 2002, Lau et al., 2009, Dominguez et al., 2004). *S. cerevisiae* Not4 is a stable subunit of the yeast Ccr4-Not complex, but CNOT4 does not

appear to be a stable component of the human Ccr4-Not complex (Lau et al., 2009a). NOT4 has an important role in cellular protein solubility and has been proposed to be involved in co-translational quality control. The role of NOT4 in protein quality control is independently from the Ccr4 deadenylase subunit (Halter et al., 2014, Panasenko, 2014).

In yeast, the Ccr4-Not complex was originally identified as a transcription factor. It appears that non-enzymatic roles of the Ccr4-Not complex are involved in in transcription regulation. The Ccr4-Not complex can bind to the general transcription factor TFIID, TATA box binding protein (TBP) and TBP-associated factors (Tafs) (Collart and Panasenko, 2011). The role of the human complex in transcriptional regulation is less well defined.

1.6 The BTG/TOB protein family

In human cells, the BTG/TOB family is composed of six members (BTG1, BTG2/PC3/Tis21, BTG3/Ana, BTG4/PC3B, TOB/TOB1, and TOB2) (Winkler, 2010). These proteins share a conserved N-terminal domain and anti-proliferative activity (Matsuda et al., 2001, Tirone, 2001, Winkler, 2010). The conserved N-terminal BTG domain covers 104-106 amino acids. The BTG domain acts as a protein-protein interactions module (Winkler, 2010). Sequence alignments of members of the BTG/TOB protein showed that Tob1 and Tob2 are the most closely related, followed by BTG1 and BTG2, then BTG3 and BTG4 (Figure 1.11A) (Winkler, 2010). Tob1 and Tob2 have the largest C terminal domains which contains the PAM motif that mediates the interaction with the poly(A) binding protein (PABP)(Ezzeddine et al., 2007, Mauxion et al., 2008, Funakoshi et al., 2007). BTG1 and BTG2 have the shortest C-terminal which interacts with the protein-arginine N-methyltransferase (Lin et al., 1996).

The crystal structure of the BTG domain of Tob1 has shown in complex with human Caf1/CNOT7. The interaction of Caf1/CNOT7 with Tob1 occurs via the amino-terminal BTG domain of Tob1 (Horiuchi et al., 2009). Other

research also provided the crystal structure of BTG2 . Alignment of the crystal structure of Tob1 in complex with Caf1/CNOT7 (PDB accession number 2D5R), human Tob1 (PBD accession number 2Z15) and human BTG2 (PBD accession number 3DJU) shows that the BTG domain of Tob1 is very similar with BTG2. The interactive surface of BTG2 and Tob1 with Caf1/CNOT7 is far away from the active site of the deadenylase protein (Figure 1.11B). In vertebrata, BTG2/TOB proteins are the best characterized partner of Caf1/CNOT7 protein (Mauxion et al., 2008, Winkler, 2010). Interaction of BTG2/TOB protein with Caf1/CNOT7 mediates the recruitment of Ccr4-Not complex to mRNA target. Figure 1.11 presents the model of nuclease sub-complex in association with Tob1.

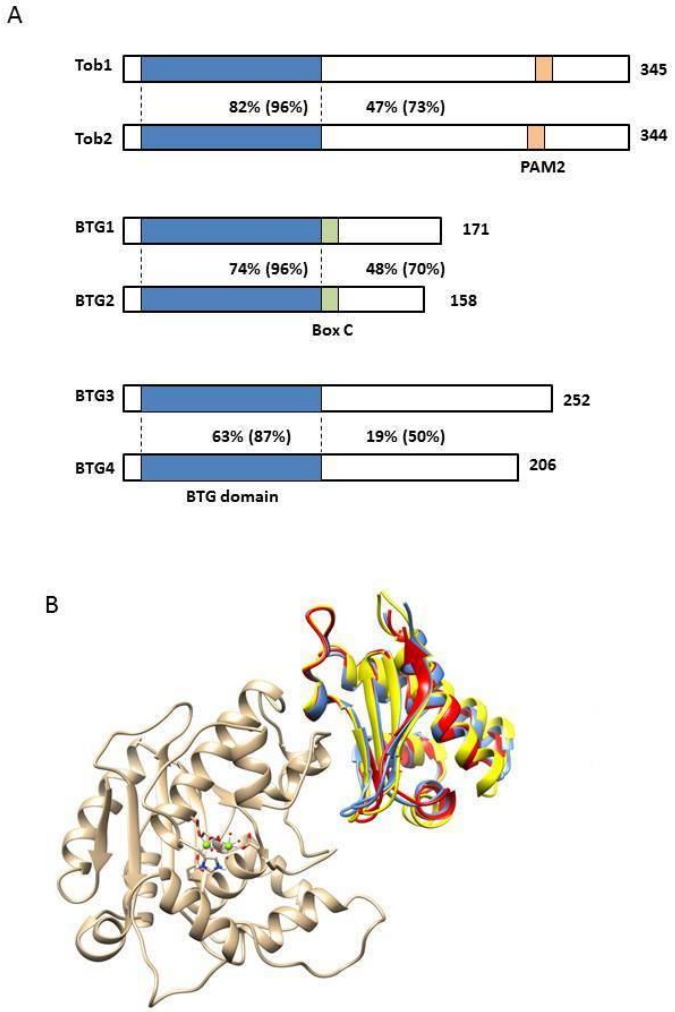

Figure 1.11 Schematic overview of the BTG/TOB protein family. A. The diagram is based on amino acid sequences. The BTG domain is highlighted (blue), the conserved PAM motif (orange) and the Box C motif (light green). The size of amino acids and percentage of identical (similar) amino acids is also shown. **B.** Model of the Caf1-BTG2 complex. Shown are Caf1 (tan), Tob1 (BTG domain, in complex with Caf1; red), Tob1 (BTG domain; blue), and BTG2 (yellow). The model of Caf1/BTG2 complex was generated by the alignment of the TOB1-Caf1 structure (PDB accession number 2D5R), Tob1 (PDB accession number 2Z15) and BTG2 (PDB accession number 3DJU). Structure was visualized using the UCSF Chimera package (http://cgl.ucsf.edu/chimera; (Pettersen et al., 2004).

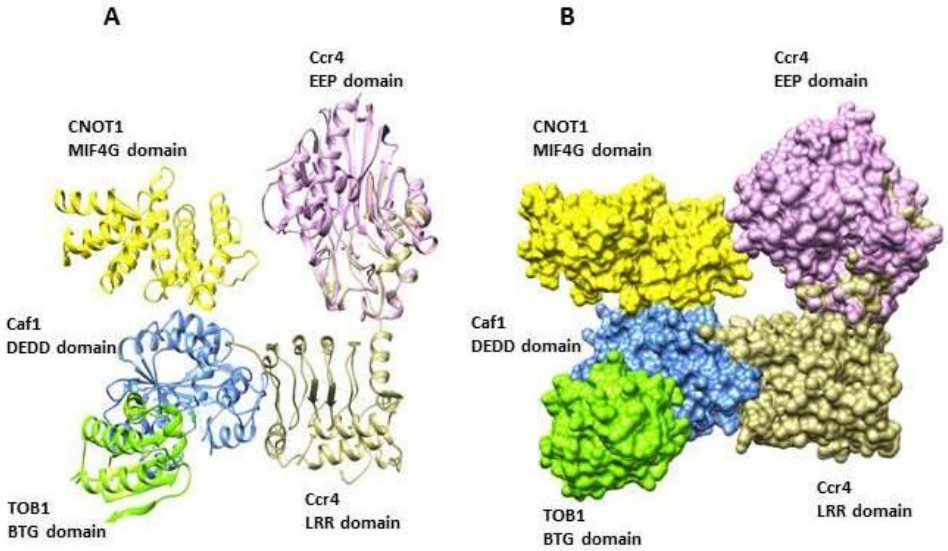

Figure 1.12 Model of the nuclease sub-complex in association with BTG domain of Tob1. Indicated are the CNOT1 MIF4G domain (yellow), Ccr4 EEP domain (pink), Ccr4 LRR domain (tan), Caf1 DEDD domain (blue) and TOB1 BTG domain (green). The model was provided by alignment of the Tob-Caf1 structure (PDB accession number 2D5R), the MIF4G domain in complex with Caf1/CNOT7 (PDB accession number 4GMJ), and the EEP nuclease domain of human Ccr4/CNOT6L (PDB accession number 3NGO) on the structure of the yeast Not1-Caf1-Ccr4 complex (PDB accession number 4B8C). Structure was visualized using the UCSF Chimera package (http://cgl.ucsf.edu/chimera; (Pettersen et al., 2004).

1.6.1 The role of the BTG/TOB protein in mRNA deadenylation and turnover

The BTG domain of the BTG/TOB protein can bind to the subunits of the Ccr4-Not complex, Caf1a/CNOT7 and Caf1b/CNOT8 enzymes (Collart and Panasenko, 2011, Doidge et al., 2012b, Goldstrohm and Wickens, 2008, Bartlam and Yamamoto, 2010). The ability of BTG/TOB proteins to interact with Caf1a/CNOT7 and Caf1b/CNOT8 suggests a role in mRNA deadenylation and turnover. Consistent with the findings above, it was shown that BTG2 and Tob1 contribute to mRNA deadenylation and decay (Ezzeddine et al., 2007, Mauxion et al., 2008, Ezzeddine et al., 2012). Analysis of the crystal structure of the Tob1–Caf1a complex indicated that the association of human Caf1 was mediated by both Box A and Box B of Tob which are located in a region contacting the interaction surface with CNOT7(Horiuchi et al., 2009). Analysis of amino acid substitutions of residues in both Box A and Box B in these regions of BTG2 and Tob1 domains disrupts the interaction with Caf1/CNOT7 (Horiuchi et al., 2009). This interaction is away from the catalytic site of the deadenylase, and allows the C-terminal domain of the BTG/TOB proteins to be available to associate with other RNA-binding proteins (Winkler, 2010). Until now, the effect of BTG/TOB proteins on mRNA turnover is still under debate. *In vitro* tests indicated that BTG2 inhibits the deadenylation activity of the Caf1, and this inhibitory role may be achieved via the direct interaction of these two proteins. Further research showed that a BTG2 mutant could not interact with Caf1 .

Tob, the other member of the TOB/BTG family also shows an interaction with the CCR4-NOT complex and inhibits the deadenylase activity *in vitro* (Miyasaka et al., 2008). In contrast, other studies determined that there was no effect on the deadenylation activity of hCaf1 in the presence of Tob138 (Horiuchi et al., 2009). *In vivo* studies using mouse NIH 3T3 fibroblasts indicated that Tob enhances mRNA deadedenylation. Tob interacts with the Caf1 and the cytoplasmic poly (A) binding protein, PABPC1. The interaction

between Tob with PABPC1 is necessary for the deadenylation-enhancing effect of the Tob protein (Ezzeddine et al., 2007). Other studies demonstrate that BTG2 is a general activator of mRNA decay *in vivo* (Mauxion et al., 2008). The exact mechanism of how BTG2 or Tob proteins increase the mRNA deadenylation remains to be determined. It has been shown that the C terminal region of Tob contains a PABP binding motif that associates with PABPC1, it can recruit the poly(A) tail of mRNA to the Ccr4-Not complex to facilitate the efficient degradation(Ezzeddine et al., 2007).

1.6.2 The role of the BTG/TOB protein in cancer and tumourigenesis

BTG/TOB proteins have been identified as important factors in preventing cancer and tumourigenesis. The BTG2 protein is a direct target for the tumour suppressor p53. Tob1 inhibits cell growth by suppressing the expression of Cyclin D1. Phosphorylation of Tob1 at serine 152, 154 and 164 by the Ras-signalling component Erk1/Erk2 causes Tob1 protein to lose its anti-proliferative activity (Boiko et al., 2006, Suzuki et al., 2002). Mice lacking Tob1 developed spontaneous carcinogenesis higher than the wild-type. Cyclin D1 expression in mRNA is increased in the absence of Tob1 protein. In human cancers the level of Tob1 is often decreased (Yoshida et al., 2003a) and the induction of Tob1 expression by peritoneal injection suppressed pancreatic cancer (Yanagie et al., 2009). Expression of BTG3 (Ana) is relatively high in the lung. In human lung cancer cell lines the expression of BTG3 protein is reduced. Mice lacking BTG3 also display an increased incidence of lung tumours (Yoneda et al., 2009).

In human kidney and breast carcinomas, the expression of BTG2 was found to be significantly reduced (Boiko et al., 2006). Furthermore, analysis of human clinical samples indicated that BTG1 and BTG2 are mutated in non-Hodgkin lymohomas (Morin et al., 2011, Waanders et al., 2012). However, the effect of this mutation on their functions is still unclear. It was observed that BTG1 plays a role in the differentiation of myeloid cells. Recently it was

shown that BTG1 can be used as a biomarker for monitoring the remission state of patients suffering from acute myeloid leukemia, the expression of BTG1 can only be detected in normal cells or cells from patients in complete remission (Cho et al., 2004).

1.6.3 The role of the BTG/TOB protein in bone morphology

Bone remodelling is controlled by the precise coordination of osteoblasts and osteoclasts. Disruption of bone remodelling leads to metabolic bone diseases. Osteoporosis, which is characterised by bone mass reduction, is the effect of the imbalance of bone formation and resorption. Proliferation and differentiation of osteoblasts is controlled by the bone morphogenic proteins (BMPs), which are members of the transforming growth factor β (TGF-β) superfamily. Tob protein inhibits signalling of BMPs through an interaction with Smad transcription factor. In the presence of Tob protein, this signalling is suppressed. In osteoblast cells, Tob1 co-localises with Smad 1, 5 and 8 transcription factors in nuclear bodies (Yoshida et al., 2000, Yoshida et al., 2003b). It has been shown that CNOT7, which interacts with Tob1, is also involved in bone metabolism. Caf1/CNOT7 null mice display an increasing of bone density. In osteoblasts, CNOT7 suppress bone mass and inhibits BMP actions (Washio-Oikawa et al., 2007). In contrast, the absence of Tob2 protein decreased bone mass and increased the number of differentiated osteoclast cells. Tob2 regulates bone formation via an interaction with the Vitamin D receptor which reduces the expression of RANKL (a vitamin D induced gene). Reduction of RANKL expression increases the number of differentiated osteoclast cells (Ajima et al., 2008).

1.7 Aims of the study

While the Ccr4-Not complex is well-characterised as a major enzyme involved in eukaryotic mRNA deadenylation, it is unclear whether the Ccr4 (encoded in vertebrata by CNOT6 or CNOT6L) and Caf1 (encoded by CNOT7 or CNOT8 in vertebrates) catalytic subunits work cooperatively, or whether the nuclease components have unique roles in deadenylation. In *Saccharomyces cerevisiae*, Ccr4 is the main catalytic subunit, which does not appear to require the enzymatic activity of Caf1. In agreement with this notion, point mutations that inactivate the catalytic activity of Caf1 do not affect deadenylation (Tucker et al., 2001, Tucker et al., 2002, Chen et al., 2002, Viswanathan et al., 2004). However, the enzyme activity of Caf1 contributes to deadenylation in other eukaryotes, including the fission yeast *Schizosaccharomyces pombe* and the filamentous yeast *Aspergillus nidula* (Takahashi et al., 2007, Morozov et al., 2010).

The aim of this study is to understand in more detail the mechanism of deadenylation by the human Ccr4-Not complex. Specifically, we focussed on the role of the catalytic components. To this end, we first developed a new quantitative and sensitive method to assess the activity of deadenylase enzymes in vitro. We then used this assay to characterise novel potential small-molecule inhibitors of the Caf1/CNOT7 subunit. Such compounds may become useful tools to investigate the contribution of the Caf1 subunit in deadenylation. Finally, we aimed to express and purify a nuclease module composed of BTG2-Caf1/CNOT7-Ccr4/CNOT6L using *Escherichia coli* and to use the purified sub-complex to understand the requirements and relative contributions of the Ccr4 and Caf1 catalytic subunits.

1.8 Experimental approaches

First, we aim to develop a better method to evaluate the deadenylase activity of the Ccr4-Not complex in vitro. There are several disadvantages when using current methods. For instance, gel-based assays are difficult to quantify and are laborious. On the other hand, assays based on methylene blue colorimetry are relatively insensitive and requires high protein and substrate concentrations. For these reasons, we used a fluorescence-based approach to develop an assay which is sensitive, quantitative and suitable for micro-well formats. The method is based on quenching via Förster (Fluorescence) resonance energy transfer (FRET), which can occur when fluorophores with spectral overlap are in close proximity. Specifically, we used a combination of fluorescein and tetramethylrhodamine (TAMRA). Using this combination, quenching can occur, because the emission spectrum of fluorescein overlaps with the excitation spectrum of TAMRA (Figure 1.13).

For the fluorescence-based deadenylase assay, a 5' fluorescein-labelled RNA substrate was used in combination with a 3' TAMRA-labelled DNA probe. The active enzyme would degrade and shorten the poly(A) tail of the RNA substrate and this would prevent the DNA probe to anneal to the substrate. Therefore, fluorescence of the substrate-conjugated fluorescein can be detected. By contrast, in the absence of enzyme activity, no poly(A) tail degradation occurs. Consequently the TAMRA conjugated DNA probe would bind perfectly to the substrate and quench fluorescence.

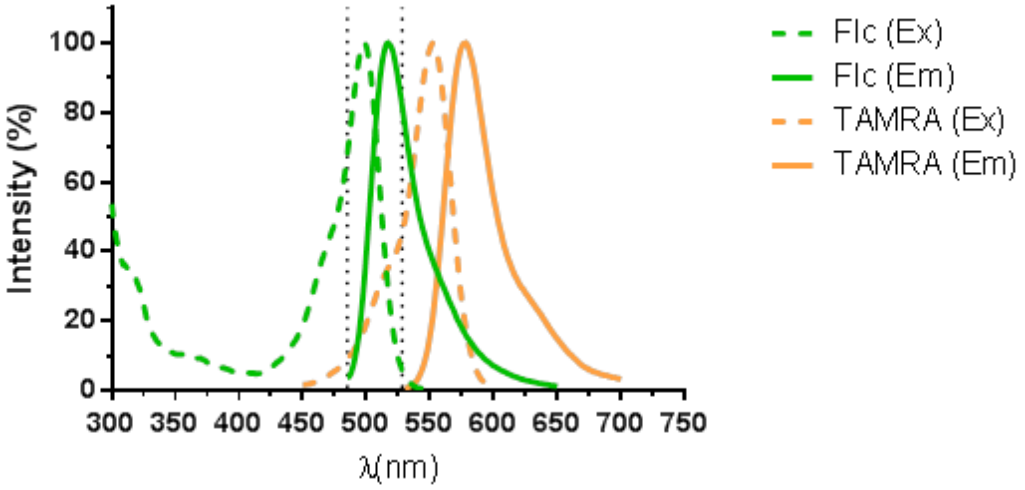

Figure 1.13 Emission and excitation spectra of fluorescein and TAMRA. Emision spectrum of fluorescein overlaps with the excitation spectrum of TAMRA resulted quenching. Excitation and emission data of Flc and TAMRA were obtained from http://www.lifetechnologies.com.

Then, the new method was used to discover and characterise small molecule inhibitors for the Caf1/CNOT7 enzyme. These compounds will be a first step towards cell-permeable inhibitors that could become highly useful tools to understand in more detail the role of the Caf1 subunit in deadenylation. Cell-permeable inhibitors could complement siRNA-based techniques in various ways. For example, whereas siRNA knockdown affects both enzymatic and structural roles, active-site inhibitors would only affect the activity of Caf1.

Finally, we used a bacterial expression system that allowed the purification of a nuclease sub-complex from the bacterial lysate using a combination of different affinity tags. Specifically, we used an *Escherichia coli* strain expressing the T7 bacteriophage RNA polymerase when isopropyl-β-D-1-thiogalactopyranoside (IPTG) is added to the culture medium. The plasmids used required T7 polymerase or endogenous RNA polymerase for the expression of components of the nuclease sub-complex (Figure 1.14). To

maintain two different expression plasmids, different selection markers (ampicillin and chloramphenicol) and compatible origins of replications were used.

The recombinant nuclease sub-complex was purified by using two different affinity tags. The *glutathione S-transferase* (GST) tag is composed of 220 amino acids (approximately 26 kDa). It has high affinity for reduced glutathione, which can be immobilised to a solid agarose support. Alternatively, a His tag containing a stretch of six histidine residues was used. Purification of His-tagged proteins is facilitated by the affinity of the hexahistidine stretch for bivalent transition metals such as Ni^{2+} or Co^{2+}.

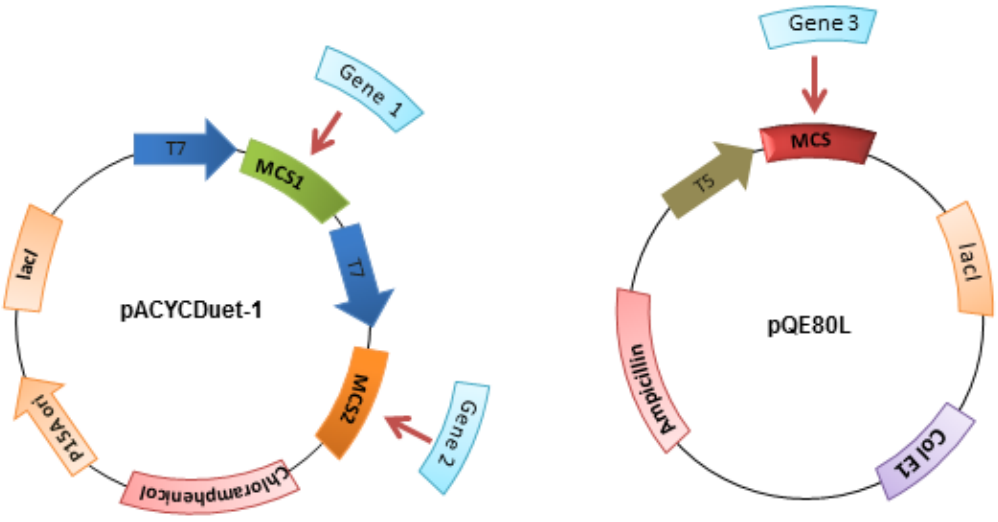

Figure 1.14 Schematic of vectors used for co-expression of Caf1/CNOT7, Ccr4/CNOT6(L) and BTG2. pACYCDuet-1 and pQE80L vectors were used for expression of trimeric protein complex. pACYCDuet-1 vector contains two multi cloning sites (MCS), P15A replicon, *lacI* gene and chloramphenicol resistance gene. Each of MCS is preceded by a T7 promoter/lac operator. pQE80L contains multi cloning site, *lacI* gene, ColE1 and ampicillin resistance gene.

Once a procedure for the purification of a nuclease module was established, the role of the Caf1 and Ccr4 subunits was investigated using the new fluorescence-based assay, chemical inhibition using newly characterised inhibitors of Caf1/CNOT7 and well-characterised inactivating amino acid substitutions in the active site of Caf1 and Ccr4, respectively.

-

Chapter 2

Materials and Methods

Chapter 2. Materials and Methods

2.1 Bacterial growth and transformation

2.1.1 Reagents, stock solutions and buffers

Lysogeny Broth (LB): 10 g/L tryptone, 5 g/L yeast extract, 5 g/L NaCl, pH 7.2 (NaOH). LB agar included 15 g/L bacterial agar. The medium was sterilized using an autoclave and stored at room temperature.

Ampicillin 1000X stock solution : 100 mg/ml in 50% ethanol/water. Stored at -20°C

Chloramphenicol 1000X stock solution: 34 mg/ml in 100% ethanol, stored at -20°C.

IPTG: Isopropyl β-D-1-thiogalactopyranoside in H_2O, sterilized by filtration (0.22 μM pore size)

X-Gal solution: solution of 5-bromo-4-chloro-3-indolyl-B-D-galactopyranoside (50 mg/ml in dimethylformide), from Promega. Stored at -20°C.

2.1.2 Culture of *Escherichia coli*

Escherichia coli strain DH5α was used for DNA manipulations; *Escherichia coli* strain BL21 (DE3) for protein expression. *Escherichia coli* was streaked onto agar plate (containing appropriate antibiotic) and grown overnight at 37°C. The plate contained colonies were stored at 4°C for a few weeks. To prepare liquid culture, a single colony was grown in LB medium containing appropriate antibiotic, incubated at 37°C, 200 rpm, overnight. For large scale cultures glass conical flakes were used.

2.1.3 Preparation of *Escherichia coli* competent cells

Escherichia coli DH5α or BL21 (DE3) were prepared for transformation using calcium chloride. A single colony of *Escherichia coli* was used to inoculate 5 ml of LB medium, grown at 37°C, 200 rpm for overnight. Then, the culture was diluted (1:60) in LB medium and grown until the OD (600 nm) was 0.5. The culture was incubated on ice for 10 minutes in 50 ml falcon tubes. Cells were harvested by centrifugation at 4000 rpm, 4°C for 10 minutes. Cell pellets were re-suspended in 50ml 0.1M MgCl and centrifuged at 4000 rpm for 10 min. Cell pellet was then re-suspended in 8.3ml of 0.1M CaCl and incubated for 20 min. The pellets were again centrifuged at 4000 rpm for 10min, 4°C .
The cell pellets were then combined into 8.6ml of 0.1M CaCl, to which 1.4 ml sterile Glycerol was added. The suspension of cells was then distributed into 200 µl aliquots in sterile microfuge tubes before being snap frozen in liquid nitrogen and stored at -80°C.

2.1.4 Transformation of competent cells

Competent cells (50 µl) were used for plasmid transformation and 100 µl of competent cell were used for ligation or mutagenesis transformation. For transforming plasmids, <500 ng of DNA was used, and for transforming ligations or mutagenesis reactions, 10 µl of ligation reaction mix was used. Competent cell was added with DNA or ligation product, followed by heat shocking at 42°C in water bath for 90 seconds and then placed on ice for 2 minutes. LB media (1 ml) was added to the competent cell before incubating for an hour at shaking incubator 37°C. For plasmid transformation, 100 µl of the cell suspension was spread onto LB agar plates (containing the appropriate antibiotic). For ligations or mutagenesis transformations the culture was spun for 1-2 minutes at 6000 rpm until pellet form, 900 µl of supernatant was removed and the cells were re-suspended in the remaining 100 µl. Finally, the resuspended pellet spread onto LB agar plates (containing the appropriate antibiotic) followed by overnight incubation at 37°C.

2.2 Molecular biology

2.2.1 Reagents, stock solutions and buffers

TE buffer: 10 mM Tris-HCl pH 8.0, 1mM EDTA.

Oligonucleotides : Primers were dissolved in TE to make 100 μM solution and stored at -20^{0}C.

6 × Ficoll loading dye : 16% Ficoll, 0.2% orange G in H_2O and stored at room temperature.

5× TBE : 40 mM Tris base, 40 mM boric acid, 1 mM EDTA, pH 8.0, stored at room temperature.

2.2.2 DNA plasmid preparation

Macherey-Nagel plasmid mini prep kits (Cat# 740588.250) were used for the small scale preparation of plasmid DNA. A single bacterial colony was picked and used to inoculate 2 ml LB in appropriate antibiotic, grow overnight in orbital shaker 200 rpm, at 37°C. The overnight culture was then spun in a microtufuge tube for 1-2 minutes at 6000 rpm until pellet form. The plasmid DNA was then extracted using Macherey-Nagel plasmid mini prep kits. Details of manufacturer's instructions can be found in the Macherey-Nagel plasmid mini prep handbook. Plasmids were eluted in 50μl of elution buffer pre-warmed to 70°C. The concentration of plasmid DNA was measured using a Nanodrop ND-1000 spectrophotometer, then stored at -20°C.

2.2.3 Determination of DNA concentration

The concentration of plasmid DNA was determined using the NanoDrop ND-100 UV-Vis Spectrophotometer (NanoDrop Technologies). To estimate DNA

purity was used A_{260}/A_{280} value. A ratio between 1.8 – 2.0 was acceptable for DNA sample.

2.2.4 Agarose gel electrophoresis

A 0.8% agarose gel (w/v) was prepared by dissolving 0.4 g of agarose in 50 ml of 0.5 X TBE. Five microlite of ethidium bromide was added to the gel before it was poured into a gel tank equipped with an appropriate comb. Each DNA sample was mixed with 6 fold Ficoll dye and pipetted into the appropriate wells. Samples were loaded alongside 5 µl of NEB standard 1 Kb DNA ladder diluted to 0.2 µg/µl and run at 80V. Bands were then visualised using an ultraviolet transluminator (BioRad Gel Doc 2000) and BioRad Quantity One computer software.

2.2.5 Restriction enzyme digestion of DNA

To create compatible ends for cloning and to verify newly created plasmids, DNA plasmid was digested using restriction endonuclease. All restriction enzymes and buffers were supplied by NEB and followed the instruction provided.

To verify new plasmid from ligation products, 100 ng of plasmid DNA was digested in 20 µl total reaction volume. For digesting large amount of DNA for cloning, 5 µg of plasmid DNA was digested for 2 hours at 37°C.

2.2.6 Extraction and purification of DNA from agarose gel

To purify the fragment of DNA from agarose gel, the DNA bands were cut from the agarose gel using a scalpel. Extraction of DNA from agarose gel, and purification of DNA from reaction mixture was carried out using Machery-Nagel Nucleospion PCR clean up, gel extraction and purification kit, following the instructions provided

2.2.7 DNA fragment ligation

Ligation of DNA fragments using T4 DNA ligase was carried out to create recombinant plasmids. Ligation of vector to insert used approximately 100 ng of digested vector DNA and a 3-fold excess insert concentration (Table 2.1). The reaction was carried out overnight at room temperature.

Reagent/component	Volume
100 ng template DNA	-
3-fold excess insert DNA	-
10× T4 DNA Ligase buffer	1.5 µl
T4 DNA Ligase enzyme	1.0 µl
H_2O	Up to 15 µl

Table 2.1 Standard ligation reaction

2.2.8 DNA transformation

Competent cells (100 µl) were added to 10 µl of DNA (ligation product), followed by a heat shock in a 42°C water bath for 90 seconds and then placed on ice for 2 minutes. LB media (1 ml) was added to the competent cell before incubating for an hour at shaking incubator 37°C. The culture was then spun for 1-2 minutes at 6000 rpm until pellet form, the media was removed, and the pellet was resuspended in the remaining media. Finally, the resuspended pellet was plated on LB plate containing antibiotic followed by overnight incubation at 37°C.

2.2.9 Polymerase Chain Reaction (PCR)

PCR was performed using a Peqlab Primus 96 advanced thermal cycler. A standard reaction set up is indicated in Table 2.2 and Table 2.3. Sample were initially denatured at 95°C for 5 minute followed by 30 cycle of a denaturing step 95°C for 15 second, annealing at 50°C for 30 second, then elongation at 72°C for 2 minutes. At the end of this process, a final elongation step for 10

min at 72°C was included. The primers used are shown in Table 2.4 and 2.7. To check the PCR product was the correct size, some of the reaction was loaded onto a 0.8% agarose gel.

Volume (µl)	**Reagent**
2	10 mM dNTPs
1	Phusion enzyme
20	5× phusion Buffer HF
1	1 µM forward primer (Sigma), 100 µM stock in TE
1	1 µM reverse primer (Sigma), 100 µM stock in TE
x	100 ng DNA template
Up to 100	Nuclease free H_2O

Table 2.2 Standard reaction set up of PCR using the Phusion DNA polymerase

Volume (µl)	**Reagent**
1	10 mM dNTPs
0.5	Taq DNA polymerase
2.5	10× Taq pol buffer
1	1 µM forward primer (Sigma), 100 µM stock in TE
1	1 µM reverse primer (Sigma), 100 µM stock in TE
4	culture
15	Nuclease free H_2O

Table 2.3 Standard reaction set up of PCR using Taq DNA polymerase

Name	Sequence (5'-3')
BamH1 CNOT6LGS	AAAAGGATCCAATGCGTCTGATTGGCATGCCG
BamH1 CNOT7GS	AAAAGGATCCAATGCCGGCCGCCACCG
PQE30L RV	GTTCTGAGGTCATTACTGG

Table 2.4 Primer sequences used for amplification of CNOT7 and CNOT6L cDNAs

Name	Sequence (5'-3')
pACYCDuetUP1	GGATCTCGACGCTCTCCT
DuetDown1	GATTATGCGGCCGTGTACAA
DuetUP2	TTGTACACGGCCGCATAATC
T7 terminator	GCTAGTTATTGCTCAGCGG

Table 2.5 Primer sequences used for amplification and DNA sequencing of MCS1 and MCS2 of pACYCDuet-1

Name	Sequence (5'-3')
GST•CNOT6L _FR	AAAACCATGGGCTCCCCTATACTAGGTTATTGG
pGEX4T1 Rv	CCGGGAGCTGCATGTGTCAGAGG

Table 2.6 Primer sequences used for amplification of GST•CNOT6L

Name	Sequence (5'-3')
NcoI-CNOT6L_FR	AAAACCATGGGCCGTCTGATTGGCATGCCGAAAG
PQE30L RV	GTTCTGAGGTCATTACTGG

Table 2.7 Primer sequences used for amplification of untagged CNOT6L

2.2.10 Site-directed mutagenesis

For site-directed mutagenesis, primers with the desired mutations were designed (Table 2.8) using the PrimerX programme (http://www.bioinformatics.org/primerx) using the primer design protocol optimised for the Stratagene Quikchange protocol. Reactions were set up as shown in Table 2.2. Reactions were initially incubated at 95°C for 5 min followed by 30 cycles consisting of a denaturing step of 95°C for 15 sec, annealing at 50°C for 30 sec, then elongation at 72°C for 1 min/0.5 kb. A final elongation step for 10 min at 72°C was included at the end. The annealing temperature could be varied between 40°C and 60°C to optimise the reaction efficiency.

To remove template DNA from site directed mutagenesis reactions, the enzyme DpnI was used. DpnI (2µl) was added to each 50µl mutagenesis reaction and incubated at 37°C for 2 h. Ten microlitres of the reaction was then loaded and run on a 0.8% agarose gel. The remaining sample was then used to transform *E. coli* DH5α before DNA isolation and sequencing to confirm the presence of the desired mutations.

Name	**Sequence (5'-3')**
CNOT7_D40A FW	CTACGTTGCGATGGCGACCGAATTTCCGGG
CNOT7_D40A RV	CCCGGAAATTCGGTCGCCATCGCAACGTAG
CNOT6L_E240A FW	GCGGATATTATCAGTCTGCAGGCGGTGGAAACCGAAC AGTATTTTAC
CNOT6L_E240A RV	GTAAAATACTGTTCGGTTTCCACCGCCTGCAGACTGAT AATATCCGC
CNOT6_E240A FW	CGTGAGTCTGCAGGCGGTTGAAACCGAACCAG
CNOT6_E240A RV	CTGTTCGGTTTCAACCGCCTGCAGACTCACG

Table 2.8 Primer sequences used for site directed-mutagenesis

2.2.11 List of plasmids

	Abbreviation	MCS[1] 1	MCS[1] 2
1	pACYCDuet-1 M01	His•CNOT7	CNOT6L
2	pACYCDuet-1 M02	His•CNOT6L	CNOT7
3	pACYCDuet-1 M03	His•CNOT6L	CNOT7 D40A
4	pACYCDuet-1 M04	His•CNOT6L E240A	CNOT7
5	pACYCDuet-1 M05	His•CNOT6L E240A	CNOT7 D40A
6	pACYCDuet-1 M06	GST•CNOT6L	CNOT7
7	pACYCDuet-1 M07	GST•CNOT6L	CNOT7 D40A
8	pACYCDuet-1 M08	GST•CNOT6L E240A	CNOT7
9	pACYCDuet-1 M09	GST•CNOT6L E240A	CNOT7 D40A
10	pACYCDuet-1 M10	CNOT6L	CNOT7
11	pACYCDuet-1 M11	CNOT6L	CNOT7 D40A
12	pACYCDuet-1 M12	CNOT6L E240A	CNOT7
13	pACYCDuet-1 M13	CNOT6L E240A	CNOT7 D40A
14	pACYCDuet-1 M14	GST•CNOT6	CNOT7
15	pACYCDuet-1 M15	GST•CNOT6	CNOT7 D40A
16	pACYCDuet-1 M16	GST•CNOT6 E240A	CNOT7
17	pACYCDuet-1 M17	GST•CNOT6 E240A	CNOT7 D40A

Table 2.9 List of plasmids

[1] Multiple cloning site

2.3 Protein expression and purification

2.3.1 Reagents, stock solutions and buffers

Lysogeny Broth (LB) media and agar: 10 g/L tryptone, 5 g/L yeast extract, 5g/L NaCl, pH 7.2 (NaOH)

Ampicillin 1000× stock solution: 100mg/ml in 50% ethanol/water. Stored at -20°C.

Chloramphenicol 1000× stock solution: 34 mg/ml in 100% ethanol, stored at -20°C.

IPTG (Isopropyl β-2-1-thiogalactopyranoside)

NaCl (Sodium chloride)

β-mercapthoethanol

Tris-HCl

Imidazole

2.3.2 Protein Expression : His-Tagged Caf1/CNOT7 and Ccr4b /CNOT6L ΔLRR Expression

Plasmids pQE80L-CNOT7, pQE80L-CNOT7 D40A, pQE80L-CNOT6L ΔLRR and pQE80L-CNOT6L E240A ΔLRR were transformed into *Eschericia coli* strain BL21 (DE3). A single colony was growth into 1 ml of LB containing 100 μg/ml ampicilin for 6 hours at 37°C and then the starter culture was used to inoculate 100 ml LB containing 100 μg/ml ampicilin, incubated at 37°C, overnight. The pre-culture, then was diluted to 2 L of LB at 37°C until the optical density (600 nm) was between 0.6 and 0.8. Expression was then induced by the addition of 0.2 mM isopropyl β-D-1-thiogalactopyranoside for 3 hours at 30°C. The cells were harvested by centrifugation (6000 rpm) using a Sorvall SLC-6000 SUPER-LITE rotor at 4°C for 15 minutes. The supernatant was discarded, and then the bacterial pellet was resuspended in 30 ml of ice-

cold extraction buffer (20 mM Tris-Hcl pH 7.8, 500 mM NaCl, 10% glycerol, 1 mM β-mercaptoethanol). Cells were frozen and keep at -80°C until further use. The bacterial suspension was thawed and then lysed on ice using a Qsonica XL2000, using five 30s on/30s off cycles. The crude lysate was then transferred into Sorvall tubes and then centrifuged in a SS-34 rotor at 10000 rpm at 4°C for 30 minutes to remove insoluble material. The supernatant was collected and stored until further use at -80°C.

2.3.3 Purification of His-Tagged Caf1/CNOT7 and Ccr4b /CNOT6L ΔLRR Proteins

The histidine-tagged Caf1/CNOT7 and Ccr4b /CNOT6L ΔLRR proteins were purified in a single step using HisTrap column (GE Life Science; 1ml bed volume). Before use, 1 ml His Trap HP columns were washed with 3–5 column volumes of distilled water, then equilibrated with 5 column volumes of extraction buffer (20 mM Tris-HCl pH 7.8, 500 mM NaCl, 10% glycerol, 1 mM β-mercaptoethanol). The soluble lysate was then applied to the column using a syringe at an approximate flow rate of 2-3 drops per second (>1ml/min). Subsequently, the column was washed using a syringe filled with using 10 ml wash buffer (20 mM Tris-HCl pH 7.8, 500 mM NaCl, 10% glycerol, 1 mM β-mercaptoethanol, 10 mM imidazole). Finally, elution buffer (20 mM Tris-HCl pH 8, 500 mM NaCl, 10% glycerol, 1 mM β-mercaptoethanol, 250 mM imidazole) was added (approximately 5-6 ml) to elute the protein and fractions of 1 ml were collected. Elution fractions were analysed by sodium dodecyl sulphate-polyacryl-amide gel electhrophoresis SDS-PAGE and coomassie staining (Invitrogen Bio-Safe Staining Kit). The protein concentrations were assessed using Bio-Rad Protein Assay Reagent and stored until further use at -80°C.

2.3.4 Protein Expression : His•CNOT6L-CNOT7 and His•CNOT7-CNOT6L expression

Plasmids pACYCDuet-1 His•CNOT6L/CNOT7 dan pACYCDuet-1 His•CNOT7/CNOT6L were transformed into *Escherichia coli* strain BL21 DE3 cell. A single colony was growth into 1 ml of LB containing 34 µg/ml chloramphenicol for 6 hours at 37°C. The starter culture was then used to inoculate 100 ml LB containing 34 µg/ml chloramphenicol at 37°C, overnight. The pre-culture, then was diluted to 2 L of LB at 37˚C until the optical density (600 nm) was between 0.6 and 0.8. Expression was then induced by the addition of 0.2 mM isopropyl β-D-1-thiogalactopyranoside for 3 hours at 30°C. The cells were harvested by centrifugation (6000 rpm) using a Sorvall SLC-6000 SUPER-LITE rotor at 4°C for 15 minutes. The supernatant was discarded, and then the bacterial pellet was resuspended in 30 ml of ice-cold extraction buffer (20 mM Tris-Hcl pH 7.8, 250 mM NaCl, 5% glycerol, 1 mM β-mercaptoethanol). Cells were frozen and keep at -80°C until further use. The bacterial suspension was thawed and then cells were lysed on ice using a Qsonica XL2000, using five 30s on/30 s off cycles. The crude lysate was cleared by centrifugation using a SS-34 rotor spun at 10000 rpm at 4°C for 30 minutes to remove insoluble material. The supernatant was collected and stored until further use at -80°C.

2.3.5 Lysis of His•CNOT6L-CNOT7 protein complex by subjection of the cells to sucrose shock.

Plasmids pACYCDuet-1 His•CNOT6L/CNOT7 and pACYCDuet-1 His•CNOT7/CNOT6L were transformed into *Eschericia coli* strain BL21 DE3 cell. A single colony was growth into 1 ml of LB containing 34 µg/ml chloramphenicol for 6 hours at 37°C. The starter culture was then used to inoculate 100 ml LB containing 34 µg/ml chloramphenicol at 37°C, overnight. The pre-culture, then was diluted to 2 L of LB at 37°C until the optical density (600 nm) was between 0.6 and 0.8. Expression was then induced by the

addition of 0.1 mM isopropyl β-D-1-thiogalactopyranoside for overnight at room temperature. The cells were harvested by centrifugation (6000 rpm) using a Sorvall SLC-6000 SUPER-LITE rotor at 4°C for 15 minutes. The supernatant was discarded, and then the bacterial pellet was resuspended in sucrose buffer (5 mM HEPES, 20% sucrose, 1mM EDTA pH 8), 5ml sucrose buffer/gram pellet. The suspension was then re-pellet by centrifugation (7000 rpm) at 4°C for 30 minutes. The supernatant was then discarded and the bacterial pellet was resuspended in extraction buffer (20 mM Tris-HCl pH 7.8, 250 mM NaCl, 5 % glycerol, 1 mM β-mercaptoethanol), 1.5ml extraction buffer/gram pellet, followed by freezing at -80°C. The bacterial suspension was thawed and then lysed on ice using a Qsonica XL2000, using five 30s on/30s off cycles. The crude lysate was then transferred into Sorvall tubes and then centrifuged in a SS-34 rotor at 10000 rpm, 4°C for 30 minutes to remove insoluble material. The supernatant was collected and stored until further use at -80°C.

2.3.6 Purification of His•CNOT6L-CNOT7 and His•CNOT7-CNOT6L protein complexes.

His•CNOT6L-CNOT7 and His•CNOT7-CNOT6L protein complexes were purified in a single step using HisTrap column (GE Life Science; 1ml bed volume). Before use, 1 ml His Trap HP columns were washed with 3–5 column volumes of distilled water, then equilibrated with 5 column volumes of extraction buffer (20 mM Tris-HCl pH 7.8, 250 mM NaCl, 5% glycerol, 1 mM β-mercaptoethanol). The soluble lysate was then applied to the column using a syringe at an approximate flow rate 0f 2-3 drops per second (>1ml/min). Subsequently, the column was washed using a syringe filled with using 10 ml wash buffer (20 mM Tris-HCl pH 7.8, 250 mM NaCl, 5% glycerol, 1 mM β-mercaptoethanol, 20 mM imidazole). Finally, elution buffer (20 mM Tris-HCl pH 8, 250 mM NaCl, 5% glycerol, 1 mM β-mercaptoethanol, 250 mM imidazole) was added (approximately 5-6 ml) to elute the protein

and fractions of 1 ml were collected. Elution fractions were analysed by sodium dodecyl sulphate-polyacryl-amide gel electhrophoresis SDS-PAGE and coomassie staining (Invitrogen Bio-Safe Staining Kit). The protein concentrations were assessed using Bio-Rad Protein Assay Reagent and stored until further use at -80°C.

2.3.7 Expression of GST•CNOT6L-CNOT7 protein complex.

Plasmid pACYCDuet-1 GST•CNOT6L/CNOT7 was transformed into *Eschericia coli* strain BL21 DE3 cell. A single colony was growth into 1 ml of LB containing 34 µg/ml chloramphenicol for 6 hours at 37°C. The starter culture was then used to inoculate 100 ml LB containing 34 µg/ml chloramphenicol at 37°C, overnight. The pre-culture, then was diluted to 2 L of LB at 37°C until the optical density (600 nm) was between 0.6 and 0.8. Expression was then induced by the addition of 0.1 mM isopropyl β-D-1-thiogalactopyranoside for overnight at room temperature. The cells were harvested by centrifugation (6000 rpm) using a Sorvall SLC-6000 SUPER-LITE rotor at 4°C for 15 minutes. The supernatant was discarded, and then the bacterial pellet was resuspended in 40 ml of ice-cold lysis buffer (20 mM Tris-HCl pH 7.8, 100 mM NaCl, 10% glycerol, 1 mM β-mercaptoethanol). Cells were frozen and keep at -80°C until further use. The bacterial suspension was thawed and then cells were lysed on ice using a Qsonica XL2000, using five 30s on/30 s off cycles. The crude lysate was cleared by centrifugation using a SS-34 rotor spun at 10000 rpm, 4°C for 30 minutes to remove insoluble material. The supernatant was collected and stored until further use at -80°C.

2.3.8 Purification of GST•CNOT6L-CNOT7 protein complex

Purification of GST•CNOT6L-CNOT7 protein complex was carried out using affinity chromatography. Soluble lysate was incubated with glutathione

agarose by mixing gently for overnight at 4°C (cold room). The glutathione-agarose/lysate mixture was spun, and the supernatant containing unbound protein was removed. Then, the glutathione-agarose/lysate suspension was applied to the column holder followed by washing using 10 ml of wash buffer (20 mM Tris-HCl pH 7.8, 500 mM NaCl, 10 % glycerol, 1 mM β-mercaptoethanol). Finally, protein was eluted using lysis buffer containing 10 mM reduced glutathione and the fractions was collected every 0.8 ml. Elution fractions were analysed by sodium dodecyl sulphate-polyacryl-amide gel electhrophoresis (SDS-PAGE) and coomassie staining (Invitrogen Bio-Safe Staining Kit). The protein concentrations were assessed using Bio-Rad Protein Assay Reagent and stored until further use at -80°C.

2.3.9 Expression of His•BTG2-CNOT7-CNOT6L protein complex

Plasmids pACYCDuet-1 CNOT6L/CNOT7 and pQE80L-BTG2 were co-transfered into BL21 (DE3) using selection with the chloramphenicol and ampicillin antibiotics. A single colony containing the pACYCDuet-1 CNOT6L/CNOT7 and pQE80L-BTG2 plasmid was used to inoculate a starter culture for protein expression. The pre-culture, was then grown in the presence of chloramphenicol (34 μg/ml) and ampicilin (100 μg/ml) at 37°C until the OD (600 nm) was between 0.6-0.8. IPTG (final concentration of 0.1 mM) was added to the culture at room temperature for overnight to induce the expression of the protein. The cells were harvested by centrifugation (6000 rpm) using a Sorvall SLC-6000 SUPER-LITE rotor at 4°C for 15 minutes. The supernatant was discarded, and then the bacterial pellet was resuspended in 30 ml of ice-cold lextraction buffer (20 mM Tris-HCl pH 7.8, 250 mM NaCl, 5 % glycerol, 1 mM β-mercaptoethanol). Cells were frozen and keep at -80°C until further use. The bacterial suspension was thawed and then cells were lysed on ice using a Qsonica XL2000, using five 30s on/30 s off cycles. The crude lysate was cleared by centrifugation using a SS-34 rotor

spun at 10000 rpm at 4°C for 30 minutes to remove insoluble material. The supernatant was collected and stored until further use at -80°C.

2.3.10 Purification of His•BTG2-CNOT7-CNOT6L protein complex

Purification of His•BTG2-CNOT7-CNOT6L protein complex was carried out in two step purifications, using Co^{2+} agarose followed by gel filtration (Superdex 200 16/60; GE Health). First purification, soluble lysate was incubated overnight with Co^{2+} agarose beads in extraction buffer (20 mM Tris-HCl pH 7.8, 250 mM NaCl, 5 % glycerol, 1 mM β-mercaptoethanol) at 4°C. The cobalt/protein lysate mixture was centrifuged (1500 rpm) for 5 minutes, 4°C, then supernatant containing unbinding protein was discharged. The cobalt/protein lysate mixture was washed using 10 ml extraction buffer, followed by centrifugation (1500 rpm) for 5 minutes, 4°C. The cobalt/protein lysate was resuspended in 5 ml extraction buffer, then poured into a column holder. Thus, approximately 6 ml of elution buffer (20 mM Tris-HCl pH 7.8, 250 mM NaCl, 5 % glycerol, 1 mM β-mercaptoethanol, 20 mM imidazole) was added and 0.5 ml fractions were collected. Elution fractions were analysed by SDS-PAGE analysis and coomassie staining (Invitrogen Bio-Safe Staining Kit). The protein concentrations were assessed using Bio-Rad Protein Assay Reagent.

Second purification was carried out using gel filtration. Protein fractions from the first purification (14 mg protein, 6 ml) was concentrated until 3.5 ml, then applied on the gel filtration column (a Superdex 200 16/60 gel filtration column equilibrated with 20 mM Tris-HCl (pH 7.8), 150 mM NaCl, 5 % glycerol and 1 mM β-mercaptoethanol). Elution protein was collected in fraction at 2.5 ml. Protein were analysed using SDS-PAGE analysis and coomassie staining (Invitrogen Bio-Safe Staining Kit).

2.3.11 Expression of His•BTG2-CNOT7-GST•CNOT6L protein complex

Plasmids pACYCDuet-1 GST•CNOT6L/CNOT7 and pQE80L-BTG2 were co-transfered into BL21 (DE3) using selection with the chloramphenicol and ampicillin antibiotics. A single colony containing the pACYCDuet-1 GST•CNOT6L/CNOT7 and pQE80L-BTG2 plasmids was used to inoculate a starter culture for protein expression. The pre-culture, was then grown in the presence of chloramphenicol (34 μg/ml) and ampicilin (100 μg/ml) at 37°C until the OD (600 nm) was between 0.6-0.8. IPTG (final concentration of 0.1 mM) was added to the culture at room temperature for overnight to induce the expression of the protein. The cells were harvested by centrifugation (6000 rpm) using a Sorvall SLC-6000 SUPER-LITE rotor at 4°C for 15 minutes. The supernatant was discarded, and then the bacterial pellet was resuspended in 30 ml of ice-cold lextraction buffer (20 mM Tris-HCl pH 7.8, 250 mM NaCl, 5 % glycerol, 1 mM β-mercaptoethanol). Cells were frozen and keep at -80°C until further use. The bacterial suspension was thawed and then cells were lysed on ice using a Qsonica XL2000, using five 30s on/30s off cycles. The crude lysate was cleared by centrifugation using a SS-34 rotor spun at 10000 rpm at 4°C for 30 minutes to remove insoluble material. The supernatant was collected and stored until further use at -80°C.

2.3.12 Purification of His•BTG2-CNOT7-GST•CNOT6L protein complex

Purification of His•BTG2-CNOT7-GST•CNOT6L protein complex was carried out in two step purifications, using Co^{2+} agarose followed by GST affinity chromatography. Soluble lysate was incubated overnight with Co^{2+} agarose beads in extraction buffer (20 mM Tris-HCl pH 7.8, 250 mM NaCl, 5 % glycerol, 1 mM β-mercaptoethanol) at 4°C. The cobalt/protein lysate mixture was centrifuged for 5 minutes, 1500 rpm, 40°C, then supernatant containing unbinding protein was discharged. The cobalt/protein lysate mixture was washed using 10 ml wash buffer (20 mM Tris-HCl pH 7.8, 250 mM NaCl, 5 % glycerol, 1 mM β-mercaptoethanol, 20 mM imidazole), followed by

centrifugation (1500 rpm) for 5 minutes, 4°C. The cobalt/protein lysate was resuspended in 5 ml extraction buffer, then poured into a column holder. Thus, approximately 6 ml of elution buffer (20 mM Tris-HCl pH 7.8, 250 mM NaCl, 5 % glycerol, 1 mM β-mercaptoethanol, 20 mM imidazole) was added and 0.5 ml fractions were collected. Elution fractions were analysed by SDS-PAGE analysis and coomassie staining (Invitrogen Bio-Safe Staining Kit). The protein concentrations were assessed using Bio-Rad Protein Assay Reagent. Further purification was carried out by GST affinity purification, using Pierce® GST Spin Purification Kit (Thermo Scientific). Elution fractions from the cobalt agarose column were applied to GST/spin column containing 0.2 ml resin and incubated for 60 minutes at 4°C on an end-over-end mixes. After washing using wash buffer (20 mM Tris-HCl pH 7.8, 500 mM NaCl, 10 % glycerol, 1 mM β-mercaptoethanol), bound proteins was eluted from the resin by adding buffer (20 mM Tris-HCl pH 7.8, 100 mM NaCl, 10% glycerol, 1 mM β-mercaptoethanol) containing 10 mM reduced glutathion. Elution fractions were analysed by 14% SDS-PAGE and coomassie staining (Invitrogen Bio-Safe Staining Kit). The protein concentrations were assessed using Bio-Rad Protein Assay Reagent and store at -80°C until further use.

2.3.13 Expression and purification of His•BTG2-CNOT7-GST•CNOT6 protein complex

Expression and purification of His•BTG2-CNOT7-GST•CNOT6 protein complex was carried out using the same procedure in His•BTG2-CNOT7-GST•CNOT6L protein complex.

2.4 Protein analysis

2.4.1 Reagents, stock solutions and buffers for use in protein analysis

Upper buffer (4×): 0.5M Tris base, 0.4% SDS, pH 6.8; store at room temperature

Lower buffer (4×): 1.5M Tris base, 0.4% SDS, pH 8.8; store at room temperature

Running buffer (10×): 0.25M Tris Base, 1.0% SDS, 1.92M glycine, store at room temperature

Transfer buffer (10×): 0.25M Tris Base, 1.92M glycine, store at room temperature

SDS loading buffer (4×): 50% upper buffer, 40% glycerol, 1% β-merchaptoethanol, 1.25% Bromophenolblue (0.1%), 0.25% H_2O; store stock at -20°C. Small aliquots were store at -4°C

Tris buffer saline supplemented with 0.05% Tween-20 (TBST): 50 mM Tris-HCl pH7.8, 150 m NaCl, 0.1% Tween-20. Store at room temperature

10% APS: 10% ammonium persulphate (APS) in H_2O.

2.4.2 Bradford assay to determine protein concentration

A Bradford assay was used to determine protein concentration. The Bio-Rad protein reagent (Bio-Rad Laboratories GmbH) was diluted 1:5 with H_2O before use. BSA dissolved in water was used for protein standard curve. Ten microlitres of protein sample was added to 990 µl of 1x Bradford reagent, vortexed and incubated for 1 minute room temperature. Samples were transferred to 1ml microfuge and the absorbance were read at optical density (600 nm). The standard curve was obtained by linear regression analysis using Microsoft Excel and used to calculate the protein concentration of the samples.

2.4.3 Sodium dodecyl sulphate polyacrylamide gel electrophoresis (SDS-PAGE) analysis

Proteins were analysed using SDS-PAGE in the invitrogen X-Cell sureLock Mini cell system. SDS-PAGE gels were prepared to the appropriate percentage resolving gel (Table 2.10) based on the molecular mass of the protein of interest. Separating gels were cast in gel cassettes (Invitrogen) leaving 1.5 cm room at the top for the stacking gel to be cast. The separating gel was cast first and allowed to set for 30 minutes before the stacking gel was applied, and then the appropriate comb inserted and the gel left to set for further 30 minutes. The wells were washed with 1x running buffer prior to use. Protein extract were denatured by boiling for 5 minutes in 4x SDS sample buffer (50% upper buffer, 40% glycerol, 1% β-mercaptoethanol, 1.25% bromophenol blue (0.1%), 0.25% H2O) immediately before loading. Gels were run in 1x running buffer (10×- 0.25M Tris Base, 1.0% SDS, 1.92M glycine) at 180V for approximately 1-1.5h.

	Resolving Gel			Stacking Gel
	10%	**12%**	**14%**	**4%**
Protein MW range, kDa	30-200	20-150	10-80	
40% acrylamide: Bisacrylamide (29:1)	2.0ml	2.4ml	2.8ml	300µl
4x Lower buffer	2.0ml	2.0ml	2.0ml	-
4x Upper buffer	-	-	-	750µl
H_2O	4.0ml	3.6ml	3.2ml	1950µl
10% APS	80µl	80µl	80µl	60µl
TEMED	8µl	8µl	8µl	6µl

Table 2.10 Preparation of SDS-PAGE gels

2.4.4 Western Blot Analysis

Protein separated on SDS-PAGE gels for western blotting were transferred to nitrocellulose (Whatman Protran 0.45µm) membranes using the Invitrogen X-Cell SureLock Mini Cell system for 1 hour at 25V in 1x transfer buffer (6.04 g Tris Base, 28.8 g glycine, 200 ml methanol and 1.6 L ddH2O). The membrane was then blocked using dried milk in 1X TBST (TBS, supplemented with 0.1% Tween20) for 1 hour at room temperature while mixing on a platform shaker. The membrane was then transferred to a 5ml Falcon tube containing 5ml of the appropriate primary antibody solution (Table 2.11) followed by incubating overnight at 4°C on a rotating shaker. Membranes were then washed 3 times for 5 minutes with TBST, transferred to the secondary antibody solution (Table 2.12) and incubated at room temperature for 1 hour on a platform shaker. The membrane was then wash again 3 times with TBST, placed between the 2 sheets of plastic wallet before

addition of an enhance chemiluminescence detection kit (PIERCE), after 1 minute incubation, the signals were detected using a Fujifilm LAS-4000 digital imaging system. Image analysis was carried out using ImageJ.

2.4.5 List of antibodies used for Western blotting

Primary Antibodies	Dilution	Supplier
Anti-CNOT7 (rabbit)	1/5000	Eurogentec[1]
Anti-CNOT6L (rabbit)	1/5000	Eurogentec[2]
Anti-CNOT6 (rabbit)	1/5000	Eurogentec[3]
Anti-BTG2 H-50 (goat)	1/1000	Santa Cruz

Table 2.11 Primary antibodies used for western blotting.

Antibodies were diluted in TBST containing 5% dried milk powder.

[1,2,3] These antibodies were custom-made and are not commerically available. The antibodies were generated using synthetic peptides; [1]Caf1/CNOT7: (C)NGTGNAYEEEANKQS (16 AA), [2]Ccr4b/CNOT6L: ASSRPGSPTADPNSIP (16 AA), [3]Ccr4a/CNOT6: SIEMPSGKPHLGTEK(C) (16 AA).

Secondary Antibodies	Dilution	Supplier
Anti-Rabbit HRP	1/1000	Santa Cruz (sc-2004)
Anti-Goat HRP	1/1000	Santa Cruz (sc-2020)

Table 2.12 Secondary antibodies used for western blotting. Antibodies were diluted in TBST containing 5% dried milk powder.

2.5 Deadenylation assay

2.5.1 Reagents, stock solutions and buffers

Purified deadenylase enzyme in extraction buffer

Fluorescent RNA substrate (5'- Flc-CCUUUCCAAAAAAAAA -3') (Eurogentec)

Fluorescent DNA probe (5'- TTTTTTTTTGGAAAGG-TAMRA -3') (Eurogentec)

5× reaction buffer: 100 mM Tris-HCl pH 7.8, 25% glycerol, 5 mM β-mercapto-ethanol

20 mM $MgCl_2$, Nuclease-free water

SDS (Sodium dodecyl sulpate)

RNA Loading buffer (95% formamide, 0.025% SDS, 0.025% bromophenol blue, 0.025% xylene cyanol FF, 0.025% ethidium bromide, 0.5mM EDTA)

40% acrylamide:bisacrylamide (19:1) solution

10% ammonium persulphate (APS) in H_2O.

Urea, TEMED (Tetramethylethylenediamine)

2.5.2 Deadenylase assay using denaturing polyacrylamide gel electrophoresis

In this assay the total reaction has a final volume of 10 µl. It contained 4 µl of protein (diluted in extraction buffer), 1 µl of 20 mM $MgCl_2$, 4 µl of 1x reaction buffer (20 mM Tris-HCl pH 7.9, 10% glycerol, 1 mM β-mercaptoethanol) and 1 µl RNA substrate at final concentration of 0.1 µM. The reaction samples were incubated for 60 minutes at 30°C and stopped by addition of 12 µl of RNA loading buffer (95% formamide, 0.025% SDS, 0.025% bromophenol blue, 0.025% xylene cyanol FF, 0.025% ethidium bromide, 0.5mM EDTA). The reaction samples were then heated for 3 minutes at 85°C and 5 µl of each sample was loaded into a well on a the 20% acrylamide:bisacrylamid (19:1)/50 % urea gel (Table 2.13). The gel was run using the invitrogen X-

Cell SureLock Mini cell system, at 200V for approximately 1.5 hours or until the loading dye was ¾ bottom of the gel. A Fujifilm LAS-4000 was used for imaging the gel.

Reagent		**Volume**
20 % acrylamide:bisacrylamide (19:1)		6.0 ml
5 × TBE		2.4 ml
Urea	6.0 g	
TEMED	12 µl	
APS (10%)		120 µl
Total volume		**12 ml**

Table 2.13 The 20% gel formula for deadenylation assay (gel-based format)

2.5.3 Fluorescence-based deadenylase assay

The total reaction in a final volume of 10 µl contained 4 µl of enzyme (diluted in extraction buffer), 1 µl of 20 mM MgCl2, 4 µl of 1x reaction buffer (20 mM Tris-HCl pH 7.9, 10% glycerol, 1 mM β-mercaptoethanol) and 1 µl RNA substrate at a final concentration of 0.1 µM. The reaction samples were incubated for 60 minutes at 30°C, followed by adding with 10 µl of stop/probe mix (1 µl of SDS 10%, 4 µl of TE and 5 µl of DNA probe at a final concentration of 0.1 µM). Subsequently, the fluorescence was measured using a Biotek Synergy HT plate reader. The settings of the plate reader were: Greiner 384 Fluotrac, temperature set point: 25, detection method: fluorescence, read type: Endpoint. The filter sets: Excitation: 485/20, Emission: 528/20, Optics position: Top, Sensitivity: 90.

2.6 Characterization of drug-like small molecule inhibitors of the Caf1/CNOT7 enzyme

2.6.1 Reagents, stock solutions and buffers

Purified deadenylase enzyme in extraction buffer

Fluorescent RNA substrate (5'- Flc-CCUUUCCAAAAAAAAA -3') (Eurogentec)

Fluorescent DNA probe (5'- TTTTTTTTTGGAAAGG-TAMRA -3') (Eurogentec)

5× reaction buffer: 100 mM Tris-HCl pH 7.8, 25% glycerol, 5 mM β-mercapto-ethanol

20 mM $MgCl_2$, Nuclease-free water

SDS (Sodium dodecyl sulpate)

RNA loading buffer (95% formamide, 0.025% SDS, 0.025% bromophenol blue, 0.025% xylene cyanol FF, 0.025% ethidium bromide, 0.5mM EDTA)

2.6.2 Determination of the IC_{50} value of compounds

Serial concentrations of compound were pre-incubated with 0.4μM Caf1/CNOT7 for 15 minutes at room temperature. After addition of RNA substrate (final concentration of 1.0μM), the reaction mixture were incubated for 60 minutes at 30°C. The reactions were stopped by the addition of an equal volume of solution containing SDS and DNA probe (final concentration of 3μM). Data analysis and curve-fitting were carried out using Microsoft Excel 2007 and Graphpad Prism 6.0.

2.6.3 Gel based analysis for validation the inhibitory activity of small molecule inhibitor

Caf1/CNOT7 (0.4μM) was incubated with RNA substrate (1.0μM) in the presence and absence of the identified compounds for 60 minutes at 30°C. The reaction were stopped by addition of RNA loading buffer (95% formamide, 0.025% SDS, 0.025% bromophenol blue, 0.025% xylene cyanol FF, 0.025% ethidium bromide, 0.5mM EDTA). The reaction samples were then heated for 3 minutes at 85°C and 5 μl of each sample was analysed by denaturing PAGE using a the 20% acrylamide:bisacrylamid (19:1) gel containing 50% (w/v) urea. Polyacrylamide gel s (8x8 cm; Invitrogen Xcell system) were pre-run for 30 min at 200 V before sample loading. Flc-labelled RNA was visualized by epifluorescence using a Fujifilm LAS-4000 imager equipped with an Epi-Blue illuminator (460 nm).

2.6.4 Selectivity of small molecule inhibitors of CNOT7 enzyme

To assess the selectivity of the compounds, we used fluorescence-based assay. We tested the effect of the compounds on the activity of the DEDD type deadenylase, PARN, and the EEP type enzyme, Ccr4b/CNOT6L. Enzymes and RNA substrate were incubated in the presence of the identified compounds for 60 minutes at 30°C. The reaction mixtures were then stopped by addition of a solution containing SDS and DNA probe. Fluorescence was measured using a BioTek Synergy HT plate reader as described in section 2.5.3.

Chapter 3

Fluorescence-based Assay for Quantitative Analysis of Deadenylase Enzyme Activity

Chapter 3. A Fluorescence-based Assay for Quantitative Analysis of Deadenylase Enzyme Activity

3.1 Introduction

In vitro deadenylase assays are useful to identify and characterize the properties of deadenylase enzymes as well as to study control mechanisms of mRNA deadenylation. There are various benefits of in vitro deadenylase assay as compared to in vivo assays. In vitro approaches allow the study of purified deadenylase enzymes and are useful for determining the kinetics and cofactor requirements of deadenylase enzymes (Chen et al., 2002, Viswanathan et al., 2003, Andersen et al., 2009, Goldstrohm and Wickens, 2008). The effect of substrate structure and RNA sequences can also be examined using this approach. In vitro assays are also useful to study the effect of amino acid substitutions on the enzyme activity (Bianchin et al., 2005, Viswanathan et al., 2003).

There are several methods that have been used for deadenylase assays. The first method is based on labelling of substrate RNA using radioactive isotopes or fluorescent groups. In the latter method, synthesized 5'-fluorescent dye-labeled RNA substrate was used as a substrate for the enzymatic reaction. The reaction sample is analyzed by size separation using denaturing gel electrophoresis (Chen et al., 2002, Viswanathan et al., 2003). Deadenylase activity is determined by detecting the degradation of RNA substrate. This assay is widely used, because of its high sensitivity and also relative simplicity, although it is difficult to quantify and laborious. An alternative method is based on methylene blue colorimetry. In this method, after adding methylene blue, intercalation of methylene blue to RNA will cause a shift of the absorbance maximum of methylene blue (Greiner-Stoeffele et al., 1996, Liu and Yan, 2008). This method is non-radioactive and less time consuming as compared to product analysis based on gel electrophoresis. However, the

disadvantage of this method is that it is relatively insensitive and requires high protein and substrate concentrations.

Recently, a new method based on size-exclusion chromatography (SEC) was described. In this method, after enzymatic reaction, the reaction samples were separated by size-exclusion chromathography. Using this method the product and substrate can be separated and quantified (Balatsos et al., 2012). The size-exclusion chromathography assay was applied to study purified enzymes and also complex enzymes, such as protein mixtures or crude cell extracts. However, this method is relatively time consuming, particularly when multiple samples require analysis.

The purpose of this study was to develop an in vitro deadenylase assay based on fluorescence which is sensitive, quantitative and suitable for micro-well formats. The fluorescence-based deadenylase assay is based on end-point measurement and suitable for 96- and 384-well microplate formats.

3.2 Deadenylation activity of purified Caf1/CNOT7

3.2.1 Protein purification

Wild-type and catalytically inactive Caf1/CNOT7 enzymes were used to develop the fluorescent assay. Purified proteins were prepared using the prokaryotic expression vector pQE80L containing a codon optimised CNOT7 cDNA. A single colony of *E. coli* BL21 containing plasmid pQE80L-CNOT7 or pQE80L-CNOT7 D40A was used to inoculate a starter culture for protein expression. The pre-culture, was then grown in 1 L of Lysogeny Broth (LB) at 37°C until the OD_{600} was between 0.6-0.8. Then, isopropyl-β-D-1-thiogalactopyranoside (IPTG; final concentration of 0.2 mM) was added to the culture to induce the expression of the protein.

Protein purification was carried out using immobilised metal affinity chromatography (IMAC). For this, a His-Trap HP cartridge (GE Healthcare) was used. Soluble lysate was applied to the column using a syringe followed by washing using 10 ml of wash buffer containing 10 mM imidazole. Elution buffer containing 250 mM imidazole was added (approximately 5-6 ml) while collecting 1 ml fractions. The catalytically inactive version, Caf1/CNOT7 D40A was purified in parallel using the same conditions. The amount of protein was measured with Bio-Rad Protein Assay Reagent (Table 3.1) and the purity was analysed by sodium dodecyl sulphate-polyacryl-amide gel electrophoresis SDS-PAGE followed by Coomassie blue staining (Figure 3.1).

3.2.2 Deadenylation activity of Caf1/CNOT7

A gel-based deadenylation assay was used to confirm the activity of Caf1/CNOT7 enzyme. For the gel-based assay, a fluorescent RNA oligonucleotide containing nine adenosine residues at the 3'end (5'-Flc-CCUUUCCAAAAAAAAA-3') was used as the substrate. In this assay the total reaction has a final volume of 10 µl.

As shown in Figure 3.2, incubation of RNA substrate in the presence of 0.3 μM Caf1/CNOT7 resulted in limited RNA degradation, and increasing the amount of enzyme increased the RNA degradation. Addition of 1.2 μM Caf1/CNOT7 resulted in complete degradation in 60 minutes. To check that the observed deadenylase activity is indeed due the specific activity of purified Caf1/CNOT7, we also incubated the RNA substrate with the inactive version of Caf1/CNOT7. The catalytically inactive version contained a point mutation at position 40 where the aspartic acid residue is substituted for alanine (D40A). Asp-40 is required for chelation of Mg^{2+} ions in the active site and necessary for enzyme activity (Horiuchi et al., 2009, Jonstrup et al., 2007, Liu and Yan, 2008, Thore et al., 2003).

The result indicated that there is no degradation of the RNA substrate at any concentration of the catalytically inactive version of Caf1/CNOT7 D40A. Thus, the Asp-40 residue is critical for the activity of CNOT7 and the observed RNA degradation is specifically due to the activity of Caf1/CNOT7.

Protein	Fraction	Concentration (mg/ml)
CNOT7	# 1	6.0
	# 2	8.0
	# 3	2.0
CNOT7 D40A	# 1	5.9
	# 2	6.9
	# 3	1.2

Table 3.1 Concentration of purified Caf1/CNOT7 and Caf1/CNOT7 D40A. One litre of overnight culture of BL21 induced with 0.2 mM IPTG was used to purify the indicated proteins using a 1 ml His Trap™ column. The concentration of eluted protein was measured using Bio-Rad Protein Assay Reagent.

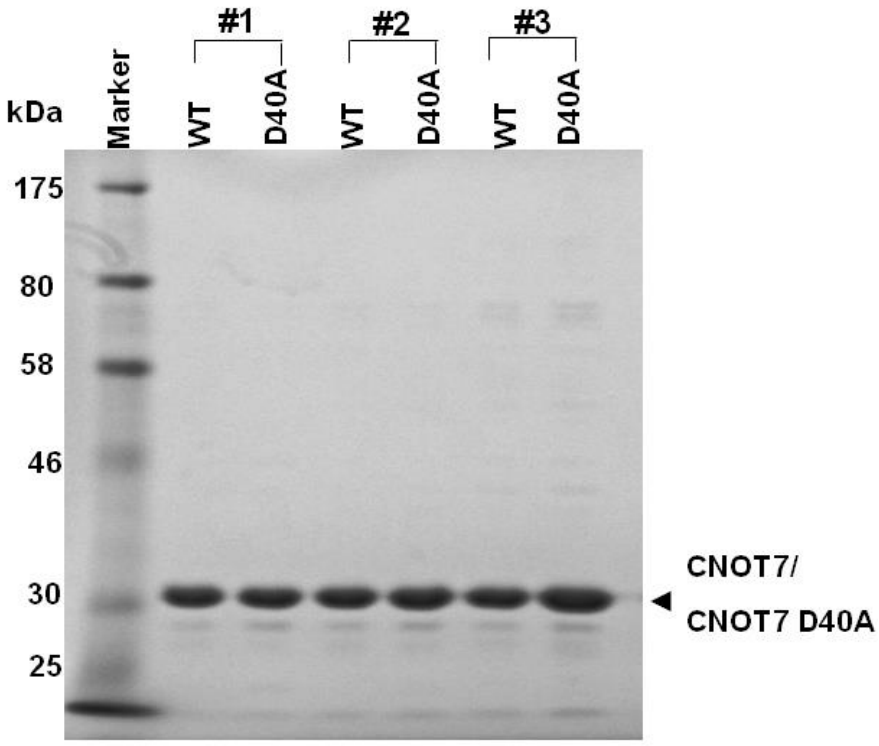

Figure 3.1 Purified Caf1/CNOT7 and Caf1/CNOT7 D40A proteins. Proteins were purified from an overnight culture of BL21 (1L) induced with 0.2 mM IPTG using a 1 ml His Trap column. The column was washed with 10 ml of buffer containing 10 mM imidazole. Fractions were collected during elution using buffer containing 250 mM imidazole and samples were analysed by 10% SDS-PAGE. Protein were visualised by staining with Coomassie Brilliant Blue.

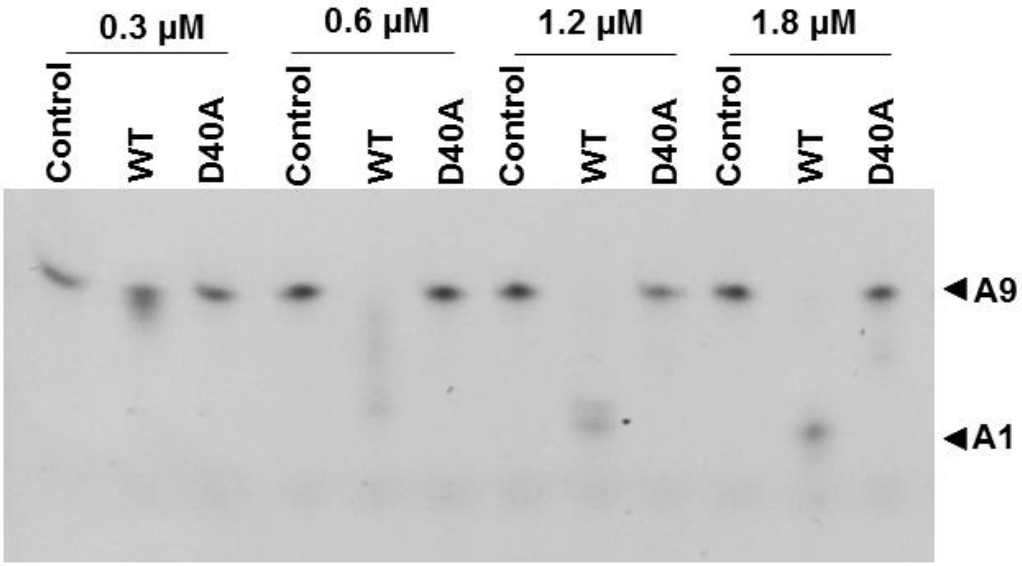

Figure 3.2 Deadenylase activity of Caf1/CNOT7. Proteins were incubated with RNA substrate at 30°C for 60 minutes. Then, RNA loading buffer was added to the reaction mixtures. Reaction mixtures were then separated on a denaturing 20% acrylamide:bisacrylamide (19:1)/50% urea gel. Indicated are reactions without enzyme (Control), and reactions containing wild-type enzyme (WT) and a catalytically inactive version of Caf1/CNOT7 (D40A). Also indicated are intact (A9) and degraded RNA substrate (A1).

3.2.3 A fluorescence-based assay for deadenylase activity

Previous reports indicated that short RNA oligonucleotides are recognised as substrates of deadenylase enzymes *in vitro* (Horiuchi et al., 2009, Anderson and Kedersha, 2009). This was confirmed as shown in section 3.2.2. Based on these findings, we designed a fluorescence-based substrate detection method. This assay used three components: purified enzyme, a fluorescent RNA substrate (5'-Flc-CCUUUCCAAAAAAAAA-3') and a DNA probe containing a 3' fluorophore (5'TTTTTTTTTGGAAAGG-TAMRA-3').

Purified enzyme and RNA substrate were incubated at 30°C for 60 minutes. A TAMRA-conjugated DNA probe mix containing 10% SDS, was used to stop the reaction. A fluorescence plate reader was used to measure the fluorescence. The active enzyme would degrade and shorten the poly(A) tail of the RNA substrate and this would prevent the DNA probe to anneal to the substrate. Therefore, fluorescence of the substrate-conjugated fluorophore can be detected (Figure 3.3). By contrast, in the absence of enzyme activity, no poly(A) tail degradation occurs. Consequently the TAMRA labelled probe would bind perfectly to the substrate and quench fluorescence.

The wild-type and catalytically inactive version of Caf1/CNOT7 were used to verify the method. Figure 3.4A indicated that Caf1/CNOT7 displayed deadenylase activity. The mutant type, Caf1/CNOT7 D40A did not show activity at any concentration, indicating that the observed activity was due to Caf1/CNOT7 and no contaminating enzyme activity was present. We also did the assay with different incubation times (0, 2, 5, 10, 25 and 60 minutes). As expected, the fluorescence increased with increasing incubation time. Already after 10-20 minutes, the signal was significantly above background (Figure 3.4B).

To assess the suitability of the fluorescence-based assay for quantitative analysis, we carried out a kinetic analysis of the Caf1/CNOT7 enzyme activity. A fixed amount of Caf1/CNOT7 was incubated with increasing RNA substrate concentration, and fluorescence as a function of time was measured. Each

substrate concentration was analyzed in duplicate. After obtaining the initial rate of reaction by linear regression, the substrate concentration was then plotted versus the initial rate of reaction. Finally, by using non-linear regression, we derived the K_m of Caf1/CNOT7, (10.6 ± 2.9 μM) (Figure 3.5). This K_m value indicated that Caf1/CNOT7 exhibits a relatively low deadenylase activity.

Figure 3.3 The principle of fluorescence-based assay. Enzymes were incubated with RNA substrate for 60 minutes at 30°C. The reaction was terminated by adding DNA probe mix containing 10% SDS, then fluorescence was measured using a Biotek Synergy HT plate reader. In the presence of active enzyme, the RNA substrate was degraded preventing the annealing of the DNA-TAMRA probe. Thus, substrate fluorescence is detected. In the absence of enzyme activity, the probe anneals to the RNA substrate, thereby quenching substrate fluorescence.

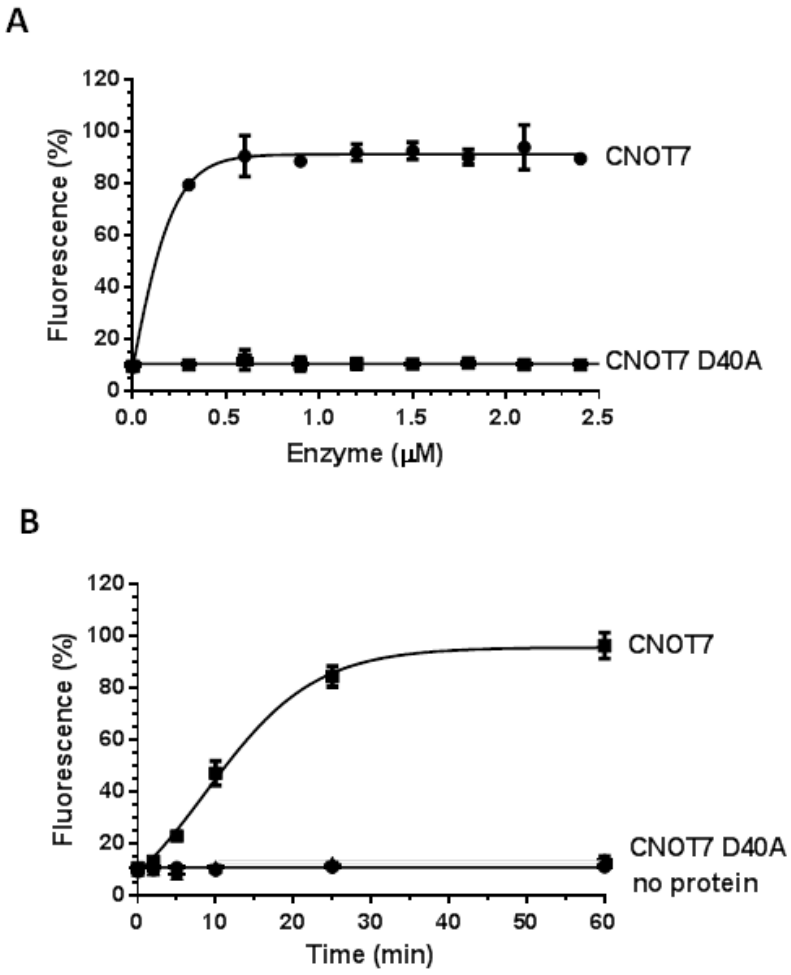

Figure 3.4 Deadenylation activity of Caf1/CNOT7 and Caf1/CNOT7 D40A. **(A)** Caf1/CNOT7 displays deadenylase activity. The indicated concentration of Caf1/CNOT7 and Caf1/CNOT7 D40A was incubated with RNA substrate for 60 minutes at 30°C. A stop/probe mix containing 10% SDS, TE and a five-fold molar excess of DNA probe (5'TTTTTTTTTGGAAAGG-TAMRA-3') was added to stop the reactions and detect enzyme activity. **(B)** Deadenylation activity of Caf1/CNOT7 as a function of time. RNA substrate was incubated with 0.6 μM wild-type or inactive Caf1/CNOT7 at 30°C for 0, 2, 5, 10, 25 and 60 minutes. DNA probe mix was added and fluorescence was measured. Error bars represent standard deviations (n = 3), multiple wells done on the same day.

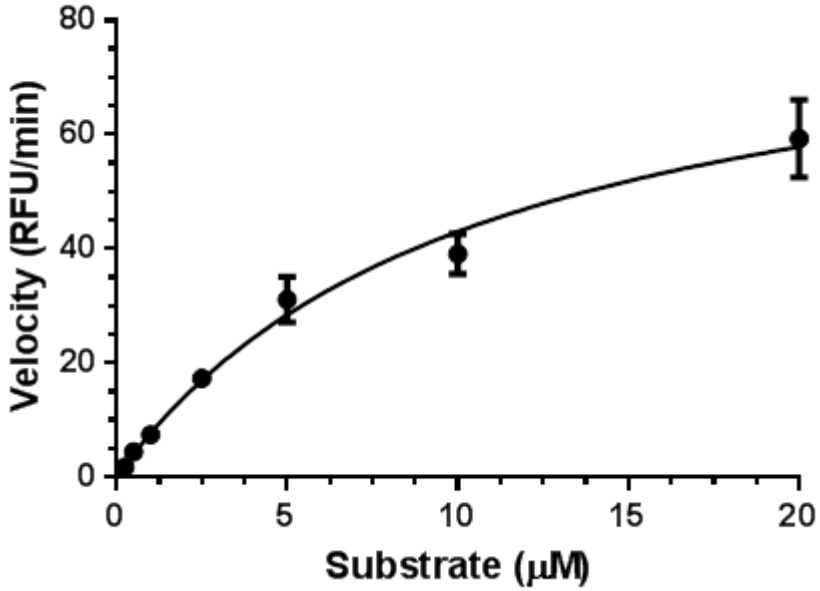

Figure 3.5 Determination the K_m of Caf1/CNOT7 using the fluorescence-based assay. Caf1/CNOT7 (0.4 μM) enzyme was incubated with different concentration of RNA substrate (0.25, 1.0, 2.5, 5.0, 10, 15 and 20 μM). Each substrate was incubated for different times (0, 2, 5, 10, 25 and 60 minutes) and analyzed in duplicate. After obtaining the initial rate of reaction by linear regression, the substrate concentration was then plotted versus the initial rate of reaction. The values obtained were fitted by non-linear regression analysis to the Michaelis-Menten equation and used for determine the K_m (10.6 ± 2.9 μM). Error bars represent standard deviations (n = 3), multiple wells done on the same day.

3.2.4 Optimization of fluorescence-based assay

In order to determine the stability of signal in the assay after the addition of DNA probe, the signal was measured every 30 minutes for 4 hours. The result indicated that the signal remained stable for at least 4 hours after addition of the DNA probe (Figure 3.6A).

Furthermore, to ascertain the most suitable DNA probe concentration, we also optimized the amount of DNA probe for the fluorescent assay (Figure 3.6B). In this assay, a fixed amount of RNA substrate (0.1 μM) was used. Solutions containing increasing concentrations of DNA probe (0.03, 0.1, 0.3, 0.5 and 0.9 μM) and SDS were added to terminate the enzymatic reaction. The results showed that from the addition of 0.1 μM DNA probe was sufficient when using a concentration of 0.1 μM of RNA substrate. Thus, an equimolar amount of DNA probe is the minimum quantity that must be added to the reaction.

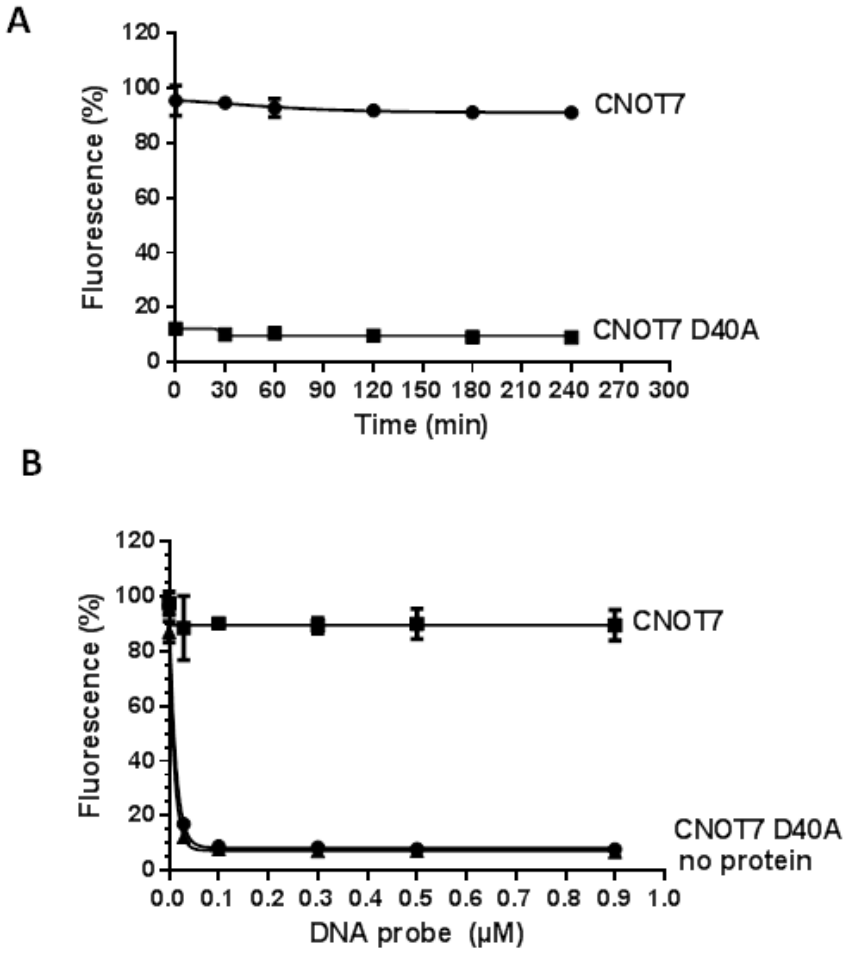

Figure 3.6 Optimization of the fluorescence-based assay. (A) The stability of the signal in the fluorescent assay. The reaction mixture containing wild-type or inactive Caf1/CNOT7 and the RNA substrate (final concentration of 0.1 μM) was incubated for 60 minutes at 30°C. After addition of stop/probe mix, the signal was measure every 30 minutes for 4 hours. **(B)** Optimization of DNA probe concentration in the fluorescence-based assay**.** The wild-type or inactive Caf1/CNOT7 was incubated with 0.1 μM RNA substrate at 30°C for 60 minutes. Different concentrations of DNA probe (0.03, 0.1, 0.3, 0.5 and 0.9 μM) were used to stop and probe the enzymatic reaction. Error bars represent standard deviations (n = 3, multiple wells done on the same day.

3.3 Deadenylation activity of purified Ccr4b/CNOT6L ΔLRR

3.3.1 Protein purification of Ccr4b/CNOT6L ΔLRR

To find out whether the fluorescence-based assay is also suitable for other deadenylase enzymes, we next used the EEP type enzyme Ccr4b/CNOT6L lacking the amino-terminal leucine-rich repeat (LRR) domain (Ccr4b/CNOT6L ΔLRR). Ccr4b/CNOT6L displays deadenylase activity both in vitro and in vivo. This enzyme is localized mainly in the cytoplasm (Morita et al., 2007). We used Ccr4b/CNOT6L ΔLRR, because initial experiments indicated that full length Ccr4b/CNOT6L was not soluble (Figure 5.2, Chapter 5). In human, the LRR domain of CNOT6L is not required for the deadenylation activity of Ccr4b/CNOT6L enzyme (Wang et al., 2010). Here, we also purified the catalytically inactive version of Ccr4b/CNOT6L E240A. Previous research indicated that mutation of Glu240 in this enzyme abolished the deadenylation activity (Wang et al., 2010).

Thus, a single colony of *E. coli* BL21 containing plasmid pQE80L-CNOT6L ΔLRR or pQE80L-CNOT6L ΔLRR E240A was used to inoculate a starter culture for protein expression. To induce the expression of the protein, IPTG (final concentration of 0.2 mM) was added to the culture. Protein purification of truncated Ccr4b/CNOT6L ΔLRR and the inactive type Ccr4b/CNOT6L ΔLRR E240A was carried out using immobilized metal affinity chromatography (IMAC). The soluble lysate (obtained from 1L culture) was first applied onto a 1 ml His Trap HP column (GE Healthcare) using a syringe. Wash buffer containing 10 mM imidazole was used to remove nonspecific binding of bacterial proteins. Bound protein was eluted with 6 ml elution buffer containing 250 mM imidazole and collected in 1 ml fractions. The protein of interest eluted in fraction 1, 2 and 3 (Figure 3.7). SDS-PAGE analysis indicated that there were small amounts of impurities in both wild-type and mutant type of Ccr4b/CNOT6L ΔLRR. The protein concentration was measured using Bio-Rad Protein Assay Reagent (Table 3.2)

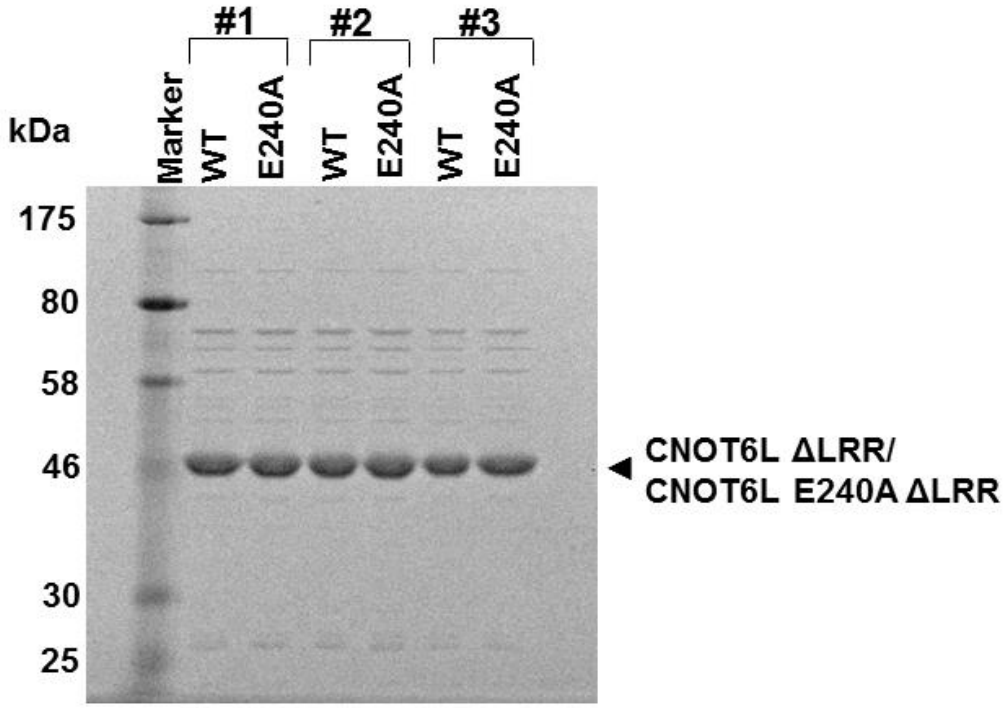

Figure 3.7 Analysis of purified Ccr4b/CNOT6L ΔLRR and Ccr4b/CNOT6L E240A ΔLRR proteins. Overnight culture of BL21 (1L) induced with IPTG (final concentration of 0.2 mM) was used to purify the indicated proteins using a 1 ml His Trap column. The column was washed with 10 ml of wash buffer containing 10 mM imidazole. Bound protein was eluted with 6 ml elution buffer containing 250 mM imidazole and collected in 1 ml fractions. Proteins were analysed by 10% SDS-PAGE, then visualised by staining with Coomassie Brilliant Blue.

Protein	Fraction	Concentration (mg/ml)
CNOT6L	# 1	0.54
	# 2	1.2
	# 3	0.26
CNOT6L E240A	# 1	1.6
	# 2	5.6
	# 3	1.0

Table 3.2 Concentration of purified Ccr4b/CNOT6L and Ccr4b/CNOT6L E240A. Overnight culture of BL21 (1L) induced with IPTG (final concentration of 0.2 mM) was used to purify the indicated proteins using a 1 ml His Trap HP column. The protein concentrations were measured using the Bio-Rad Protein Assay Reagent.

3.3.2 Deadenylase activity of Ccr4b/CNOT6L

A gel based assay was carried out to confirm the activity of Ccr4b/CNOT6L ΔLRR. Purified Ccr4b/CNOT6L ΔLRR enzyme was incubated with RNA substrate. Then, the enzymatic reaction was terminated by adding RNA loading dye, followed by size separation using denaturing gel electrophoresis. The results showed that while the wild-type Ccr4b/CNOT6L ΔLRR enzyme degraded the RNA oligonucleotide substrate, no degradation of the RNA substrate was observed at any concentration in the presence of inactive Ccr4b/CNOT6L ΔLRR E240A. At a concentration of 1.2 μM CNOT6L ΔLRR, all RNA substrate was degraded. These results indicate that the observed deadenylase activity was specifically due to Ccr4b/CNOT6L ΔLRR and that no contaminating nuclease from *E. coli* was present (Figure 3.8).

3.3.3 Fluorescence-based detection of deadenylase activity of Ccr4b/CNOT6L

In agreement with the gel based assay, that the deadenylase activity of Ccr4b/CNOT6L ΔLRR was also observed using the fluorescence-based assay while Ccr4b/CNOT6L ΔLRR E240A did not show activity (Figure 3.9A). The fluorescence was dependent on the incubation time and enzyme concentration (Figure 3.9A and 3.9B).

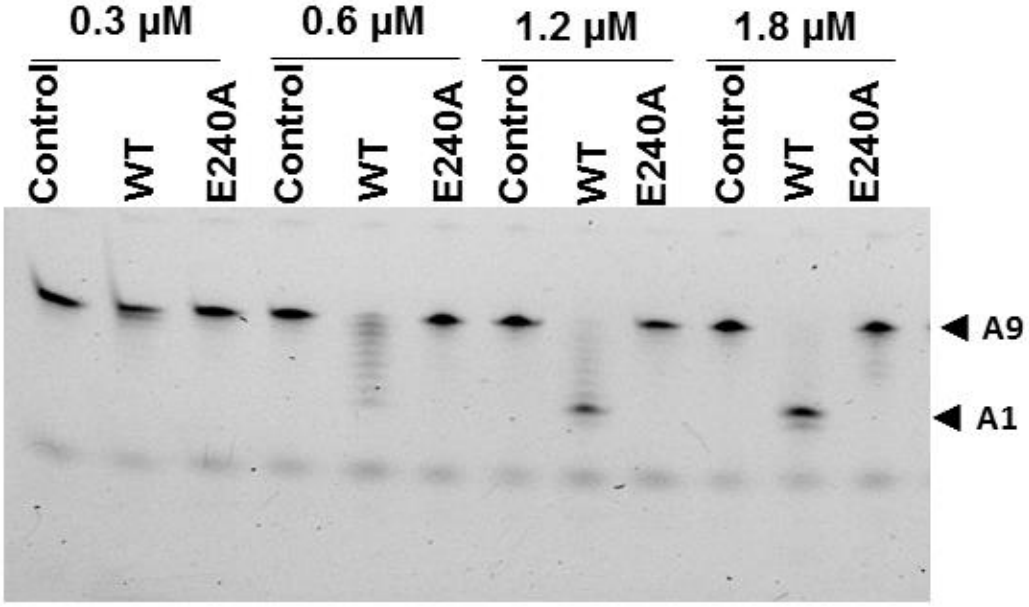

Figure 3.8 Deadenylase activity of Ccr4b/CNOT6L ΔLRR. Wild-type and inactive CNOT6L ΔLRR containing the amino acid substitution E240A were incubated with 0.1 µM RNA substrate at 30°C for 60 minutes. Then, RNA loading buffer was added followed by heat treatment. The reaction mixtures were then fractionated on a 20% acrylamide:bisacrylamide (19:1)/50% urea gel. Indicated are control reaction without enzyme (Control), wild-type (WT), catalytically inactive version of Ccr4b/CNOT6L ΔLRR (E240A). Also indicated are the intact (A9) and degraded RNA substrate (A1).

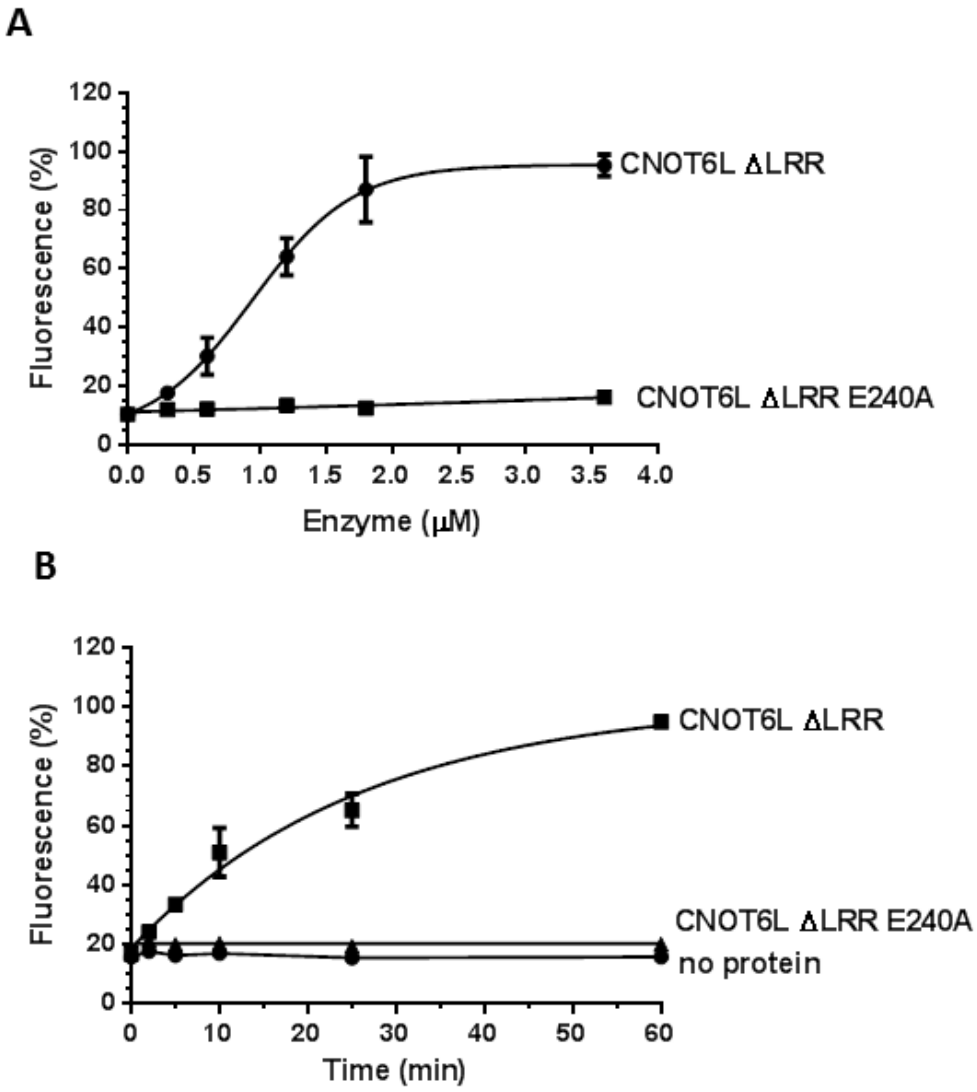

Figure 3.9 Flurescence-based detection of the deadenylase activity of Ccr4b/CNOT6L ΔLRR. (A) Concentration dependent deadenylation by Ccr4b/CNOT6L ΔLRR. Increasing concentrations of wild-type and inactive Ccr4b/CNOT6L ΔLRR were incubated with RNA substrate for 60 minutes at 30°C. **(B)** Time dependent deadenylase activity of Ccr4b/CNOT6L ΔLRR. Enzymes were incubated with 0.1 μM RNA substrate at 30°C for different incubation time (0, 2, 5, 10, 25 and 60 minutes). Error bars represent standard deviations (n = 3), multiple wells done on the same day.

3.4 Deadenylation activity of purified PARN

Finally, we also used another DEDD type enzyme, PARN, to validate the new fluorescence-based assay. PARN is a member of DEDD family of nucleases that dependent on a divalent metal ions for enzyme activity (Korner et al., 1998). Site-directed mutagenesis indicated that $Asp^{28,}$ Glu^{30}, Asp^{292} and Asp^{382} residues are essential for catalytic activity of PARN. These residues are required for the binding of divalent metal ions to PARN (Ren et al., 2002b, Ren et al., 2004, Wu et al., 2005).

Wild-type PARN, as well as inactive PARN containing the D28A amino acid substitution were a generous gift of Mrs Blessing Airhihen (School of Pharmacy, University Of Nottingham). Initially, to confirm the deadenylase activity of the enzyme, we again used a gel based assay. The results of the assay indicated that the wild-type of PARN enzyme degraded the RNA substrate at much lower concentrations than Caf1/CNOT7 or Ccr4/CNOT6L. No RNA substrate degradation was observed at any concentration of inactive PARN containing the amino acid substitution D28A (Figure 3.10).

Fluorescence-based detection of PARN enzyme activity corresponded to the results obtained with the gel based assay. As shown in Figure 3.11A, fluorescence was measured after incubation with wild type of PARN while no fluorescence was observed when RNA substrate was incubated with inactive PARN D28A, even in the presence of relatively high concentrations (Figure 3.11B). Thus, the fluorescence was time and concentration dependent.

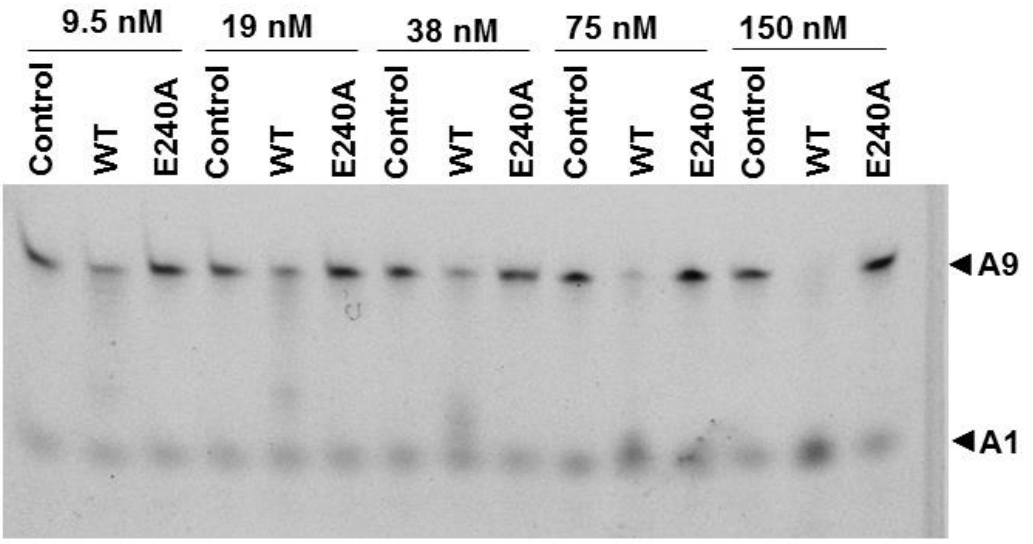

Figure 3.10 Deadenylase activity of PARN enzyme. Wild-type enzyme and inactive PARN containing the amino acid substitution D28A were incubated with 0.1 μM RNA substrate at 30°C for 60 minutes. Then, RNA loading buffer was added to the reaction sample followed by heat treatment. The reaction mixtures were then fractionated on a denaturing 20% acrylamide:bisacrylamide (19:1)/50% urea gel. Indicated are control reaction without enzyme (Control), wild-type (WT) and catalytically inactive PARN (D28A). Also indicated are intact (A9) and degraded RNA substrate (A1).

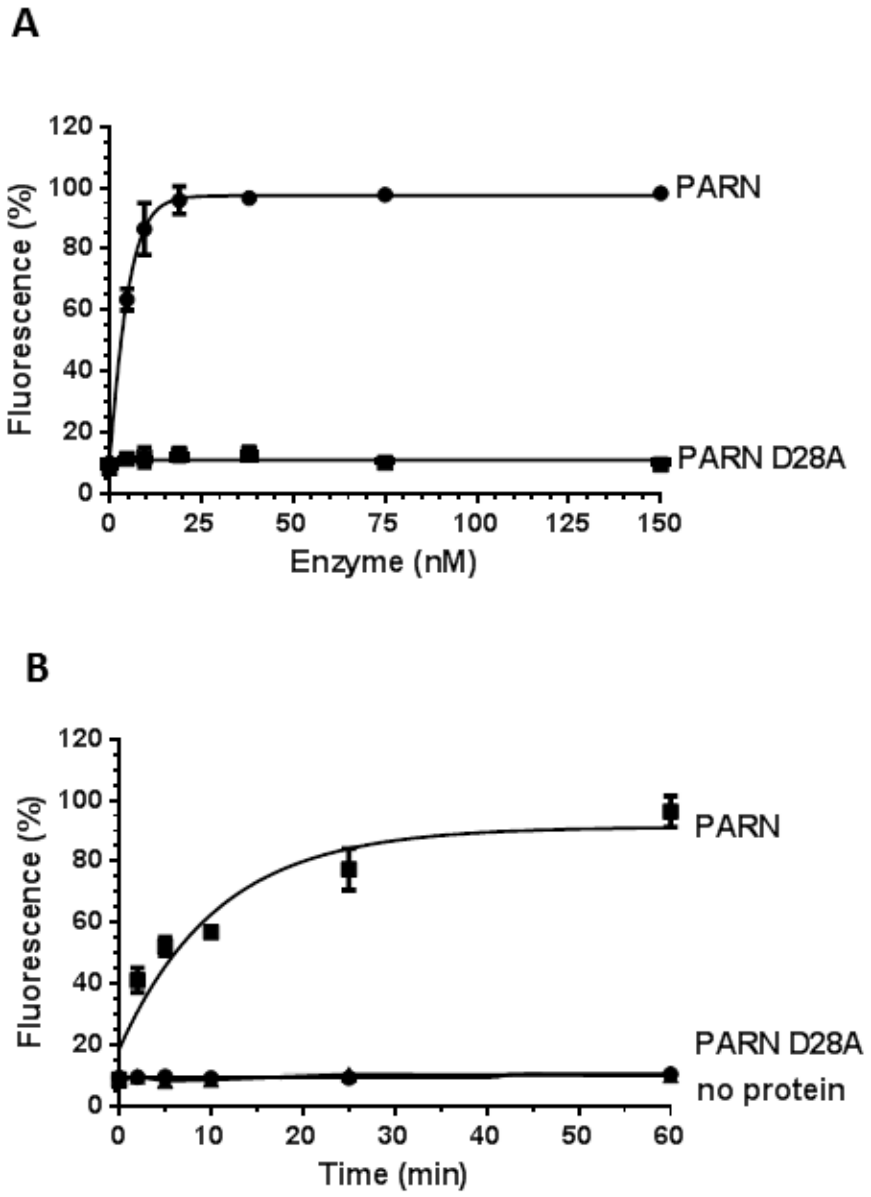

Figure 3.11 Fluorescence-based detection of the deadenylase activity of PARN. **(A)** Concentration dependent deadenylation by PARN. Increasing concentrations of wild-type and inactive PARN were incubated with 0.1 μM RNA substrate for 60 minutes in 30°C. **(B)** Time-dependent deadenylase activity of PARN. Enzyme was incubated with 0.1 μM RNA substrate at 30°C at different incubation times (0, 2, 5, 10, 25 and 60 minutes). Error bars represent standard deviations (n = 3), multiple wells done on the same day.

3.5 Discussion

In this chapter, a novel fluorescence-based assay to facilitate the biochemical analysis of deadenylase enzyme is described. The principle of this assay is based on fluorescence resonance energy transfer (FRET). FRET can occur if there is a significant overlaps of the emission spectrum of a donor fluorophore and the absorption spectrum of an acceptor. FRET is strongly dependent on the distance between the donor and acceptor molecules, which must be in close proximity. In this study, the quenching of the fluorescence signals of the fluorescein tagged RNA substrate (donor) by TAMRA tagged DNA probe (acceptor) was used.

Wild-type and mutant Caf1/CNOT7, PARN and also Ccr4b/CNOT6L ΔLRR were used to validate the fluorescence-based assay method. We noted that the enzymatic activity of PARN, Caf1/CNOT7 and Ccr4b/CNOT6L differs significantly, as judged based on the minimum enzyme concentration required for complete degradation of the RNA oligonucleotide substrate. The assay can be used to quantitatively determine the deadenylase activity of purified enzyme and also for multi-well formats. Based on the optimisation work of the fluorescence-based assay, the ratio of DNA probe and RNA substrate must be at least 1:1. However, increasing the molar excess of the DNA probe did not reduce background signal. The fluorescence signal can be measure for at least 4 hours after adding the DNA probe. This may increase the usefulness of the assay, because there is no requirement to have immediate access to a fluorescence spectrophotometer. In addition, this may be relevant when carrying out large numbers of reactions in parallel, for instance when screening compound libraries.

When compared with previously described methods, such as analysis based on gel electrophoresis, methylene blue colourimetry or size-exclusion chromatography (Greiner-Stoeffele et al., 1996, Chen et al., 2002, He and Yan, 2012), the fluorescence-based assay has significant advantages. Due to the sensitivity of the fluorescence-based assay, enzyme activity can be detected

at much lower concentrations and in smaller reaction volumes as compared with methylene blue colourimetry or size-exclusion chromatography. Furthermore, this new assay is fast and less laborious when compared with methods using gel electrophoresis or chromatography. Thus, because of the suitability for plate-based format, using this method can be used to evaluate a large number of reactions in parallel with less effort when compared with previous methods. However, there are some possible disadvantages of this new assay. First, other components could interfere with the fluorescence detection. Therefore we need to validate this method using another method, such as gel-based assay. Second, the short poly(A) tail of the substrate oligo used in this assay may cause difficulty when assessing the activity of some enzymes. For example, the Pan2-Pan3 enzyme does not efficiently degrade the final 20-25 nt (Lowell et al., 1992, Wolf and Passmore, 2014).

Chapter 4

Application of the fluorescence-based deadenylase enzyme assay: Characterization of drug-like small molecule inhibitors of the Caf1/CNOT7 enzyme

Chapter 4. Application of the fluorescence-based deadenylase enzyme assay: Characterization of drug-like small molecule inhibitors of the Caf1/CNOT7 enzyme

4.1 Introduction

Divalent metal ions are important for the catalysis and stability of the structure of many nucleotydyl-transfer enzymes, including polymerases, nucleases and phosphatases. Some enzyme uses two metal ions for their catalytic activity, while others just utilize one of metal ion (Beese and Steitz, 1991, He et al., 2011, Sissi and Palumbo, 2009). Poly(A)-Specific Ribonuclease (PARN) and Caf1/CNOT7 are examples of Mg(II)-dependent deadenylases that degrade poly(A) tails, releasing 5'-AMP (Goldstrohm and Wickens, 2008). As well as in the case for the PARN enzyme, the metal ions of Caf1/CNOT7 are coordinated by four amino acid residues, one glutamate and three aspartate residues (Astrom et al., 1991, Korner and Wahle, 1997, Thore et al., 2003, Jonstrup et al., 2007, Horiuchi et al., 2009, Winkler and Balacco, 2013). Based on biochemical and structural analysis, it has been proposed that these enzymes use the two metal ions for their catalytic activity (Ren et al., 2004, Wu et al., 2005).

There are few examples of Mg^{2+} -dependent enzymes that can be inhibited by small molecule inhibitors. It has been reported that aminoglycosides and natural purine nucleotides inhibit PARN activity (Ren et al., 2002a, Balatsos et al., 2009a). Further research identified that synthetic nucleoside analogues containing a fluoro-glucopyranosyl sugar moiety and benzoyl-modified cytosine or adenine inhibit human PARN (Balatsos et al., 2009b). However, until now no inhibitors of Caf1/CNOT7 have been reported.

To obtain further insight into the biological roles of deadenylase enzymes, small molecules such as potent, selective and cell permeable inhibitors are desirable. Thus, to discover inhibitors of the Caf1/CNOT7 enzyme, two

approaches were carried out. First, we screened a sub-set (1440 compounds) of a large compound library (83086 compounds, Managed Chemical Compound Collection, MCCC; Dr I. Kaur, School of Pharmacy, University of Nottingham), which were prioritised by virtual library screening (Dr G. Jadhav, School of Pharmacy, University of Nottingham). As a second approach, analogues of Caf1/CNOT7 inhibitors were synthesised (Dr G. Jadhav & Prof P.M. Fisher, School of Pharmacy, University of Nottingham). To synthesize these compounds, we referred to previous research of FEN1 (Flap Endonuclease-1) enzyme (Tumey et al., 2005). FEN1 is a divalent metal (Mg^{2+} or Mn^{2+}) dependent enzyme involved in base excision repair (BER), the main pathway for mammalian cells to repair DNA damage caused by alkylating agent (Tumey et al., 2005, Parikh et al., 1999). Tumey et al. reported that compounds which contain an *N*-hydroxy urea structure inhibited FEN1 by coordination of the metal ions needed for FEN1 activity (Tumey et al., 2005). They proposed two possible binding mechanisms of compounds and the metal ions (Figure 4.1) (Tumey et al., 2005). Thus, several compounds were identified with similarity to the reported FEN1 inhibitors from the National Cancer Institute Open Repository Collection containing over 140000 compounds with potential anticancer activity (National Cancer Institute, USA) (Dr G. Jadhav, School of Pharmacy, University of Nottingham). Based on the activity of these compounds, analogues were then synthesized to find more potent and selective Caf1/CNOT7 inhibitors.

These combined approaches led to the discovery and characterisation of several selective small-molecule inhibitors of Caf1/CNOT7. In addition, we also identified inhibitors that were able to inhibit both Caf1/CNOT7 and the highly related PARN deadenylase. These compounds may be pan-DEDD type deadenylase inhibitors.

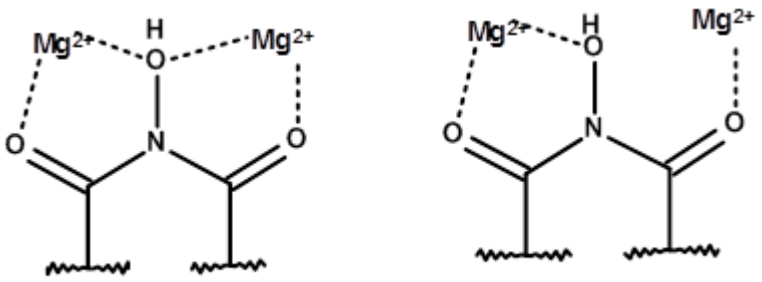

Figure 4.1. Two possible binding mechanisms of N-hydroxy urea analogues to active site divalent metal ions of DNA and RNA nuclease enzymes.

4.2 Discovery of small molecule inhibitors of Caf1/CNOT7 enzyme by compound library screening

To screen a compound collection for inhibitors of Caf1/CNOT7 (Dr. I. Kaur, School of Pharmacy, University of Nottingham), virtual library screening was initially carried out to prioritize candidates (Dr. G. Jadhav, University of Nottingham). This collection contains a highly diverse set of 83086 lead-like compounds. For the virtual screening, the coordinates of an X-ray crystal structure of the Caf1–NOT1 complex (Petit et al., 2012b) (Protein Data Bank entry 4GMJ, chain C) were used to construct a docking receptor with Sybyl 8.0 (www.tripos.com) software. Compounds were docked to this receptor using the genetic optimization for ligand docking (GOLD)(37) program (www.ccdc.cam.ac.uk) in standard parameter mode.

Using this procedure, 1440 predicted hits were selected for bioassays. Thus, these compounds were subjected to (automated) screening using liquid handling robotics (Dr. I. Kaur, University of Nottingham). This step produced 11 compounds that were selected for further analysis. Three of the compounds had very low inhibitory activity (estimated IC_{50}>500 μM). Two compounds precipitated and were discarded. The remaining six compounds, NCC-0001590, NCC-0007277, NCC-00019223, NCC-00039069, NCC-00010651 and NCC-00037292, were characterised in more detail.

4.2.1 Determination of the IC_{50} value of compounds identified by screening

To determine the IC_{50} values of NCC-0001590, NCC-0007277, NCC-00019223, NCC-00039069, NCC-00010651, and NCC-00037292, serial concentrations of compound were pre-incubated with Caf1/CNOT7 for 15 minutes at room temperature. After addition of RNA substrate, the reaction mixtures were incubated for 60 minutes at 30°C. The reactions were then stopped by the addition of a solution containing SDS and DNA probe. Data analysis and curve-fitting were carried out using Microsoft Excel 2007 and

Graphpad Prism 6.0. The results showed that all the analysed compounds have IC_{50} values <250 μM. NCC-00037292 was the most potent compound with an IC_{50} value of 14.6±3.1 μM (Figure 4.2 and Table 4.1).

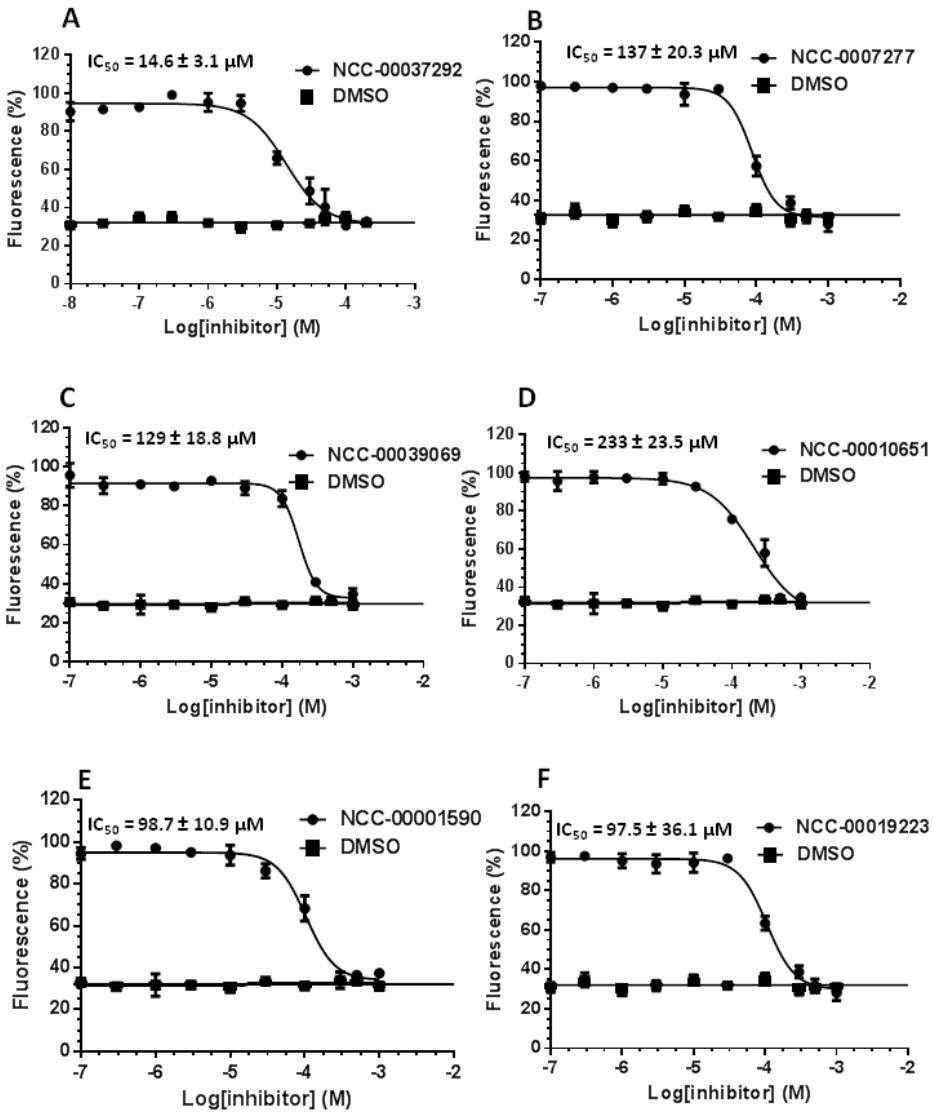

Figure 4.2 IC_{50} values of compounds identified by screening of a compound library. Shown are dose-response curves of reactions containing **(A)** NCC-00037292; **(B)** NCC-00007277; **(C)** NCC-00039069; **(D)** NCC-00010651; **(E)** NCC-00001590 and **(F)** NCC-00019223. Compounds were pre-incubated for 15 min at room temperature with Caf1/CNOT7 followed by addition of RNA substrate. The reaction mixture was incubated for 60 min at 30°C, DNA probe mixture containing SDS was then added to stop the reactions. Fluorescence was measure using a BioTek Synergy HT plate reader. Data analysis and curve-fitting were carried out using Microsoft Excel 2007 and Graphpad Prism 6.0. Error bars represent standard deviations (n = 3).

Compound	IC_{50} (μM)
NCC-00001590 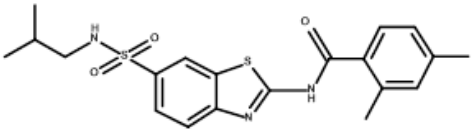	98.7 ± 10.9
NCC-00007277 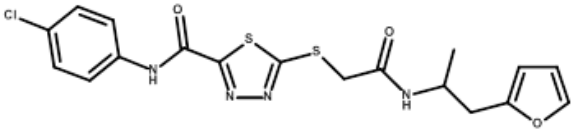	137 ± 20.3
NCC-00019223 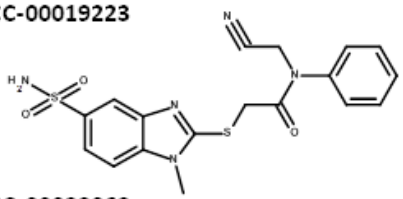	97.5 ± 36.1
NCC-00039069 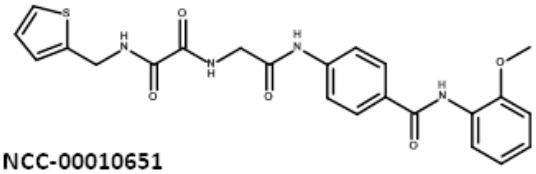	129 ± 18.8
NCC-00010651 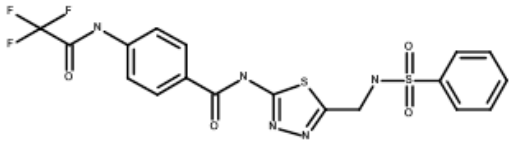	233 ± 23.5
NCC-00037292 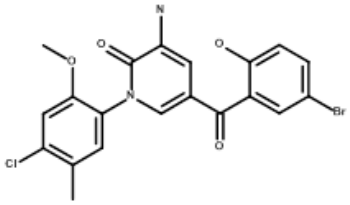	14.6 ± 3.1

Table 4.1 Structure and the IC_{50} values of compounds identified by screening of a compound library. The IC_{50} values are obtained from at least three replicate experiments. Data analysis and curve-fitting were carried out using Microsoft Excel 2007 and Graphpad Prism 6.0.

Furthermore, to ensure that the identified compounds were bona fide inhibitors of the Caf1/CNOT7 enzyme, and also to eliminate the possibility of interference of fluorescence measurement, we used gel-based assays (Figure 4.3). Caf1/CNOT7 was incubated with RNA substrate in the presence and absence of the identified compounds for 60 minutes at 30°C. The reactions were stopped by addition of RNA loading buffer. The reaction samples were then heated for 3 minutes at 85°C and 3 µl of each sample was loaded into a well of a 20% acrylamide:bisacrylamide (19:1)/50% urea gel. A Fujifilm LAS-4000 imager was used for gel visualisation. As predicted, in the absence of inhibitor, Caf1/CNOT7 degraded the RNA substrate, whereas in the control reaction that did not contain Caf1/CNOT7 enzyme, RNA substrate remained intact. Importantly, degradation of RNA substrate was greatly reduced in the presence of identified compounds. This confirmed that the identified compounds inhibited the deadenylase activity of Caf1/NOT7 enzyme (Figure 4.3).

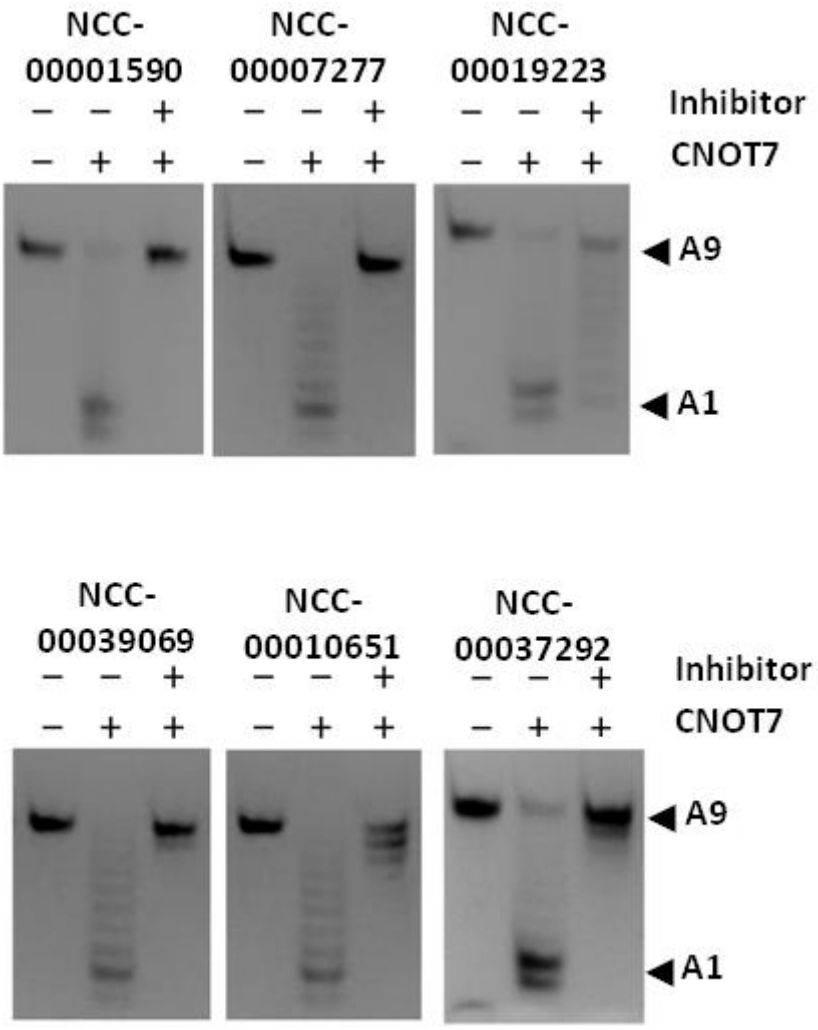

Figure 4.3 Validation of inhibitory activity using gel-based product analysis. Compounds (300 μM of NCC-00001590, NCC-00007277, NCC-00019223, NCC-00039069, NCC-00010651 and 100μM of NCC-00037292) were incubated with Caf1/CNOT7 enzyme (0.4 μM) and RNA substrate (1.0 μM) for 60 min 30°C. The enzymatic reactions were then inactivated by the addition of RNA loading buffer and heating at 85°C for 3 min. Products were separated by denaturing PAGE and directly visualized by epifluorescence. Indicated are the intact RNA substrates (A9) and the reaction product containing a single 3' adenosine residue (A1).

4.2.2 Selectivity of compounds identified by screening

In order to assess whether the identified compounds were selective for Caf1/CNOT7 or whether they were more general deadenylase inhibitors, we tested the effect of the compounds on the activity of the DEDD type deadenylase, PARN, and the EEP type enzyme, Ccr4b/CNOT6L. For this purpose, we also used the fluorescence-based assay. Enzymes and RNA substrate were incubated in the presence of the identified compounds for 60 minutes at 30°C. The reaction mixtures were then stopped by addition of a solution containing SDS and DNA probe. Fluorescence was measured using a BioTek Synergy HT plate reader. The results showed that compounds NCC-00039069 and NCC-00001590 are selective inhibitors as they only inhibit Caf1/CNOT7 and did not inhibit the activity of Ccr4b/CNOT6L and PARN (Figure 4.4C and E). However, compounds NCC-00007277, NCC-00019223 and NCC-00037292 exhibited less selectivity and partially inhibited the activity of Ccr4b/CNOT6L and PARN enzymes (Figure 4.4A, D and F). Compound NCC-00010651 inhibited all three deadenylase enzyme, although it did not completely inhibit the Ccr4b/CNOT6L and PARN activity (Figure 4.4B).

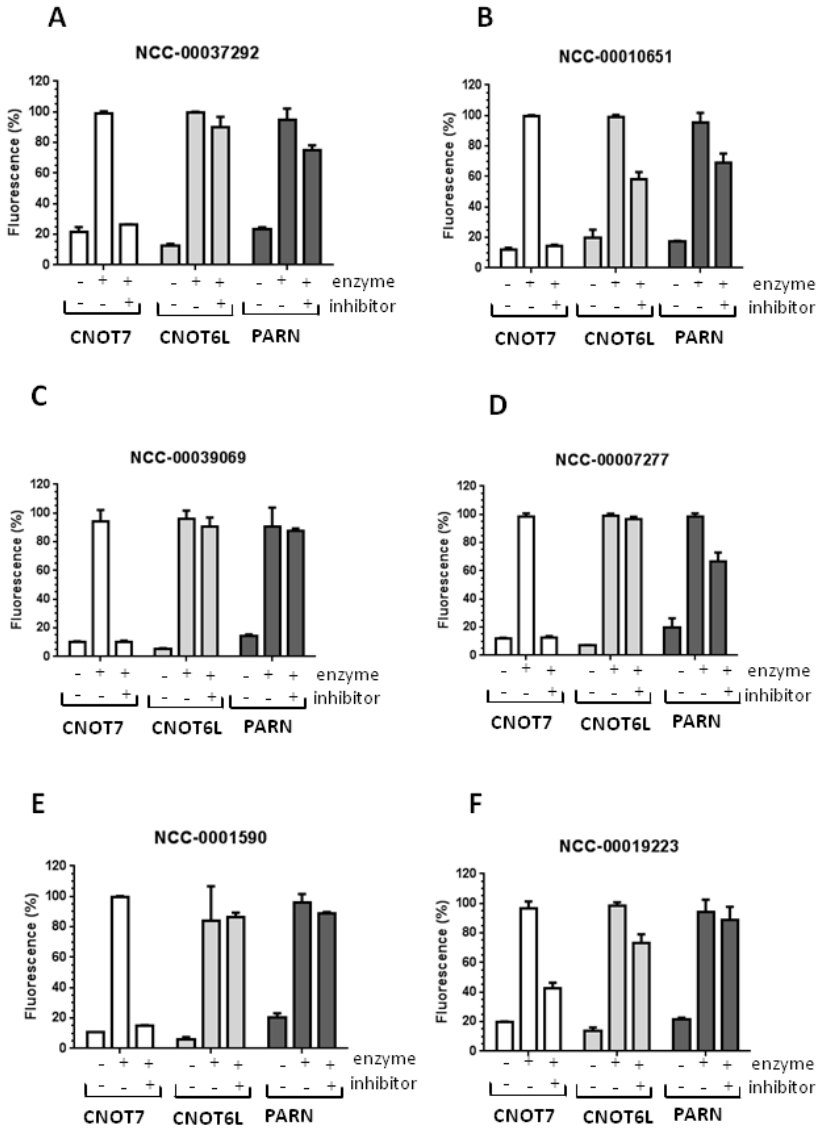

Figure 4.4 Selectivity of Caf1/CNOT7 inhibitors. The activity of the Caf1/CNOT7, CNOT6L and PARN enzymes was assessed in the presence of compounds **(A)** NCC-00037292 (100 μM, final concentration); **(B)** NCC-00010651; **(C)** NCC-00039069; **(D)** NCC-00007277; and **(E)** NCC-00001590 (300 μM, final concentration). Enzymes were pre-incubated with the indicated compounds at room temperature for 15 minutes followed by incubation with RNA substrate (1.0 μM) for 60 min 30°C. Fluorescence was measure after addition of DNA probe mixture containing SDS (0.5% final concentration). Error bars represent standard deviations (n = 3), multiple wells done on the same day.

4.3 Discovery of small molecule inhibitors of Caf1/CNOT7 enzyme based on similarity

As an alternative approach to find additional small molecule inhibitors for the Caf1/CNOT7 enzyme, a similarity search was carried out based on known inhibitors of the Mg^{2+} dependent enzyme FEN1 (Tumey et al., 2005). It was proposed that compounds which contained an N-hydroxy urea structure inhibited FEN1 by coordination of the two metal ions needed for enzyme activity. Because the activity of Caf1/CNOT7enzyme also requires two metal ions, it was hypothesized that N-hydroxy urea compounds may also inhibit Caf1/CNOT7. Based on the presence of an N-hydroxy diketone structure, five compounds from the National Cancer Institute compound repository (Developmental Therapeutics Program, NCI, USA) were selected for further analysis (Dr G. Jadhav, School of Pharmacy, University of Nottingham). Then, IC_{50} values of the five compounds were determined using the fluorescence-based assay (Figure 4.5). Compound 193557 and 85703 have IC_{50} values >250 μM. Interestingly, replacement of the methyl group of compound 85703 by a benzyl group, increased the inhibitory activity around 10-fold (compound 86353). Based on the results, it was decided to synthesize a series of 1-hydroxy-3,7-*N*-substituted-purine-2,6-dione (Figure 4.5) analogues to find more potent and selective inhibitors of Caf1/CNOT7 enzyme (Dr G. Jadhav & Prof P.M. Fischer, School of Pharmacy, University of Nottingham).

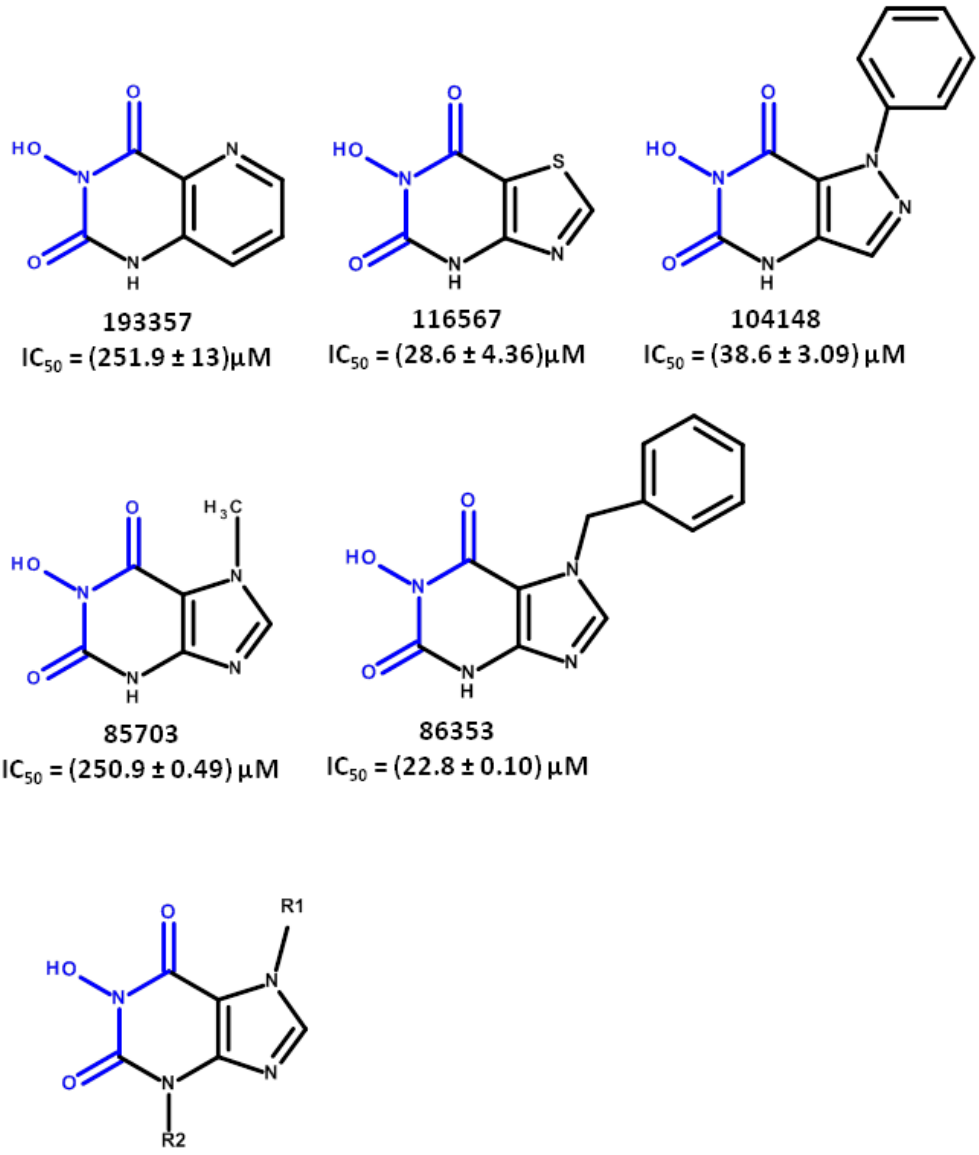

Figure 4.5 Structure and IC_{50} values of selected compounds from the National Cancer Institute compound repository. Highlighted is the N-hydroxy urea substructure for the screening of compounds from National Cancer Institute (Bethesda, USA).

4.3.1 Analysis and preliminary SAR of 1-hydroxy purines

A series of 1-hydroxy-3,7-*N*-substituted-purine-2,6-dione analogues were synthesised and made available for profiling (Dr. G. Jadhav & Prof. P.M. Fisher, School of Pharmacy, University of Nottingham). In total, 13 compounds were characterized (Table 4.2). First, IC_{50} values of the synthesised compounds were determined using the fluorescence-based assay. Serial dilutions of compound were pre-incubated with Caf1/CNOT7 for 15 minutes at room temperature. After addition of RNA substrate, the reaction mixtures were incubated for 60 minutes at 30°C, the reactions were stopped by the addition of a solution containing SDS and DNA probe. Data analysis was carried out using Microsoft Excel 2007 and GraphPad Prism 6.0.

Compound GPJMRC007 (R1= benzyl) proved to be have an IC_{50} of 6.5 μM (Figure 4.6A). The inhibitory activity of GPJMRC007 was thus around 4-fold more potent than compound 86353. The addition of methyl benzyl (compound GPJMRC066) resulted in increased potency, approximately 10-fold compared to compound 86353(IC_{50} = 2.4 μM; Figure 4.6B). Addition of methyl benzyl at R1 and methyl at R2, compound GPJMRC070, resulting a compound with higher potency, around 6-fold compared to compound 86353 (IC_{50} = 4.4 μM, Figure 4.6C). Furthermore, addition of methyl benzyl at R1 and propyl benzyl at R2, compound GPJMRC071, resulted in increased potency, around 20-fold (Figure 4.6D). This compound, GPJMRC071 displayed IC_{50} value of 1.2 μM.

Substitution of R1 using meta-methyl pyridine (GPJMRC033), resulted in increased potency, around 4-fold compared to compound 86353 (Figure 4.7A). Potency of this analogue was the same with GPJMRC007, IC_{50} value of 6.5 μM. However, substitution of R1 using para-methyl pyridine, GPJMRC042, resulted in a compound with un-changed potency (IC_{50} = 23.2 μM; Figure 4.7B). Substitution of ortho-methyl pyridine at R1, GPJMRC044, increased potency, approximately 2-fold (IC_{50} = 10.8 μM; Figure 4.7C). Furthermore, substitution at R1 using a longer chain, para-ethyl pyridine,

GPJMRC067, resulted in increased potency around 20-fold (IC_{50} = 1.5 μM; Figure 4.7D).

Substitution of cyclohexane at R1 (GPJMRC032), resulting in a compound with un-changed potency, IC_{50} value of 28 μM (Figure 4.8A and Table 4.1). Moreover, addition of longer chain at R1 using propyl benzyl, compound GPJMRC043, resulted in slightly increase potency (2-fold; IC_{50} = 13.2 μM;) (Figure 4.8B).

Addition of R1 using ethyl phenyl ether (GPJMRC055) or ortho-ethyl thiophene (GPJMRC054) resulting compounds which have higher potency than compound 86353 with IC_{50} values of 7.8 μM and 6.5 μM, respectively (Figure 4.9A and Figure 4.9C). However, substitution of propoxybutane at R1, GPJMRC047, resulted in a compound with un-changed potency (IC_{50} = 20.6 μM; Figure 4.9B).

The potency of the series of analogues is summarised in Table 4.2.

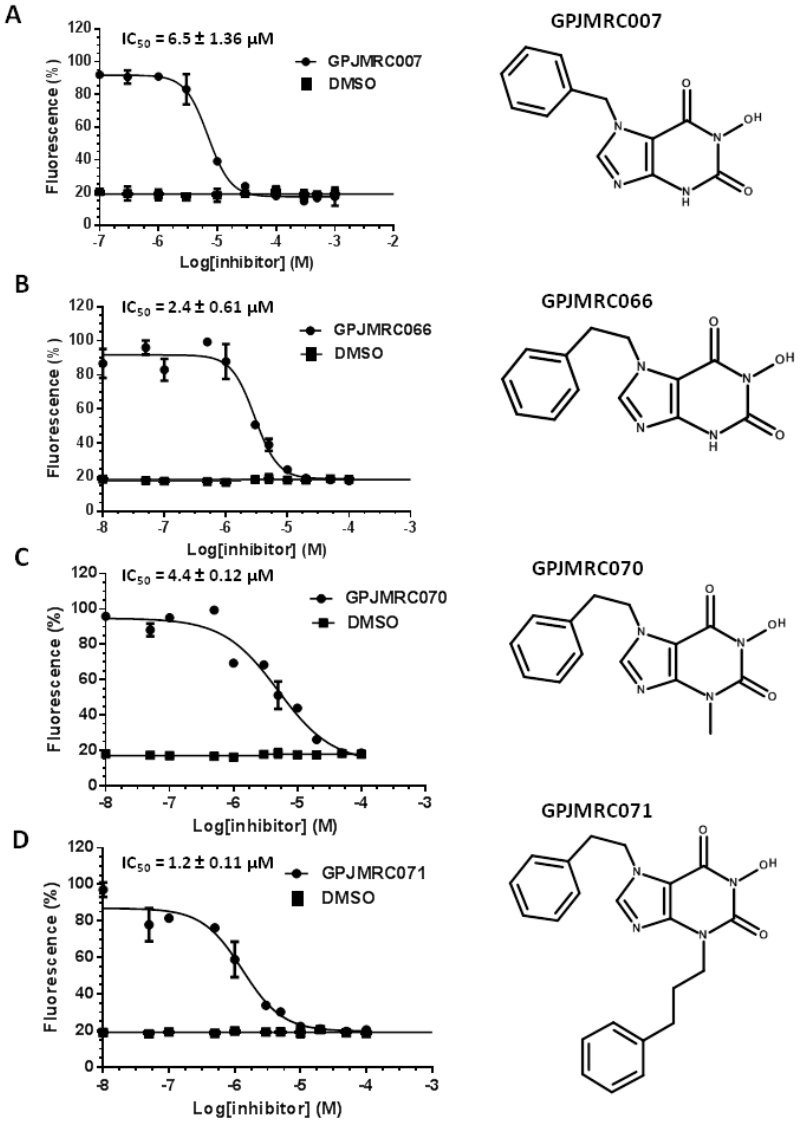

Figure 4.6 Determination of IC_{50} values of (A) GPJMRC007, (B) GPJMRC066, (C) GPJMRC070, and (D) GPJMRC071.

Compounds were pre-incubated for 15 min at room temperature with Caf1/CNOT7 followed by addition of RNA substrate. The reaction mixture was incubated for 60 min at 30°C. DNA probe mixture containing SDS was then added to stop the reaction. Fluorescence was measure using a BioTek Synergy HT plate reader. Data analysis and curve-fitting were carried out using Microsoft Excel 2007 and Graphpad Prism 6.0. Error bars represent standard deviations (n = 3), multiple wells done on the same day.

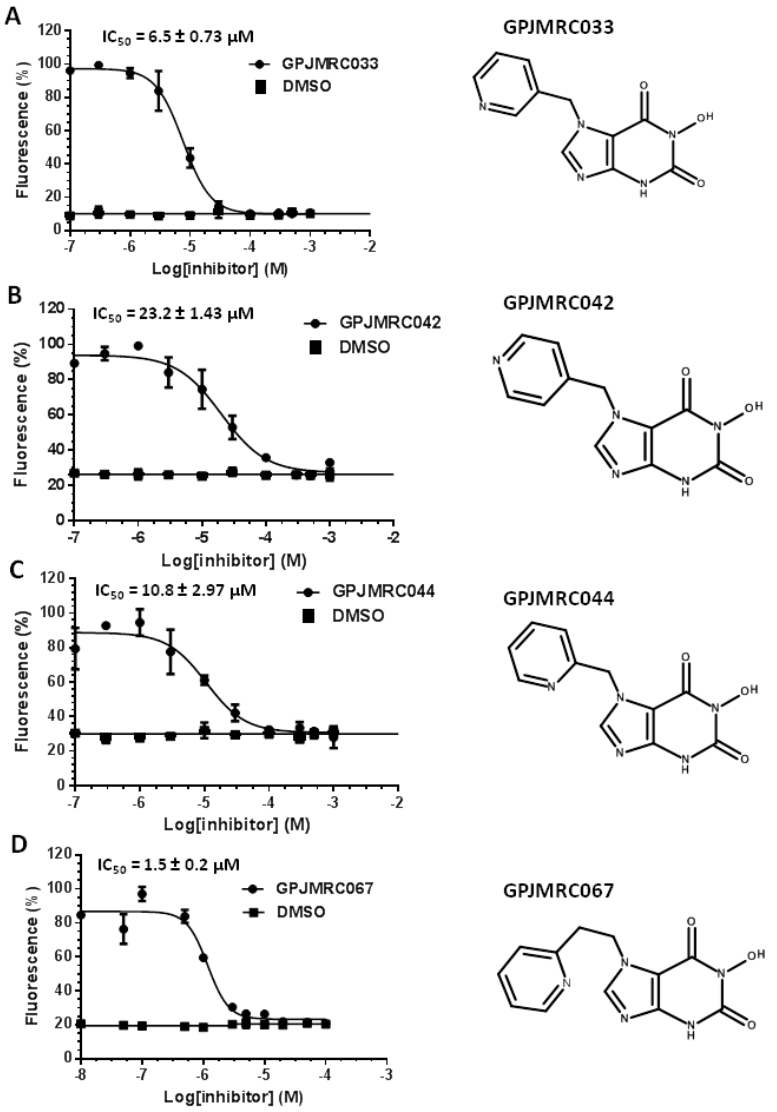

Figure 4.7 Determination of IC_{50} values of (A) GPJMRC033, (B) GPJMRC042, (C) GPJMRC044 and (D) GPJMRC067.

Compounds were pre-incubated for 15 min at room temperature with Caf1/CNOT7 followed by addition of RNA substrate. The reaction mixture was incubated for 60 min at 30°C. DNA probe mixture containing SDS was then added to stop the reaction. Fluorescence was measure using a BioTek Synergy HT plate reader. Data analysis and curve-fitting were carried out using Microsoft Excel 2007 and Graphpad Prism 6.0. Error bars represent standard deviations (n = 3), multiple wells done on the same day.

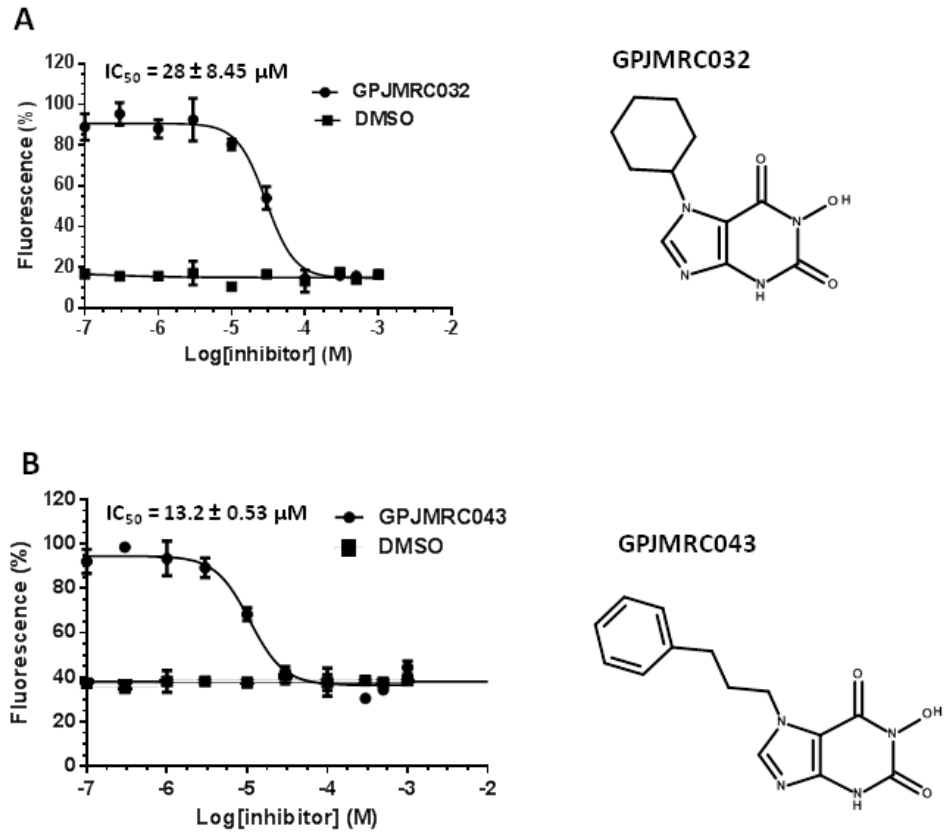

Figure 4.8 Determination of IC_{50} values of (A) GPJMRC032 and (B) GPJMRC043. Compounds were pre-incubated for 15 min at room temperature with Caf1/CNOT7 followed by addition of RNA substrate. The reaction mixture was incubated for 60 min at 30°C. DNA probe mixture containing SDS was then added to stop the reaction. Fluorescence was measure using a BioTek Synergy HT plate reader. Data analysis and curve-fitting were carried out using Microsoft Excel 2007 and Graphpad Prism 6.0. Error bars represent standard deviations (n = 3), multiple wells done on the same day.

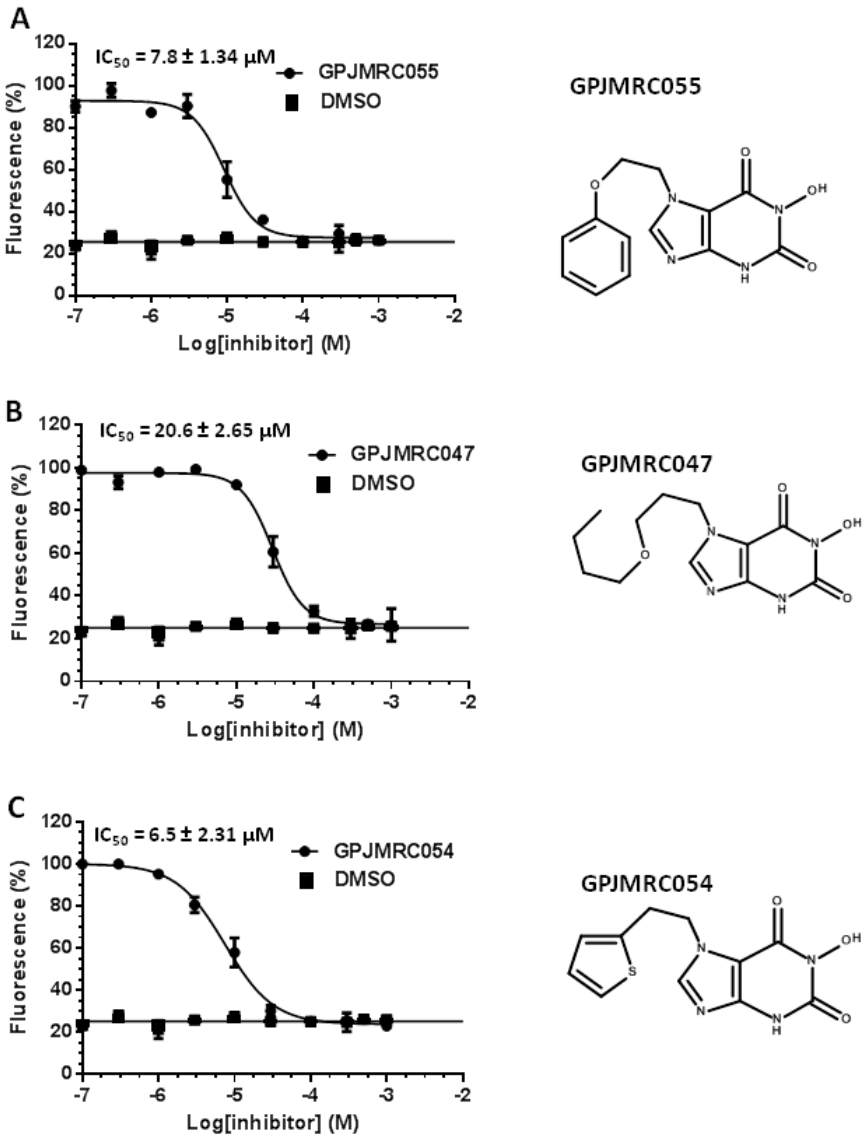

Figure 4.9 Determination of IC_{50} values of (A) GPJMRC055, (B) GPJMRC047 and (C) GPJMRC054. Compounds were pre-incubated for 15 min at room temperature with Caf1/CNOT7 followed by addition of RNA substrate. The reaction mixture was incubated for 60 min at 30°C. DNA probe mixture containing SDS was then added to stop the reaction. Fluorescence was measure using a BioTek Synergy HT plate reader. Data analysis and curve-fitting were carried out using Microsoft Excel 2007 and Graphpad Prism 6.0. Error bars represent standard deviations (n = 3), multiple wells done on the same day.

Compound	R1	R2	IC_{50} (μM)
GPJMRC007	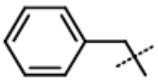	H	6.5 ± 1.36
GPJMRC032	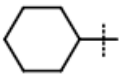	H	28 ± 8.45
GPJMRC033	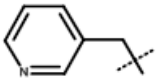	H	6.5 ± 0.73
GPJMRC042	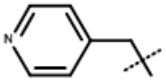	H	23.2 ± 1.43
GPJMRC043	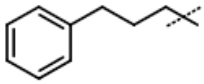	H	13.2 ± 0.53
GPJMRC044	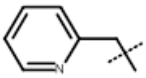	H	10.8 ± 2.97
GPJMRC047	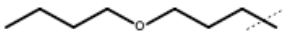	H	20.6 ± 2.65
GPJMRC054	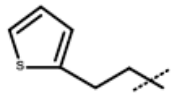	H	6.5 ± 2.31
GPJMRC055	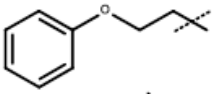	H	7.8 ± 1.34
GPJMRC066	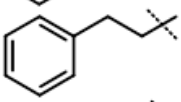	H	2.4 ± 0.61
GPJMRC067	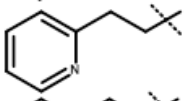	H	1.5 ± 0.2
GPJMRC070	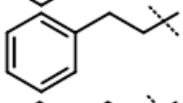	CH_3	4.4 ± 0.12
GPJMRC071	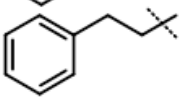	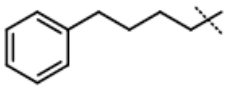	1.2 ± 0.11

Table 4.2 Structure and IC_{50} values of 1-hydroxy-3,7-*N*-substituted-3,7-dihydro-1*H*-purine-2,6-dione analogues

4.3.2 Selectivity of 1-hydroxy-3,7-*N*-substituted-purine-2,6-dione analogues

To assess whether the synthesized analogues were selective for Caf1/CNOT7 or whether they are more general deadenylase inhibitors, we tested the effect of the compounds on the activity of PARN and Ccr4b/CNOT6L. Enzymes and RNA substrate were incubated in the presence of synthesized compounds for 60 minutes at 30°C. The reaction mixture was then stopped by addition of a solution containing SDS and DNA probe. Fluorescence was measure using a BioTek Synergy HT plate reader. None of the compounds inhibited the Ccr4b/CNOT6L enzyme (Figure 4.10B). Compounds GPJMRC007, GPJMRC033, GPJMRC042 and GPJMRC044 were selective inhibitors. They only inhibited Caf1/CNOT7 and did not inhibit the activity of Ccr4b/CNOT6L or PARN (Figure 4.10). However, compounds GPJMRC047, GPJMRC054 and GPJMRC055 displayed less selectivity and partially inhibited the activity PARN enzyme. Compounds GPJMRC032, GPJMRC043, GPJMRC066, GPJMRC067, GPJMRC070 and GPJMRC071 inhibited both Caf1/CNOT7 and PARN (Figure 4.10).

To further investigate the selectivity of GPJMRC007, GPJMRC033, GPJMRC042 and GPJMRC044, we then determined the IC_{50} values of the compounds using the PARN enzyme. The results showed that the identified compounds exhibited >10-fold selectivity for Caf1/CNOT7 over PARN (Figure 4.11 and Table 4.3).

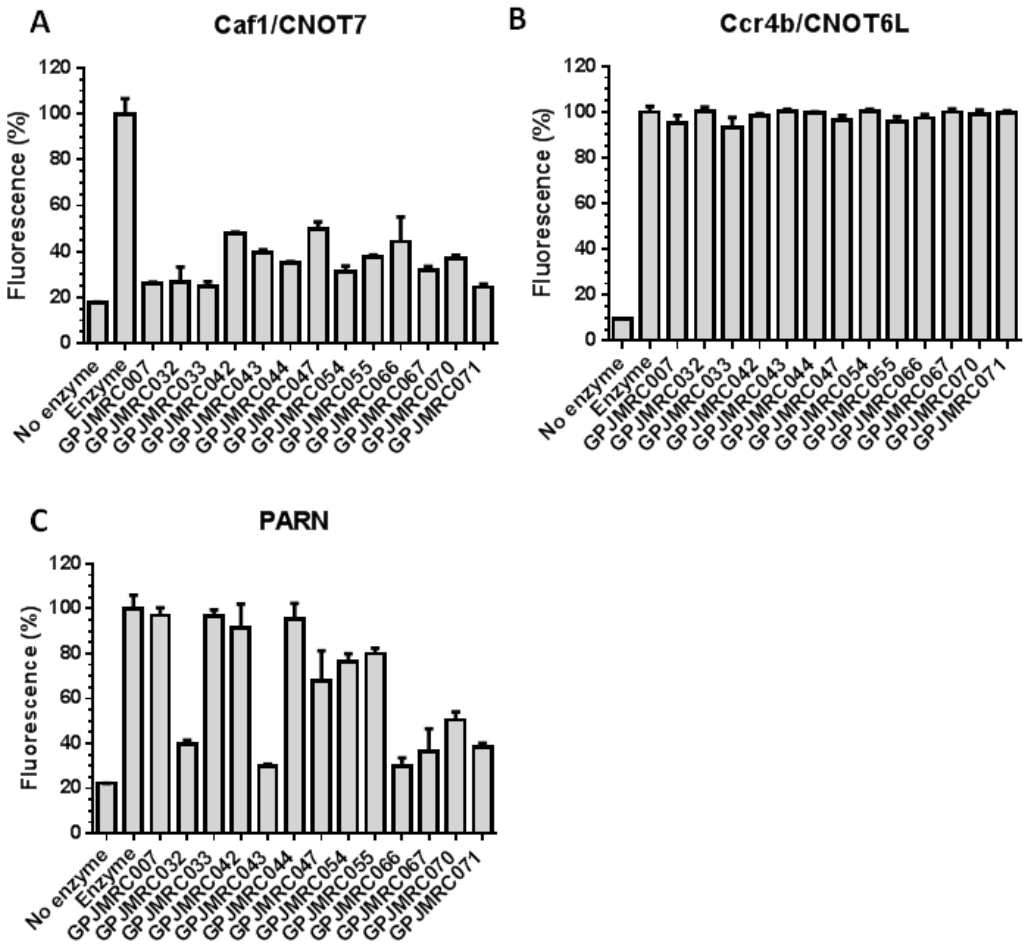

Figure 4.10 Selectivity of compounds GPJMRC007, GPJMRC033, GPJMRC042 and GPJMRC044. The activity of **(A)** Caf1/CNOT7, **(B)** Ccr4b/CNOT6L and **(C)** PARN was assessed in the presence of synthesized compounds. Enzymes were pre-incubated with the indicated compounds at room temperature for 15 minutes followed by incubation with RNA substrate (1.0 μM) for 60 min 30^0C. Fluorescence was measured after addition of DNA probe mixture containing SDS (0.5% final concentration). Error bars represent standard deviations (n = 3), multiple wells done on the same day.

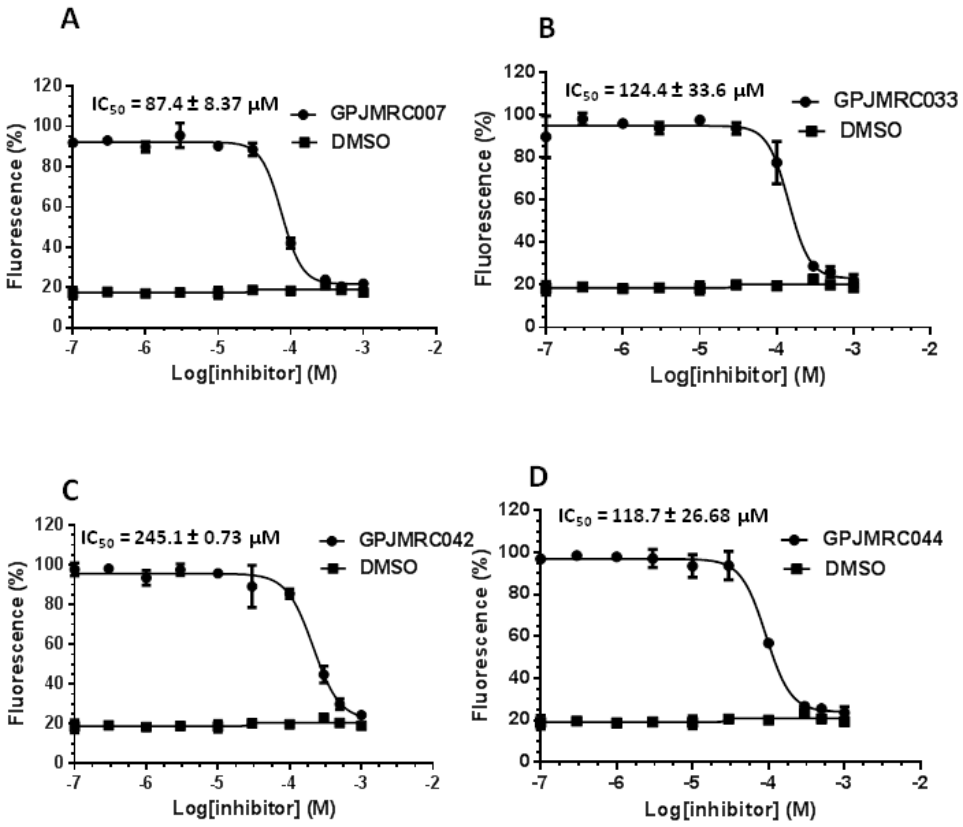

Figure 4.11 Determination of IC_{50} values of (A) GPJMRC007, (B) GPJMRC033, (C) GPJMRC042 and (D) GPJMRC044 into PARN enzyme. Compounds were pre-incubated for 15 min at room temperature with PARN followed by addition of RNA substrate. The reaction mixture was incubated for 60 min at 30°C. DNA probe mixture containing SDS was then added to stop the reaction. Fluorescence was measure using a BioTek Synergy HT plate reader. IC_{50} values were determined by data analysis and curve-fitting using Microsoft Excel 2007 and Graphpad Prism 6.0. Error bars represent standard deviations (n = 3), multiple wells done on the same day.

Compound	IC_{50} CNOT7 (μM)	IC_{50} PARN (μM)
GPJMRC007	6.5 ± 1.36	87.4 ± 8.37
GPJMRC033	6.5 ± 0.73	124.4 ± 33.66
GPJMRC042	23.2 ± 1.43	245.1 ± 0.73
GPJMRC044	10.8 ± 2.97	118.7 ± 26.86

Table 4.3 Selective inhibition of Caf1/CNOT7 by GPJMRC007, GPJMRC033, GPJMRC042 and GPJMRC044. The IC_{50} values are obtained from at least three replicate experiments. Data analysis and curve-fitting were carried out using Microsoft Excel 2007 and Graphpad Prism 6.0.

4.4 Discussion

In mice, Caf1/CNOT7 plays a role in bone metabolism, by suppressing bone mineralisation and BMP action (Washio-Oikawa et al., 2007). Caf1/CNOT7 could represent a potential molecule target for drug that enhances bone mass and density. In addition, small molecule inhibitors of enzymes can be used as powerful tools to obtain more insight into protein function.

Here, compounds that inhibit Caf1/CNOT7 were characterised. The compounds were identified using two approaches: (i) the screening of a compound library; and (ii) the synthesis of a series of 1-hydroxy-3,7-*N*-substituted-3,7-dihydro-1*H*-purine-2,6-dione analogues. We demonstrated the use of the fluorescence-based assay for characterization of Caf1/CNOT7 inhibitors. It was shown that selectivity of the inhibitor compounds can be obtained. Using the first approach we identified a potent compound, NCC-00037292, which has IC_{50} value 14.6 μM and five inhibitors with relatively low potency (IC_{50} around 100 μM). These compounds will be useful for the biochemical analysis of deadenylase enzymes. Based on preliminary molecular modelling analysis, it is likely that the identified compounds bind in the active site, thus blocking interaction with the RNA substrate. Further analysis indicated that compound NCC-00037292 partially inhibited other deadenylase enzymes, Ccr4b/CNOT6L and PARN. It would be interesting to find more potent and selective Caf1/CNOT7 inhibitors by generating analogues of NCC-00037292 to further explore a structure-activity relationship.

In addition, analogues of compound 85703 (National Cancer Institute, USA) were synthesized. Four compounds were identified which are selective inhibitors: GPJMRC007, GPJMRC033, GPJMRC042 and GPJMRC044. These compounds only inhibited Caf1/CNOT7, but did not inhibit Ccr4b/CNOT6L and PARN. GPJMRC007 and GPJMRC033 are the most potent compounds. It would be very interesting to test the selectivity of these compounds using another DEDD-type deadenylase enzyme for example, the PAN2 enzyme. We

also identified more potent compound which were not selective: GPJMRC066, GPJMRC067, GPJMRC070 and GPJMRC071.

These small molecule inhibitors will be useful as tool compounds to understand more detail the mechanism of deadenylase enzyme. For example, we already used the compounds to investigate deadenylation by the trimeric protein complex, His•BTG2-Caf1/CNOT7-GST•Ccr4b/CNOT6L (Chapter 6).

Recently, inhibitors of the PARN deadenylase enzyme were reported (Balatsos et al., 2009b, Balatsos et al., 2012). As in the case for Caf1/CNOT7 enzyme, PARN also contains a DEDD domain and requires Mg^{2+} for its enzymatic activity (Ren et al., 2004). Nucleoside analogues could inhibit PARN activity. These analogues act as competitive inhibitors of PARN. Importantly, increasing of Mg^{2+} could not return the deadenylase activity of PARN enzyme (Balatsos et al., 2009b). It will be interesting to assess whether these nucleoside analogues are selective inhibitors of PARN or whether they also inhibit other DEDD-type deadenylase enzyme, such as Caf1/CNOT7 and PAN2 or the EEP-type enzyme, Ccr4b/CNOT6L.

In conclusion, the utility of the fluorescence-based deadenylase assay for the characterisation of small molecule inhibitors of the Caf1/CNOT7 enzyme was demonstrated. The small molecule inhibitors will be highly useful as chemical tools for the study of post-transcriptional gene regulation.

Chapter 5

Expression and Purification of a Nuclease sub-complex of Human Ccr4-Not Containing Caf1/CNOT7 and Ccr4b/CNOT6L

Chapter 5. Expression and Purification of a Nuclease sub-complex of Human Ccr4-Not Containing Caf1/CNOT7 and Ccr4b/CNOT6L

5.1 Introduction

The conserved core of the Ccr4-Not complex consists of at least two modules: a catalytic module and the NOT module. The catalytic module contains two deadenylase subunits. One of these subunits is a member of the Endonuclease-Exonuclease-Phosphatase (EEP) family (Ccr4a/CNOT6 or Ccr4b/CNOT6L), while the second is an RNAseD DEDD type nuclease (either Caf1/CNOT7 or Pop2/CNOT8). The catalytic subunits are tethered to the non-catalytic components via interactions between the Caf1 subunit and the MIF4G (middle domain of initiation factor 4G) domain located in the N-terminal half of NOT1. The NOT module consists of the NOT2 and NOT3 heterodimer bound to the C-terminus of NOT1. Because the interaction of the two modules is mediated by NOT1, NOT1 acts as the scaffold protein of the complex (Tucker et al., 2001, Tucker et al., 2002, Lau et al., 2009b, Bartlam and Yamamoto, 2010, Collart and Panasenko, 2011, Petit et al., 2012).

Previous work presented the crystal structure of human Caf1-Not1 (Petit et al., 2012). In this structure, the NOT1 domain contains five helical hairpins that form a MIF4G fold. The interaction of NOT1 MIF4G with Caf1 leaves the catalytic site of Caf1 fully accessible to RNA substrates. For the crystallisation, the NOT1-Caf1 complex was obtained by incubating the purified Caf1 and NOT1 MIF4G domain, which were then purified by gel filtration (Petit et al., 2012).

Recent research also provided the crystal structure of the yeast Not1-Caf1-Ccr4 protein complex. The complex was reconstituted by mixing the purified MIF4G domain of Not1, Caf1 and Ccr4 followed by purification using size exclusion chromatography. The Not1-Caf1-Ccr4 protein complex is

established by the consecutive binary interactions between the Not1 MIF4G domain and the Caf1 nuclease, and between Caf1 and the leucine rich repeat (LRR) domain of Ccr4, respectively (Basquin et al., 2012).

Caf1/CNOT7 and Pop2/CNOT8 associate with a group of antiproliferative proteins, which constitute the TOB/BTG family. This family of six proteins is characterised by an N-terminal BTG domain, which is involved in protein-protein interactions with either Caf1/CNOT7 and Pop2/CNOT8. Previous research provided the crystal structure of the human Tob-Caf1/CNOT7 protein complex. The protein complex was obtain by co-expressing the N-terminal residues of Tob comprising the BTG domain and intact Caf1/CNOT7 in *E. coli* BL21(DE3). The crystal structure of Tob-Caf1/CNOT7 complex indicated that Box A and Box B in the BTG domain of Tob mediate the association with Caf1/CNOT7. The complex formation of Tob-Caf1/CNOT7 is important for the antiproliferative activity of Tob1, but it is not required for the deadenylase activity of Caf1/CNOT7 enzyme (Horiuchi et al., 2009, Ezzeddine et al., 2012, Doidge et al., 2012b).

In MCF7 cells, combined knockdown of Ccr4a/CNOT6 and Ccr4b/CNOT6L reduced cell proliferation and decreased the viability of the cells (Mittal et al., 2011). Using siRNA-mediated knockdown, it was also shown that the *CNOT7* and *CNOT8* genes encoding the Caf1 deadenylase subunit of the Ccr4-Not complex are also important for cell proliferation (Aslam et al., 2009). Comparison of genome-wide mRNA expression profiles of Caf1 (CNOT7/CNOT8) and Ccr4 (CNOT6/CNOT6L) knockdown cells suggest that the deadenylase subunits of Ccr4-Not have distinct roles in deadenylation and mRNA degradation (Mittal et al., 2011).

To further explore whether the Caf1 and Ccr4 subunits have unique or cooperative roles in deadenylation, the aim of this work was to develop a strategy to obtain a purified Ccr4b/CNOT6L-Caf1/CNOT7 deadenylase complex for the characterisation of the Ccr4-Not deadenylase module by using a biochemical approach.

Five strategies were used to express a Ccr4b/CNOT6L-Caf1/CNOT7 protein complex (Figure 5.1). First, we aimed to reconstitute the complex with purified Caf1/CNOT7 and Ccr4b/CNOT6L. However, expression of (GST-tagged) Ccr4b/CNOT6L containing the LRR domain indicated that the protein was not soluble in bacterial lysates. Secondly, we tried co-expression of (His-tagged) CNOT6L and CNOT7 in *E.coli* BL21(DE3). This strategy was not successful because we were unable to produce pure protein possibly due to a chaperone contamination. A third strategy involved co-expression of (GST-tagged) CNOT6L and CNOT7 in *E. coli.* Using this method, a putative chaperone contamination was revealed. Although it was possible to remove the majority of the contaminants by washing with buffers containing ATP and urea, the purity obtained was unsatisfactory. Thus, a forth strategy was performed by co-expression of (un-tagged) CNOT6L-CNOT7 and His-BTG2 in *E. coli*. In combination with size exclusion chromatography, this strategy produced a trimeric complex containing BTG2, Caf1/CNOT7 and Ccr4b/CNOT6L as well as a dimeric complex containing BTG2 and Caf1/CNOT7. The last strategy was based on co-expression of GST-Ccr4b/CNOT6L, Caf1/CNOT7 and His-BTG2. By using consecutive immobilised metal and glutathione affinity chromatography, a trimeric complex with the expected stoichiometric ratio was obtained.

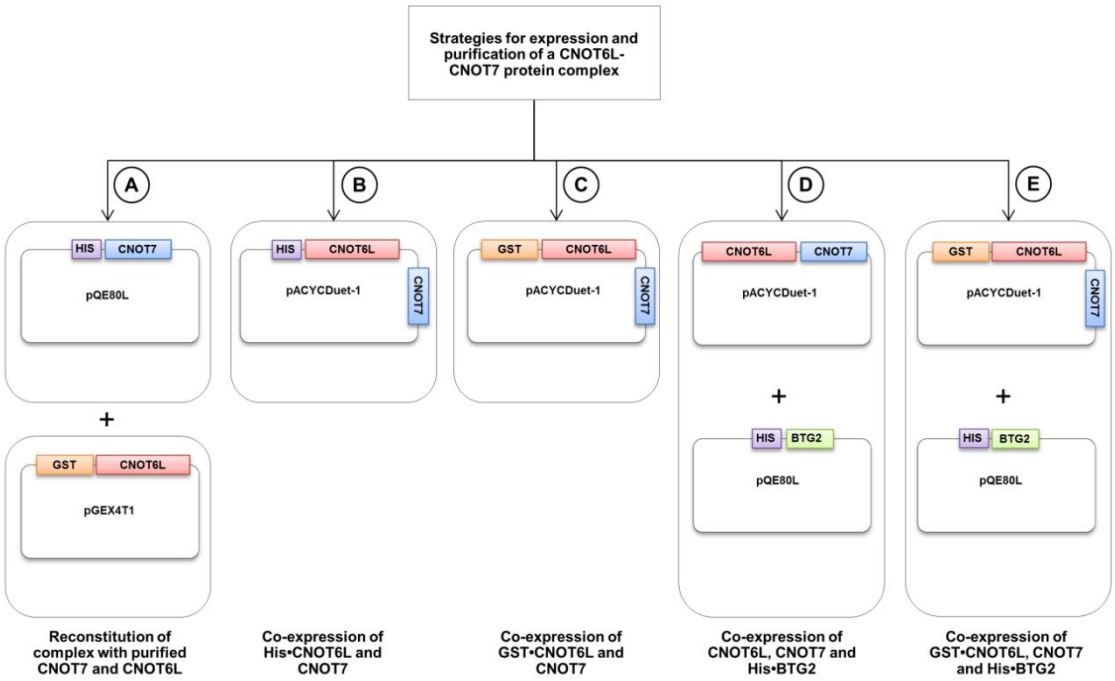

Figure 5.1 Strategies for the purification of a Caf1/CNOT7•Ccr4b/CNOT6L protein complex. (A) Reconstitution of a Caf1•Ccr4 complex with purified His-Caf1/CNOT7 and GST-Ccr4b/CNOT6L. **(B)** Co-expression and purification of His-Ccr4b/CNOT6L•Caf1/CNOT7. **(C)** Co-expression and purification of GST-Ccr4b/CNOT6L•Caf1/CNOT7. **(D)** Co-expression and purification of His•BTG2-Ccr4b/CNOT6L•Caf1/CNOT7. **(E)** Co-expression and purification of His•BTG2-GST-Ccr4b/CNOT6L•Caf1/CNOT7.

5.2 Reconstitution of a nuclease complex using purified Caf1/CNOT7 and Ccr4b/CNOT6L

Purification of Caf1/CNOT7 was initiated by transferring plasmid pQE80L-CNOT7 into BL21(DE3). A single colony of *E. coli* BL21 containing plasmid pQE80L-CNOT7 was used to inoculate a starter culture for protein expression. Protein purification was carried out using immobilised metal affinity chromatography (IMAC). We successfully purified the Caf1/CNOT7 protein which is >90% homogeneous (Figure 3.1, Chapter 3).

Then, we tried to express full length Ccr4a/CNOT6 and Ccr4b/CNOT6L. Plasmid pGEX4T1-CNOT6 or pGEX4T1-CNOT6L was transformed in *E. coli* BL21(DE3), and a single colony was used to inoculate a starter culture. The pre-culture was then grown in 1 L of LB containing 100 µg/ml ampicillin at 37°C until the OD(600 nm) was between 0.6-0.8. To induce expression of the protein, IPTG (final concentration of 0.2 mM) was added to the culture for 3 hours at 30°C. Cells were harvested by centrifugation and the cell pellet was resuspended in extraction buffer. Cells were frozen and kept at -80°C until further use. After thawing the bacterial suspension, the cells were lysed on ice using a sonicator. The crude lysate (total lysate) was centrifuged to remove insoluble material. The supernatant was collected as soluble lysate. SDS-PAGE analysis of the total lysate and soluble lysate indicated that full length (GST-tagged) Ccr4a/CNOT6 and Ccr4b/CNOT6L were insoluble in bacterial lysates (Figure 5.2). Based on the result, no further attempts were made to express full length Ccr4a/CNOT6 or Ccr4b/CNOT6L. Instead, co-expression of Ccr4b/CNOT6L and Caf1/CNOT7 in *E. coli* was attempted.

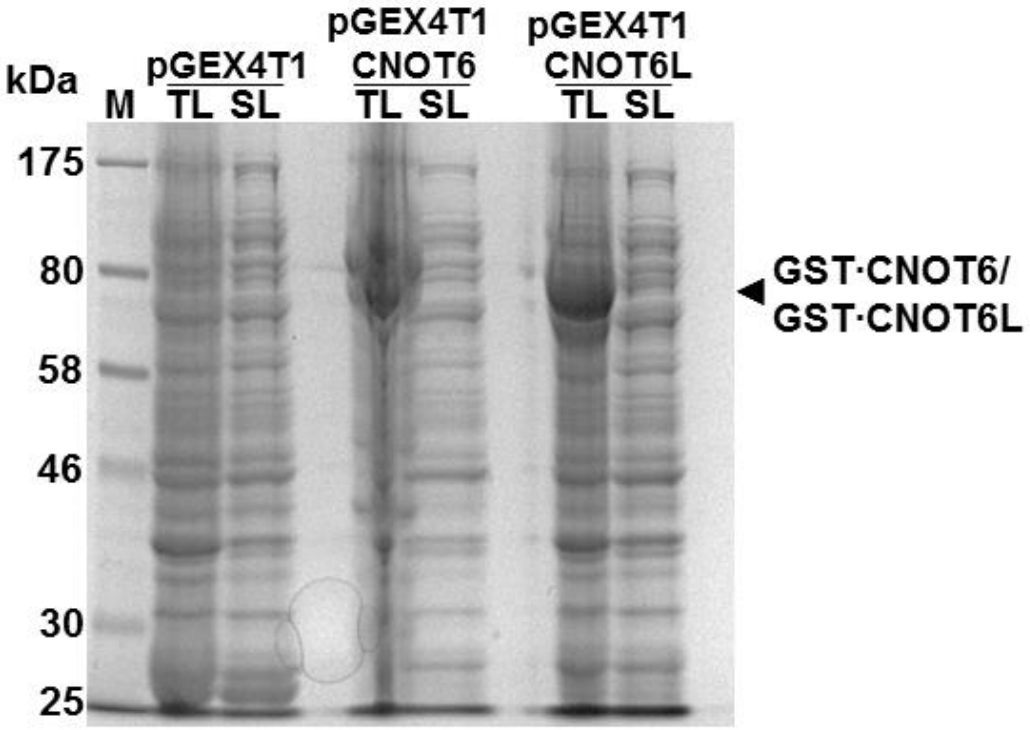

Figure 5.2 GST-tagged Ccr4a/CNOT6 and Ccr4b/CNOT6L are not soluble in bacterial lysates. Lysates were obtained from 1 litre of culture of BL21(DE3) after expression was induced for 3 h with 0.2 mM IPTG. Lysates (10 μl) were analysed by 10% SDS-PAGE followed by staining with Coomassie Briliant Blue. Indicated are the marker (M), total lysate (TL) and soluble lysate (SL).

5.3 Co-expression and purification of His-tagged Ccr4b/CNOT6L and Caf1/CNOT7

5.3.1 Generation of bacterial expression vectors

Because the reconstitution of a nuclease complex using purified Caf1/CNOT7 and Ccr4b/CNOT6L was not successful, we constructed plasmids for co-expression. Vector pACYCDuet-1, which contains two multiple cloning sites (MCS) and is suitable for co-expression, was used for dual expression of (His-tagged) Ccr4b/CNOT6L and Caf1/CNOT7 in *E. coli* BL21 (DE3). The CNOT7 and CNOT6L cDNAs used were codon-optimised for expression in *E. coli* (Genscript). Initially, two plasmids were generated, plasmid pACYCDuet-1 M01 with CNOT7 inserted into MCS 1 and CNOT6L in MCS 2 and plasmids pACYCDuet-1 M02 with CNOT6L in MCS 1 and CNOT7 in MCS 2 (Figure 5.3). Firstly, the CNOT7 and CNOT6L cDNAs were PCR amplified and then digested using restriction enzymes BamHI (5') and SalI (3'). Next, the restriction digested CNOT7 cDNA (858 bp) and CNOT6L cDNA (1668 bp) were subcloned into MCS 2 of pACYCDuet-1 (4.0 kb), which was digested using the BglII and XhoI restriction sites. The presence of the CNOT7 and CNOT6L cDNAs in MCS 2 of pACYCDuet-1 was confirmed by digesting the plasmids using PstI and EcoRI, respectively. Digestion of pACYCDuet1/CNOT7 using PstI resulted in two fragments (4.0 kb and 800 bp), while digestion of pACYCDuet-1/CNOT6L with EcoRI also resulted in two fragments (4.5kb and 1.1 kb). Subsequently, the CNOT7 and CNOT6L cDNAs were subcloned into the BamHI and SalI restriction sites of MCS 1. To confirm the correct ligation of the cDNA fragments in MCS1, pACYCDuet-1 M01 and pACYCDuet-1 M02 were digested using BamHI and SalI. Digestion of both plasmids using BamHI and SalI enzymes resulted in two fragments as expected. The plasmids were verified by DNA sequencing.

Plasmids pACYCDuet-1 expressing catalytically inactive variants of Ccr4b/CNOT6L and Caf1/CNOT7 were also constructed. The catalytically

inactive version of Caf1/CNOT7, D40A, and the catalytically inactive version of Ccr4b/CNOT6L, E240A, was used. The construction of the plasmid containing a single mutation, pACYCDuet-1 His•CNOT6L/CNOT7 D40A (pACYCDuet-1 M03) was carried out by sub-cloning a CNOT7 D40A cDNA into MCS 2 followed by subcloning a CNOT6L cDNA into MCS 1, as described above. To construct plasmid pACYCDuet-1 His·CNOT6L E240A/CNOT7 (pACYCDuet-1 M04), which contains a single inactivating mutation in the CNOT6L cDNA, CNOT6L was removed from MCS 1 of pACYCDuet-1 M02 plasmid using the BamHI and SalI restriction enzymes. A cDNA encoding the inactive version of Ccr4b/CNOT6L (E240A) was then inserted into MCS 1. Furthermore, the double mutant plasmid pACYCDuet-1 His•CNOT6L E240A/CNOT7 D40A (pACYCDuet-1 M05) was constructed by removing the CNOT6L cDNA from MCS 1 of pACYCDuet-1 M03 using BamHI and SalI and replaced with the mutant cDNA (Table 5.1). All plasmids were verified by DNA sequencing.

Plasmid	Caf1/CNOT7	Ccr4b/CNOT6L
pACYCDuet-1 M02	WT	WT
pACYCDuet-1 M03	D40A	WT
pACYCDuet-1 M04	WT	E240A
pACYCDuet-1 M05	D40A	E240A

Table 5.1 Derivatives of plasmid pACYCDuet-1 His·CNOT6L/CNOT7.

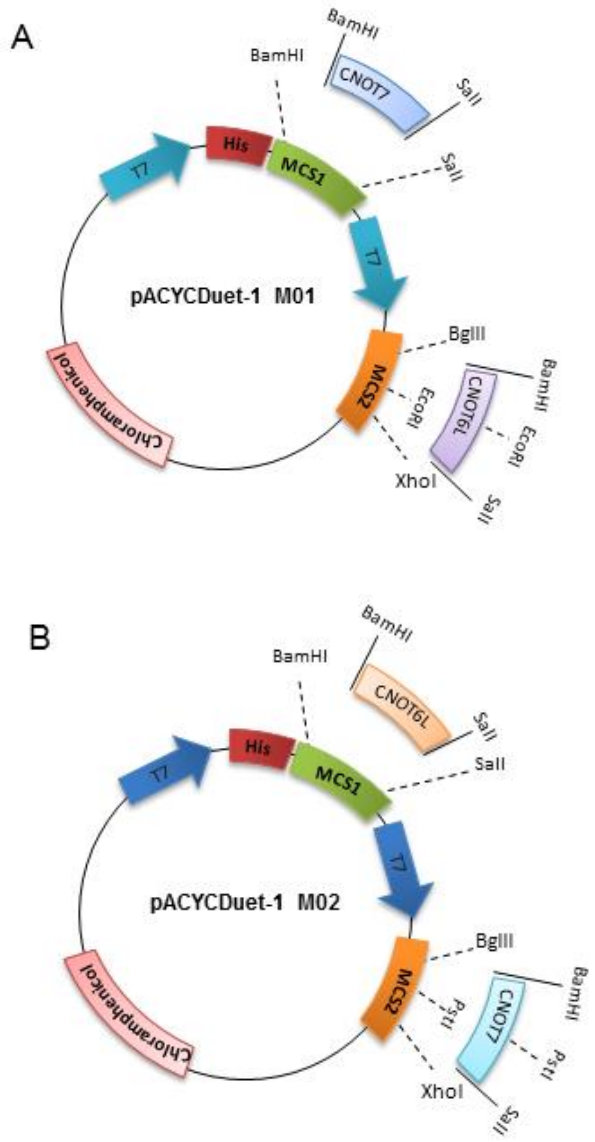

Figure 5.3 Generation of bacterial expression vectors containing the CNOT7 and CNOT6L cDNAs. The pACYCDuet-1 vector was used to generate plasmids pACYCDuet-1 M01 and pACYCDuet-1 M02. (A) Generation of plasmid pACYCDuet-1 M01. CNOT6L (BamHI-SalI) was subcloned into multiple cloning site 2 (MCS 2) of pACYCDuet-1 (BglII-XhoI). Next, CNOT7 (BamHI-SalI) was subcloned into MCS 1(BamHI-SalI). (B) Generation of pACYCDuet-1 M02. CNOT7 (BamHI-SalI) was subcloned into MCS 2 of pACYCDuet-1 (BglII-XhoI). Then, CNOT6L was inserted into MCS 1(BamHI-SalI).

5.3.2 Protein expression and purification

Protein expression was initiated by transferring plasmid pACYCDuet-1 M01 or pACYCDuet-1 M02 into *E. coli* BL21(DE3) cells. For each plasmid, a single colony of *E. coli* BL21(DE3) was used to inoculate a starter culture for protein expression. The pre-culture was then grown in 1 L of LB containing 34 μg/ml chloramphenicol at 37°C until the OD(600 nm) was between 0.6-0.8. Then, IPTG (final concentration of 0.2 mM) was added to the culture to induce protein expression for 3 hours at 30°C. Analysis of total lysates obtained before and after 3 hours of addition of IPTG showed the synthesis of proteins with expected molecular weight (Figure 5.4A).

Protein purification was carried out using immobilised metal affinity chromatography (IMAC). The soluble lysate was applied to a His Trap column using a syringe with a flow rate of approximately 2-3 drops per second. Then, the column was washed using 10 ml of wash buffer containing 20 mM imidazole. Protein was eluted with 5 ml of elution buffer containing 250 mM imidazole and collected in 1 ml fractions. The purity of the protein complex was verified using SDS-PAGE and staining with Coomassie Brilliant Blue (Figure 5.4B). The result of SDS-PAGE analysis indicates that only the fractions obtained from cells containing plasmid pACYCDuet-1 M02 (pACYCDuet-1 His•CNOT6L/CNOT7) showed bands corresponding to both Ccr4b/CNOT6L and Caf1/CNOT7 on the gel. The Ccr4b/CNOT6L protein was observed as a single band at ~60 kDa and the Caf1/CNOT7 protein appeared as a single band at ~30 kDa. However, there were still a lot of impurities present in the fractions containing the His•Ccr4b/CNOT6L-Caf1/CNOT7 protein complex.

On the other hand, the fractions obtained from cells containing plasmid pACYCDuet-1 M01 (pACYCDuet-1 His•CNOT7/CNOT6L), only a single band corresponding to Caf1/CNOT7 (~30 kDa) was detected on the gel, and no Ccr4b/CNOT6L band was visible (Figure 5.4B). Therefore, the pACYCDuet-1 M02 plasmid was used for subsequent protein expression.

To improve the purity of the protein complex, we tried to optimize the conditions of the purification process. Firstly, we modified the wash buffer by increasing the volume of wash buffer and also increasing the imidazole concentration. Increasing the volume of wash buffer (20 ml) could increase the purity of the elution fractions, however, increasing the imidazole in the wash buffer (40 mM imidazole) significantly reduced the yield of protein in the elution fractions (Figure 5.5A).

In addition, it was tried to re-purify the protein complex using a second round of IMAC. Firstly, elution buffer containing 250 mM imidazole was removed from the protein fractions using a PD10 desalting column. Then, the protein was applied to a His Trap column using a syringe at flow rate of approximately 2-3 drops per second. After washing using 10 ml wash buffer containing 20 mM imidazole, the protein was eluted with 5 ml elution buffer and 1 ml fractions were collected. SDS-PAGE analysis showed that the fractions were more pure after the second round of IMAC, but there was still a significant level of contaminating proteins present (Figure 5.5B).

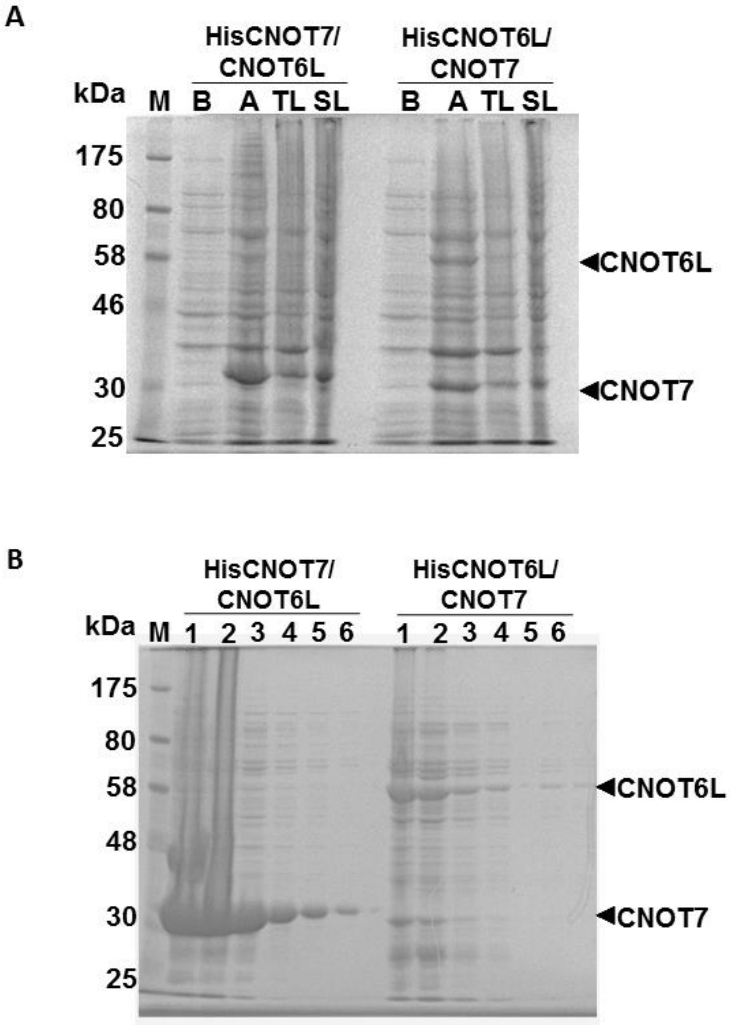

Figure 5.4 Expression and purification of His•Ccr4b/CNOT6L-Caf1/CNOT7 and His•Caf1/CNOT7-Ccr4b/CNOT6L protein complexes. **(A)** Total lysates of cells expressing His-Ccr4b/CNOT6L, Caf1/CNOT7 and His-Caf1/CNOT7, Ccr4b/CNOT6L, respectively. Protein expression was induced with 0.2 mM IPTG for 3 hours at 30°C. Samples were analysed by 10% SDS-PAGE. Proteins were visualised by staining with Coomassie Briliant Blue. Indicated are lysates before adding IPTG (B), lysates after 3 hours induction with IPTG (A), total lysate (TL) and soluble lysate (SL). **(B)** Purification of dimeric His•Caf1/CNOT7-Ccr4b/CNOT6L and His•Ccr4b/CNOT6L-Caf1/CNOT7 protein complexes by immobilised metal affinity chromatography**.** Indicated are the marker (M) and protein elution fractions (1-6).

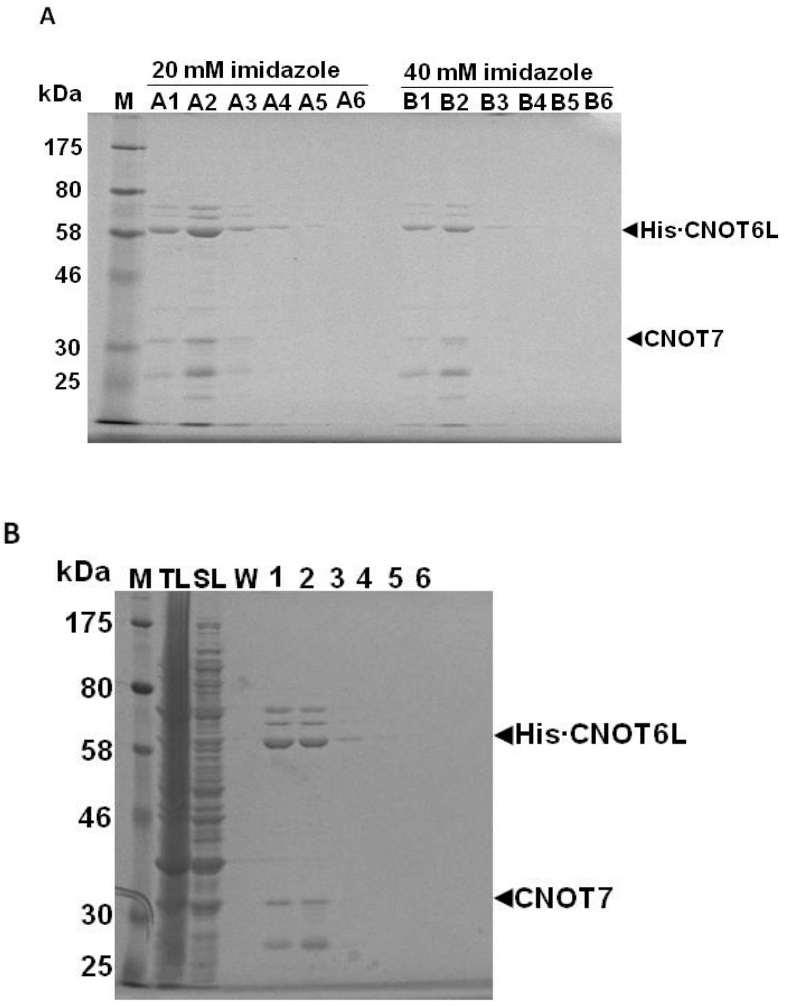

Figure 5.5 Optimization of the purification of the His•Ccr4b/CNOT6L-Caf1/CNOT7 protein complex. (A) Increasing amount of imidazole in the wash buffer reduced the concentration of the protein of interest. One litre of overnight culture of BL21 induced with 0.2 mM IPTG was used for the purification of His•Ccr4b/CNOT6L-Caf1/CNOT7. After washing with buffer containing 20 mM or 40 mM imidazole, protein was eluted using buffer containing 250 mM imidazole (A1-A6; B1-B6). **(B)** Re-purification of His•Ccr4b/CNOT6L-Caf1/CNOT7 protein complex. After desalting using a PD 10 column, elution fractions 1 and 2 were re-purified using a second round of immobilised metal affinity chromatography. Indicated are total lysate (TL), soluble lysate (SL), and protein elution fractions (1-6).

Finally, a different extraction method was carried out with the aim to increase the purity of the target protein. Previous research showed that removing the periplasmic material before lysis increased the purity of the protein of interest (Magnusdottir et al., 2009). IMAC is sensitive to the presence of metal chelators which are present in the periplasmic space of *E. coli*. To remove the periplasmic material, *E. coli* cells were subjected to an osmotic shock, using buffer containing 20% sucrose, before cell lysis. Figure 5.7A showed that this method increased the purity of the protein of interest. Interestingly, measurements using Bradford assay indicated that the concentration of the protein of interest increased almost doubled (Table 5.2).
To confirm that the bands were indeed Ccr4b/CNOT6L and Caf1/CNOT7 and to detect possible degradation products (protein with N-terminal and C-terminal deletions), western blot analysis was carried out. Protein samples were separated by 10% SDS-PAGE and western blot analysis was conducted using Anti-CNOT6L and Anti-CNOT7 primary antibodies (Figure 5.6B).
However, because the purification of His•Ccr4b/CNOT6L-Caf1/CNOT7 using IMAC did not result in pure protein, we tried to express and purify the GST• Ccr4b/CNOT6L-Caf1/CNOT7 protein complex by glutathione affinity chromatography.

Method of purification	**Protein concentration (mg/ml)**
Lysis without removal of periplasmic material	Fraction 1 = 0.23 Fraction 2 = 0.29
Removal of periplasmic material before lysis using sucrose buffer	Fraction 1 = 0.47 Fraction 2 = 0.49

Table 5.2 Removal of the periplasmic material from the bacterial cells increased the concentration of the protein of interest.

One litre of overnight culture of BL21 induced with 0.2 mM IPTG at 30°C for 3 hours was subjected to affinity chromatography. The concentration of protein was measured using the Bio-Rad protein assay reagent.

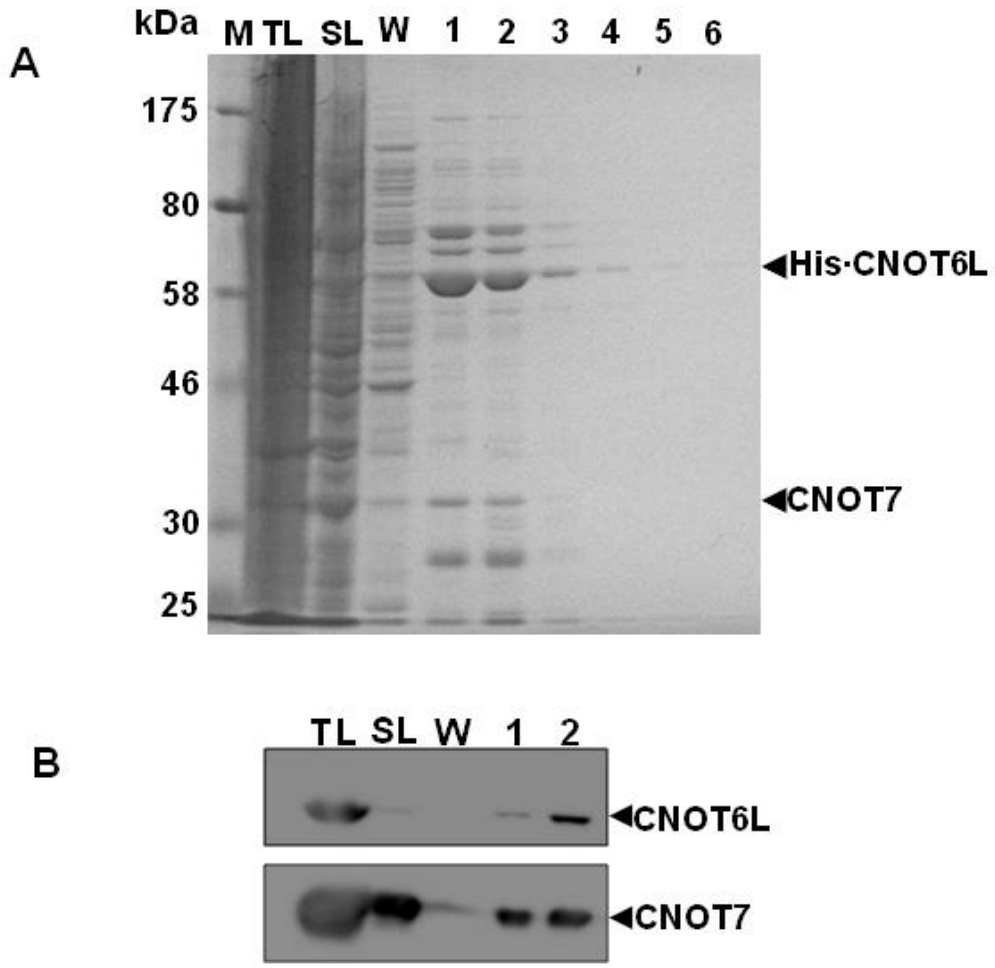

Figure 5.6 Purification of His•Ccr4b/CNOT6L-Caf1/CNOT7 following the removing of periplasmic material. (A) SDS-PAGE analysis of purified His•Ccr4b/CNOT6L-Caf1/CNOT7 protein complex. Cells were subjected to an osmotic shock before lysis to remove the periplasmic material. Proteins were analysed by 10% SDS-PAGE and visualised by staining with Coomassie Briliant Blue. **(B)** Western blot analysis of Ccr4b/CNOT6L-Caf1/CNOT7. Protein samples were separated by 10% SDS-PAGE. Western blot analysis was conducted using Anti-CNOT6L and Anti-CNOT7 primary antibodies. A molecular weight marker was used to confirm the size of the protein. Indicated are total lysate (TL), soluble lysate (SL), wash (W), protein elution fractions (1-6).

5.4 Expression and purification using GST-tagged Ccr4b/CNOT6L and Caf1/CNOT7

5.4.1 Cloning strategy

To construct plasmid pACYCDuet-1 GST•CNOT6L/CNOT7 (pACYCDuet-1 M06) (Figure 5.7), we used pACYCDuet-1 M02 as the initial plasmid. Construction of the plasmid was carried out by replacing the His•CNOT6L fragment from MCS 1 of pACYCDuet-1 M02 with GST-CNOT6L. Removal of His•CNOT6L was conducted by digesting pACYCDuet-1 M02 using NcoI and NotI. Then, a CNOT6L cDNA was PCR amplified to include an NcoI restriction site and the GST-tag. To amplify the GST•CNOT6L cDNA, plasmid pGEX4T1-CNOT6L was used as template. The PCR product was digested using the restriction enzymes NcoI and NotI and subcloned into the NcoI and NotI restriction sites of pACYCDuet-1 M02. To confirm the correct ligation of the cDNA fragment in MCS 1, plasmid pACYCDuet-1M06 was digested using NcoI and NotI enzymes. Finally, PCRs were conducted to amplify MCS 1 of plasmid pACYCDuet-1 M06 for sequencing. To amplify MCS 1, ACYCDuetUP1 and DuetDOWN primers were used.

Derivatives of plasmid pACYCDuet-1 M06 containing cDNAs encoding inactive Ccr4b/CNOT6L and Caf1/CNOT7 were also constructed. Construction of plasmid pACYCDuet-1 GST•CNOT6L/CNOT7 D40A (pACYCDuet-1 M07) was carried out as described above by using plasmid pACYCDuet-1 M03 containing the D40A mutation in the CNOT7 cDNA as a starting point. Plasmids pACYCDuet-1 GST•CNOT6L E240A/CNOT7 (pACYCDuet-1 M08) containing the single E240A mutation in CNOT6L, and pACYCDuet-1 GST•CNOT6L E240A/CNOT7 D40A (pACYCDuet-1 M09) containing cDNAs encoding inactive nucleases were constructed as described above using pGEX4T1-CNOT6 E240A as a template and inserting the GST•CNOT6L E240A cDNA (NcoI-NotI) in MCS 1 of plasmids pACYCDuet-

1M02 and pACYCDuet-1M03, respectively. All plasmids were verified by DNA sequencing (Table 5.3).

Plasmid	Caf1/CNOT7	Ccr4b/CNOT6L
pACYCDuet-1 M06	WT	WT
pACYCDuet-1 M07	D40A	WT
pACYCDuet-1 M08	WT	E240A
pACYCDuet-1 M09	D40A	E240A

Table 5.3 Derivatives of plasmid pACYCDuet-1 GST·CNOT6L/CNOT7.

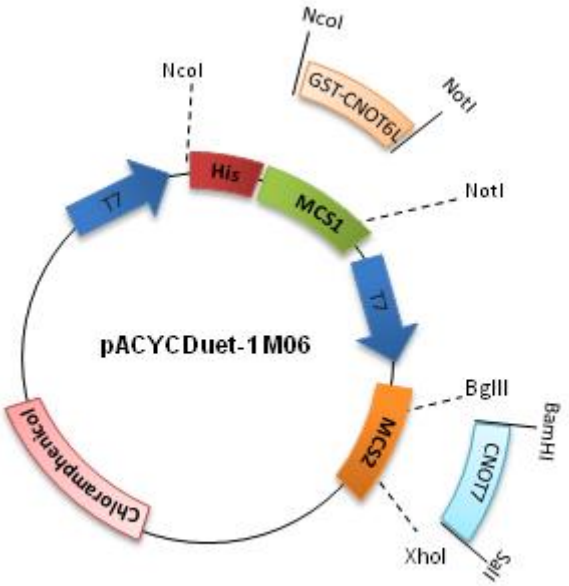

Figure 5.7 Generation of plasmid pACYCDuet-1 GST•CNOT6L/CNOT7. Vector pACYCDuet-1 was used to generate pACYCDuet-1 GST·CNOT6L/CNOT7 plasmid. CNOT7 (BamHI-SalI) was present in MCS 2 (BglII-XhoI). GST-CNOT6L was inserted into MCS 1 using the NcoI and NotI restriction sites thereby removing the sequences encoding the hexahistidine tag.

5.4.2 Protein expression and purification

To optimize the purification of the GST•Ccr4b/CNOT6L-Caf1/CNOT7 protein complex, a single colony of *E. coli* BL21 containing plasmid pACYCDuet-1 M06 was used to inoculate a starter culture for protein expression. The pre-culture, was then grown in 1 L of LB containing 34 μg/ml chloramphenicol at 37°C until the OD (600 nm) was between 0.6-0.8. Then, protein expression was induced by adding IPTG (final concentration of 0.1 mM) and incubation was continued overnight at room temperature.

Purification of the GST•Ccr4b/CNOT6L-Caf1/CNOT7 protein complex was carried out by incubating the soluble lysate with glutathione agarose by gently mixing overnight at 4°C (cold room). The glutathione-agarose/lysate mixture was spun at low speed, and the supernatant containing unbound protein was removed. Then, the glutathione-agarose suspension was washed using 10 ml of wash buffer. Elution of the protein was performed by adding 5-6 ml lysis buffer containing 10 mM reduced glutathione and 0.8 ml fractions were collected. SDS-PAGE analysis indicated that there was a major impurity with an apparent molecular weight of ~60 kDa (Figure 5.8). This is consistent with the presence of the GroEL chaperone in the purified mixture.

Optimization was performed to remove the putative chaperone contamination. Previous work has shown that washing with ATP and adding urea to partially denature proteins in the sample could remove chaperone contaminations (Thain et al., 1996, Rohman and Harrison-Lavoie, 2000). Thus, the soluble lysate was initially incubated with glutathione agarose (equilibrated in lysis buffer) containing 2 mM ATP by gently mixing overnight at 4°C. The glutathione-agarose/lysate suspension was subjected to centrifugation and the supernatant containing unbound protein was removed. To remove the remaining unbound protein, glutathione-agarose mixture was washed using lysis buffer followed by washing using 10 ml of wash buffer. Elution of the protein was performed by adding 5-6 ml lysis buffer containing 10 mM reduced glutathione and 0.8 ml fractions were

collected. However, while the purity of the elution fractions was improved, the addition of ATP alone was only partially removed the putative chaperone contamination (Figure 5.9).

Next, we included a washing step using wash buffer containing urea to partially denature proteins before elution with reduced glutathione. As shown in Figure 5.10, adding 5mM ATP in the lysis buffer and the presence of 1.5M urea in the wash buffer removed the majority of the putative chaperone contamination.

Furthermore, we tried an incubation step in the purification process to further remove the putative chaperone contamination. Soluble lysate was incubated overnight with glutathione-agarose (equilibrated in lysis buffer containing 5mM ATP) at 4°C. The glutathione-agarose/protein lysate-ATP mixture was then incubated at 37°C for 15 or 30 minutes before washing. Then, lysis buffer containing 10 mM reduced glutathione was added to elute the protein. While this method increased the purity of the protein samples, it also reduced the yield of the protein of interest and could not completely remove the putative chaperone contamination (Figure 5.11).

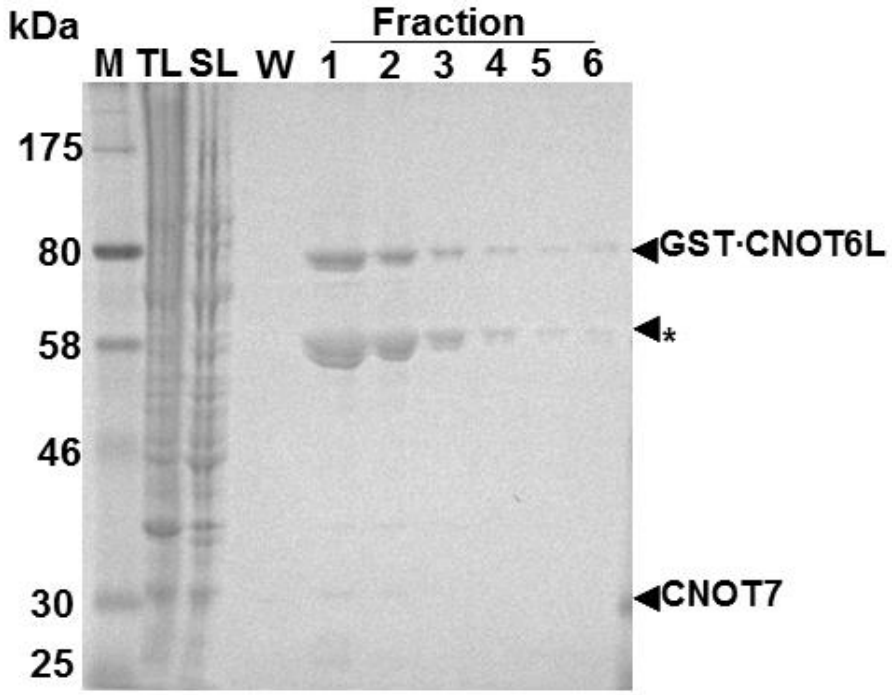

Figure 5.8 A putative GroEL chaperone contamination is present in glutathione affinity purified GST•Ccr4b/CNOT6L-Caf1/CNOT7. One litre of overnight culture of BL21(DE3) induced with IPTG (final concentration of 0.1 mM) was used for glutathione affinity purification. Fractions were collected during elution and samples were analysed by 12% SDS-PAGE. Protein were visualised by staining with Comassie Briliant Blue. Indicated are the marker (M), total lysate (TL), soluble lysate (SL), final wash fraction (W), and elution fractions 1-6. The putative GroEL chaperone contamination is indicated with an asterisk (*).

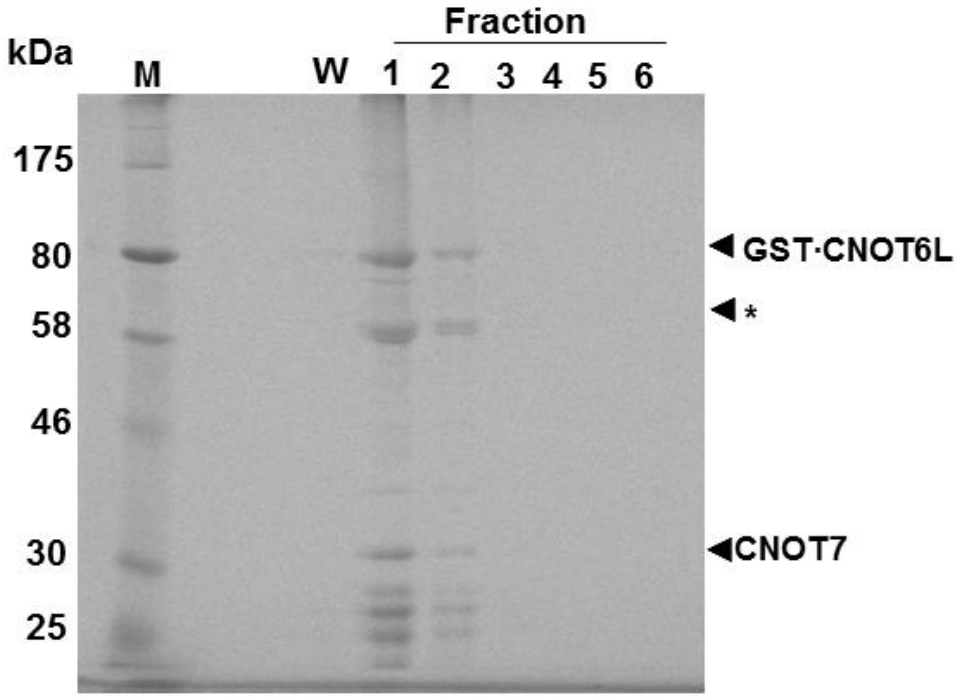

Figure 5.9 Addition of ATP partly removes the putative GroEL chaperone contamination in glutathione affinity purified GST•Ccr4b/CNOT6L-Caf1/CNOT7. One litre of overnight culture of BL21(DE3) induced with IPTG (final concentration of 0.1 mM) was used for glutathione affinity purification. Soluble lysate was incubated with glutathione agarose (equilibrated in lysis buffer) containing 2 mM ATP by gently mixing overnight at 4°C. After washing using 10 ml wash buffer, eluted fractions were collected. Samples were analysed by 12% SDS-PAGE. Protein were visualised by staining with Coomassie Briliant Blue. Indicated are the marker (M), final wash fraction (W), and elution fractions 1-6. The putative GroEL chaperone contamination is indicated with an asterisk (*).

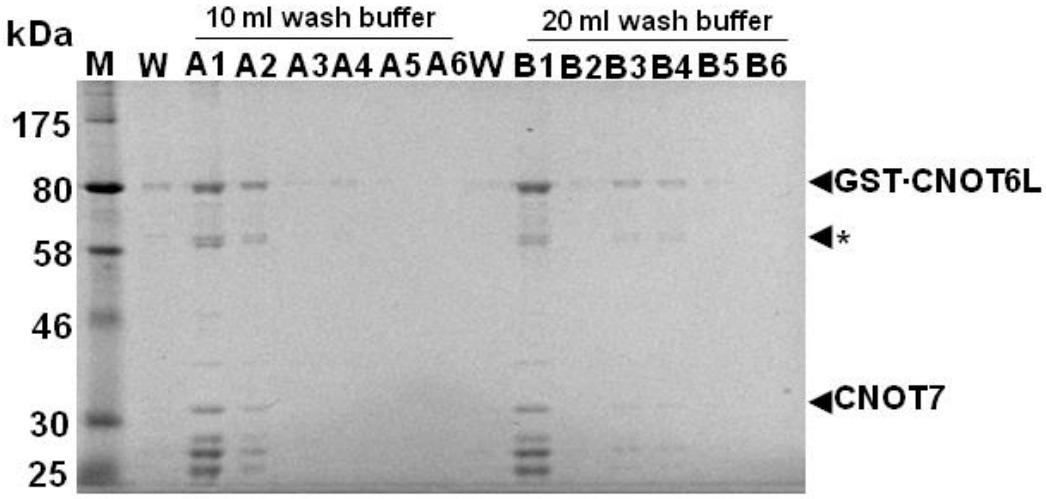

Figure 5.4 Partial removal of the putative GroEL chaperone contamination in glutathione affinity purified GST•Ccr4b/CNOT6L-Caf1/CNOT7 by adding ATP and urea in the washing process. Overnight culture of BL21(DE3) induced with IPTG (final concentration of 0.1 mM) was used for glutathione affinity purification. Lysis buffer containing 5 mM ATP and wash buffer containing 1.5 M urea were used. The first column was washed with 10 ml of wash buffer (A1-A6) and the second column was washed with 20 ml of wash buffer (B1-B6). Fractions were collected during elution and samples were analysed by 12% SDS-PAGE. Protein were visualised by staining with Coomassie Briliant Blue. Indicated are the marker (M) and final wash fraction (W). The putative GroEL chaperone contamination is indicated with an asterisk (*).

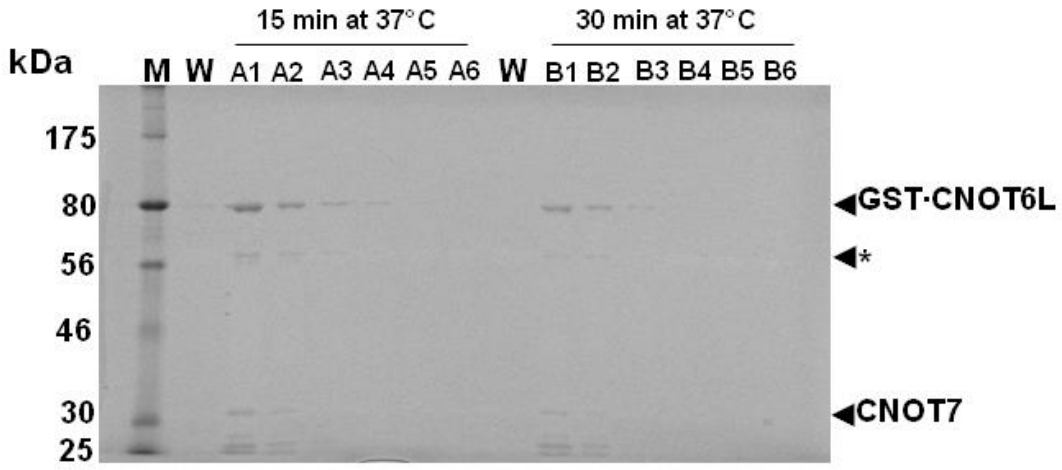

Figure 5.5 Partial removal of the putative GroEL chaperone contamination in glutathione affinity purified GST•Ccr4b/CNOT6L-Caf1/CNOT7 by addition of ATP and incubation at 37°C. Overnight culture of BL21(DE3) induced with IPTG (final concentration of 0.1 mM) was used for glutathione affinity purification. Lysis buffer containing 5 mM ATP and wash buffer containing 1.5 M urea were used. The bound protein was incubated for 15 minutes (A1-A6) or 30 minutes (B1-B6) before washing. Fractions were collected during elution and samples were analysed by 12% SDS-PAGE. Protein were visualised by staining with Coomassie Briliant Blue. Indicated are the marker (M) and final wash fraction (W). The putative GroEL chaperone contamination is indicated with an asterisk (*).

5.5 Expression and purification of a trimeric nuclease sub-complex using His-tagged BTG2

Because the purification of GST•Ccr4b/CNOT6L-Caf1/CNOT7 using glutathione affinity chromatography did not result in sufficiently pure protein, we tried co-expression of His•BTG2, Ccr4b/CNOT6L and Caf1/CNOT7.

5.5.1 Cloning strategy

To construct plasmid pACYCDuet-1 CNOT6L/CNOT7 (pACYCDuet-1 M10), plasmid pACYCDuet-1 GST•CNOT6L/CNOT7 (pACYCDuet-1 M6) was used as the starting point (Figure 5.12A). Firstly, CNOT6L cDNA was amplified by PCR to include the NcoI restriction site at the 5' end. Then, the PCR product was digested using the restriction enzymes NcoI and SalI. The restriction digested CNOT6L cDNA was then sub-cloned into the NcoI and SalI restriction sites of pACTCDuet-1 M6 replacing GST-CNOT6L in MCS 1. All sequences encoding affinity tags were removed. To confirm the correct ligation of the cDNA fragments, plasmid pACYCDuet-1 M10 was digested using NcoI and SalI. Finally, PCRs were conducted to amplify MCS 1 of plasmid pACYCDuet-1 M10 for DNA sequencing. To amplify MCS 1, primers ACYCDuetUP1 and DuetDOWN were used.

Derivatives of plasmid pACYCDuet-1 M10 containing cDNAs encoding inactive Ccr4b/CNOT6L and Caf1/CNOT7 were also constructed. Construction of plasmid pACYCDuet-1 CNOT6L/CNOT7 D40A (pACYCDuet-1 M07) was carried out as described above by using plasmid pACYCDuet-1 M11 containing the CNOT7 D40A cDNA in MCS 2 as a starting point. Plasmids pACYCDuet-1 CNOT6L E240A/CNOT7 (pACYCDuet-1 M12) containing the single E240A mutation in CNOT6L, and pACYCDuet-1 CNOT6L E240A/CNOT7 D40A (pACYCDuet-1 M13) containing two mutant cDNAs encoding inactive nucleases were constructed as described above by inserting a CNOT6L E240A cDNA (NcoI-SalI) in MCS 1 of plasmids pACYCDuet-1 M06 and

pACYCDuet-1 M07, respectively (Table 5.4). All plasmids were verified by DNA sequencing.

To express His-tagged BTG2, plasmid pQE80L-BTG2 was constructed (Figure 5.13B). To construct the plasmid, firstly, a human BTG2 cDNA was amplified by PCR. Then, the PCR product was digested using the restriction enzymes BamHI and SalI followed by ligation of the BTG2 cDNA into the corresponding restriction sites of vector pQE80L. Plasmid pQE80L contains an ampicillin resistance gene as well as the ColE1 replication origin, which are compatible with the chloramphenicol resistance gene and the P15A replication origin of the pACYCDuet-1 vector. Thus, the combination of these two vectors allows the co-expression of His•BTG2, Ccr4/CNOT6L, and Caf1/CNOT7 in bacterial cells.

Plasmid	Caf1/CNOT7	Ccr4b/CNOT6L
pACYCDuet-1 M10	WT	WT
pACYCDuet-1 M11	D40A	WT
pACYCDuet-1 M12	WT	E240A
pACYCDuet-1 M13	D40A	E240A

Table 5.4 Derivatives of plasmid pACYCDuet-1 CNOT6L/CNOT7.

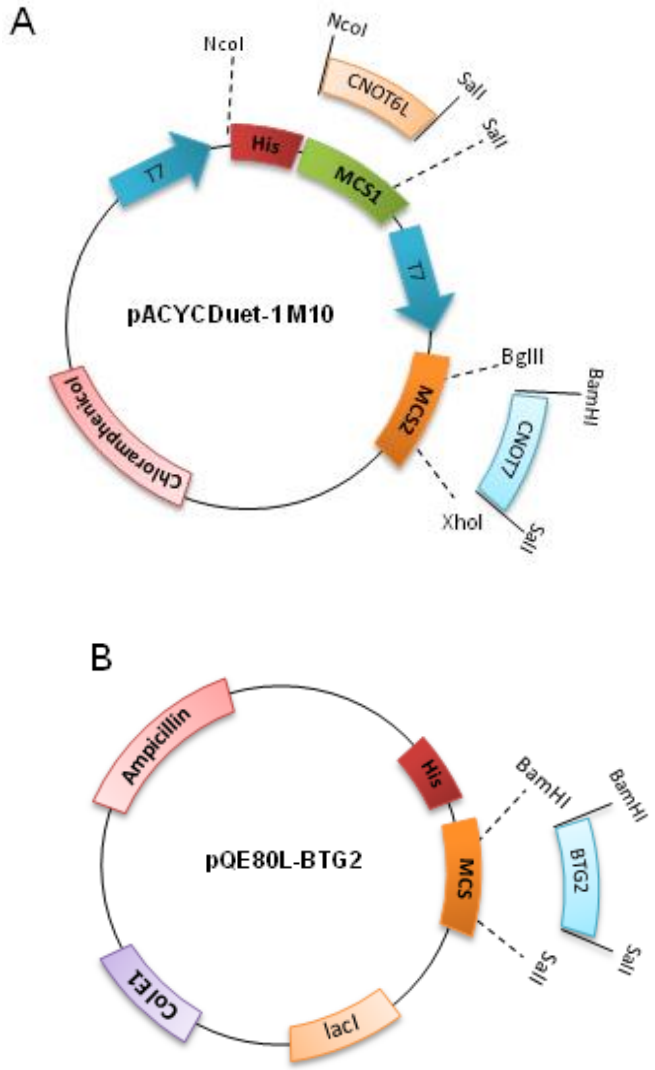

Figure 5.12 Generation of bacterial expression vectors. (A) Generation of plasmid pACYCDuet-1 CNOT6L/CNOT7. The CNOT7 cDNA (BamHI-SalI) was inserted into the BglII and XhoI restriction sites of MCS 2. The CNOT6L cDNA was inserted into the NcoI and NotI restriction sites of MCS 1. **(B)** Generation of plasmid pQE80L-BTG2. The BTG2 cDNA was subcloned into the multiple cloning site of pQE80L using the BamHI and SalI restriction sites.

5.5.2 Protein expression and purification

Expression of the His•BTG2-Caf1/CNOT7-Ccr4b/CNOT6L trimeric protein complex was performed using plasmids pACYCDuet-1 CNOT6L/CNOT7 and pQE80L-BTG2. The plasmids were co-transformed into BL21 (DE3) using selection with the antibiotics chloramphenicol and ampicillin. A single colony containing the pACYCDuet-1 CNOT6L/CNOT7 and pQE80L-BTG2 plasmids was used to inoculate a starter culture for protein expression. The pre-culture, was then grown in the presence of chloramphenicol (34 µg/ml) and ampicillin (100 µg/ml) at 37°C until the OD (600 nm) was between 0.6-0.8. IPTG (final concentration of 0.1 mM) was added to the culture and the incubation was continued overnight at room temperature to induce protein expression.

Purification of the His•BTG2-Caf1/CNOT7-Ccr4b/CNOT6L protein complex was carried out in two steps: His-tagged purification and gel filtration (Figure 5.14A). The soluble lysate was incubated overnight with Co^{2+}-agarose beads at 4°C (cold room). The Co^{2+}-agarose/protein mixture was spun, and the supernatant containing unbound protein was removed. Then, the Co^{2+}-agarose/protein mixture was washed using 10 ml of wash buffer. Elution of the protein was performed by adding 5-6 ml elution buffer containing 250 mM imidazole and 0.5 ml fractions were collected. SDS-PAGE analysis showed that there were three proteins present in the elution fractions with molecular weights corresponding to Ccr4b/CNOT6L, Caf1/CNOT7 and His-BTG2. The putative chaperone contamination appeared to be completely absent (Figure 5.13B: see also Figure 5.15B). The staining intensity of the protein bands suggested that the purified protein fractions did not only contain the trimeric protein complex (His-BTG2•Caf1/CNOT7•Ccr4b/CNOT6L) but also a dimeric protein complex composed of His-BTG2•Caf1/CNOT7. To separate the dimeric and trimeric protein complexes, gel filtration was employed using a Superdex 200 16/60 gel filtration column. Protein complexes (14 mg, 6 ml) were concentrated to

3.5 ml, and then applied onto the gel filtration column. Eluted proteins were collected in 3 ml fractions. As shown in Figure 5.15A, the UV profile of the gel filtration run showed three dominant peaks. We expected that peak I (at 47 ml) is the void volume of a Superdex 200 column and therefore peak I would contain aggregated protein with very high molecular weight. SDS-PAGE analysis showed that peak II contained His-BTG2, Caf1/CNOT7 and Ccr4b/CNOT6L. Based on the staining intensity, this peak (fraction 20) appeared to contain a trimeric nuclease complex with a 1 : 1 : 1 stoichiometry. Peak III appeared to contain the dimeric His•BTG2-Caf1/CNOT7 complex (Figure 5.15B).

It is possible that the GST domain in this complex could mediate dimerization. The trimeric proteins joined together by the GST domain would form a complex of double the size, around 280 kDA. The dimer would probably come off the gel filtration at about 55ml, in between the void volume (peak I) and the trimeric protein (peak II).

Thus, co-expression of Caf1/CNOT7, Ccr4b/CNOT6L and His·BTG2 allowed the purification of a trimeric BTG2•Caf1/CNOT7-Ccr4b/CNOT6L nuclease module, as well as a dimeric BTG2•Caf1/CNOT7 complex using a two-step procedure involving consecutive immobilised metal affinity purification and size exclusion chromatography.

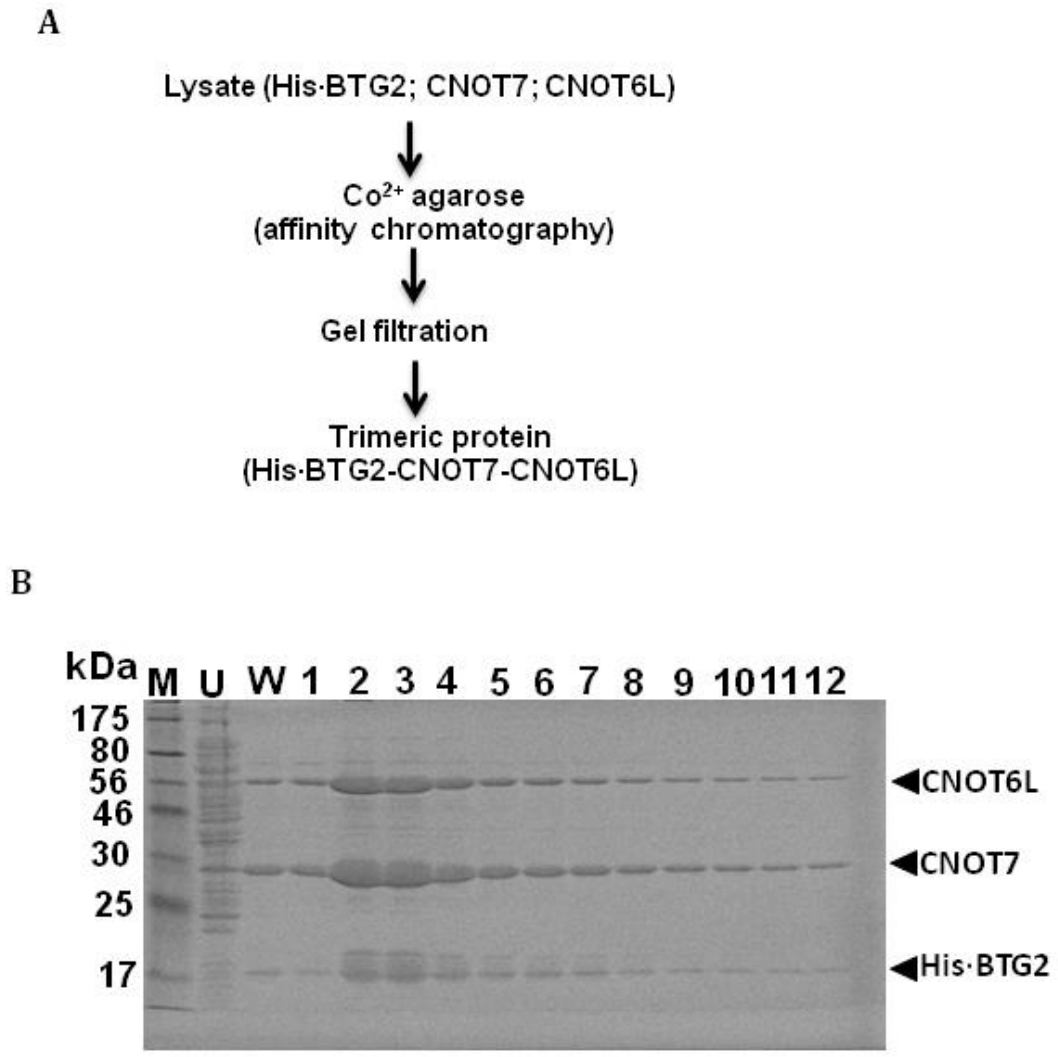

Figure 5.63 Purification of a His•BTG2-Caf1/CNOT7-Ccr4/CNOT6L protein complex. (A) Schematic of the two step purification strategy. (B) Purification of the His•BTG2-Caf1/CNOT7-Ccr4/CNOT6L protein complex using immobilised metal affinity chromatography. Overnight culture of BL21(DE3) induced with IPTG (final concentration of 0.1 mM) was used for Co2+-affinity chromatography. Fractions (0.5 ml) were collected during elution. Then purified protein was analyzed by 14% SDS-PAGE and visualised by staining with Coomassie Briliant Blue. Indicated are marker (M), unbound protein (U), wash (W), and elution fractions (1-12).

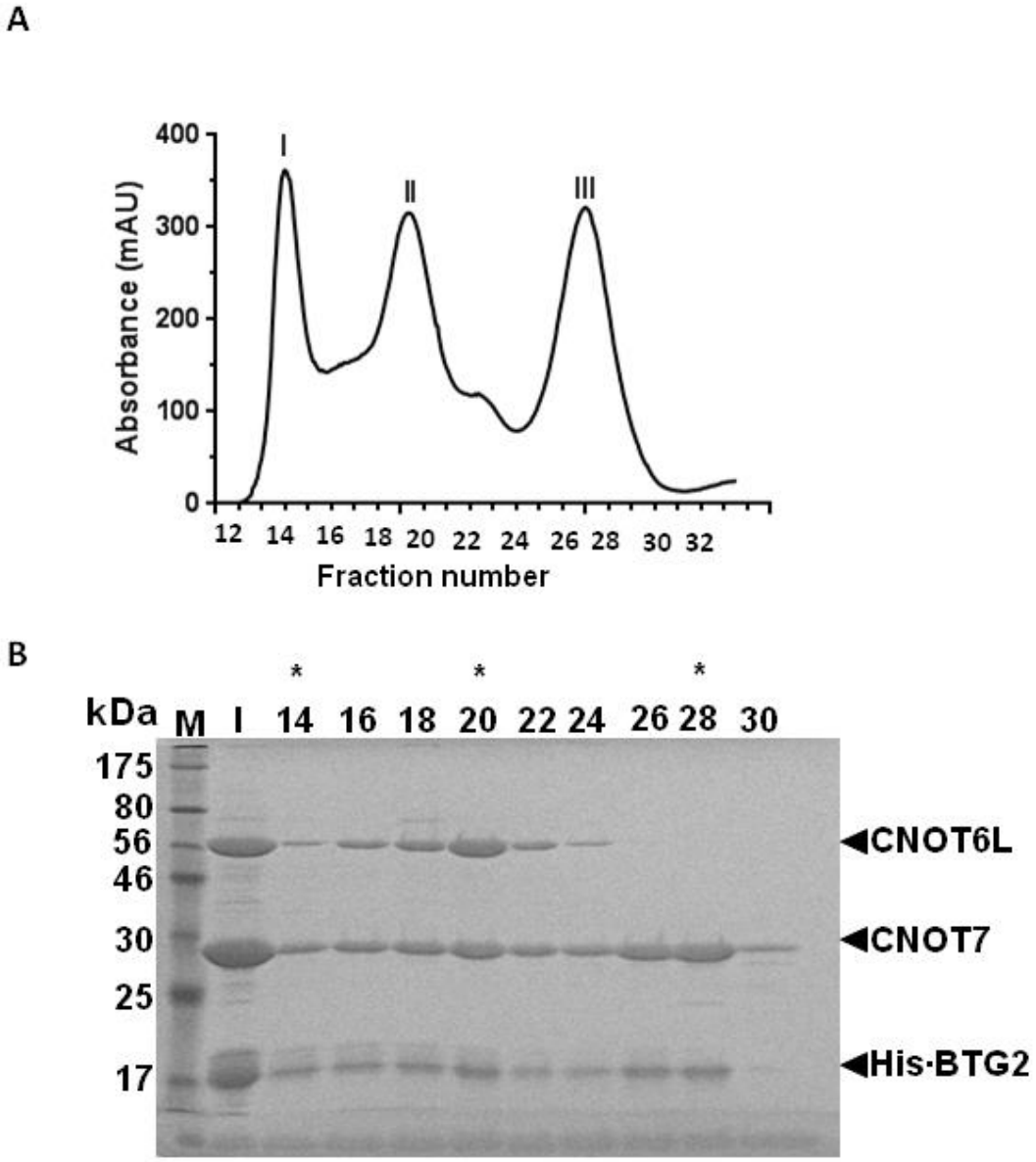

Figure 5.14 Purification of a His•BTG2-Caf1/CNOT7-Ccr4/CNOT6L protein complex using gel filtration. (A) Gel filtration profile. Elution fractions of Co^{2+}-affinity chromatography were applied onto a Superdex 200 16/60 gel filtration column. Eluted protein was collected in 3 ml fractions. **(B)** SDS-PAGE analysis of gel filtration fractions. Elution fractions were analyzed by 14% SDS-PAGE. Proteins were visualised by staining with Coomassie Briliant Blue. Indicated are marker (M), input in to gel filtration column (I) and gel filtration fractions (14-30).

5.6 Expression and purification of a trimeric nuclease sub-complex using His-tagged BTG2 and GST-tagged Ccr4b/CNOT6L

As a final strategy, co-expression of His•BTG2, GST•Ccr4b/CNOT6L and Caf1/CNOT7 was carried out to purify a trimeric nuclease module using successive immobilised metal and glutathione affinity chromatography (Figure 5.16A). First, plasmids pACYCDuet-1 M06 and pQE80L-BTG2 were co-transformed into BL21 (DE3) using selection with chloramphenicol and ampicillin. A single colony containing plasmids pACYCDuet-1 M06 and pQE80L-BTG2 was used to inoculate a starter culture for protein expression. The pre-culture was then grown in 2 L of LB containing chloramphenicol (34 µg/ml) and ampicilin (100 µg/ml) at 37°C until the OD (600 nm) was between 0.6-0.8. IPTG (final concentration of 0.1 mM) was then added to the culture to induce protein expression. First, immobilised metal affinity chromatography was done using Co^{2+}-agarose beads. Soluble lysate was incubated overnight with Co^{2+}-agarose beads in extraction buffer at 4˚C. After washing, bound proteins were eluted from the Co^{2+}-agarose beads with 5-6 ml of elution buffer containing 250 mM imidazole. Eluted proteins were collected in 0.5 ml fractions. SDS-PAGE analysis showed that the putative GroEL chaperone contamination was completely absent using this method (Figure 5.15). However, the staining intensity of the protein bands suggested that the elution fractions did not only contain the trimeric complex, but also the dimeric His•BTG2-Caf1/CNOT7 protein complex.

To isolate the trimeric complex, glutathione affinity purification was carried out exploiting the presence of the GST-tag fused to Ccr4b/CNOT6L. Thus, elution fractions from the Co^{2+}-agarose column were applied onto a GST affinity spin column containing 0.2 ml resin and incubated for 60 minutes at 4°C on an end-over-end mixer. After washing, bound proteins were eluted from the resin by adding buffer containing 10 mM reduced glutathion. Based

on the staining intensity of the protein bands, the elution fractions appeared to contain a trimeric nuclease complex with a 1 : 1 : 1 stoichiometry.
Thus, two procedures for the expression and purification of a trimeric BTG2-Caf1/CNOT7-Ccr4/CNOT6L nuclease module are described in this chapter.

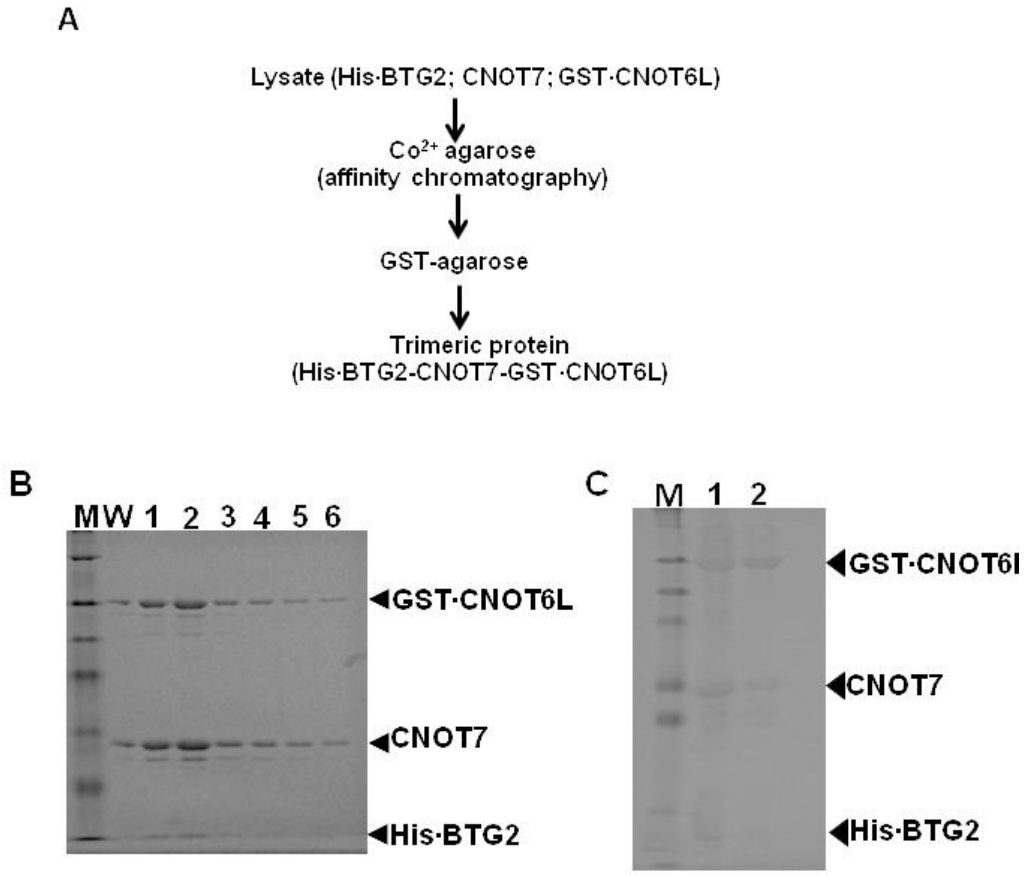

Figure 5.75 Purification of a His•BTG2-Caf1/CNOT7-GST•Ccr4/CNOT6L protein complex. (A) Schematic of two step purification strategy of a His•BTG2-Caf1/CNOT7-GST•Ccr4/CNOT6L protein complex **(B)** Purification of His•BTG2-Caf1/CNOT7-GST•Ccr4/CNOT6L using immobilised metal affinity chromatography. Overnight culture of BL21(DE3) induced with IPTG (final concentration of 0.1 mM) was used for Co^{2+}-affinity chromatography. Fractions (1 ml) were collected during elution. Then, purified protein was analysed by 14% SDS-PAGE and visualised by staining with Coomassie Briliant Blue. Indicated are marker (M), final wash (W), and elution fractions (1-6). **(C)** Analysis of purified His•BTG2-Caf1/CNOT7-GST•Ccr4/CNOT6L protein complex. Purified protein was separated by 14% SDS-PAGE. Protein were visualised by staining with Coomassie Briliant Blue. Indicated are the pooled Co^{2+}-agarose elution fractions (1) and the combined elution fractions of the glutathione-agarose column (2).

5.7 Discussion

In this chapter, different methods are described for the purification of human Ccr4b/CNOT6L-Caf1/CNOT7 deadenylase complexes. Initially, we tried to reconstitute the complex using purified His•Caf1/CNOT7 (Chapter 3) and full length GST•Ccr4b/CNOT6L. This was unsuccessful, because GST•Ccr4b/CNOT6L (as well as GST•Ccr4a/CNOT6) was insoluble in bacterial lysates. Next, we tried co-expression of His•Ccr4b/CNOT6L-Caf1/CNOT7. When these proteins were co-expressed in BL21 (DE3) and purified using immobilized metal affinity chromatography (IMAC), we did not obtain samples of sufficient purity. SDS-PAGE analysis also indicated that the protein complex did not appear to show the correct stoichiometry.

Moreover, we tried a different extraction method to increase the protein yield. It has been reported that immobilized metal affinity chromatography (IMAC) is very sensitive to metal chelators (Chaga, 2001). Because these are mainly present in the periplasmic space of *E. coli*, removal of the periplasmic material can result in increased yield and purity (Magnusdottir et al., 2009). However, while this method increased the yield of the protein of interest, the purified protein was still insufficiently pure. Following the co-expression and purification of GST•Ccr4b/CNOT6L-Caf1/CNOT7, which was subsequently carried out, it was concluded retrospectively that a putative GroEL chaperone contamination was present in these protein fractions, which co-migrates with His•Ccr4b/CNOT6L in SDS-PAGE. Several methods have been suggested to remove GroEL chaperone contaminations during the purification of GST fusion proteins, for example by adding ATP (Thain et al., 1996) or the addition of urea to the bacterial lysate and wash buffers (Rohman and Harrison-Lavoie, 2000). The combined use of ATP and urea containing wash buffers was successful to remove the majority of the putative GroEL chaperone contamination from fractions containing purified GST•Ccr4b/CNOT6L-Caf1/CNOT7 deadenylase complexes.

Interestingly, co-expression of (GST•)Ccr4b/CNOT6L, Caf1/CNOT7 and His•BTG2 successfully removed the putative GroEL chaperone contamination without the need for ATP and urea-containing wash buffers. This suggested that by co-expression of BTG2, a natural interaction partner of Caf1/CNOT7, the chaperone did not bind to the Ccr4b/CNOT6L-Caf1/CNOT7 complex. Two procedures for the expression and purification of a trimeric BTG2•Caf1/CNOT7-Ccr4/CNOT6L nuclease module are described in this chapter. The first is based on sequential immobilised metal affinity chromatography followed by gel filtration. This procedure can be used to obtain both trimeric His•BTG2-Caf1/CNOT7-Ccr4b/CNOT6L and dimeric His•BTG2-Caf1/CNOT7. The second procedure is based on successive immobilised metal and glutathione affinity chromatography. This procedure is faster and allows the handling of multiple samples in parallel.

In summary, two strategies for the co-expression and purification of a human BTG2-Caf1/CNOT7-Ccr4b/CNOT6L protein complex were developed. This is the first time a procedure for the expression and purification of a nuclease module of the human Ccr4-Not complex is described. A previous method was reported for the reconstitution of the yeast nuclease module comprising the MIF4G domain of Not1, Caf1 and Ccr4 (Basquin et al., 2012). The latter method is relatively time consuming as compared to the strategy described here, which is easier and faster. The isolation of a human BTG2-Caf1/CNOT7-Ccr4b/CNOT6L nuclease module is a first step towards the reconstitution of the complete human Ccr4-Not complex.

Chapter 6

The enzyme activities of Ccr4 and Caf1 are both required for the deadenylase activity of a human Ccr4-Not nuclease sub-complex

Chapter 6. The enzyme activities of Ccr4 and Caf1 are both required for the deadenylase activity of a human Ccr4-Not nuclease sub-complex

6.1 Introduction

A key step in the mRNA degradation pathway begins with shortening of the poly(A) tail by deadenylase enzymes. This is often the rate limiting step. Pioneering work identified that the Ccr4-Not complex is the major deadenylase in *Saccharomyces cerevisiae* (Tucker et al., 2001). The enzyme complex contains two deadenylase subunits, Caf1 and Ccr4. In vertebrates, each of these subunits is encoded by two paralogous genes: Caf1 is encoded by *CNOT7* or *CNOT8*, while *CNOT6* and *CNOT6L* encode the highly related Ccr4 subunits (Wilusz et al., 2001, Parker and Song, 2004, Doidge et al., 2012a, Winkler and Balacco, 2013, Wahle and Winkler, 2013).

In vitro studies in human and yeast indicated that Ccr4 has a strong preference for poly (A) residues (Chen et al., 2002, Wang et al., 2010). The crystal structure of the catalytic domain of human Ccr4b/CNOT6L showed that there are two Mg^{2+} ions in the active site. The Mg^{2+} ions are coordinated by five conserved residues, asparagine, glutamate, two aspartates and histidine (Wang et al., 2010). Substitutions of these amino acids involved in the coordination of metal ions abolished the deadenylation activity of Ccr4b/CNOT6L (Chen et al., 2002, Wang et al., 2010).

As in the case for Ccr4, Caf1 also requires Mg^{2+} ions for its enzymatic activity. The metal ions are coordinated by four amino acid residues, a glutamate and three aspartate residues. Substitution of these amino acids eliminates the enzymatic activity (Thore et al., 2003, Jonstrup et al., 2007, Horiuchi et al., 2009).

Currently, it is unclear whether the Ccr4 and Caf1 nuclease subunits have unique roles, or whether they cooperate in mRNA deadenylation. In the yeast

Saccharomyces cerevisiae, Ccr4 is the main catalytic subunit. In agreement with this notion, point mutations that inactivate the catalytic activity of Caf1 complement the phenotype of *Caf1Δ* cells and do not affect deadenylation (Tucker et al., 2001, Tucker et al., 2002, Chen et al., 2002, Viswanathan et al., 2004). However, the enzyme activity of Caf1 contributes to deadenylation in other eukaryotes, including the fission yeast *Schizosaccharomyces pombe* and the filamentous yeast *Aspergillus nidulan* (Takahashi et al., 2007, Morozov et al., 2010). In human cells, there are marked differences in the genome-wide expression profiles of Caf1 and Ccr4-knockdown cells, respectively, suggesting that the Caf1 and Ccr4 subunits have unique roles in the regulation of mRNA levels (Aslam et al., 2009, Mittal et al., 2011). Consistent with this notion, the active sites of Caf1 and Ccr4 are not located closely together in a minimal nuclease module consisting of the budding yeast Not1 MIF4G domain, Caf1 and Ccr4 (Basquin et al., 2012).

Caf1 has been shown to interact with members of the Tob/BTG family, which are characterised by the presence of an N-terminal BTG domain, which mediates the interaction between the BTG/TOB and Caf1 proteins. It is still debated what the effect is of BTG/TOB proteins on the deadenylase activity of the Ccr4-Not complex. In vitro analysis indicated that BTG2 can suppress the deadenylase activity of Caf1 . Tob can also inhibit the deadenylase activity of the Ccr4-Not complex in vitro (Miyasaka et al., 2008). Nevertheless, it has also been reported that there is no effect on the deadenylation activity of Caf1/CNOT7 in the presence of the N-terminal 138 amino acids comprising the BTG domain of Tob (Horiuchi et al., 2009). Moreover, Tob and BTG2 were identified as general activators of mRNA deadenylation using cell-based approaches (Ezzeddine et al., 2007, Mauxion et al., 2008).

In this chapter, we determined the deadenylase activity of the His•BTG2-Caf1/CNOT7-GST•Ccr4b/CNOT6L protein complex. The activity of the protein complex was higher than the individually isolated subunits or the dimeric His•BTG2-Caf1/CNOT7 protein complex. Interestingly, the activity of

the trimeric protein complex required the enzyme activity of both deadenylase subunits, Caf1/CNOT7 and Ccr4b/CNOT6L. Inactivation of either subunit completely abolished the enzymatic activity of the protein complex. In addition, no deadenylase activity was observed when the trimeric complex was incubated in the presence of small molecule inhibitors that are selective towards Caf1/CNOT7.

The same results were observed when we assessed the deadenylase activity of the highly related His•BTG2-Caf1/CNOT7-GST•Ccr4a/CNOT6 protein complex. The activity of this protein complex also required the catalytic activity of both subunits, Ccr4a/CNOT6 and Caf1/CNOT7.

6.2 Expression and purification of His•BTG2-Caf1/CNOT7-GST•Ccr4b/CNOT6L protein complexes containing inactive deadenylase subunits

To investigate the deadenylase activity of the His•BTG2-Caf1/CNOT7-GST•Ccr4b/CNOT6L protein complex, we used plasmids pACYCDuet-1 M07 and pACYCDuet-1 M08 containing single base pair mutations (CNOT7 D40A or CNOT6L E240A), and, pACYCDuet-1 M09 plasmid containing both mutations (Section 5.3.1).

Expression and purification of the protein complexes was done using the same procedure that we used for the expression and purification of wild type His•BTG2-Caf1/CNOT7-GST•Ccr4b/CNOT6L protein complex (Section 5.5). The above plasmids were co-transformed with pQE80L-BTG2 into BL21 (DE3) using medium containing chloramphenicol (34 μg/ml) and ampicillin (100 μg/ml). A single colony was used to inoculate a starter culture (100 ml) for protein expression. The pre-culture, was then grown in LB media containing chloramphenicol (34 μg/ml) and ampicillin (100 μg/ml) at 37°C until the OD (600 nm) was between 0.6-0.8. IPTG (final concentration of 0.1 mM) was added to the culture and left overnight at room temperature to induce protein expression.

The purification of protein complexes was conducted by using a two step purification strategy. First, purification was performed using immobilized metal affinity chromatography (IMAC) followed by GST affinity purification using glutathione agarose. The purified complexes were analysed by SDS-PAGE, and then stained using Coomassie Brilliant Blue (Figure 6.1A). There were three bands visible in agreement with the predicted molecular weights. GST-Ccr4b/CNOT6L (wild type or E240A) was observed at ~80 kDa, Caf1/CNOT7 (wild type or D40A) was detected at ~30 kDa and His-BTG2 was observed at ~17 kDa. However, minor impurities were detected at around 25 kDa. Based on the staining intensity, SDS-PAGE analysis indicated that all the protein complexes had correct stoichiometric ratio. It is estimated that the purity of the isolated His•BTG2-Caf1/CNOT7-GST•Ccr4b/CNOT6L protein complexes was >90%. Furthermore, to confirm the identity of the protein bands, western blots analysis was carried out using anti-CNOT6L, anti-CNOT7 and anti-His primary antibodies (Figure 6.1B).

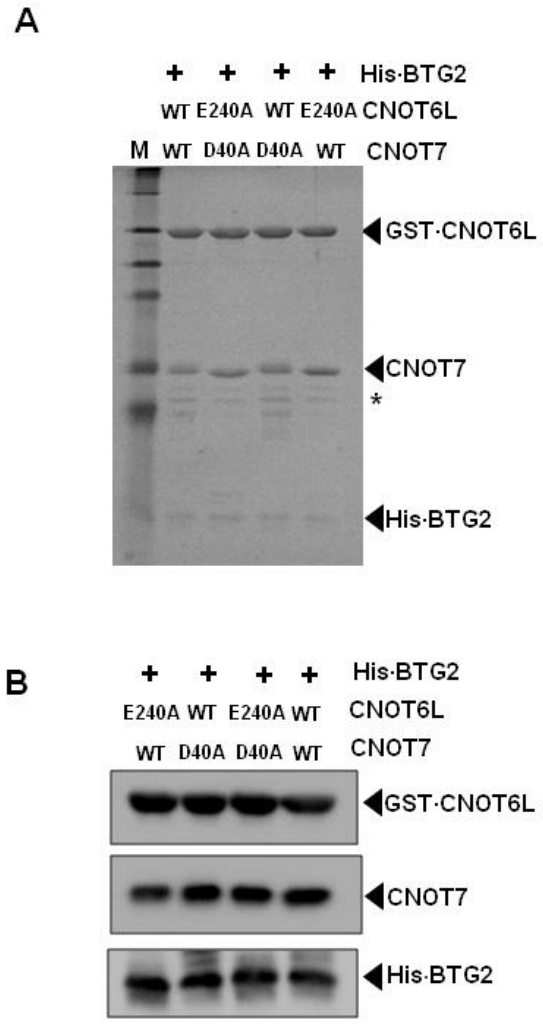

Figure 6.1 Analysis of purified His•BTG2-Caf1/CNOT7-GST•Ccr4b/CNOT6L protein complexes. (A) SDS-PAGE analysis of wild type and variant His•BTG2-Caf1/CNOT7-GST•Ccr4b/CNOT6L protein complexes. Proteins (2 µg) were separated by 14% SDS-PAGE and stained using Coomassie Briliant Blue. Impurities are indicated by an asterisk. **(B)** Western blot analysis of His•BTG2-Caf1/CNOT7-GST•Ccr4b/CNOT6L protein complexes. Protein samples were separated by 14% SDS-PAGE and western blot analysis was conducted using anti-CNOT6L, anti-CNOT7 and anti-His primary antibodies.

6.3 The His•BTG2-Caf1/CNOT7-GST•Ccr4b/CNOT6L protein complex displays deadenylase activity

In order to assess the activity of the purified His•BTG2-Caf1/CNOT7-GST•Ccr4b/CNOT6L complex, the fluorescence-based deadenylase assay was used (Chapter 3). Increasing concentrations of wild type His•BTG2-Caf1/CNOT7-GST•Ccr4b/CNOT6L complex, or a variant complex with inactive enzymatic subunits was incubated with Flc-labelled RNA substrate for one hour at 30°C. Then, a solution containing SDS and TAMRA-labelled DNA probe was added. Fluorescence was detected after incubation with the isolated wild type protein complex in a concentration-dependent manner (Figure 6.2). As predicted, no fluorescence was observed when the RNA substrate was incubated in the presence of a catalytically inactive protein complex. This result indicated that the isolated wild type protein complex has deadenylase activity, and there are no contaminating activities from *E. coli* remain after the purification procedure (Figure 6.2).

Then, we compared the activity of the trimeric complex with the isolated deadenylase subunits, Caf1/CNOT7, Ccr4b/CNOT6L ΔLRR and the dimeric His•BTG2-Caf1/CNOT7 complex. The Caf1/CNOT7 and Ccr4b/CNOT6L ΔLRR protein were successfully purified using IMAC and glutathione affinity chromatography, respectively (Chapter 3). The His•BTG2-Caf1/CNOT7 dimeric protein complex was obtained following co-expression of His-BTG2, Caf1/CNOT7and Ccr4b/CNOT6L and purification using sequential IMAC and gel filtration chromatography (Chapter 5). First, I compared the purified proteins by SDS-PAGE analysis. Proteins (2μg) were separated by SDS-PAGE, then, Coomassie Brilliant Blue (Figure 6.3A) was used to visualise the protein bands. Using the staining method, it was difficult to detect BTG2 protein band because the size of the protein (17 kDa). Therefore, SYPRO Ruby was also used to stain the gel (Figure 6.3B). As shown in Figure 6.3B, using SYPRO Ruby staining, the BTG2 protein could be detected more clearly as compared to Coomassie Brilliant Blue staining. SDS-PAGE analysis showed that

concentration of Caf1/CNOT7 and the dimeric His•BTG2-Caf1/CNOT7 complex were comparable, however the concentration of the trimeric protein complex was slightly lower.

Western blot analysis was carried out to confirm the identity and concentration of the Caf1/CNOT7 and Ccr4b/CNOT6L proteins. Proteins (2µg) were separated by SDS-PAGE, and western blot analysis was then done using anti-CNOT7 and anti-CNOT6L primary antibodies. The result indicated that the concentration of the Caf1/CNOT7 monomer and in the dimeric protein complex were comparable, but the concentration of Caf1/CNOT7 in the trimeric protein complex was slightly lower (Figure 6.4A).

To determine the deadenylase activity of the monomeric subunits, as well as the dimeric His•BTG2-Caf1/CNOT7 and trimeric His•BTG2-Caf1/CNOT7-GST•Ccr4b/CNOT6L protein complexes, proteins were incubated with Flc-labelled substrate for 60 minutes. Then, a solution containing SDS and TAMRA-labelled DNA probe was added. Three different enzyme concentrations were used (250, 350 and 450 nM). Ccr4b/CNOT6L ΔLRR displayed the lowest deadenylase activity when it was compared with Caf1/CNOT7, or the dimeric His•BTG2-Caf1/CNOT7 and trimeric His•BTG2-Caf1/CNOT7-GST•Ccr4b/CNOT6L protein complexes (Figure 6.4B). The result also indicated that the His•BTG2-Caf1/CNOT7 complex was more active than the Caf1/CNOT7 monomer. Furthermore, even though the concentration of the trimeric His•BTG2-Caf1/CNOT7-GST•Ccr4b/CNOT6L complex was lower, it showed the highest activity (Figure 6.4B).

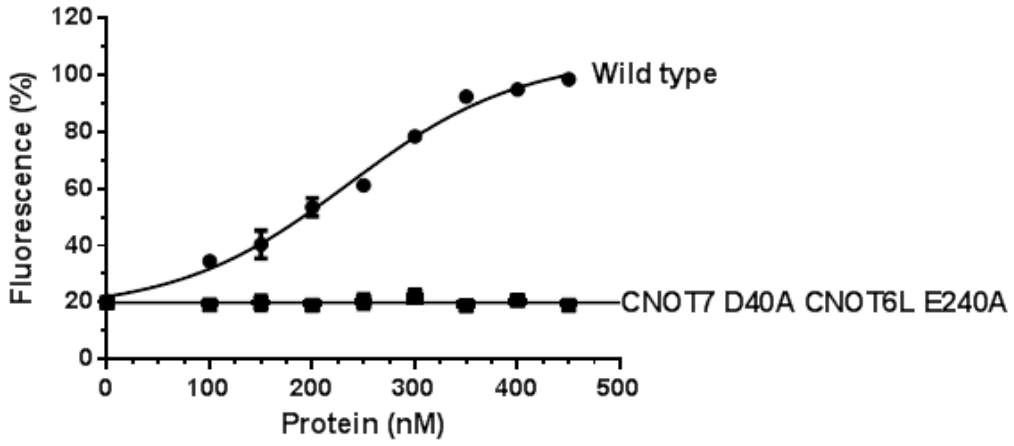

Figure 6.2 The His•BTG2-Caf1/CNOT7-GST•Ccr4b/CNOT6L protein complex displays deadenylase activity. Wild type and protein complex containing two inactive deadenylase subunits were incubated with RNA substrate (1 μM) for 60 minutes at 30°C. The total reaction volume was 10 μl. A stop/probe mix containing 1% SDS, TE and a 5-fold molar excess of DNA probe was added. A BioTek Synergy HT plate reader was used to measure the fluorescence.

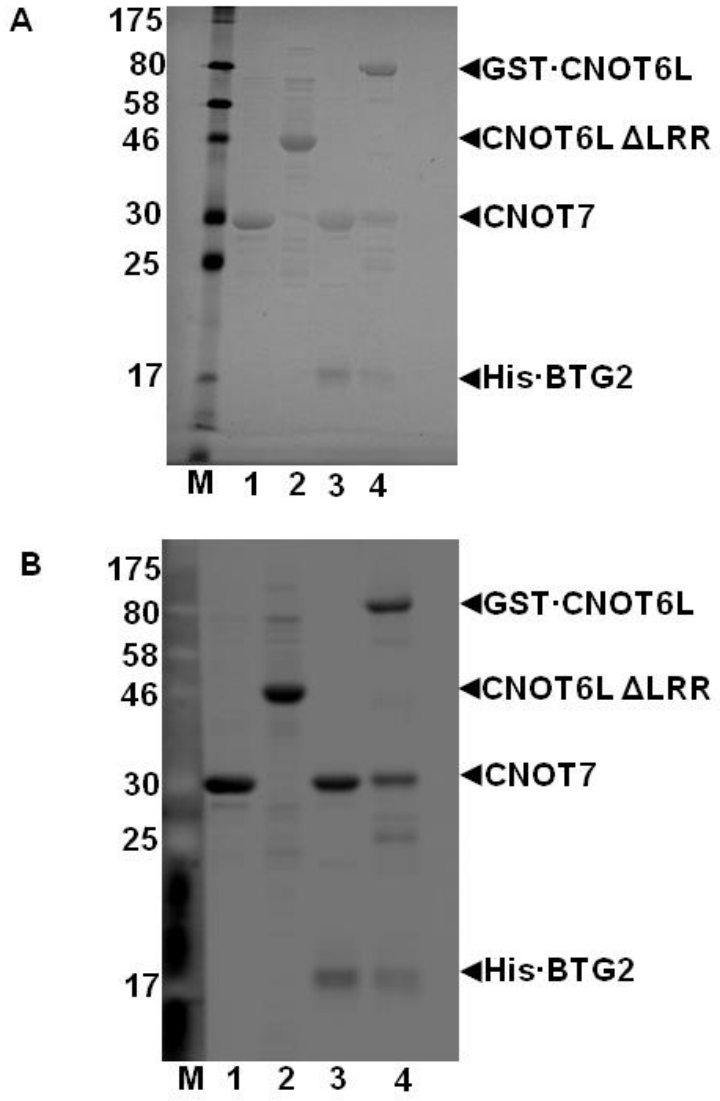

Figure 6.3 Analysis of purified monomeric Caf1/CNOT7 and Ccr4b/CNOT6L ΔLRR, dimeric His•BTG2-Caf1/CNOT7 and trimeric His•BTG2-Caf1/CNOT7-GST•Ccr4b/CNOT6L. (A, B) SDS-PAGE analysis of purified Caf1/CNOT7 (1), Ccr4b/CNOT6L ΔLRR (2), dimeric His•BTG2-Caf1/CNOT7 (3) and trimeric His•BTG2-Caf1/CNOT7-GST•Ccr4b/CNOT6L (4). Proteins (2 μg) were analysed by 14% SDS-PAGE gel, then stained using **(A)** Coomassie Brilliant Blue, or **(B)** SYPRO Ruby.

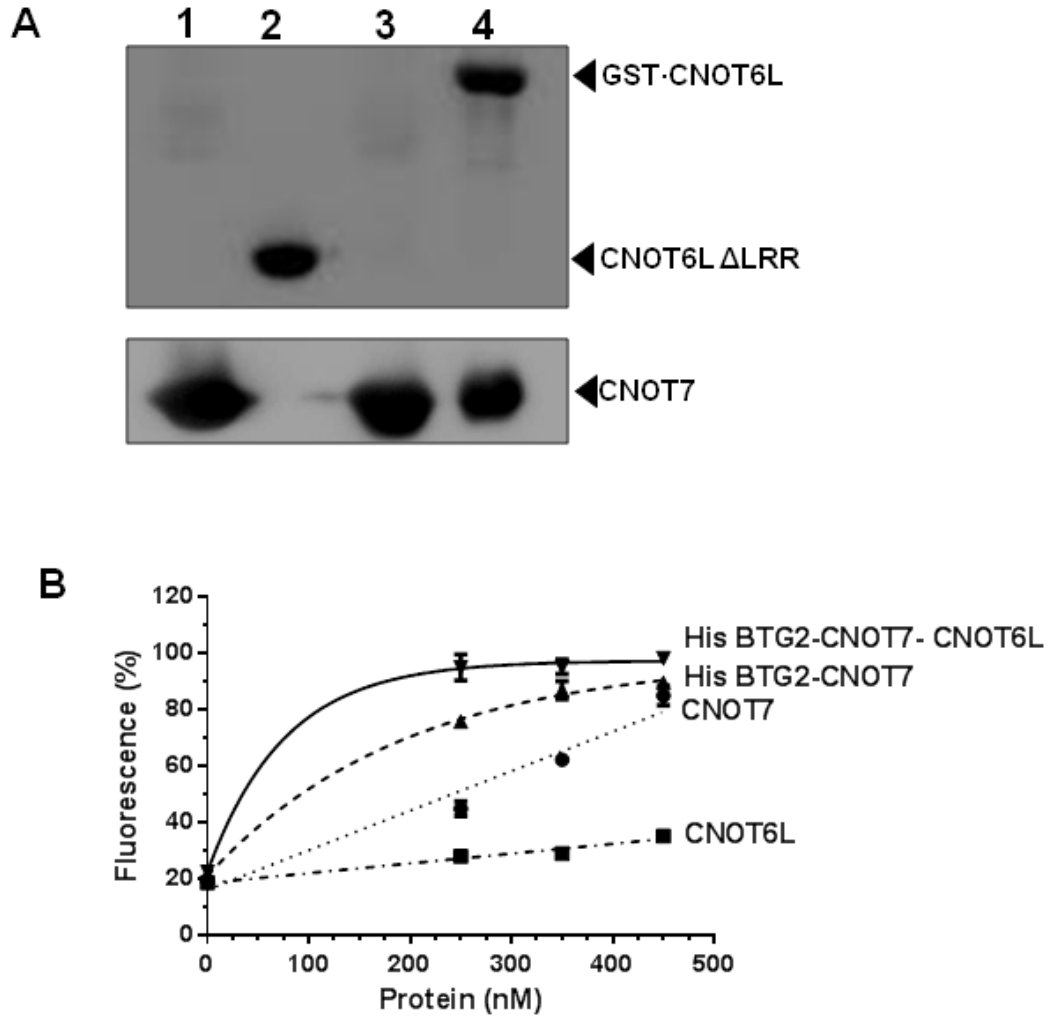

Figure 6.4 Activity of purified deadenylase enzymes. (A) Western blot analysis of purified monomeric Caf1/CNOT7 (1), Ccr4b/CNOT6L ΔLRR (2), dimeric His•BTG2-Caf1/CNOT7(3) and trimeric His•BTG2-Caf1/CNOT7-GST•Ccr4b/CNOT6L (4). Protein samples were separated by 14% SDS-PAGE gel and western blot analysis was conducted using anti-CNOT6L and anti-CNOT7 primary antibodies. **(B)** Trimeric His•BTG2-Caf1/CNOT7-GST•Ccr4b/CNOT6L protein complex is more active than monomeric Caf1/CNOT7, Ccr4b/CNOT6L ΔLRR, or dimeric His•BTG2-Caf1/CNOT7. Proteins were incubated with RNA substrate for 60 minutes at 30°C, then a solution containing SDS and DNA probe was added. A BioTek Synergy HT plate reader was used to measure the fluorescence.

6.4 The contribution of the deadenylase subunits to the activity of a trimeric BTG2•Caf1/CNOT7•Ccr4b/CNOT6L protein complex

To determine the contribution of each deadenylase subunit to the activity of a trimeric BTG2•Caf1/CNOT7•Ccr4b/CNOT6L protein complex, we compared the deadenylase activity of the wild type protein complex and three variants containing catalytically inactive subunits. Three different proteins complexes containing catalytically inactive subunits were investigated. First, a protein complex containing a catalytically inactive version of Caf1/CNOT7 (amino acid substitution D40A). Second, a protein complex containing a catalytically inactive version of Ccr4b/CNOT6L (amino acid substitution E240A). Third, a protein complex containing catalytically inactive versions of both Caf1/CNOT7 and Ccr4b/CNOT6L. We compared three different concentrations of the protein complexes (250, 350 and 450 nM). Proteins were incubated with Flc-labelled RNA substrate for one hour at 30°C, then the enzymatic reaction was stopped by adding TAMRA-labelled DNA probe containing SDS. As shown in Figure 6.5A, fluorescence was only detected in the presence of the wild type protein complex. Surprisingly, protein complexes containing catalytically inactive Caf1/CNOT7 or Ccr4b/CNOT6L displayed no deadenylase activity, and were indistinguishable from complexes where both nuclease components were inactive.

Further analysis using a gel-based assay confirmed that there was degradation of RNA substrate in the presence of wild type protein complex, but degradation of RNA substrate was not observed in the presence of variant complexes containing one or two inactive nuclease subunits (Figure 6.5B). These data suggest that the activity of the trimeric BTG2•Caf1/CNOT7•Ccr4b/CNOT6L protein complex requires both Caf1/CNOT7 and Ccr4b/CNOT6L in vitro.

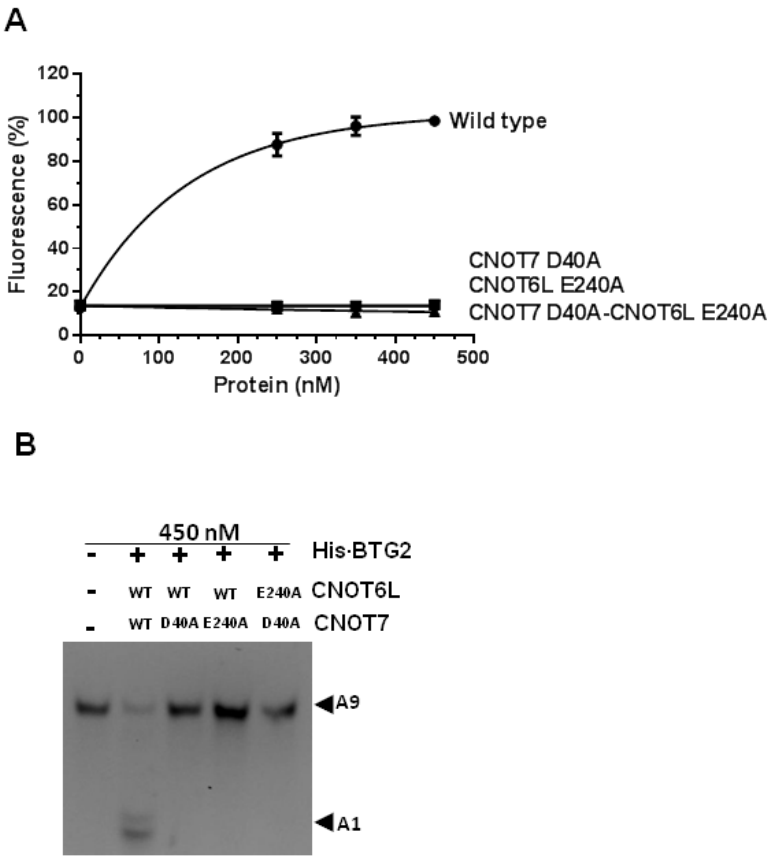

Figure 6.5 The deadenylase activity of a trimeric BTG2-Caf1/CNOT7-Ccr4b/CNOT6L protein complex requires the activity of both Caf1/CNOT7 and Ccr4b/CNOT6L. (A) Fluorescence-based deadenylation assay of wild type and variant BTG2-Caf1/CNOT7-Ccr4b/CNOT6L protein complexes. Proteins were incubated with RNA substrate for 60 minutes at 30°C. Then a solution containing SDS and DNA probe was added to stop and fluorescence measured. **(B)** Gel-based deadenylation assay of wild type and variant BTG2-Caf1/CNOT7-Ccr4b/CNOT6L protein complexes. Equal amounts of wild-type and mutant protein (450 nM) were incubated with RNA substrate (1 μM). After 60 min incubation at 30°C, the reaction mixture was subjected to denaturing PAGE and visualized using epifluorescence. Indicated are the intact RNA substrates (A9) and the product containing a single adenosine residue (A1).

6.5 Pharmacological inhibition of Caf1/CNOT7 abolishes the activity of a BTG2-Caf1/CNOT7-Ccr4b/CNOT6L complex

In order to further investigate the role of the Caf1/CNOT7 subunit on the activity of protein complex, seven small molecule inhibitors of Caf1/CNOT7 enzyme were tested. Four compounds from the screening of library compounds were tested (Chapter 4). These compounds, NCC-0007277, NCC-00001590, NCC-00010651, and NCC-00039069 have IC_{50} values of 137, 98, 233 and 129 μM, respectively. Three synthesised compounds, GPJMRC007, GPJMRC033, GPJMRC044 (Chapter 4) were also used to investigate the effect of the Caf1/CNOT7 subunit on the activity of the trimeric protein complex. The synthesised compounds have IC_{50} values of 6.82, 6.5 and 10.58 μM, respectively (Chapter 4). As a negative control, the analogue GPJMRC039, which does not display inhibitory activity towards Caf1/CNOT7 was used. All the compounds used in this work did not inhibit the Ccr4b/CNOT6L enzyme (Chapter 4).

The trimeric protein complex was incubated with the presence or absence of 300 μM of NCC compounds or 30 μM of GPJMRC compounds for 15 minutes at room temperature. RNA substrate was then added to the reaction mixture. After 60 minutes incubation at 30°C, a solution containing DNA probe and SDS was added. As shown in Figure 6.6A, using a concentration of 300 μM, NCC-00001590 completely inhibited the activity of the trimeric protein complex. However, compounds NCC-00039069, NCC-00007277 and NCC-00010651 partially inhibited the activity of protein complex, which correlated with their IC_{50} values. The results were confirmed using a gel-based analysis of the reaction products (Figure 6.6B).

As expected, analogue GPJMRC039 did not inhibit the activity of the trimeric protein complex. However, compounds GPJMRC007, GPJMRC033 and GPJMRC044 strongly inhibited the deadenylase activity of the His•BGT2-Caf1/CNOT7-GST•Ccr4b/CNOT6L protein complex (Figure 6.7A). The results were also confirmed using a gel-based analysis of the reaction products

(Figure 6.7B). These results are consistent with the notion that Caf1/CNOT7 activity is required for the activity of the trimeric complex.

To further investigate the role of subunits on the deadenylase activity of protein complex, we assessed the contribution of the Ccr4a/CNOT6 subunit, which is highly related to Ccr4b/CNOT6L.

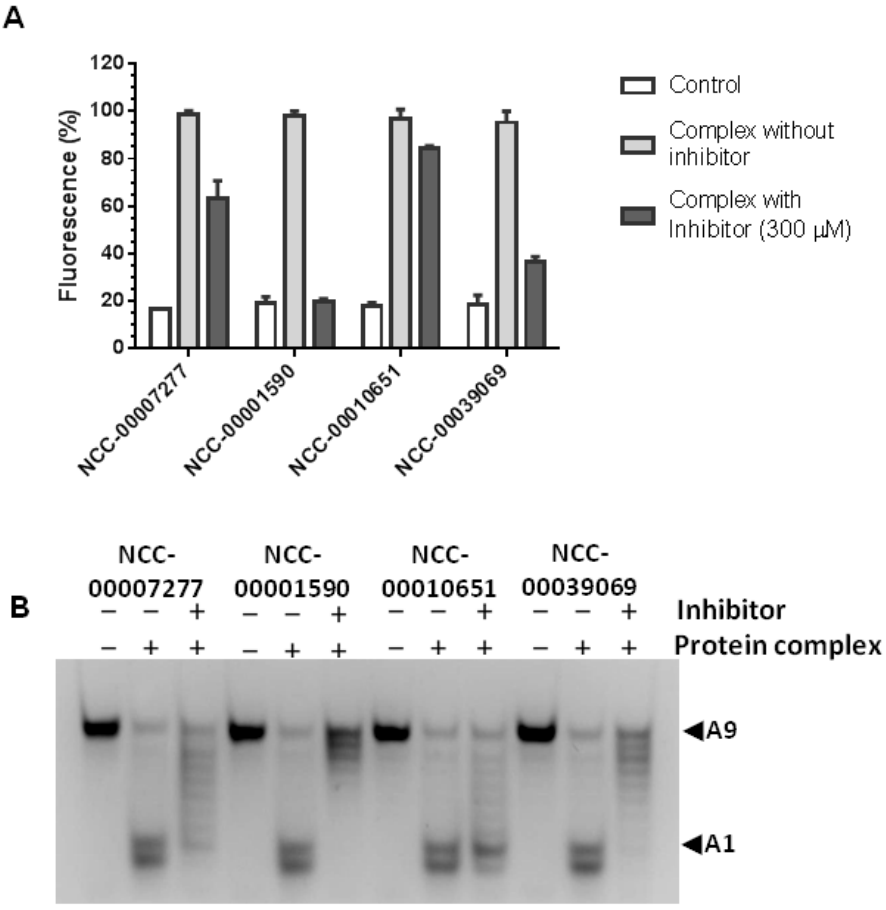

Figure 6.6 Effect of selective small molecule inhibitors of Caf1/CNOT7 on the activity of a BGT2-Caf1/CNOT7-Ccr4b/CNOT6L protein complex. (A) Inhibition of the deadenylase activity of a BGT2-Caf1/CNOT7-Ccr4b/CNOT6L protein complex by selective small molecule inhibitors of Caf1/CNOT7. Proteins were pre-incubated with the indicated compounds at room temperature for 15 min. After addition of Flc-labelled substrate RNA, reactions were incubated at 30°C for 60 min. Fluorescence was measured after addition of solution containing SDS and TAMRA-labelled probe. **(B)** Product analysis by a gel-based assay. Proteins were pre-incubated with the indicated compounds at room temperature for 15 min. After incubation at 30°C for 60 min, enzymatic reactions were terminated by heating at 85°C for 3 min. Products were separated by denaturing PAGE and directly visualized by epifluorescence. Indicated are the intact RNA substrates (A9) and the reaction product containing a single adenosine residue (A1).

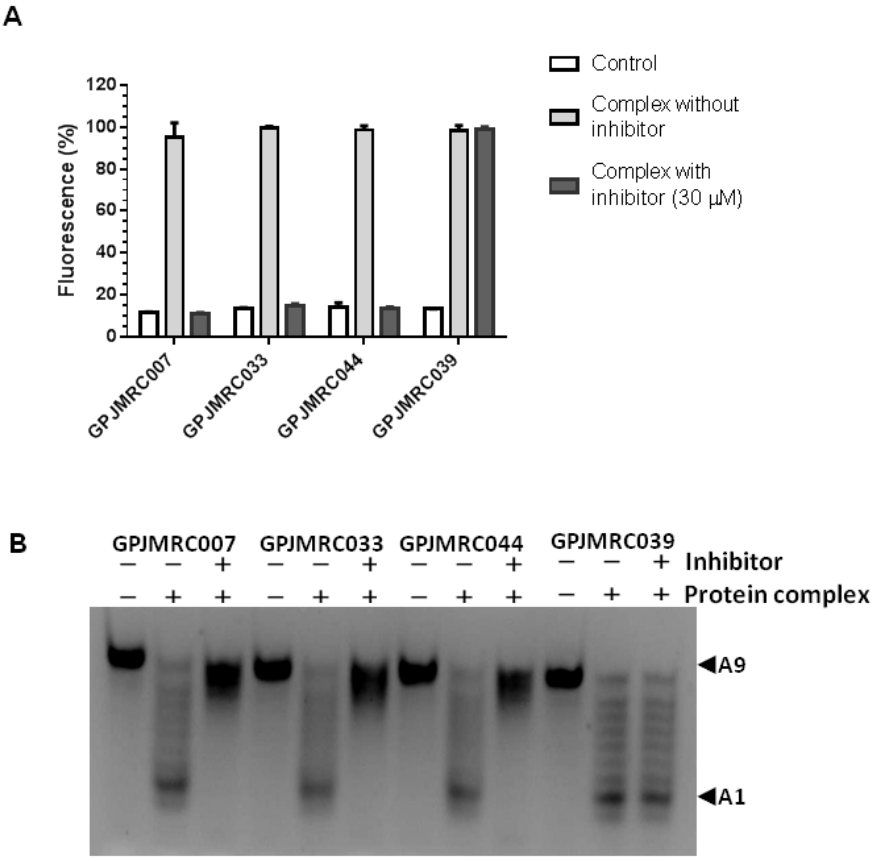

Figure 6.7 Effect of new synthetic Caf1/CNOT7 inhibitors on the activity of a BGT2-Caf1/CNOT7-Ccr4b/CNOT6L protein complex. (A) A Fluorescence-based assay to assess the effect of Caf1/CNOT7 inhibitors on the activity of a BGT2-Caf1/CNOT7-Ccr4b/CNOT6L protein complex. Proteins were pre-incubated with the indicated compounds at room temperature for 15 min. After addition of Flc-labelled substrate RNA, reactions were incubated at 30°C for 60 min. Fluorescence was measured after addition of solution containing SDS and TAMRA-labelled probe. **(B)** Product analysis by a gel-based assay. Proteins were pre-incubated with the indicated compounds at room temperature for 15 min. After incubation at 30°C for 60 min, enzymatic reactions were terminated by heating at 85°C for 3 min. Products were separated by denaturing PAGE and directly visualized by epifluorescence. Indicated are the intact RNA substrates (A9) and the reaction product containing a single adenosine residue (A1).

6.6 Deadenylase activity of a BTG2-Caf1/CNOT7-Ccr4a/CNOT6 protein complex

To further explore the contribution of the Ccr4 subunit to the deadenylase activity of the nuclease module of Ccr4-Not, we assessed the deadenylase activity of a trimeric nuclease protein complex containing the Ccr4a/CNOT6 subunit, which is highly related to Ccr4b/CNOT6L.

6.6.1 Generation of bacterial expression vectors

To construct plasmid pACYCDuet-1 GST-CNOT6/CNOT7 (pACYCDuet-1 M14), pACYCDuet-1 M06 was used as the initial plasmid. Firstly, the GST-Ccr4b/CNOT6L cDNA was removed from pACYCDuet-1 M06 by digestion using NcoI and NotI. Then, the CNOT6 cDNA was amplified by PCR to include an NcoI restriction site and a GST-tag. Plasmid pGEX4T1-CNOT6 was used as a template to amplify the GST-CNOT6 cDNA. The PCR product was digested using the NcoI and NotI restriction enzymes, then subcloned into the NcoI and NotI restriction sites of pACYCDuet-1 (Figure 6.8). The correct ligation of the cDNA fragments in MCS 1 of pACYCDuet-1 was confirmed by restriction enzyme digestion using NcoI and NotI enzymes. Finally, PCRs were conducted to amplify the GST-CNOT6 of plasmid pACYCDuet-1 M14 for sequencing. To amplify the GST-CNOT6 cDNA, primers ACYCDuetUP1 and DuetDOWN were used.

Derivatives of plasmid pACYCDuet-1 M14 were also constructed. To construct plasmid pACYCDuet-1 GST-CNOT6/CNOT7 D40A (pACYCDuet-1 M15), pACYCDuet-1 M07 was used as a starting point. To construct pACYCDuet-1 GST-CNOT6 E240A/CNOT7 plasmid (pACYCDuet-1 M16), the GST·CNOT6 E240A cDNA was amplified and sub-cloned into the NcoI and NotI restriction sites of pACYCDuet-1 M06. PCRs were conducted to amplify the GST·CNOT6 E240A of the pACYCDuet-1 M16 plasmid for sequencing. To amplify GST-CNOT6, ACYCDuetUP1 and DuetDOWN primers were used. A plasmid containing two mutations, pACYCDuet-1 GST-CNOT6L

E240A/CNOT7 D40A (pACYCDuet-1 M17), was also constructed (Table 6.1). All plasmids with site-directed mutations were verified by DNA sequencing.

Plasmid	Caf1/CNOT7	Ccr4a/CNOT6
pACYCDuet-1 M14	WT	WT
pACYCDuet-1 M15	D40A	WT
pACYCDuet-1 M16	WT	E240A
pACYCDuet-1 M17	D40A	E240A

Table 6.1 Derivatives of plasmid pACYCDuet-1 CNOT6/CNOT7.

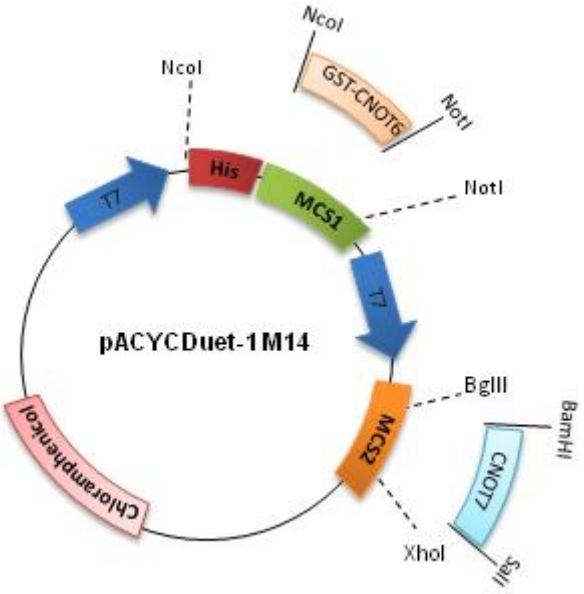

Figure 6.8 Generation of plasmid pACYCDuet-1 GST-CNOT6/CNOT7. Vector pACYCDuet-1 was used to generate pACYCDuet-1 GST-CNOT6/CNOT7. A CNOT7 cDNA (BamHI-SalI) was inserted in the BglII and XhoI restriction sites of MCS 2. The GST-CNOT6 cDNA was inserted into the NcoI and NotI restriction sites of MCS 1.

6.6.2 Expression and purification of a His•BGT2-Caf1/CNOT7-GST•CNOT6 protein complex

Co-expression of His•BTG2, Caf1/CNOT7 and GST•CNOT6 was initiated by co-transformation of plasmids pACYCDuet-1 M14 and pQE80L-BTG2 into BL21 (DE3) cells. A single colony containing plasmids pACYCDuet-1 M14 and PQE80L-BTG2 was used to inoculate a starter culture for protein expression. The pre-culture was then grown in 2 L of LB containing chloramphenicol (34 µg/ml) and ampicillin (100 µg/ml) at 37°C until the OD (600 nm) was between 0.6-0.8. IPTG (final concentration of 0.1 mM) was added to the culture to induce the expression of the proteins. Purification of the protein complex was conducted using a two-step purification (Chapter 5). First, immobilized metal ion affinity chromatography (IMAC) was performed followed by GST-affinity purification using glutathione-agarose. Based on the staining intensities of the protein bands, SDS-PAGE analysis showed that protein complexes appeared to have the expected stoichiometric ratio (1 : 1 : 1) and that the purity of the protein complexes was >90% (Figure 6.9A and Figure 6.9B). Western blot analysis confirmed the identity of the proteins (Figure 6.9C).

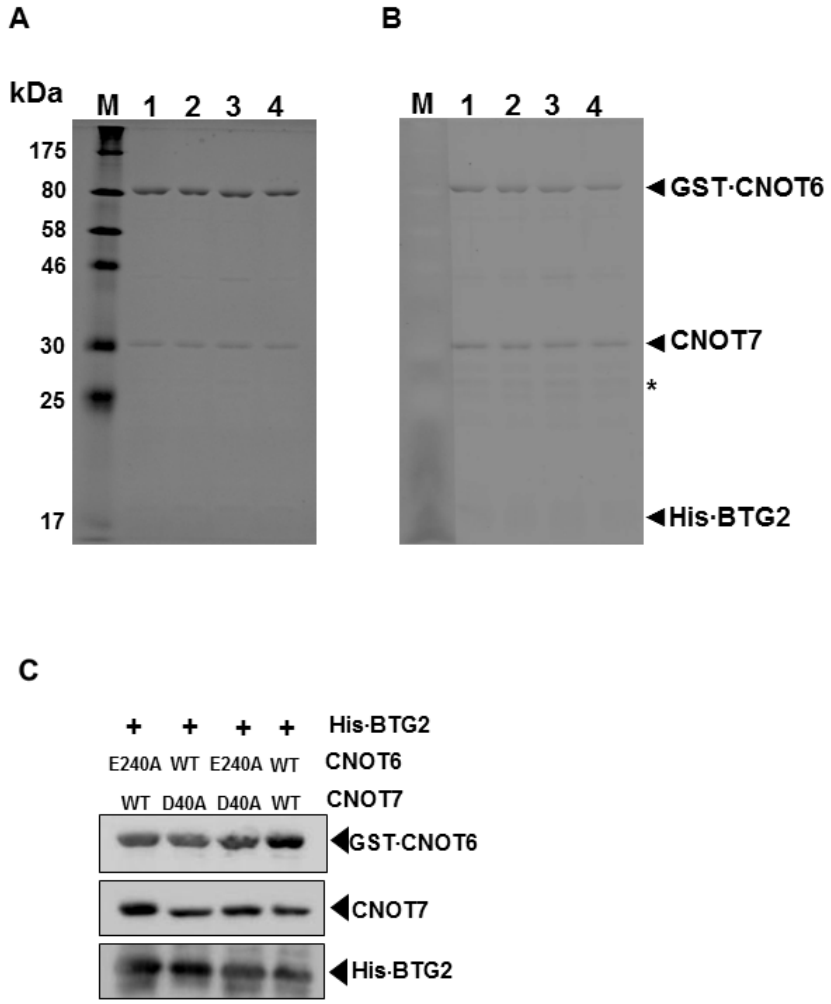

Figure 6.9 Analysis of purified protein complexes. (A, B) SDS-PAGE analysis of purified His•BTG2-Caf1/CNOT7-GST•CNOT6 protein complexes. Equal amounts of proteins were analyzed by 14% SDS-PAGE and stained using **(A)** Coomassie Brilliant Blue, or **(B)** SYPRO Ruby. Indicated are wild type protein (1), protein complex containing inactive version of CNOT7 D40A (2), protein complex containing inactive version of Ccr4a/CNOT6 E240A (3) and protein complex containing inactive version of Caf1/CNOT7 D40A and Ccr4a/CNOT6 E240A (4). **(C)** Western blot analysis of wild type and variant His•BTG2-Caf1/CNOT7-GST•CNOT6 protein complexes. Protein samples were separated by 14% SDS-PAGE and western blot analysis was conducted using anti-CNOT6, anti-CNOT7 and anti-His primary antibodies.

6.6.3 His•BTG2-Caf1/CNOT7-GST•CNOT6 protein complex displays deadenylase activity

The fluorescence-based assay was used to determine the deadenylase activity of the His•BTG2-Caf1/CNOT7-GST•Ccr4a/CNOT6 protein complex. Different concentrations of the wild type protein complex and the variant containing inactive nuclease subunits were incubated with Flc-labelled RNA substrate for an hour at 30°C. Then, a solution containing SDS and TAMRA-labelled DNA probe was added. Fluorescence was detected after incubation of the substrate with the wild type protein complex. As expected, no fluorescence was observed when the RNA substrate was incubated. This result indicated that the isolated wild type protein complex has deadenylase activity, and there are no contaminating activities from *E. coli* present in the purified protein samples (Figure 6.10A). Product analysis using a gel based assay also demonstrated that the RNA substrate was degraded in the presence of the wild type of protein complex, but remained intact in the absence of protein, or in the presence of protein complex containing inactive subunits (Figure 6.10B).

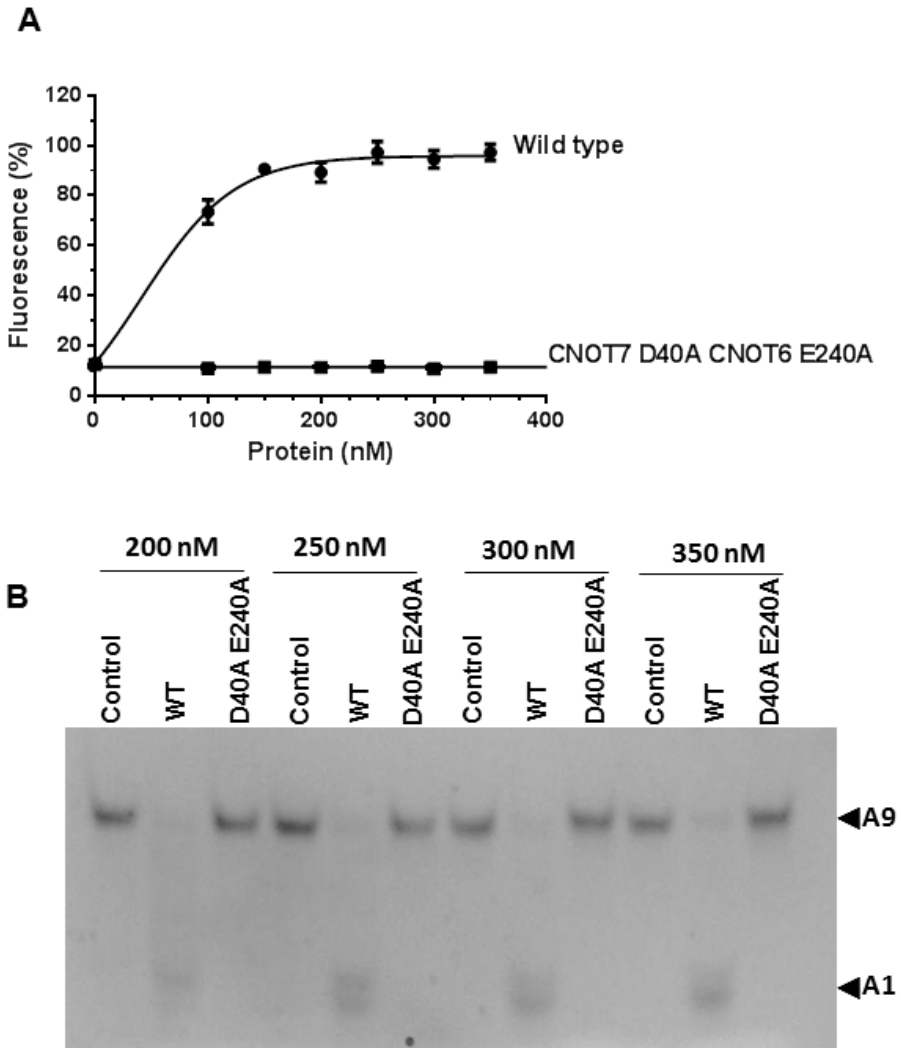

Figure 6.10 Deadenylase activity of His•BTG2-Caf1/CNOT7-GST•Ccr4a/CNOT6 protein complex. (A) Fluorescence-based assay to determine deadenylase activity of His•BTG2-Caf1/CNOT7-GST•Ccr4a/CNOT6. Wild type and variant His•BTG2-Caf1/CNOT7-GST•Ccr4a/CNOT6 protein complexes containing inactive nuclease subunits were incubated with RNA substrate for 60 minutes at 30°C. A stop/probe mix containing SDS and DNA probe was added and fluorescence measured. **(B)** Product analysis by gel-based assay to confirm the deadenylase activity of His•BTG2-Caf1/CNOT7-GST•Ccr4a/CNOT6. Proteins were incubated with RNA substrate at 30°C for 60 minutes, then enzymatic reactions were terminated by heating at 85°C for 3 min. Products were separated by denaturing PAGE and directly visualized by epifluorescence. Indicated are the intact RNA substrates (A9) and the reaction product containing a single adenosine residue (A1).

To determine the role of the nuclease subunits on the activity of the His•BTG2-Caf1/CNOT7-GST•Ccr4a/CNOT6 protein complex, we compared the deadenylase activity of wild type and three variant protein complexes containing inactive deadenylase subunits. We assessed the activity using three different concentrations of protein complex (150, 250 and 350 nM). Proteins were incubated with Flc-labelled RNA substrate for one hour at 30°C. Then the enzymatic reactions were stopped by adding TAMRA-labelled DNA probe containing SDS (0.5% final concentration). As shown in Figure 6.11A, fluorescence was only detected in the presence of the wild type protein complex. As was the case for the His•BTG2-Caf1/CNOT7-GST•Ccr4b/CNOT6L protein complex, all three variant protein complexes containing catalytically inactive deadenylase subunits did not show any deadenylase activity. The catalytically inactive versions of either Caf1/CNOT7 or Ccr4a/CNOT6 completely deleted the activity of the protein complex. Gel-based assays confirmed that there was degradation of RNA substrate in the presence of wild type protein complex, which was not observed in the presence of any of the variant protein complexes (Figure 6.11B). Together these data suggest that the activity of the protein complex requires both Caf1/CNOT7 and Ccr4a/CNOT6.

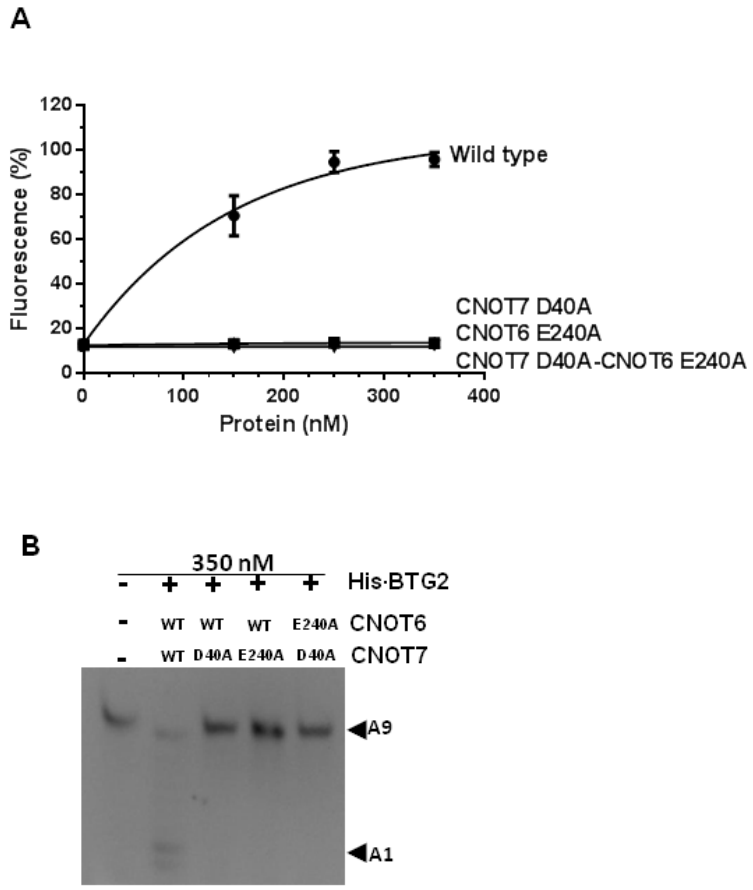

Figure 6.11 Deadenylase activity of the His•BTG2-Caf1/CNOT7-GST•Ccr4a/CNOT6 protein complex requires the activity of both Caf1/CNOT7 and Ccr4a/CNOT6. (A) Fluorescence-based deadenylation assay of wild type and variant His•BTG2-Caf1/CNOT7-GST•Ccr4a/CNOT6 protein complexes. Proteins were incubated with RNA substrate for 60 minutes at 30°C. Then a solution containing SDS and DNA probe was added and fluorescence measured. **(B)** Gel-based deadenylation assay of wild type and variant His•BTG2-Caf1/CNOT7-GST•Ccr4a/CNOT6 protein complexes. Equal amounts of wild-type and mutant protein (350 nM) were incubated with RNA substrate (1 μM). After 60 min incubation at 30°C, the reaction mixture was subjected to denaturing PAGE and visualized using epifluorescence. Indicated are the intact RNA substrates (A9) and the product containing a single adenosine residue (A1).

6.7 Discussion

Having successfully purified Caf1/CNOT7, Ccr4b/CNOT6L ΔLRR (Chapter 3), the dimeric His•BTG2-Caf1/CNOT7 complex, and the trimeric His•BTG2-Caf1/CNOT7-GST•Ccr4b/CNOT6L protein complex (Chapter 5), it was possible to compare the deadenylase activities of the protein samples.

In vitro analysis demonstrated that the dimeric His•BTG2-Caf1/CNOT7 protein complex was more active than the Caf1/CNOT7 monomer. This was surprising, because it has been reported that BTG2 and its family member Tob can inhibit the activity of Caf1/CNOT7. However, the result is in agreement with the findings that BTG2 and Tob can act as general activators of mRNA deadenylation (Ezzeddine et al., 2007, Mauxion et al., 2008).

The trimeric His•BTG2-Caf1/CNOT7-GST•Ccr4b/CNOT6L nuclease module was more active than the dimeric His•BTG2-Caf1/CNOT7 complex suggesting that the Ccr4b/CNOT6L does contribute to the activity of the trimeric nuclease complex. To understand the relative contributions of the Caf1/CNOT7 and Ccr4b/CNOT6L subunits in more detail, well characterised amino acid substitutions, D40A of Caf1/CNOT7 and E240A of Ccr4b/CNOT6L, were used. Residue Asp-40 is critical for the activity of Caf1/CNOT7 (Wang et al., 2010, Thore et al., 2003) and residue Glu-240 is important for the deadenylase activity of the Ccr4b/CNOT6L enzyme (Wang et al., 2010).

Nuclease modules containing inactive Caf1/CNOT7 did not display deadenylase activity and were indistinguishable from complexes with no active nuclease subunit. To further investigate this result, we tested the effect of Caf1/CNOT7 inhibition in the protein complex using small molecule inhibitors, which inhibited the deadenylase activity of the trimeric nuclease complex. Thus, it was concluded that Caf1/CNOT7 is required for the activity of a BTG2-Caf1/CNOT7-Ccr4b/CNOT6L complex. This result indicates a marked difference to the situation in *Saccharomyces cerevisiae*. In yeast, Caf1 deadenylase activity is not required for its in vivo function and the Ccr4

subunit is the main deadenylase subunit of the Ccr4-Not complex (Chen et al., 2002, Tucker et al., 2002, Viswanathan et al., 2004).

Even though the activity of isolated Ccr4b/CNOT6L ΔLRR was low, it also makes a major contribution to the deadenylase activity of the trimeric nuclease complex, because complexes containing inactive Ccr4b/CNOT6L did not display any activity and were indistinguishable from trimeric modules with no active nuclease subunit. To further investigate the role of the Ccr4 subunit, a trimeric BTG2-Caf1/CNOT7-Ccr4a/CNOT6 complex was characterised showing that active Ccr4a/CNOT6 is also required for the deadenylase activity of the complex. It would be interesting to establish the effect of Ccr4 (CNOT6/CNOT6L) inhibition on the activity of the nuclease module using pharmacological tools. Thus, it can be concluded that the activities of the BTG2-Caf1/CNOT7-Ccr4a/CNOT6 and BTG2-Caf1/CNOT7-Ccr4b/CNOT6L nuclease modules require the activity of both the Caf1/CNOT7 and the Ccr4a/CNOT6 or Ccr4b/CNOT6L nuclease subunits.

This conclusion is surprising, because several results indicated that the nuclease subunits have unique roles. Firstly, as mentioned above, the catalytic activity of Caf1 is dispensable in *Saccharomyces cerevisiae*, indicating that the enzyme activity of Ccr4 is sufficient for deadenylation (Chen et al., 2002, Tucker et al., 2002, Viswanathan et al., 2004). In addition, knockdown of the Caf1 paralogues in human cells differentially affects gene expression as compared to knockdown of the Ccr4 paralogues (Aslam et al., 2009, Mittal et al., 2011). Also, the isolated Caf1 protein or the purified EEP domain of Ccr4 are active ribonuclease enzymes. Finally, the structural analysis of a minimal nuclease module composed of the yeast MIF4G domain of Not1, Caf1 and Ccr4 indicated that the active sites of Caf1 and Ccr4 are not in close proximity (Basquin et al., 2012). While we only investigated the role of a nuclease sub-complex, it may be likely that both enzyme activities are also required in the context of the complete Ccr4-Not complex, although we

cannot exclude that the accessory subunits of the Ccr4-Not complex modulate the activity of the nuclease module.

In summary, we conclude that the activities of the Caf1/CNOT7-Ccr4b/CNOT6L or Caf1/CNOT7-Ccr4a/CNOT6 deadenylase modules (i) are not inhibited by BTG2; and (II) require the activities of both the Caf1/CNOT7 and the Ccr4a/CNOT6 or Ccr4b/CNOT6L nuclease subunits.

Chapter 7

Concluding Remarks and Future Outlook

Chapter 7. Concluding Remarks and Future Outlook

In this work, a new in vitro deadenylase assay is described, which is sensitive, quantitative and suitable for small volumes and micro-well plate formats (Chapter 3). The new method was used for the discovery of small molecule inhibitors of the Caf1/CNOT7 deadenylase enzyme and the characterization of analogues (Chapter 4). Furthermore, it was used to investigate whether both catalytic subunits of the Ccr4-Not complex work cooperatively or whether the subunits have unique roles in deadenylation. To achieve this, a method is described to express and purify a nuclease module of the Ccr4-Not complex consisting of BTG2-Caf1/CNOT7-Ccr4/CNOT6L from bacterial cells (Chapter 5). Deadenylase activity of the trimeric protein complex and individually isolated subunits were assessed using the fluorescence-based assay showing that the activity of the nuclease complex is higher as compared to the monomeric subunits. The analysis of purified complexes containing well-characterised inactivating amino acid substitutions demonstrated that the enzyme activities of Caf1 and Ccr4 are both required for deadenylation. This was confirmed by applying the discovered small molecule inhibitors of Caf1/CNOT7 as well as the analysis of the highly related BGT2-Caf1/CNOT7-Ccr4/CNOT6 protein complex (Chapter 6).

7.1 A fluorescence-based assay to assess deadenylase activity

In vitro deadenylase assays are useful to identify and characterize deadenylase enzymes. There are several limitations with the previously described in vitro deadenylase assays. Gel-based assays are expensive, laborious and time consuming. Moreover, it is difficult to obtain quantitative information from gels or use gel-based detection for high throughput screening of libraries compound collections (Chen et al., 2002, Viswanathan et al., 2003). The methylene blue method, which is based on a shift in the absorbance maximum of methylene blue upon RNA binding, is relatively insensitive and requires high enzyme concentrations (Greiner-Stoeffele et al.,

1996, Liu and Yan, 2008). The recently published method based on Size-Exclusion Chromatography (SEC) is also time consuming, laborious, and relatively insensitive (Balatsos et al., 2012).

Therefore, a new fluorescence-based method was developed (Chapter 3). This method is based on *Förster* resonance energy transfer (FRET). The principle of this assay is the complementarity of the DNA probe and RNA substrate in the absence of deadenylase activity, resulting in the close proximity of fluorescein (Flc) conjugated to the RNA substrate and a tetramethylrhodamine (TAMRA) moiety attached to the DNA probe. In the absence of substrate degradation, fluorescence of the Flc moiety is quenched. In contrast, in the presence of deadenylase enzyme activity, degradation of the RNA substrate prevents efficient annealing of the DNA probe. In this situation, Flc-mediated fluorescence can be detected. The fluorescence-based assay is sensitive, can be used for quantitative analysis and is suitable for screening compound libraries and the characterisation of small molecule inhibitors.

7.2 Small molecule inhibitors of the Caf1/CNOT7 deadenylase enzyme

Caf1/CNOT7 is one example of an enzyme, which requires the presence of Mg^{2+} ions for its activity (Thore et al., 2003, Jonstrup et al., 2007, Horiuchi et al., 2009, Winkler and Balacco, 2013). Although few inhibitors of such enzymes have been described, it may be possible to identify small-molecule inhibitors of Mg^{2+}-dependent RNA/DNA nucleases as evidenced by the reported inhibitors of FEN-1, a DNA structure-specific endonuclease, as well as the Human Immunodeficiency Virus (HIV)-encoded RNAse H enzyme. In Chapter 4, the utility of the fluorescence-based assay for the discovery and characterisation of small molecule inhibitors of the Caf1/CNOT7 enzyme is described.

Through library screening, one inhibitor with relatively high affinity was identified. However, this compound was not selective as the compound

partially inhibited both Ccr4/CNOT6L and PARN. Five compounds with relatively low potency were also identified. Furthermore, we characterised four synthetic analogues, which are selective inhibitors of Caf1/CNOT7. These compounds were N-hydroxy diketone purine analogues, which are predicted to interact with the Mg^{2+} ions in the active site of Caf1/CNOT7, thus blocking interactions with the RNA substrate. These small molecule inhibitors may be useful as tool compounds to understand in more detail the cellular roles of deadenylase enzymes. It has been reported that *Cnot7* knockout mice display enhanced bone formation (Washio-Oikawa et al., 2007). Thus, Caf1/CNOT7 may be a potential novel target for drugs that increase bone density. The discovered inhibitors may be a first step towards such therapeutics.

7.3 The enzyme activities of Caf1/CNOT7 and Ccr4/CNOT6L are both required for deadenylation by the human Ccr4-Not nuclease module

The Ccr4-Not complex, which contains two catalytic subunits, is a major deadenylase enzyme involved in the shortening and removal of the poly(A) tail of mRNA. However, it has been unclear whether the catalytic nuclease subunits cooperate in deadenylation, or whether they have unique roles.

To further investigate the relative contributions of the Caf1/CNOT7 and Ccr4/CNOT6L nuclease subunits, we first developed strategies to express and purify a nuclease sub-complex containing the Caf1/CNOT7 and Ccr4/CNOT6L catalytic components (Chapter 5). Initially, plasmids for co-expression of Ccr4/CNOT6L and Caf1/CNOT7 were generated using the pACYCDuet-1 vector (Merck). We succeeded in obtaining a purified Ccr4-Not nuclease module by co-expressing Caf1/CNOT7, Ccr4/CNOT6L and BTG2, whose interaction with Caf1/CNOT7 is well characterised (Mauxion et al., 2008, Winkler, 2010). Trimeric His•BTG2-Caf1/CNOT7-Ccr4/CNOT6L and dimeric His•BTG2-Caf1/CNOT7 were obtained using consecutive immobilised metal affinity chromatography and gel filtration. Alternatively, we obtained a

purified His•BTG2-Caf1/CNOT7-GST•Ccr4/CNOT6L nuclease module by consecutive immobilised metal and glutathione affinity chromatography.

In Chapter 6, we provide evidence that the deadenylase activities of both Caf1/CNOT7 and Ccr4b/CNOT6L are required for deadenylation. The findings are based on the newly developed strategy for expression and purification of a trimeric His•BTG2-Caf1/CNOT7-GST•Ccr4/CNOT6L protein complex. This strategy allowed the analysis of purified protein complexes containing one catalytically inactive subunit (either Caf1/CNOT7 or Ccr4b/CNOT6L) or two inactive subunits (both Caf1/CNOT7 and Ccr4b/CNOT6L). Three independent approaches indicate that the deadenylase activity of both subunits is required: (i) the analysis of trimeric protein complex, BTG2-Caf1/CNOT7-Ccr4b/CNOT6L; (ii) the effect of Caf1/CNOT7 inhibitors on the deadenylase activity of trimeric protein complex; (iii) the analysis of a highly related BTG2-Caf1/CNOT7-Ccr4/CNOT6 protein complex. The conclusion that both Caf1/CNOT7 and Ccr4/CNOT6L are required for the deadenylase activity of the trimeric protein complex is surprising, because several reports indicated that the nuclease subunit have unique roles. In *Saccharomyces cerevisiae*, the Ccr4 subunit is the main deadenylase and the activity of Caf1 (Pop2) is not required for the deadenylation process (Chen et al., 2002, Tucker et al., 2002, Viswanathan et al., 2004). In addition, the phenotypes and gene expression profiles of breast cancer cells upon knockdown of Caf1 (CNOT7/CNOT8) are distinct from those of Ccr4 (CNOT6/CNOT6L) knockdown cells (Mittal et al., 2011, Aslam et al., 2009). Moreover, structural analysis of a minimal nuclease containing yeast Not1 (MIF4G domain), Caf1 and Ccr4 indicated that the active sites of Caf1 and Ccr4 are not in close proximity (Basquin et al., 2012). The data presented in Chapter 6 also indicate that the activity of a BTG2-Caf1/CNOT7 dimeric protein complex is higher than that of the monomeric Caf1/CNOT7 protein. In addition, a BTG2-Caf1/CNOT7-Ccr4b/CNOT6L trimeric protein complex was also more active than His·BTG2-CNOT7 or any of the

monomeric subunits. This data was unexpected, because it was previously reported that BTG2 is able to inhibit the deadenylase activity of Caf1/CNOT7 . However, our finding is in agreement with the finding that BTG2 is a positive regulator of mRNA deadenylation (Horiuchi et al., 2009, Mauxion et al., 2008).

Taken together, the data presented in Chapter 6 supports a model in which the nuclease subunits of the Ccr4-Not complex cooperate in deadenylation. We speculate that the deadenylase activity of the complex requires the consecutive action of Caf1/CNOT7 and Ccr4b/CNOT6L, possibly to prevent product inhibition by AMP (Figure 7.1).

Even though Caf1/CNOT7 and Ccr4/CNOT6L have low activity in vitro (Chapter 3), the enzyme activity might be higher in cells because of the stimulation of other proteins. Some proteins, for example the BTG/Tob proteins and tritetrapolin (TTP) protein interact with sub-units of the Ccr4-Not complex in order to mediate the recruitment of the Ccr4-Not complex to specific mRNAs. Tob1 protein acts as mediator for interaction with the C-terminal domain of PABP. Through this interaction, Tob1 facilitates the recruitment of the Ccr4-Not complex to specific RNA (Ezzeddine et al., 2007, Funakoshi et al., 2007, Mauxion et al., 2008, Hosoda et al., 2011). TTP acts as bridge to mediate the recruitment of Ccr4-Not complex via an interaction with the scaffold protein CNOT1. TTP binds to AREs and activate mRNA decay (Fabian et al., 2013). Thus, the apparent affinity of Ccr4-Not to specific mRNAs may be significantly increased by these mechanisms. Moreover, it may be possible that the non-catalytic subunits of the Ccr4-Not complex may also stimulate its associated deadenylase activity. Caf1 and Ccr4 subunits may also have roles independent of Ccr4-Not.

In summary, the work presented in this thesis describes the successful development of a new fluorescence-based method to assess deadenylase activity. The utility of the method for the discovery and characterisation of Caf1/CNOT7 inhibitors is demonstrated. Finally, a strategy for the expression

and purification of a trimeric BTG2•Caf1/CNOT7•Ccr4b/CNOT6L nuclease module is reported. The analysis of this complex using the fluorescence-based assay indicates that the enzyme activity of both Caf1/CNOT7 and Ccr4/CNOT6(L) is required for deadenylase activity of the nuclease module.

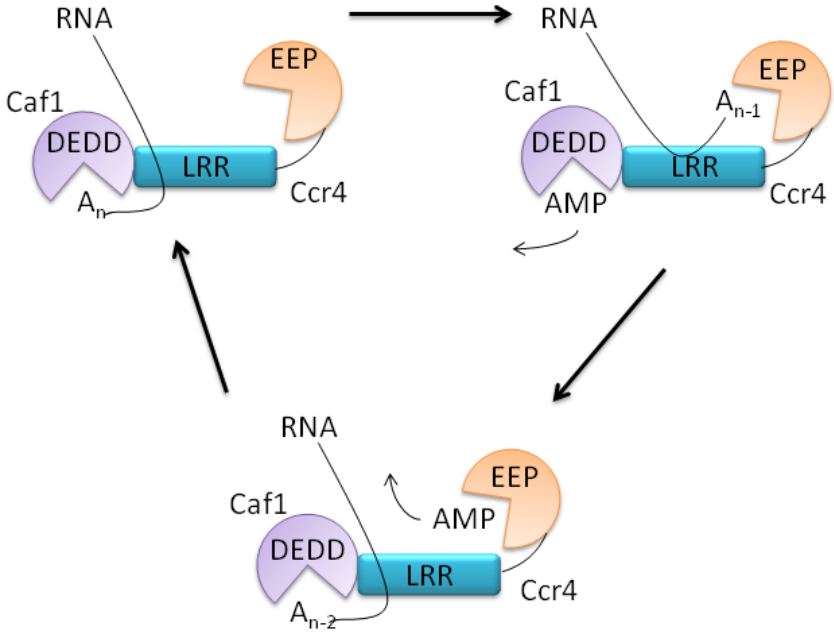

Figure 7.1 Model for deadenylation by the Ccr4-Not complex. A speculative schematic model for deadenylation mediated by the nuclease module of the Ccr4-Not complex. In this model, both catalytic subunits participate and concecutive action by the Caf1(CNOT7/CNOT8) and Ccr4 (CNOT6/CNOT6L) subunits is required. Significant conformations change in the substrate RNA or the nuclease components may be required.

7.4 Future outlook

The work described in this thesis presents a new method for the fluorescence-based measurement of deadenylase activity. We used the new method to assess the deadenylase activity of Caf1/CNOT7, Ccr4b/CNOT6L and PARN. We believe that this method can also be used to determine the deadenylase activities of other enzymes, such as, for example, Pop2/CNOT8, which is highly related to Caf1/CNOT7, Pan2 and the Pan2-Pan3 complex. Because Pan2-Pan3 enzyme does not efficiently degrade the final 20-25 nt (Lowell et al., 1992, Wolf and Passmore, 2014), the substrate must be longer than 25 A residues when this assay is used to assess its enzyme activity. This might be achieved by extending the oligonucleotide substrate using *E. coli* polyA polymerase, in combination with probes recognising oligo(A). In addition, it should be relatively straightforward to adapt the assay for the characterisation of a wide variety of exo- and endonucleases, such as Smg6, which is involved in nonsense-mediated decay, and the exosome-associated Dis3 and Dis3L1 subunits, which display both exonuclease activity (associated with the central RNB domain) and endonuclease activity (residing in the N-terminal PIN domain).

One application of the fluorescence-based assay is the discovery and characterisation of small molecule inhibitors (Chapter 4). Cell-permeable, small molecule inhibitors may be used as research tools that are complementary to other approaches, such as siRNA-mediated knockdown. The specific advantage of small molecule inhibitors is their ability to inhibit the enzymatic activity of proteins without interfering with structural roles. Chemical tools are underused in the study of post-transcriptional gene regulation and a toolbox of molecules inhibiting the ribonuclease activities of various nucleases involved in mRNA degradation and RNA quality control would be extremely valuable. Furthermore, small molecule inhibitors can also guide the development of new therapeutic agents. For example, previous

research indicated that *Cnot7* knockout mice have increased bone density (Washio-Oikawa et al., 2007). Based on this, further investigations of small molecule inhibitors of Caf1/CNOT7 using animal models would be interesting in the field of osteoporosis.

The characterisation of the activity of a small set of proteins containing amino acid substitutions is a second application of the fluorescence-based assay (Chapter 6). In combination with the development of a method to express and purify a trimeric nuclease module of human Ccr4-Not (Chapter 5), this led to the surprising finding that both Caf1 and Ccr4 are required for deadenylation by a human Ccr4-Not nuclease module. The use of selective small molecules of Caf1 and Ccr4 would be useful to investigate roles for Caf1 or Ccr4 that are independent of Ccr4-Not. Moreover, this finding illustrates that the molecular mechanism of deadenylation by Ccr4-Not is not well understood. Further structural information on the BTG2•Caf1/CNOT7•Ccr4b/CNOT6Lcomplex and biophysical investigations are required, which will be facilitated by the availability of a purified human Ccr4-Not nuclease module.

References

Ajima, R., Akiyama, T., Usui, M., Yoneda, M., Yoshida, Y., Nakamura, T., Minowa, O., Noda, M., Tanaka, S., Noda, T. & Yamamoto, T. 2008. Osteoporotic bone formation in mice lacking tob2; involvement of Tob2 in RANK ligand expression and osteoclasts differentiation. *FEBS Lett,* 582**,** 1313-8.

Albert, T. K., Hanzawa, H., Legtenberg, Y. I., de Ruwe, M. J., van den Heuvel, F. A., Collart, M. A., Boelens, R. & Timmers, H. T. 2002. Identification of a ubiquitin-protein ligase subunit within the CCR4-NOT transcription repressor complex. *EMBO J,* 21**,** 355-64.

Albert, T. K., Lemaire, M., van Berkum, N. L., Gentz, R., Collart, M. A. & Timmers, H. T. 2000. Isolation and characterization of human orthologs of yeast CCR4-NOT complex subunits. *Nucleic Acids Res. 2000 Feb 1;28(3):809-17.*

Andersen, K. R., Jonstrup, A. T., Van, L. B. & Brodersen, D. E. 2009. The activity and selectivity of fission yeast Pop2p are affected by a high affinity for Zn2+ and Mn2+ in the active site. *RNA. 2009 May;15(5):850-61. Epub 2009 Mar 23.*

Anderson, P. & Kedersha, N. 2009. RNA granules: post-transcriptional and epigenetic modulators of gene expression. *Nat Rev Mol Cell Biol. 2009 Jun;10(6):430-6.*

Aslam, A., Mittal, S., Koch, F., Andrau, J. C. & Winkler, G. S. 2009. The Ccr4-Not Deadenylase Subunits CNOT7 and CNOT8 Have Overlapping Roles and Modulate Cell Proliferation. *Molecular Biology of the Cell,* 20**,** 3840-3850.

Astrom, J., Astrom, A. & Virtanen, A. 1991. In vitro deadenylation of mammalian mRNA by a HeLa cell 3' exonuclease. *Embo j,* 10**,** 3067-71.

Balatsos, N., Vlachakis, D., Chatzigeorgiou, V., Manta, S., Komiotis, D., Vlassi, M. & Stathopoulos, C. 2012. Kinetic and in silico analysis of the slow-binding inhibition of human poly(A)-specific ribonuclease (PARN) by novel nucleoside analogues. *Biochimie,* 94**,** 214-21.

Balatsos, N. A., Anastasakis, D. & Stathopoulos, C. 2009a. Inhibition of human poly(A)-specific ribonuclease (PARN) by purine nucleotides: kinetic analysis. *J Enzyme Inhib Med Chem,* 24**,** 516-23.

Balatsos, N. A., Vlachakis, D., Maragozidis, P., Manta, S., Anastasakis, D., Kyritsis, A., Vlassi, M., Komiotis, D. & Stathopoulos, C. 2009b. Competitive inhibition of human poly(A)-specific ribonuclease (PARN) by synthetic fluoro-pyranosyl nucleosides. *Biochemistry. 2009 Jul 7;48(26):6044-51.*

Bartlam, M. & Yamamoto, T. 2010. The structural basis for deadenylation by the CCR4-NOT complex. *Protein Cell. 2010 May;1(5):443-52. Epub 2010 Jun 4.*

Basquin, J., Roudko, V. V., Rode, M., Basquin, C., Seraphin, B. & Conti, E. 2012. Architecture of the Nuclease Module of the Yeast Ccr4-Not Complex: the Not1-Caf1-Ccr4 Interaction. *Mol Cell. 2012 Sep 5.*

Bawankar, P., Loh, B., Wohlbold, L., Schmidt, S. & Izaurralde, E. 2013. NOT10 and C2orf29/NOT11 form a conserved module of the CCR4-NOT complex that docks onto the NOT1 N-terminal domain. *RNA Biol,* 10**,** 228-44.

Beese, L. S. & Steitz, T. A. 1991. Structural basis for the 3'-5' exonuclease activity of Escherichia coli DNA polymerase I: a two metal ion mechanism. *Embo j,* 10**,** 25-33.

Behm-Ansmant, I., Rehwinkel, J., Doerks, T., Stark, A., Bork, P. & Izaurralde, E. 2006. mRNA degradation by miRNAs and GW182 requires both CCR4:NOT deadenylase and DCP1:DCP2 decapping complexes. *Genes Dev,* 20**,** 1885-98.

Bentley, D. L. 2005. Rules of engagement: co-transcriptional recruitment of pre-mRNA processing factors. *Curr Opin Cell Biol,* 17**,** 251-6.

Bianchin, C., Mauxion, F., Sentis, S., Seraphin, B. & Corbo, L. 2005. Conservation of the deadenylase activity of proteins of the Caf1 family in human. *RNA. 2005 Apr;11(4):487-94.*

Boeck, R., Tarun, S., Jr., Rieger, M., Deardorff, J. A., Muller-Auer, S. & Sachs, A. B. 1996. The yeast Pan2 protein is required for poly(A)-binding protein-stimulated poly(A)-nuclease activity. *J Biol Chem,* 271**,** 432-8.

Boiko, A. D., Porteous, S., Razorenova, O. V., Krivokrysenko, V. I., Williams, B. R. & Gudkov, A. V. 2006. A systematic search for downstream mediators of tumor suppressor function of p53 reveals a major role of BTG2 in suppression of Ras-induced transformation. *Genes Dev,* 20**,** 236-52.

.

Brown, C. E., Tarun, S. Z., Jr., Boeck, R. & Sachs, A. B. 1996. PAN3 encodes a subunit of the Pab1p-dependent poly(A) nuclease in Saccharomyces cerevisiae. *Mol Cell Biol. 1996 Oct;16(10):5744-53.*

Bushati, N. & Cohen, S. M. 2007. microRNA functions. *Annu Rev Cell Dev Biol,* 23**,** 175-205.

Chaga, G. S. 2001. Twenty-five years of immobilized metal ion affinity chromatography: past, present and future. *J Biochem Biophys Methods. 2001 Oct 30;49(1-3):313-34.*

Chang, Y. F., Imam, J. S. & Wilkinson, M. F. 2007. The nonsense-mediated decay RNA surveillance pathway. *Annu Rev Biochem,* 76**,** 51-74.

Charlesworth, A., Meijer, H. A. & de Moor, C. H. 2013. Specificity factors in cytoplasmic polyadenylation. *Wiley Interdiscip Rev RNA,* 4**,** 437-61.

Chen, C. Y. & Shyu, A. B. 1995. AU-rich elements: characterization and importance in mRNA degradation. *Trends Biochem Sci. 1995 Nov;20(11):465-70.*

Chen, C. Y. & Shyu, A. B. 2011. Mechanisms of deadenylation-dependent decay. *Wiley Interdiscip Rev RNA. 2011 Mar-Apr;2(2):167-83. doi: 10.1002/wrna.40. Epub 2010 Sep 15.*

Chen, J., Chiang, Y. C. & Denis, C. L. 2002. CCR4, a 3'-5' poly(A) RNA and ssDNA exonuclease, is the catalytic component of the cytoplasmic deadenylase. *EMBO J. 2002 Mar 15;21(6):1414-26.*

Chen, J., Rappsilber, J., Chiang, Y. C., Russell, P., Mann, M. & Denis, C. L. 2001. Purification and characterization of the 1.0 MDa CCR4-NOT complex identifies two novel components of the complex. *J Mol Biol. 2001 Dec 7;314(4):683-94.*

Chen, Y., Boland, A., Kuzuoglu-Ozturk, D., Bawankar, P., Loh, B., Chang, C. T., Weichenrieder, O. & Izaurralde, E. 2014. A DDX6-CNOT1 complex and W-binding pockets in CNOT9 reveal direct links between miRNA target recognition and silencing. *Mol Cell,* 54**,** 737-50.

Cho, J. W., Kim, J. J., Park, S. G., Lee, D. H., Lee, S. C., Kim, H. J., Park, B. C. & Cho, S. 2004. Identification of B-cell translocation gene 1 as a biomarker for monitoring the remission of acute myeloid leukemia. *Proteomics,* 4**,** 3456-63.

Colgan, D. F. & Manley, J. L. 1997. Mechanism and regulation of mRNA polyadenylation. *Genes Dev. 1997 Nov 1;11(21):2755-66.*

Collart, M. A. 2003. Global control of gene expression in yeast by the Ccr4-Not complex. *Gene,* 313**,** 1-16.

Collart, M. A. & Panasenko, O. O. 2011a. The Ccr4--not complex. *Gene. 2012 Jan 15;492(1):42-53. Epub 2011 Oct 15.*

Collart, M. A. & Panasenko, O. O. 2011b. The Ccr4--not complex. *Gene,492(1):42-53. Epub 2011 Oct 15.*

Coller, J. & Parker, R. 2004. Eukaryotic mRNA decapping. *Annu Rev Biochem,* 73**,** 861-90.

Conti, E. & Izaurralde, E. 2005. Nonsense-mediated mRNA decay: molecular insights and mechanistic variations across species. *Curr Opin Cell Biol,* 17**,** 316-25.

Cooper, G. M. & Hausman, R. E. 2000. *The Cell: A Molecular Approach, Sixth Edition,* Sunderland, Massachusetts U.S.A., Sinauer Associates, Inc.

Cowling, V. H. 2010. Regulation of mRNA cap methylation. *Biochem J,* 425**,** 295-302.

Dehlin, E., Wormington, M., Korner, C. G. & Wahle, E. 2000. Cap-dependent deadenylation of mRNA. *EMBO J. 2000 Mar 1;19(5):1079-86.*

Dlakic, M. 2000. Functionally unrelated signalling proteins contain a fold similar to Mg2+-dependent endonucleases. *Trends Biochem Sci. 2000 Jun;25(6):272-3.*

Doidge, R., Mittal, S., Aslam, A. & Winkler, G. S. 2012a. Deadenylation of cytoplasmic mRNA by the mammalian Ccr4-Not complex. *Biochem Soc Trans. 2012 Aug 1;40(4):896-901.*

Doidge, R., Mittal, S., Aslam, A. & Winkler, G. S. 2012b. The anti-proliferative activity of BTG/TOB proteins is mediated via the Caf1a (CNOT7) and Caf1b (CNOT8) deadenylase subunits of the Ccr4-not complex. *PLoS One,* 7**,** e51331.

Doma, M. K. & Parker, R. 2007. RNA quality control in eukaryotes. *Cell. 2007 Nov 16;131(4):660-8.*

Dominguez, C., Bonvin, A. M., Winkler, G. S., van Schaik, F. M., Timmers, H. T. & Boelens, R. 2004. Structural model of the UbcH5B/CNOT4 complex revealed by combining NMR, mutagenesis, and docking approaches. *Structure.* United States.

Draper, M. P., Liu, H. Y., Nelsbach, A. H., Mosley, S. P. & Denis, C. L. 1994. CCR4 is a glucose-regulated transcription factor whose leucine-rich repeat binds several proteins important for placing CCR4 in its proper promoter context. *Mol Cell Biol,* 14**,** 4522-31.

Dupressoir, A., Morel, A. P., Barbot, W., Loireau, M. P., Corbo, L. & Heidmann, T. 2001. Identification of four families of yCCR4- and Mg2+-dependent endonuclease-related proteins in higher eukaryotes, and characterization of orthologs of yCCR4 with a conserved leucine-rich repeat essential for hCAF1/hPOP2 binding. *BMC Genomics. 2001;2:9. Epub 2001 Nov 22.*

Eulalio, A., Huntzinger, E. & Izaurralde, E. 2008. GW182 interaction with Argonaute is essential for miRNA-mediated translational repression and mRNA decay. *Nat Struct Mol Biol,* 15**,** 346-53.

Ezzeddine, N., Chang, T. C., Zhu, W., Yamashita, A., Chen, C. Y., Zhong, Z., Yamashita, Y., Zheng, D. & Shyu, A. B. 2007. Human TOB, an antiproliferative transcription factor, is a poly(A)-binding protein-dependent positive regulator of cytoplasmic mRNA deadenylation. *Mol Cell Biol. 2007 Nov;27(22):7791-801. Epub 2007 Sep 4.*

Ezzeddine, N., Chen, C. Y. & Shyu, A. B. 2012. Evidence providing new insights into TOB-promoted deadenylation and supporting a link between TOB's deadenylation-enhancing and antiproliferative activities. *Mol Cell Biol,* 32**,** 1089-98.

Fabian, M. R., Cieplak, M. K., Frank, F., Morita, M., Green, J., Srikumar, T., Nagar, B., Yamamoto, T., Raught, B., Duchaine, T. F. & Sonenberg, N. 2011. miRNA-mediated deadenylation is orchestrated by GW182 through two conserved motifs that interact with CCR4-NOT. *Nat Struct Mol Biol. 2011 Oct 7;18(11):1211-7. doi: 10.1038/nsmb.2149.*

Fabian, M. R., Frank, F., Rouya, C., Siddiqui, N., Lai, W. S., Karetnikov, A., Blackshear, P. J., Nagar, B. & Sonenberg, N. 2013. Structural basis for the recruitment of the human CCR4-NOT deadenylase complex by tristetraprolin. *Nat Struct Mol Biol,* 20**,** 735-9.

Funakoshi, Y., Doi, Y., Hosoda, N., Uchida, N., Osawa, M., Shimada, I., Tsujimoto, M., Suzuki, T., Katada, T. & Hoshino, S. 2007. Mechanism of mRNA deadenylation: evidence for a molecular interplay between translation termination factor eRF3 and mRNA deadenylases. *Genes Dev. 2007 Dec 1;21(23):3135-48.*

Gao, M., Fritz, D. T., Ford, L. P. & Wilusz, J. 2000. Interaction between a poly(A)-specific ribonuclease and the 5' cap influences mRNA deadenylation rates in vitro. *Mol Cell. 2000 Mar;5(3):479-88.*

Garneau, N. L., Wilusz, J. & Wilusz, C. J. 2007a. The highways and byways of mRNA decay. *Nat Rev Mol Cell Biol. 2007 Feb;8(2):113-26.*

Garneau, N. L., Wilusz, J. & Wilusz, C. J. 2007b. The highways and byways of mRNA decay. *Nat Rev Mol Cell Biol,8(2):113-26.*

Gilmartin, G. M. 2005. Eukaryotic mRNA 3' processing: a common means to different ends. *Genes Dev,* 19**,** 2517-21.

Goldstrohm, A. C., Hook, B. A., Seay, D. J. & Wickens, M. 2006. PUF proteins bind Pop2p to regulate messenger RNAs. *Nat Struct Mol Biol. 2006 Jun;13(6):533-9. Epub 2006 May 21.*

Goldstrohm, A. C. & Wickens, M. 2008. Multifunctional deadenylase complexes diversify mRNA control. *Nat Rev Mol Cell Biol. 2008 Apr;9(4):337-44. Epub 2008 Mar 12.*

Greiner-Stoeffele, T., Grunow, M. & Hahn, U. 1996. A general ribonuclease assay using methylene blue. *Anal Biochem. 1996 Aug 15;240(1):24-8.*

Halees, A. S., El-Badrawi, R. & Khabar, K. S. 2008. ARED Organism: expansion of ARED reveals AU-rich element cluster variations between human and mouse. *Nucleic Acids Res,* 36**,** D137-40.

Halter, D., Collart, M. A. & Panasenko, O. O. 2014. The Not4 E3 ligase and CCR4 deadenylase play distinct roles in protein quality control. *PLoS One.* United States.

He, G. J., Liu, W. F. & Yan, Y. B. 2011. Dissimilar roles of the four conserved acidic residues in the thermal stability of poly(A)-specific ribonuclease. *Int J Mol Sci,* 12**,** 2901-16.

He, G. J. & Yan, Y. B. 2012. A deadenylase assay by size-exclusion chromatography. *PLoS One. 2012;7(3):e33700. Epub 2012 Mar 19.*

Horiuchi, M., Takeuchi, K., Noda, N., Muroya, N., Suzuki, T., Nakamura, T., Kawamura-Tsuzuku, J., Takahasi, K., Yamamoto, T. & Inagaki, F. 2009. Structural basis for the antiproliferative activity of the Tob-hCaf1 complex. *J Biol Chem. 2009 May 8;284(19):13244-55. Epub 2009 Mar 10.*

Hosoda, N., Funakoshi, Y., Hirasawa, M., Yamagishi, R., Asano, Y., Miyagawa, R., Ogami, K., Tsujimoto, M. & Hoshino, S. 2011. Anti-proliferative protein Tob negatively regulates CPEB3 target by recruiting Caf1 deadenylase. *EMBO J. 2011 Apr 6;30(7):1311-23. Epub 2011 Feb 18.*

Houseley, J. & Tollervey, D. 2009. The many pathways of RNA degradation. *Cell,136(4):763-76.*

Huntzinger, E. & Izaurralde, E. 2011. Gene silencing by microRNAs: contributions of translational repression and mRNA decay. *Nat Rev Genet,* 12**,** 99-110.

Huntzinger, E., Kuzuoglu-Ozturk, D., Braun, J. E., Eulalio, A., Wohlbold, L. & Izaurralde, E. 2013. The interactions of GW182 proteins with PABP and deadenylases are required for both translational repression and degradation of miRNA targets. *Nucleic Acids Res,* 41**,** 978-94.

Inada, T. & Makino, S. 2014. Novel roles of the multi-functional CCR4-NOT complex in post-transcriptional regulation. *Front Genet,* 5**,** 135.

Ito, K., Inoue, T., Yokoyama, K., Morita, M., Suzuki, T. & Yamamoto, T. 2011a. CNOT2 depletion disrupts and inhibits the CCR4-NOT deadenylase complex and induces apoptotic cell death. *Genes Cells. 2011 Apr;16(4):368-79. doi: 10.1111/j.1365-2443.2011.01492.x. Epub 2011 Feb 8.*

Ito, K., Takahashi, A., Morita, M., Suzuki, T. & Yamamoto, T. 2011b. The role of the CNOT1 subunit of the CCR4-NOT complex in mRNA deadenylation and cell viability. *Protein Cell. 2011 Sep;2(9):755-63. Epub 2011 Oct 6.*

Jonstrup, A. T., Andersen, K. R., Van, L. B. & Brodersen, D. E. 2007. The 1.4-A crystal structure of the S. pombe Pop2p deadenylase subunit unveils the configuration of an active enzyme. *Nucleic Acids Res,* 35**,** 3153-64.

Korner, C. G. & Wahle, E. 1997. Poly(A) tail shortening by a mammalian poly(A)-specific 3'-exoribonuclease. *J Biol Chem. 1997 Apr 18;272(16):10448-56.*

Korner, C. G., Wormington, M., Muckenthaler, M., Schneider, S., Dehlin, E. & Wahle, E. 1998. The deadenylating nuclease (DAN) is involved in poly(A) tail removal during the meiotic maturation of Xenopus oocytes. *EMBO J. 1998 Sep 15;17(18):5427-37.*

Lau, N. C., Kolkman, A., van Schaik, F. M., Mulder, K. W., Pijnappel, W. W., Heck, A. J. & Timmers, H. T. 2009a. Human Ccr4-Not complexes contain variable deadenylase subunits. *Biochem J,422(3):443-53.*

Lau, N. C., Kolkman, A., van Schaik, F. M., Mulder, K. W., Pijnappel, W. W., Heck, A. J. & Timmers, H. T. 2009b. Human Ccr4-Not complexes contain variable deadenylase subunits. *Biochem J. 2009 Aug 27;422(3):443-53.*

Li, Z., Pandit, S. & Deutscher, M. P. 1998. 3' exoribonucleolytic trimming is a common feature of the maturation of small, stable RNAs in Escherichia coli. *Proc Natl Acad Sci U S A,* 95**,** 2856-61.

Li, Z., Pandit, S. & Deutscher, M. P. 1999. Maturation of 23S ribosomal RNA requires the exoribonuclease RNase T. *RNA,* 5**,** 139-46.

Lin, W. J., Gary, J. D., Yang, M. C., Clarke, S. & Herschman, H. R. 1996. The mammalian immediate-early TIS21 protein and the leukemia-associated BTG1 protein interact with a protein-arginine N-methyltransferase. *J Biol Chem,* 271**,** 15034-44.

Liu, H. Y., Badarinarayana, V., Audino, D. C., Rappsilber, J., Mann, M. & Denis, C. L. 1998. The NOT proteins are part of the CCR4 transcriptional complex and affect gene expression both positively and negatively. *EMBO J. 1998 Feb 16;17(4):1096-106.*

Liu, W. F. & Yan, Y. B. 2008. Biophysical and biochemical characterization of recombinant human Pop2 deadenylase. *Protein Expr Purif,* 60**,** 46-52.

Loh, B., Jonas, S. & Izaurralde, E. 2013. The SMG5-SMG7 heterodimer directly recruits the CCR4-NOT deadenylase complex to mRNAs containing nonsense codons via interaction with POP2. *Genes Dev,* 27**,** 2125-38.

Lowell, J. E., Rudner, D. Z. & Sachs, A. B. 1992. 3'-UTR-dependent deadenylation by the yeast poly(A) nuclease. *Genes Dev,* 6**,** 2088-99.

Lykke-Andersen, J. & Wagner, E. 2005. Recruitment and activation of mRNA decay enzymes by two ARE-mediated decay activation domains in the proteins TTP and BRF-1. *Genes Dev,* 19**,** 351-61.

Magnusdottir, A., Johansson, I., Dahlgren, L. G., Nordlund, P. & Berglund, H. 2009. *Enabling IMAC purification of low abundance recombinant proteins from E. coli lysates*, Nat Methods. 2009 Jul;6(7):477-8.

Mandel, C. R., Bai, Y. & Tong, L. 2008. Protein factors in pre-mRNA 3'-end processing. *Cell Mol Life Sci,* 65**,** 1099-122.

Martinez, J., Ren, Y. G., Nilsson, P., Ehrenberg, M. & Virtanen, A. 2001. The mRNA cap structure stimulates rate of poly(A) removal and amplifies processivity of degradation. *J Biol Chem. 2001 Jul 27;276(30):27923-9. Epub 2001 May 18.*

Martinez, J., Ren, Y. G., Thuresson, A. C., Hellman, U., Astrom, J. & Virtanen, A. 2000. A 54-kDa fragment of the Poly(A)-specific ribonuclease is an oligomeric, processive, and cap-interacting Poly(A)-specific 3' exonuclease. *J Biol Chem. 2000 Aug 4;275(31):24222-30.*

Matsuda, S., Rouault, J., Magaud, J. & Berthet, C. 2001. In search of a function for the TIS21/PC3/BTG1/TOB family. *FEBS Lett,* 497**,** 67-72.

Mauxion, F., Faux, C. & Seraphin, B. 2008. The BTG2 protein is a general activator of mRNA deadenylation. *EMBO J. 2008 Apr 9;27(7):1039-48. Epub 2008 Mar 13.*

Mauxion, F., Preve, B. & Seraphin, B. 2013. C2ORF29/CNOT11 and CNOT10 form a new module of the CCR4-NOT complex. *RNA Biol,* 10**,** 267-76.

McManus, C. J. & Graveley, B. R. 2011. RNA structure and the mechanisms of alternative splicing. *Curr Opin Genet Dev,* 21**,** 373-9.

Mittal, S., Aslam, A., Doidge, R., Medica, R. & Winkler, G. S. 2011. The Ccr4a (CNOT6) and Ccr4b (CNOT6L) deadenylase subunits of the human Ccr4-Not complex contribute to the prevention of cell death and senescence. *Mol Biol Cell. 2011 Mar;22(6):748-58. Epub 2011 Jan 13.*

Miyasaka, T., Morita, M., Ito, K., Suzuki, T., Fukuda, H., Takeda, S., Inoue, J., Semba, K. & Yamamoto, T. 2008. Interaction of antiproliferative protein Tob with the CCR4-NOT deadenylase complex. *Cancer Sci. 2008 Apr;99(4):755-61.*

Morin, R. D., Mendez-Lago, M., Mungall, A. J., Goya, R., Mungall, K. L., Corbett, R. D., Johnson, N. A., Severson, T. M., Chiu, R., Field, M., Jackman, S., Krzywinski, M., Scott, D. W., Trinh, D. L., Tamura-Wells, J., Li, S., Firme, M. R., Rogic, S., Griffith, M., Chan, S., Yakovenko, O., Meyer, I. M., Zhao, E. Y., Smailus, D., Moksa, M., Chittaranjan, S., Rimsza, L., Brooks-Wilson, A., Spinelli, J. J., Ben-Neriah, S., Meissner, B., Woolcock, B., Boyle, M., McDonald, H., Tam, A., Zhao, Y., Delaney, A., Zeng, T., Tse, K., Butterfield, Y., Birol, I., Holt, R., Schein, J., Horsman, D. E., Moore, R., Jones, S. J., Connors, J. M., Hirst, M., Gascoyne, R. D. & Marra, M. A. 2011. Frequent mutation of histone-modifying genes in non-Hodgkin lymphoma. *Nature,* 476**,** 298-303.

Morita, M., Oike, Y., Nagashima, T., Kadomatsu, T., Tabata, M., Suzuki, T., Nakamura, T., Yoshida, N., Okada, M. & Yamamoto, T. 2011. Obesity resistance and increased hepatic expression of catabolism-related mRNAs in Cnot3(+/-) mice. *EMBO J. 2011 Sep 6;30(22):4678-4691. doi: 10.1038/emboj.2011.320.*

Morita, M., Suzuki, T., Nakamura, T., Yokoyama, K., Miyasaka, T. & Yamamoto, T. 2007. Depletion of mammalian CCR4b deadenylase triggers elevation of the p27Kip1 mRNA level and impairs cell growth. *Mol Cell Biol. 2007 Jul;27(13):4980-90. Epub 2007 Apr 23.*

Morozov, I. Y., Jones, M. G., Spiller, D. G., Rigden, D. J., Dattenböck, C., Novotny, R., Strauss, J. & Caddick, M. X. 2010. Distinct roles for Caf1, Ccr4, Edc3 and CutA in the co-ordination of transcript deadenylation, decapping and P-body formation in Aspergillus nidulans. *Mol Microbiol,* 76**,** 503-16.

Nasertorabi, F., Batisse, C., Diepholz, M., Suck, D. & Bottcher, B. 2011. Insights into the structure of the CCR4-NOT complex by electron microscopy. *FEBS Lett. 2011 Jul 21;585(14):2182-6. Epub 2011 Jun 12.*

Nilsson, P., Henriksson, N., Niedzwiecka, A., Balatsos, N. A., Kokkoris, K., Eriksson, J. & Virtanen, A. 2007. A multifunctional RNA recognition motif in poly(A)-specific ribonuclease with cap and poly(A) binding properties. *J Biol Chem. 2007 Nov 9;282(45):32902-11. Epub 2007 Sep 4.*

Panasenko, O. O. 2014. The role of the E3 ligase Not4 in cotranslational quality control. *Front Genet,* 5**,** 141.

Parikh, S. S., Mol, C. D., Hosfield, D. J. & Tainer, J. A. 1999. Envisioning the molecular choreography of DNA base excision repair. *Curr Opin Struct Biol,* 9**,** 37-47.

Parker, R. & Song, H. 2004a. The enzymes and control of eukaryotic mRNA turnover. *Nat Struct Mol Biol. 2004 Feb;11(2):121-7.*

Parker, R. & Song, H. 2004b. The enzymes and control of eukaryotic mRNA turnover. *Nat Struct Mol Biol,11(2):121-7.*

Petit, A. P., Wohlbold, L., Bawankar, P., Huntzinger, E., Schmidt, S., Izaurralde, E. & Weichenrieder, O. 2012a. The structural basis for the interaction between the CAF1 nuclease and the NOT1 scaffold of the human CCR4-NOT deadenylase complex. *Nucleic Acids Res. 2012 Sep 12.*

Petit, A. P., Wohlbold, L., Bawankar, P., Huntzinger, E., Schmidt, S., Izaurralde, E. & Weichenrieder, O. 2012b. The structural basis for the interaction between the CAF1 nuclease and the NOT1 scaffold of the human CCR4-NOT deadenylase complex. *Nucleic Acids Res.*

Pettersen, E. F., Goddard, T. D., Huang, C. C., Couch, G. S., Greenblatt, D. M., Meng, E. C. & Ferrin, T. E. 2004. UCSF Chimera--a visualization system for exploratory research and analysis. *J Comput Chem,* 25**,** 1605-12.

Prevot, D., Morel, A. P., Voeltzel, T., Rostan, M. C., Rimokh, R., Magaud, J. P. & Corbo, L. 2001. Relationships of the antiproliferative proteins BTG1 and BTG2 with CAF1, the human homolog of a component of the yeast CCR4 transcriptional complex: involvement in estrogen receptor alpha signaling pathway. *J Biol Chem,* 276**,** 9640-8.

Proudfoot, N. J. 2011. Ending the message: poly(A) signals then and now. *Genes Dev,* 25**,** 1770-82.

Ren, Y. G., Kirsebom, L. A. & Virtanen, A. 2004. Coordination of divalent metal ions in the active site of poly(A)-specific ribonuclease. *J Biol Chem. 2004 Nov 19;279(47):48702-6. Epub 2004 Sep 8.*

Ren, Y. G., Martinez, J., Kirsebom, L. A. & Virtanen, A. 2002a. Inhibition of Klenow DNA polymerase and poly(A)-specific ribonuclease by aminoglycosides. *Rna,* 8**,** 1393-400.

Ren, Y. G., Martinez, J. & Virtanen, A. 2002b. Identification of the active site of poly(A)-specific ribonuclease by site-directed mutagenesis and Fe(2+)-mediated cleavage. *J Biol Chem. 2002 Feb 22;277(8):5982-7. Epub 2001 Dec 12.*

Rohman, M. & Harrison-Lavoie, K. J. 2000. Separation of copurifying GroEL from glutathione-S-transferase fusion proteins. *Protein Expr Purif. 2000 Oct;20(1):45-7.*

Sheets, M. D. & Wickens, M. 1989. Two phases in the addition of a poly(A) tail. *Genes Dev,* 3**,** 1401-12.

Shim, J. & Karin, M. 2002. The control of mRNA stability in response to extracellular stimuli. *Mol Cells,* 14**,** 323-31.

Shirai, Y. T., Suzuki, T., Morita, M., Takahashi, A. & Yamamoto, T. 2014. Multifunctional roles of the mammalian CCR4-NOT complex in physiological phenomena. *Front Genet,* 5**,** 286.

Sissi, C. & Palumbo, M. 2009. Effects of magnesium and related divalent metal ions in topoisomerase structure and function. *Nucleic Acids Res,* 37**,** 702-11.

Suzuki, T., J, K. T., Ajima, R., Nakamura, T., Yoshida, Y. & Yamamoto, T. 2002. Phosphorylation of three regulatory serines of Tob by Erk1 and Erk2 is required for Ras-mediated cell proliferation and transformation. *Genes Dev,* 16**,** 1356-70.

Takahashi, S., Kontani, K., Araki, Y. & Katada, T. 2007. Caf1 regulates translocation of ribonucleotide reductase by releasing nucleoplasmic Spd1-Suc22 assembly. *Nucleic Acids Res,* 35**,** 1187-97.

Thain, A., Gaston, K., Jenkins, O. & Clarke, A. R. 1996. A method for the separation of GST fusion proteins from co-purifying GroEL. *Trends Genet. 1996 Jun;12(6):209-10.*

Thore, S., Mauxion, F., Seraphin, B. & Suck, D. 2003. X-ray structure and activity of the yeast Pop2 protein: a nuclease subunit of the mRNA deadenylase complex. *EMBO Rep. 2003 Dec;4(12):1150-5. Epub 2003 Nov 14.*

Tirone, F. 2001. The gene PC3(TIS21/BTG2), prototype member of the PC3/BTG/TOB family: regulator in control of cell growth, differentiation, and DNA repair? *J Cell Physiol,* 187**,** 155-65.

Tucker, M., Staples, R. R., Valencia-Sanchez, M. A., Muhlrad, D. & Parker, R. 2002. Ccr4p is the catalytic subunit of a Ccr4p/Pop2p/Notp mRNA deadenylase complex in Saccharomyces cerevisiae. *EMBO J. 2002 Mar 15;21(6):1427-36.*

Tucker, M., Valencia-Sanchez, M. A., Staples, R. R., Chen, J., Denis, C. L. & Parker, R. 2001. The transcription factor associated Ccr4 and Caf1 proteins are components of the major cytoplasmic mRNA deadenylase in Saccharomyces cerevisiae. *Cell. 2001 Feb 9;104(3):377-86.*

Tumey, L. N., Bom, D., Huck, B., Gleason, E., Wang, J., Silver, D., Brunden, K., Boozer, S., Rundlett, S., Sherf, B., Murphy, S., Dent, T., Leventhal, C., Bailey, A., Harrington, J. & Bennani, Y. L. 2005. The identification and optimization of a N-hydroxy urea series of flap endonuclease 1 inhibitors. *Bioorg Med Chem Lett. 2005 Jan 17;15(2):277-81.*

van Hoof, A., Frischmeyer, P. A., Dietz, H. C. & Parker, R. 2002. Exosome-mediated recognition and degradation of mRNAs lacking a termination codon. *Science,* 295**,** 2262-4.

Viswanathan, P., Chen, J., Chiang, Y. C. & Denis, C. L. 2003. Identification of multiple RNA features that influence CCR4 deadenylation activity. *J Biol Chem. 2003 Apr 25;278(17):14949-55. Epub 2003 Feb 17.*

Viswanathan, P., Ohn, T., Chiang, Y. C., Chen, J. & Denis, C. L. 2004. Mouse CAF1 can function as a processive deadenylase/3'-5'-exonuclease in vitro but in yeast the deadenylase function of CAF1 is not required for mRNA poly(A) removal. *J Biol Chem,* 279**,** 23988-95.

Waanders, E., Scheijen, B., van der Meer, L. T., van Reijmersdal, S. V., van Emst, L., Kroeze, Y., Sonneveld, E., Hoogerbrugge, P. M., van Kessel, A. G., van Leeuwen, F. N. & Kuiper, R. P. 2012. The origin and nature of tightly clustered BTG1 deletions in precursor B-cell acute lymphoblastic leukemia support a model of multiclonal evolution. *PLoS Genet,* 8**,** e1002533.

Wahle, E. & Winkler, G. S. 2013a. RNA decay machines: Deadenylation by the Ccr4-Not and Pan2-Pan3 complexes. *Biochim Biophys Acta,1829(6-7):561-70*.

Wahle, E. & Winkler, G. S. 2013b. RNA decay machines: Deadenylation by the Ccr4-Not and Pan2-Pan3 complexes. *Biochim Biophys Acta. 2013 Jan 19. pii: S1874-9399(13)00007-2. doi: 10.1016/j.bbagrm.2013.01.003.*

Wang, H., Morita, M., Yang, X. N., Suzuki, T., Yang, W., Wang, J. A., Ito, K., Wang, Q. A., Zhao, C., Bartlam, M., Yamamoto, T. & Rao, Z. H. 2010. Crystal structure of the human CNOT6L nuclease domain reveals strict poly(A) substrate specificity. *Embo Journal,* 29**,** 2566-2576.

Washio-Oikawa, K., Nakamura, T., Usui, M., Yoneda, M., Ezura, Y., Ishikawa, I., Nakashima, K., Noda, T., Yamamoto, T. & Noda, M. 2007a. Cnot7-null mice exhibit high bone mass phenotype and modulation of BMP actions. *J Bone Miner Res,22(8):1217-23.*

Washio-Oikawa, K., Nakamura, T., Usui, M., Yoneda, M., Ezura, Y., Ishikawa, I., Nakashima, K., Noda, T., Yamamoto, T. & Noda, M. 2007b. Cnot7-null mice exhibit high bone mass phenotype and modulation of BMP actions. *J Bone Miner Res. 2007 Aug;22(8):1217-23.*

Wilusz, C. J., Wormington, M. & Peltz, S. W. 2001. The cap-to-tail guide to mRNA turnover. *Nat Rev Mol Cell Biol. 2001 Apr;2(4):237-46.*

Winkler, G. S. 2010. The mammalian anti-proliferative BTG/Tob protein family. *J Cell Physiol. 2010 Jan;222(1):66-72.*

Winkler, G. S. & Balacco, D. L. 2013. *Heterogeneity and complexity within the nuclease module of the Ccr4-Not complex*, Front Genet. 2013 Dec 23;4:296. eCollection 2013.

Wolf, J. & Passmore, L. A. 2014. mRNA deadenylation by Pan2-Pan3. *Biochem Soc Trans,* 42**,** 184-7.

Wu, M., Nilsson, P., Henriksson, N., Niedzwiecka, A., Lim, M. K., Cheng, Z., Kokkoris, K., Virtanen, A. & Song, H. 2009. Structural basis of m(7)GpppG binding to poly(A)-specific ribonuclease. *Structure. 2009 Feb 13;17(2):276-86.*

Wu, M., Reuter, M., Lilie, H., Liu, Y., Wahle, E. & Song, H. 2005. Structural insight into poly(A) binding and catalytic mechanism of human PARN. *Embo j,* 24**,** 4082-93.

Wu, X. & Brewer, G. 2012. The regulation of mRNA stability in mammalian cells: 2.0. *Gene,* 500**,** 10-21.

Yamashita, A., Chang, T. C., Yamashita, Y., Zhu, W., Zhong, Z., Chen, C. Y. & Shyu, A. B. 2005. Concerted action of poly(A) nucleases and decapping enzyme in mammalian mRNA turnover. *Nat Struct Mol Biol. 2005 Dec;12(12):1054-63. Epub 2005 Nov 13.*

Yanagie, H., Tanabe, T., Sumimoto, H., Sugiyama, H., Matsuda, S., Nonaka, Y., Ogiwara, N., Sasaki, K., Tani, K., Takamoto, S., Takahashi, H. & Eriguchi, M. 2009. Tumor growth suppression by adenovirus-mediated introduction of a cell-growth-suppressing gene tob in a pancreatic cancer model. *Biomed Pharmacother,* 63**,** 275-86.

Yoneda, M., Suzuki, T., Nakamura, T., Ajima, R., Yoshida, Y., Kakuta, S., Katsuko, S., Iwakura, Y., Shibutani, M., Mitsumori, K., Yokota, J. & Yamamoto, T. 2009. Deficiency of antiproliferative family protein Ana correlates with development of lung adenocarcinoma. *Cancer Sci,* 100**,** 225-32.

Yoshida, Y., Hosoda, E., Nakamura, T. & Yamamoto, T. 2001. Association of ANA, a member of the antiproliferative Tob family proteins, with a Caf1 component of the CCR4 transcriptional regulatory complex. *Jpn J Cancer Res,* 92**,** 592-6.

Yoshida, Y., Nakamura, T., Komoda, M., Satoh, H., Suzuki, T., Tsuzuku, J. K., Miyasaka, T., Yoshida, E. H., Umemori, H., Kunisaki, R. K., Tani, K., Ishii, S., Mori, S., Suganuma, M., Noda, T. & Yamamoto, T. 2003a. Mice lacking a transcriptional corepressor Tob are predisposed to cancer. *Genes Dev,* 17**,** 1201-6.

Yoshida, Y., Tanaka, S., Umemori, H., Minowa, O., Usui, M., Ikematsu, N., Hosoda, E., Imamura, T., Kuno, J., Yamashita, T., Miyazono, K., Noda, M., Noda, T. & Yamamoto, T. 2000. Negative regulation of BMP/Smad signaling by Tob in osteoblasts. *Cell,* 103**,** 1085-97.

Yoshida, Y., von Bubnoff, A., Ikematsu, N., Blitz, I. L., Tsuzuku, J. K., Yoshida, E. H., Umemori, H., Miyazono, K., Yamamoto, T. & Cho, K. W. 2003b. Tob proteins enhance inhibitory Smad-receptor interactions to repress BMP signaling. *Mech Dev,* 120**,** 629-37.

Zhang, X., Virtanen, A. & Kleiman, F. E. 2010. To polyadenylate or to deadenylate: that is the question. *Cell Cycle. 2010 Nov 15;9(22):4437-49. Epub 2010 Nov 15.*

Zhao, J., Hyman, L. & Moore, C. 1999. Formation of mRNA 3' ends in eukaryotes: mechanism, regulation, and interrelationships with other steps in mRNA synthesis. *Microbiol Mol Biol Rev,* 63**,** 405-45.

Zuo, Y. & Deutscher, M. P. 2001a. Exoribonuclease superfamilies: structural analysis and phylogenetic distribution. *Nucleic Acids Res,29(5):1017-26.*

Zuo, Y. & Deutscher, M. P. 2001b. Exoribonuclease superfamilies: structural analysis and phylogenetic distribution. *Nucleic Acids Res. 2001 Mar 1;29(5):1017-26.*